博 士 論 文

Study on Ciprofloxacin-Removal Membrane for Antibiotic Treatment in Medical Building Wastewater

2023 年 06 月

王　興国

WANG XINGGUO

Study on Ciprofloxacin-Removal Membrane for Antibiotic Treatment in Medical Building Wastewater

ABSTRACT

With the increasing use of antibiotics and the rising concentration of antibiotics in medical wastewater, the treatment of antibiotics in wastewater from medical buildings has become increasingly important. To enhance the efficiency of antibiotic removal in medical wastewater treatment, I proposed the design of a thicker membrane material with larger interconnected pores. Additionally, I attempted to synthesize a layer of adsorptive polymer on the membrane surface to enhance its affinity for antibiotic molecules. Through this approach, I successfully synthesized polymerization adsorption membranes (PAM) and tested their performance using Ciprofloxacin (CIP) as a model antibiotic. The results demonstrated the presence of adsorption capacity and permeation inhibition for CIP molecules on the PAM. Furthermore, to meet the demand for selective adsorption of specific types of antibiotic molecules, I introduced molecular imprinting technology onto the PAM membrane. This resulted in the synthesis of a Molecularly Imprinted Membrane (MIM) using CIP as a template. The MIM exhibited significantly improved absorption capacity and permeation inhibition for CIP molecules.

In Chapter 1, RESEARCH BACKGROUND AND PURPOSE OF THE STUDY, the research backgrounds of the increasing use of antibiotics and the rising concentration of antibiotics in medical wastewater are introduced in chapter 1, including the sources and distribution of antibiotics in the environment. As well as the antibiotic pollution in water resources. Then the hazards of antibiotics pollution to the environment, creature and human beings is well introduced. Researching the treatment technologies for antibiotics in medical building wastewater is of great importance. At last, the research purpose and logical framework is shown in order to support reviewers understand the content of this paper.

In Chapter 2, LITERATURE REVIEW OF ANTIBIOTIC REMOVAL, this chapter provides a comprehensive overview of past research on the removal of antibiotics from wastewater. The focus is on three primary treatment methods: biological treatment, oxidation methods, and physical methods. The biological treatment approach is cost-effective and can achieve high removal efficiencies but sensitive to environmental conditions, and have the potential for the development of antibiotic-resistant bacteria. The oxidation methods have high treatment efficiency but its energy and cost consumption are high, too. Physical methods, particularly membrane separation technology, offers high removal efficiencies, compatibility, and the potential for resource recovery. Therefore, the treatment of antibiotics by membrane technology is the focus of this study.

In Chapter 3, METHODOLOGY, in this chapter, the design of membrane synthesis methods was explored. The aim was to enhance both membrane flux and adsorption efficiency. To achieve this, the membrane thickness was increased, and a sacrificial template method was utilized to enhance the interconnected pore structure within the membrane. To address the issue of pore size affecting treatment efficiency, a plan was devised to synthesize a polymer layer on the inner and outer surfaces of the membrane to absorb antibiotic molecules. In order to ensure that the synthesized materials meet our requirements, a design for the characterization methods of the membrane materials was established. This involved conducting a series of material property characterizations, including scanning electron microscopy (SEM), X-ray photoelectron spectroscopy (XPS), Fourier-transform infrared spectroscopy (FTIR), in-situ diffuse reflectance infrared Fourier transform spectroscopy (In-situ DRIFT) and so on.

In Chapter 4, DATA RESOURCE AND MEMBRANE PERFORMANCE ANALYSIS, this chapter focused on the planning and design of testing methods for membrane performance, with ciprofloxacin selected as the target molecule for testing. The testing methods were carefully planned to evaluate the efficacy of the membranes in adsorbing and permeating ciprofloxacin.

The adsorption capacity would provide insights into the membrane's ability to remove the target molecule from the solution, while the permeation tests would assess the membrane's ability to allow or restrict the passage of the molecule through its structure. By conducting these tests and employing the provided calculation methods, the performance of the synthesized membranes could be quantitatively evaluated.

In Chapter 5, POLYMERIZATION ADSORPTION MEMBRANE, in this chapter, the synthesis of the Polymerization Adsorption Membrane (PAM) was performed. After determining the materials and characterization equipment, the PVDF-βCD-dopamine membrane (VCDM) was synthesized as a precursor, followed by ethylene modification and subsequent polymerization to obtain the desired PAM. The membrane was then subjected to material characterization, confirming the success of each reaction step. The performance testing began with isothermal adsorption tests, which revealed that the adsorption capacity of the PAM for ciprofloxacin (CIP) reached 22.04 mg g-1. Furthermore, the adsorption sites on the PAM exhibited a uniform and monolayer distribution, confirming its adsorption capability for CIP molecules. Subsequently, permeation adsorption experiments were conducted, and it was observed that the equilibrium of CIP molecules in solution was reached after 24 hours. This indicated that the PAM had an inhibitory effect on the permeation of CIP within 24 hours.

In chapter 6, MOLECULARLY IMPRINTED MEMBRANE, in this chapter, to maximize membrane utilization and address real antibiotic discharge scenarios, I enhanced the absorption capacity of the PAM membrane for a specific antibiotic molecule among various types. Through modification during synthesis, the final step incorporated molecular imprinting technology, using ciprofloxacin (CIP) as the template, resulting in the creation of a Molecularly Imprinted Membrane (MIM). Material characterization confirmed the successful synthesis at each step. In adsorption performance tests, the MIM exhibited an impressive adsorption capacity of 121.12 mg g-1 for CIP molecules. The membrane surface demonstrated a uniform monolayer

distribution of adsorption sites, with a coexistence of chemical adsorption and physical diffusion. Subsequently, selective adsorption and permeation experiments were conducted with four structurally similar but different types of antibiotics, including CIP. The results revealed that the MIM possessed significantly higher absorption capacity for CIP molecules compared to the other three types. The inhibitory effect on CIP permeation lasted for 36 hours, surpassing the 24-hour mark observed for the other types. These findings demonstrate the strong inhibitory and adsorption capabilities of the MIM specifically for CIP molecules.

In chapter 7, PERFORMANCE COMPARISON, in this chapter, in order to evaluate the performance enhancement achieved by incorporating molecular imprinting technology, a comparison of the Molecularly Imprinted Membrane (MIM) and the Polyacrylamide (PAM) membrane was conducted. Additionally, the PAM membrane was subjected to adsorption and permeation experiments involving four structurally similar but different types of antibiotics. The results of the comparison indicated that the MIM is far superior to PAM in terms of adsorption capacity, permeation inhibition, adsorption selectivity and permeation selectivity, highlighting the role played by the imprinting sites on the membrane surface. Then regeneration performance and anti-fouling tests were performed on the MIM, demonstrating comparable regenerative properties and a wider range of resistance to fouling. Taking all the findings into consideration, the as-constructed MIM exhibited superior comprehensive properties compared to similar materials, thus presenting promising prospects for broader applications.

In Chapter 8, CONCLUSION AND PROSPECT. A summarized of each Chapter is concluded.

王 興国 博士論文の構成

Study on Ciprofloxacin-Removal Membrane for Antibiotic Treatment in Medical Building Wastewater

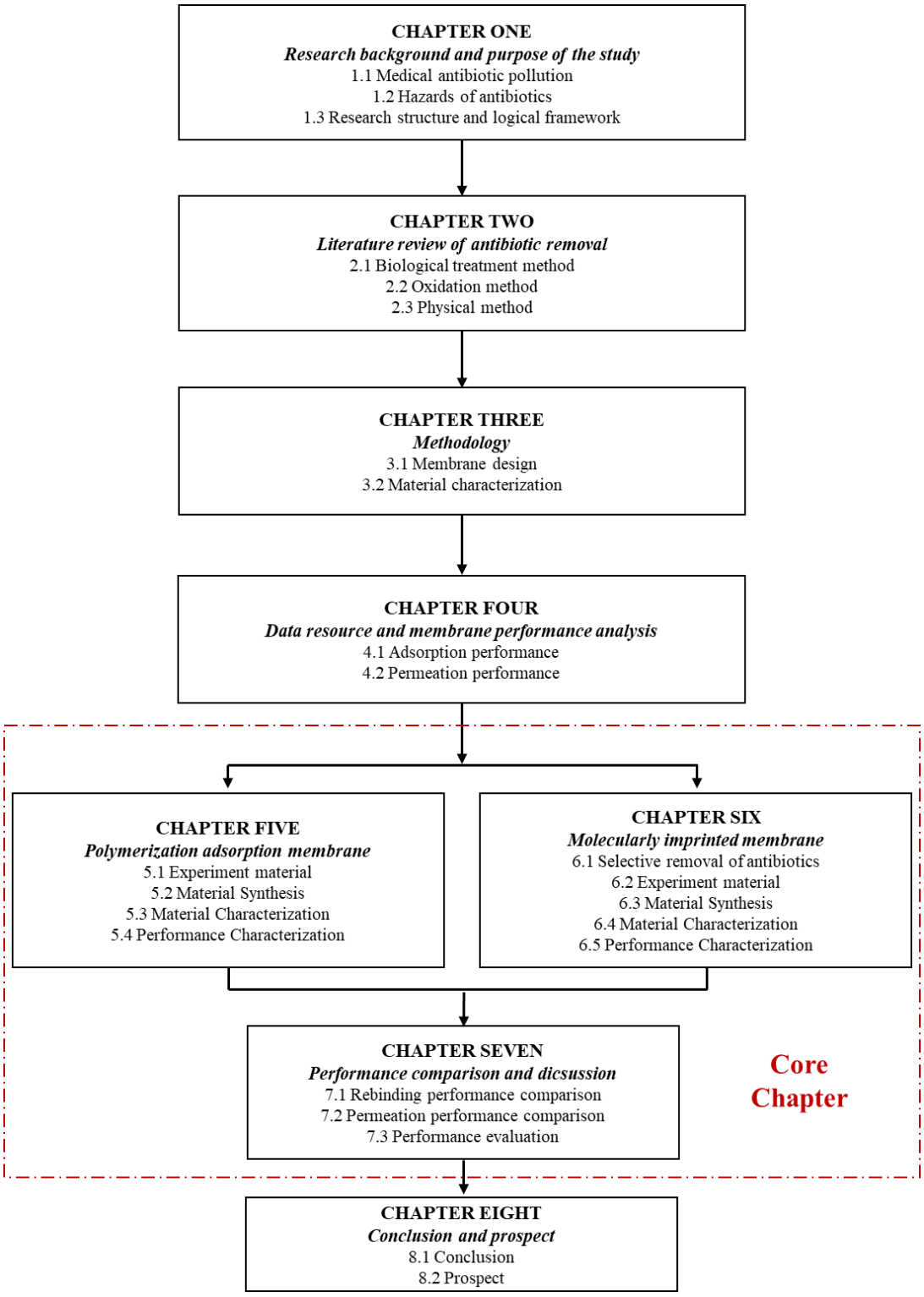

CONTENTS

Chapter 1

RESEARCH BACKGROUND AND PURPOSE OF THE STUDY

1.1 Medical antibiotic pollution

1.1.1 Background

Antibiotics are medications that fight bacterial infections. Which is used in a wide range of hospitals and residents. Between 2000 and 2015, antibiotic consumption, expressed in defined daily doses (DDD), increased 65% (21.1–34.8 billion DDDs), and the antibiotic consumption rate increased 39% (11.3–15.7 DDDs per 1,000 inhabitants per day) [1]. The residence time of antibiotics into the body is short, only a small part is absorbed into the organism for metabolism, about 60% to 90% of antibiotics in the form of prototypes or metabolites are excreted with the feces and urine. Studies have shown that more than 85% of antibiotics are transferred to the environment through sewage in the form of prodrugs and their metabolites. Currently, the range of detectable concentrations of antibiotics in wastewater has developed worldwide from the ng L^{-1} and μg L^{-1} levels to the mg L^{-1} level. And for example, the detection concentration of antibiotics in medical wastewater can reach 21 μg L^{-1} [2]. This antibiotic-laden medical effluent eventually makes its way through the sewage plant and into natural water bodies.

After antibiotics enters the water body directly or indirectly, it is still biologically active, and even if the level is only at trace level, it is still harmful to the ecological environment and human health, which can be divided into the following aspects [3]:

Drug resistance and superbugs: the residual hazards of antibiotics are mainly the induction of resistance genes, damage to aquatic ecology, and threats to human health; risk of ecological imbalance: antibiotics is toxic to many aquatic organisms, and its long-term exposure to antibiotics will inhibit their metabolic processes, and may lead to ecological imbalance due to the different sensitivity of different organisms to antibiotics; hazards to humans: antibiotics can cause adverse reactions in humans [4], such as nausea, vomiting, appetite disorders, abdominal pain, diarrhea, and other gastrointestinal reactions. Therefore, for medical buildings, it is of great importance to add antibiotic removal equipment to their drainage systems. The core technology of antibiotic removal is the subject of this paper.

1.1.2 Overview of Antibiotics

Antibiotics are mainly organic compounds produced by microorganisms (such as bacteria,

fungi, etc.) with anti-pathogenic or other activities or by synthetic or semi-synthetic analogues for the treatment and prevention of human and animal diseases caused by bacterial and microbial infections, and can also be used as growth promoters to stimulate the growth of farm animals. Since 1928 British scientist Alexander. Fleming inadvertently discovered penicillin, the emergence of antibiotics has saved countless lives and is one of the greatest inventions of mankind since the twentieth century. Due to the excellent efficacy and wide application value of antibiotics, they were soon developed rapidly.

However, in recent years, with the continuous progress of industrial and scientific development, the production and use of antibiotics are also increasing, and even the emergence of the problem of abuse has made the ecological and environmental problems caused by antibiotics increasingly become the focus of discussion. As an emerging pollutant in the environment, there are many different types of antibiotics with different physicochemical properties and scope of application, and therefore the degree of residue in the environment and the ecological risks caused， and the development of antimicrobial resistance induced also vary.

In most cases, antibiotics are highly hydrophilic and weakly volatile, and their transmission in the environment is mainly through the aqueous phase and food chain, ultimately posing a threat to human health, while the residual antibiotics in the environment have certain toxic effects on organisms that threaten the health of the ecosystem. At present, the misuse of antibiotics is relatively common, and a WHO survey shows that up to 80% of patients in z Chinese medical institutions have antibiotics in their drug list, which is much higher than the international level (about 50%), and in 2015 WHO has described the problem of antibiotic-induced drug resistance as a global public health crisis that must be addressed urgently.

1.1.3 Production and use of antibiotics

Since the 1940s, the discovery of penicillin has led to the gradual development of the antibiotic production industry. In terms of production methods, natural synthesis is the main method, supplemented by artificial synthesis, mainly by microbial fermentation, and a few antibiotics can be synthesized by chemical synthesis. At the same time, the naturally obtained antibiotics have been modified biochemically or chemically to give them superior properties. For antibiotic-producing bacteria, the two main groups include mycobacteria and

actinomycetes.

The fermentation production process of antibiotics is basically like the production process of microbial fermentation, which uses the cultivation of microorganisms to ferment them to produce antibiotics or other active pharmaceutical ingredients. Generally, a typical biological fermentation process mainly includes the steps of strain screening, seed expansion culture, microbial fermentation and extraction and purification, etc. A typical biological fermentation process is shown in Fig. 1-1. With the continuous optimization of modern biotechnology engineering, the yield of antibiotics has been effectively improved, and the components and production process of antibiotics have been effectively improved, which in turn makes the produced antibiotics more application value.

The advent of antibiotics has been a boon to save countless lives. For the present, the use of antibiotics basically falls into three areas: they can be used to treat human and animal diseases, as growth promoters, and to improve feed feeding efficiency. Globally, it has been reported that more than 100,000 tons of antibiotics are used annually [5]. China is the largest producer and user of antibiotics in the world. In 2013, the total use of antibiotics in China was reported to be about 160 million kg, which is nine times more than the use in the United States during the same period, and the per capita use of antibiotics was all more than six times that of the United Kingdom, the United States, and Canada [6]. The widely used antibiotics include sulfonamides (SAs), macrolides (MLs), quinolones (QNs), tetracyclines (TCs), and β-lactams (β-Ls), etc. A 2013 survey of five major classes of commonly used the survey of antibiotics showed that the use of antibiotics was the largest in East China and the smallest in Northwest China, in which macrolides, β-lactams and quinolones were used more in most regions.

In agriculture, animal husbandry and farming, the use of antibiotics covers almost all types of antibiotics used for human medical treatment [5], and in 2017, China ranked first in the world in the use of veterinary antibiotics (43% of the total) [7] In recent years, the use of veterinary antibiotics in China has increased year by year, and it is estimated that the proportion of the total global use of veterinary antibiotics in China will rise from 23% in 2010 to 30% in 2030 [8], while about 48% of the total use of antibiotics in China is used for human medical treatment.

The rate of antimicrobial drug use among hospital patients at all levels in China has been reported to be above 70%, far exceeding the WHO recommendation of 15%-30%. A survey of antibiotic prescriptions in 48 primary health care facilities in China showed that cephalosporins, fluoroquinolones, penicillin, imidazole and macrolides were the commonly prescribed clinical classes of antibiotics in medical use [9].

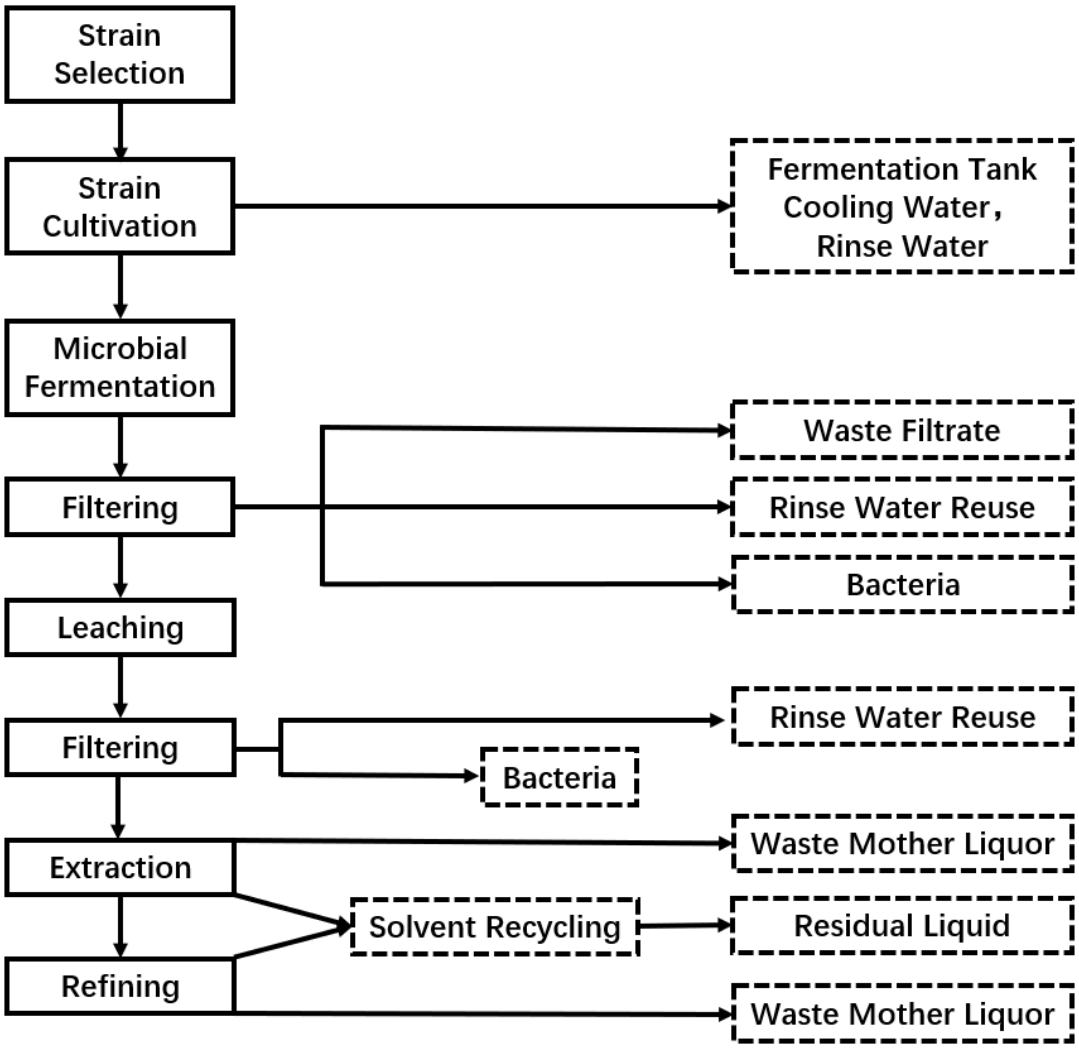

Fig. 1-1 Block figure of conventional microbial fermentation pharmacy

1.1.4 Sources and distribution of antibiotics in the environment

There are various source pathways of antibiotics in the environment, mainly including: municipal (domestic and urban wastewater), agricultural (aquaculture, animal husbandry) and pharmaceutical industries. The main sources and migration pathways of antibiotics in the environment are shown in Fig. 1-2.

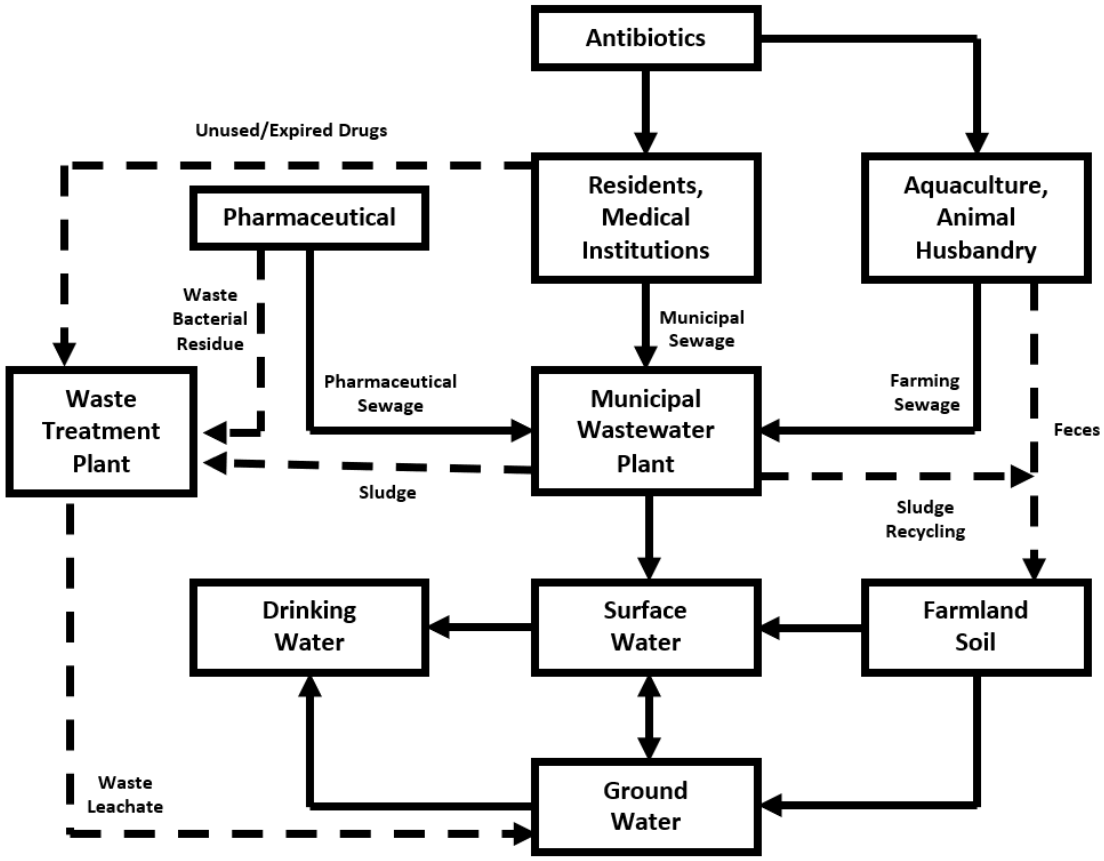

Fig. 1-2 Sources and distribution of antibiotics in the environment

After antibiotics are ingested by humans or animals, most of them cannot be metabolized by the organisms and are discharged into the sewage in their original form or as metabolites in the form of feces and urine. In China, more than half of the citizens have blind medication practices that increase the possibility of antibiotics entering the environment. To date, there have been many reports on the concentration levels of residual antibiotics in human feces and urine. Wang et al [10] quantified 18 antibiotics in the urine of 1064 children, and all antibiotics were detected, with the highest concentrations of 8 antibiotics reaching 1000 ng ml^{-1}. 19 antibiotics investigated in human feces were detected, with the highest concentrations of sulfonamides, tetracyclines, and quinolones [6]. The highest concentrations were detected in human feces [6]. These antibiotics in feces and urine are discharged with domestic sewage, which increases the load of domestic sewage, i.e., municipal sewage. It also makes municipal wastewater one of the important sources of is antibiotics.

P. Verlicchi et al. compiled 78 global articles on antibiotic concentrations in municipal wastewater, which ranged from 0.001 ug L^{-1} to 32 ug L^{-1}, with higher levels occurring in OFL

(maximum 32 ug L^{-1}), RTM (maximum 17 ug L^{-1}) and CIP (maximum 14 ug L^{-1}). Dinh et al [11] in a French sewage system of NOR, CIP, OFL, ERY and SMX were found in domestic sewage ranging from 100 ng L^{-1} to 1753 ng L^{-1}. In the coastal area of South China Sea, Chen et al [12] found that untreated domestic sewage was the major source of antibiotics followed by agricultural sewage. Zhang et al [13] investigated the source of antibiotics in Chaobai River, Beijing and found that domestic sewage was the main source of antibiotics in the rivers of the region.

Municipal wastewater is considered to be one of the major sources of antibiotics, where domestic wastewater accounts for more than 70% of municipal wastewater in the UK and US, followed by hospital wastewater 5%-20% [14], and antibiotics in domestic wastewater subsequently enter the wastewater treatment plant. A large number of studies have shown that current urban municipal wastewater plants have poor treatment capacity for antibiotics [15], and there are often varying degrees of antibiotic residues in the secondary effluent of municipal wastewater plants, and untreated antibiotics are subsequently discharged into the receiving water bodies and into the aquatic environment.

Watkinson et al [16] reported that residual concentrations of 20 antibiotics in wastewater from wastewater treatment plants in Australia could reach 10 μg L^{-1}. Antibiotics were detected in municipal wastewater plant effluent throughout China at levels up to microgramme per liter [17], and in municipal wastewater plants in the Pearl River Delta cities of southern China (e.g., Guangzhou, Shenzhen, and Hong Kong), the frequently detected and highly concentrated the antibiotic species detected frequently and at high concentrations in municipal wastewater plants in the Pearl River Delta cities of South China (e.g., Guangzhou, Shenzhen, and Hong Kong) include macrolides (e.g. ETM and AETM), fluoroquinolones (e.g. OFL and NOR), and sulfonamides (e.g. SMX) [18].Ben et al [19] investigated the antibiotic residue levels in the effluent of 14 wastewater treatment plants in large and medium-sized cities in China in 2018 and found that macrolide and quinolone antibiotics were the most abundant in the effluent of wastewater plants, with concentrations ranging from 35.3-108.4 ng L^{-1} and 1.8-253.3 ng L^{-1}, with the detection rate of macrolide antibiotics as high as 100%. Due to the limited treatment effect, this type of wastewater discharge can cause pollution to surface water, ground water and

agricultural soil.

Li [20] investigated 12 large wastewater treatment plants in China and found high ecological risks (RQ>1) for OFL, AETM, CTM, RTM, and SMX in the effluent. At the same time, substances adsorbed in activated sludge enter the environment through agricultural production activities such as composting [21]. There was a significant increase in the content and diversity of ARGs in agricultural fields after long-term application of activated sludge and chicken manure [22]. Three SAs (SMX, SPD and TMP) and three MLs (AZM, CTM and RTM) were detected in activated sludge from sewage plants in Germany and Switzerland at concentrations ranging from 0.05 to 0.2 mg Kg^{-1} [23]. Antibiotics in activated sludge can enter the environment with agricultural activities such as landfill and irrigation [24], and some antibiotics show persistence in activated sludge [25], so the contamination of antibiotics in activated sludge cannot be ignored.

In the farming industry, agricultural veterinary antibiotics are mainly used for the treatment and prevention of animal diseases, or to promote animal growth and weight gain by micro-dosing to achieve the purpose of increasing production. Currently, most farms use wastewater treatment process to treat antibiotics poorly, and for small farms without wastewater treatment facilities, antibiotic pollution may be more serious. Veterinary antibiotics, including CTC, OTC, SMZ, SDZ, and SMX, were monitored in wastewater from 27 animal farms in Jiangsu Province at concentrations up to 211 μg L^{-1} [26]. The highest level of OFL residues was found in a farm wastewater and environmental water in Jiangxi province, with concentrations up to 911 ng L^{-1}. Farm wastewater is one of the important sources in the water bodies of this region.

In addition, direct disposal of drugs (e.g., expired drugs, improper disposal of drugs) can lead to the introduction of antibiotics into municipal solid waste. Jonathan P et al [27] investigated the drug use and disposal behavior of local residents in the southeast of England and found that household waste and unused drugs were important sources of antibiotics in the environment. Bu et al [28] deduced that Beijing, Guangzhou, and Chongqing accounted for about 30-80% of the total emissions through non-wastewater routes. SMZ, NOR, OFL, RTM, PEF and AETM antibiotics were detected in 100% of solid waste and leachate from municipal landfills, with the highest levels of quinolones in solid waste. In addition, animal manure is often applied to

agricultural fields as fertilizer, which is one of the important ways for unmetabolized antibiotics to enter the soil and water environment. Zhang et al found that the levels of quinolones and tetracyclines antibiotics were significantly increased in soil applied with cattle manure. Antibiotics in soil can further migrate to surface water and groundwater through percolation and leaching, and even be absorbed by soil microorganisms and crops [24].

At the same time, discharges from the pharmaceutical industry cannot be ignored, and various wastewater discharged from the antibiotic production process (including waste filtrate, waste mother liquor, etc.) usually contain residual antibiotics and related products at high concentrations. The effluent from wastewater plants in Hebei, which receive wastewater from pharmaceutical plants, contains oxytetracycline at levels up to mg/kg, which has a high impact on the ecological environment [29].

Due to their polarity, the fraction entering the atmospheric environment will be limited. Their distribution will occur mainly in the aquatic environment [17]. Antibiotics in the water column may accumulate in the sediment with flocculation and sedimentation, etc. PPCP may also be adsorbed to activated sludge in the STP and then introduced into the environment through land application of sludge. The sediment levels in the major watersheds in China ranged from 0.1 ng L^{-1} to 1 μg L^{-1}, mostly below 100 ng L^{-1}. The high levels of TCs and QNs in the Yangtze River basin may be related to the high use of these two types of antibiotics in agricultural production in the Yangtze River basin. In contrast, the level of antibiotics in WWTP activated sludge could be as high as micro gramme per liter level. These studies suggest that PPCPs can be removed by adsorption to the sludge without being completely metabolized or degraded. This also suggests that PPCP in sediment is a potential source of non-point source pollution in surface water [24].

1.2 Hazards of antibiotics

1.2.1 Antibiotic pollution in water resources

Clean water resources play a vital role in sustaining human life and the sustainable development of society and are an important resource for the survival of life on earth. With the increase of water consumption in human production and life, the water pollution caused by the

pollutants produced is also becoming more and more serious [30-34], among which the water pollution caused by antibiotics has received more and more attention in recent years.

Antibiotic contamination in natural water bodies has a significant impact on the balance of microbial communities in water bodies, where antibiotics act as a selective agent for species in the environment and drug-resistant microorganisms become the dominant species because of unaffected growth or lack of competition [35]. Although some authors have suggested that personal medications and care products are sensitive to most antibiotics based on toxicological data and environmental concentration levels [36], Crane et al [37] summarized the chronic toxicity of human pharmaceuticals to microorganisms in the aquatic environment and showed that microalgae and cyanobacterial unicellular organisms are more sensitive to most antibiotics. Although the environmental survey data and toxicological data of antibiotics are not comprehensive, the environmental risk assessment of antibiotics has been carried out by Li et al [38], who assessed the risk of antibiotic contamination in seven major rivers in China and showed that antibiotic contamination in the Hai rivers and Yellow rivers posed a high risk to algae and invertebrates (RQ>1).

There are certain antibiotic residues (ng/L) in drinking water sources [39, 40], and although direct drinking of drinking water containing trace concentrations of antibiotics is not harmful, long-term drinking may have adverse effects on humans. As described by Van Boeckel et al [41], food animals are one of the major users of antibiotics and antibiotic resistance in these animals is increasing year by year. The accumulation of antibiotics in food animals is enriched through the food chain and eventually ingested by humans, increasing the risk of drug resistance. Antibiotics may accumulate in vegetables through water transport and passive absorption and are distributed in the order of leaves > stems > roots in vegetable plants [42]. Some antibiotics also inhibit the growth of beneficial flora in the human intestinal tract, which is harmful to human health [43]. In addition, it has been suggested that there may be a potential relationship between antibiotic use and the development of breast cancer [44].

Antibiotic contamination is an environmental contamination caused by the inability of humans or animals to fully absorb the antibiotics taken, resulting in the discharge of large amounts of antibiotics into the environment as metabolites or even in their raw state [5, 6, 30,

45].

In natural environments unaffected by human activities, microorganisms are producers of antibiotics, but the level of antibiotics produced is extremely low and belongs to the natural defense mechanism of microorganisms, so the influence of human activities is the main source of antibiotics in the current aquatic environment.

It has been reported that the residence time of antibiotics entering the organism is short and only a small portion is absorbed into the organism for metabolism, and about 60%-90% of antibiotics are excreted in the form of prototypes or metabolites with feces and urine, and eventually enter the environment through domestic sewage, medical sewage, farming sewage and production wastewater [35].

Antibiotic contamination not only causes the enhancement of bacterial resistance, but also produces certain toxicity to other organisms in the environment [30], so the research on the effective treatment of antibiotics in wastewater has an important social and scientific value.

Studies have shown that more than 85% of antibiotics is transferred to the environment through sewage and all of it is done in the form of protoplasts and their metabolites.

With the widespread use of antibiotics, antibiotics has been commonly detected in environmental water and soil. One of the main ways for antibiotics to enter the environmental soil is the arbitrary piling of livestock manure containing antibiotics antibiotics and the extensive use of organic fertilizers. Since the antibiotics cannot be completely absorbed and transformed in animals, most of the antibiotics are excreted in the form of prodrugs with manure and urine, and most of the manure is applied directly to agricultural fields without treatment, and then a large amount of antibiotics will enter the surface and water bodies with rainwater after being washed. According to statistics, the amount of antibiotics entering the soil due to manure application can reach hundreds of grams per hectare per year [51]. In order to improve the aeration, permeability, and nutrients of saline soils, additional organic fertilizers are usually applied during saline soil remediation, and antibiotics in manure contaminates the soil.

Hospital wastewater and production wastewater from medical antibiotics and antibiotics production are rapidly adsorbed by organic matter and minerals in the soil and then enriched in

the soil [52], which is one of the main ways for antibiotics to enter the environmental soil.

Due to its high residual characteristics, antibiotics is found in the environment and in plants and animals to varying degrees. Morales [53] et al. found that the level of antibiotics in Spanish soil fertilized with animal manure was 5.8 mg kg^{-1}. Lingberg [54] et al. showed that the concentration of antibiotics in municipal wastewater in the United States could be as high as 311 mg L^{-1}. Xu Weihai et al. found that antibiotics could be detected in the seawater of Port Victoria, Hong Kong. Tai Y. P. et al. found that antibiotics was present in pig manure and cow manure in Guangzhou with average levels of 152.0 μg kg^{-1} and 88.6 μg kg^{-1}. Su et al. found that antibiotics residues could be detected at different levels in soil profiles in the southeastern suburbs of Beijing, and the levels decreased and then increased with soil depth. Li Juan et al. found that antibiotics residues were found in wastewater and soil around typical pig farms in Beijing.

Currently, the range of detectable concentrations of antibiotics in wastewater worldwide has developed from nanogram per liter and microgram per liter levels to milligram per liter levels, for example, up to 21 μg L^{-1} in medical wastewater and up to 4.9 mg L^{-1} in related production wastewater [55]. The maximum detected concentration of antibiotics in the effluent from wastewater treatment plants in China was 1323 ng L^{-1}, in Brazil up to 2378 ng L^{-1} [56], and in Finland up to 4230 ng L^{-1} [57].

Antibiotics that entered sewage plants with domestic sewage, medical sewage, farming wastewater, and production wastewater are not effectively removed (e.g., there are no environmental quality and discharge standards for antibiotics in China), and eventually most of them enter surface water and pollute groundwater through the water cycle.

After antibiotics enters the water body directly or indirectly, it is still biologically active, and even if the level is only at trace level, it is still harmful to the ecological environment and human health, which can be divided into the following aspects [58]:

① Drug resistance and superbugs

The residual hazards of antibiotics are mainly the induction of resistance genes, damage to aquatic ecology, and threats to human health. The extensive use and even misuse of antibiotics

has led to a more rapid development and growing awareness of their harmful effects. The emergence of resistant bacteria (ARB), resistant bacterial genes (ARG), and antimicrobial resistance (AMR) has led to the development of resistance to antibiotics in certain disease-causing organisms, thus significantly reducing the therapeutic potential of antibiotics against human and animal pathogens [59]. In 2015, antimicrobial resistance (AMR) was recognized by WHO as a global public health crisis. Over the past 18 years, Van Boeckel et al [59], in a study of resistance in animal foods in developing countries, found that resistance in animals such as chickens and pigs has increased significantly year by year. In addition, some bacteria have been characterized as multi-drug resistant (MDR) to multiple antibiotics. For example, Tsai et al [60] isolated methicillin-resistant Staphylococcus aureus (MRSA) with multiple drug resistance in a river near a farm in Taiwan. In a shrimp farm in Vietnam, several bacteria were found to be resistant to TMP, NOR and SMX simultaneously [61].

Some of the unmetabolized antibiotics enter the natural world with the excretion of the organism, so that organisms in the natural world are affected by antibiotics for a long time and induce the production of biological resistance genes and promote the acquisition of drug resistance by pathogenic bacteria through the water cycle, food chain and other means, and even produce superbugs.

② Risk of ecological imbalance

Antibiotics is toxic to many aquatic organisms, and its long-term exposure to antibiotics will inhibit their metabolic processes, and may lead to ecological imbalance due to the different sensitivity of different organisms to antibiotics.

The mechanism of action of quinolone antibiotics is to achieve bactericidal effect by inhibiting the normal replication of bacterial DNA, which can cause acute and chronic toxicity to organisms. For example, Wu Yinbao et al. showed that enrofloxacin was acutely toxic to Daphnia magna, and all Daphnia magna died at a concentration of 120 μg mL^{-1} at a temperature of 25 ℃. Vaccaro E [62] et al. showed that enrofloxacin inhibited the liver P450 enzyme activity in sea bass. Zhang Zhe et al showed that norfloxacin had significant inhibitory effects on oxide dismutase, alkaline and acid phosphatase. Nie Xiangping et al. showed that antibiotics could

inhibit EROD enzymes in pond crucian carp. Liu Kaiyong et al. found that antibiotics residues in rats reduced their muscle protein content.

The application of animal manure and urine and municipal sewage containing antibiotics to agricultural fields can affect the growth and development of agricultural and aquatic plants. Qin Hongwei et al. investigated the toxic effects of ofloxacin on P. obliquus and showed that the growth of P. obliquus was inhibited by different concentrations of ofloxacin, and the inhibitory effect on the growth of P. obliquus increased with the increase of the concentration of ofloxacin.

Boxall [63] et al. found that enrofloxacin could inhibit the growth of carrot and lettuce. Jin Caixia et al. showed that antibiotics concentration significantly correlated with root growth inhibition in wheat, tomato and cabbage seeds, and the sensitivity of the three crops to antibiotics stress was cabbage > tomato > wheat in that order. Li Tong et al. found that root elongation inhibition and shoot elongation inhibition of maize, radish and cabbage seeds were significantly correlated with antibiotics concentrations. Wang Peng et al. found that antibiotics inhibited the growth of maize seedlings.

Antibiotics are mostly antibacterial drugs that inhibit the growth of microorganisms or directly kill them, thus changing the composition of microbial communities in the environment, affecting the decay and decomposition of manure and soil organic matter, and affecting soil fertility. The results of Wang Liping et al. showed that low concentrations of enrofloxacin stimulated soil microbial activity, while high concentrations of enrofloxacin inhibited soil microbial activity. Wang Jialong et al. showed that enrofloxacin at a concentration of 1 μg mg^{-1} in soil inhibited fibrous decomposition, ammonification, and nitrification in soil. Ma Yi et al. found that antibiotics in soil reduced the microbial carbon content and significantly affected the carbon metabolism intensity and metabolic diversity of soil microbial communities, and that antibiotics at 100 μg g^{-1} had irreversible long-term effects on the carbon metabolism function of soil microbial communities. Zhou showed that antibiotics could inhibit microbial activity and significantly reduce the abundance of species and carbon source utilization of microorganisms.

③ Hazards to humans

Antibiotics is enriched in high trophic level organisms through the food chain and its concentration is often higher than the level of antibiotics in the environment. Long-term human consumption of water or food containing antibiotics may cause intestinal diseases, allergic reactions and even affect the human immune system, posing a potential hazard to human health.

Antibiotics can cause adverse reactions in humans [37], such as nausea, vomiting, appetite disorders, abdominal pain, diarrhea, and other gastrointestinal reactions. Ding Yan showed that the higher the dose of antibiotics, the higher the incidence of intestinal reactions, and cause central system adverse reactions such as headache, dizziness, and poor sleep. Gao Weibo showed that the declining renal function in elderly patients is more likely to cause central nervous system adverse reactions to quinolones. The quinolone antibiotics also cause tendonitis and joint adverse reactions, cause toxic effects on the heart, affect cartilage development and skin health in children, and cause damage to the liver. Liang Xiu-Fen [64] showed that the energy generated by the absorption of light energy by quinolones is not only released in the skin but also becomes activated and binds to proteins in the skin in the form of semi-antigens causing allergic reactions and skin damage.

1.2.2 Analytical methods for antibiotic residues in environmental samples

Antibiotics are often present at trace levels in the environment, and environmental samples (e.g., water, sediment, soil, etc.) are complex in composition; therefore, the pretreatment process to isolate and purify trace antibiotics from the matrix becomes a critical step for analytical determination. Currently, sample pretreatment techniques have been gradually developed to include accelerated solvent extraction (ASE), supercritical extraction (SFE), solid phase extraction (SPE), solid phase microextraction (SPME), liquid-liquid microextraction (LLME) [65], matrix solid phase dispersion (MSPD), microwave-assisted extraction (MAE), ultrasound-assisted extraction (UAE), and other commonly used extraction techniques as shown in Table 1-1.

Liquid-liquid extraction (LLE), solid-phase extraction (SPE), solid-phase microextraction (SPME), and dispersive liquid-phase microextraction are the main methods used for the pretreatment of liquid samples. For the analysis of antibiotic contamination in the environment, SPE is the most used in the pretreatment of liquid samples because of its high recovery and

reproducibility, among which, C18 and Oasis HLB columns are more frequently used, and their recoveries are usually greater than 80%.

The SPE method has the advantages of high recovery, good cleanup, and high automation, but it also has the disadvantages of sorbent activation, clogging, and time consuming. Tandem connection of different SPE units can also increase the recovery of target analytes and improve the scrubbing effect.

Jia Yuan et al. used a combination of HLB, silica and MAX columns for complex water samples to achieve simultaneous multi-component analysis of antibiotics in water and activated sludge. In addition, Siedlewicz [66], Ivan Senta [67], Oya S. Okay [68], and others have successfully applied tandem columns for the analysis of antibiotics in water and activated sludge. et al. have successfully applied a combination of tandem SAX columns for the analysis of several antibiotics in sediments and soils, and the SAX columns can successfully retain other organic contaminants in the matrix. In addition, when the sample matrix composition is complex, such as humic acid and metal ions, quinolones and macrolide antibiotics can form chelates with divalent and trivalent cations, which can seriously affect the extraction efficiency.

EDTA has a wide range of coordination properties and can form chelates with almost all metal ions, so Na_2EDTA is often added during pretreatment [69]. Most of the antibiotic substances PKA<7, acidic, pH affects the chemical structure and stability of organic matter, and adjusting the pH to acidic can improve the extraction efficiency [14]. The pH is usually adjusted to 3-5 by adding acid after filtration of water samples [70, 71].

Solid-phase environmental samples are usually dehydrated by freeze-drying and aged with standards (usually one week for internal standard determination) and then extracted with a single organic solvent (usually acetonitrile or methanol) or a mixture of solvents (usually a mixture of acetonitrile or methanol with buffer solution and EDTA). Ultrasound-assisted extraction (UAE), microwave-assisted extraction (MAE), or pressurized liquid extraction (PLE) were also used to enhance the extraction efficiency as shown in Table 1-1.

UAE is a simple solid-liquid extraction technique that uses ultrasonic energy to enhance the penetration of the solvent into the solid medium and to rupture the solid by ultrasound-

generated bubbles to assist in the extraction of trace organic components from solid samples. The extraction efficiency is influenced by various factors such as ultrasonic intensity, extraction temperature, extraction time and solvent-to-solid ratio [72]. Together with the use of solid extraction columns, the recovery of antibiotics in solid phase samples can usually reach 60%-120% [13, 39, 73]. The choice of eluent also has a great influence on the recovery of different types of antibiotics.

Gao ZG compared the elution effects of pure methanol, 0.1% formic acid, methanol and 3% ammonia methanol and found that 0.1% formic acid methanol eluted best for quinolone and tetracycline antibiotics, while 3% ammonia methanol eluted best for sulfonamide antibiotics. Chen et al. used an Oasis HLB column to enrich water samples (pH=5) containing the target species with 5% ammonia-methanol elution, and the recoveries of sulfonamide, macrolide and quinolone antibiotics ranged from 75. 8% to 108%.

Physical and chemical detection methods are used to quantify and characterize different antibiotics with different functional groups. The common detection methods are: high performance liquid chromatography, gas chromatography, fluorescence, etc., and the combination techniques: high performance liquid chromatography and mass spectrometry, ultra-high performance liquid chromatography-mass spectrometry, gas chromatography-mass spectrometry, etc., such as. Among them, high performance liquid chromatography coupled with mass spectrometry has been widely used in recent years for the detection of antibiotics in the environment because of its high sensitivity, low detection limit and fast detection speed [74-76].

Different mobile phase compositions are suitable for different types of antibiotics, and the optimal separation conditions are obtained by adjusting the mobile phase composition in a gradient, i.e., by increasing the proportion of non-polar solvents in the mobile phase mixture, the analytes gradually elute from the column, thus separating the target substances with different retention times for rapid and efficient chromatographic separation. Gao ZG et al. determined 15 antibiotics of sulfonamides, quinolones and tetracyclines in surface water by UPLC-MS/MS using an external standard method with a BEH C18 column chromatographic separation using formic acid water 0.05% and pure methanol as the mobile phase.

Table 1-1 Extraction methods of common antibiotics in solid-phase matrix environment

Target	Substrate	Methods	Solvent	Column	Eluent
SDZ, SGD, STZ, SPD, SMR, SMZ, STP, SMM, SMX, ENR, SPA, DC, TC, OTC, CTC, etc.	Reservoir sediment	UAE	Citrate buffer, Acetonitrile, EDTA	HLB column	Methanol
SPD, SDZ, STZ, SMR, SMZ, STP, SFM, SMX, FLE, OFL, ENO, etc.	Soil sediment	MAE	McIlvaine, buffer, EDTA	HLB column	Methanol
RTM, ODM, AETM, TC, OTC, OFL, LOM, CIP, NOR, SMZ, SMX, SDZ, SPD, SFT	River sediment	UAE	Citrate buffer, Acetonitrile,	HLB column	Methanol
TC, OTC, DC, CTC, ETM, RTM, SMR, SDM, SMD, SMZ	Agricultural land soil	Soil samples, Extraction solution	McIlvaine, buffer, EDTA	SAX, HLB	Methanol
TC, OTC, CTC, ENR, CIP	River sediment	UAE	Citrate buffer, Organic solvents, EDTA	SAX, HLB	Oxalic acid, Methanol

Li et al. used chloramphenicol-D5 standard as an internal standard and 5 mmol L^{-1} ammonium acetate solution with methanol as the mobile phase to establish a liquid-mass tandem method for the simultaneous determination of three chloramphenicol antibiotic residues in environmental water by gradient elution. The detection limits (LOD) ranged from 0.08 to 4.2

μg kg^{-1}. Tong [77] et al. used UHPLC-Q Orbitrap to analyze the antibiotics in aquifer sediments. The gradient separation of 25 antibiotics was performed by C18 column chromatography using 0.2% formic acid and methanol as mobile phases. The EPA also used a combination of HLB column enrichment and LC-MS/MS detection for 74 PPCPs in environmental samples and biosolids such as activated sludge.

In China, antibiotic residues have also been investigated by many scholars, mostly in economically developed regions. 2007, Xu Weihai et al. investigated the residues of antibiotics in surface water in the Pearl River Basin, and the results showed that there were high concentrations of antibiotic residues in river water in the Pearl River Delta, and in summer the river water in the Pearl River Delta The residual levels of antibiotics in river water in the Pearl River Delta ranged from 11 to 67 ng L^{-1} in summer and 66 to 460 ng L^{-1} in spring.

In addition to the point-based studies of antibiotic concentrations in different watersheds and environments in different years, it is worth noting that in 2015, based on the previous work, the Guangzhou Institute of Geochemistry of the Chinese Academy of Sciences obtained the first inventory of antibiotic use and emissions in China and predicted the "antibiotic environmental concentration map" for 58 watersheds in China. In the same year, a study by the School of Public Health of Fudan University in Shanghai on the prevalence of antibiotic exposure among children in Jiangsu, Zhejiang and Shanghai attracted widespread attention. The study examined the urine of more than 1000 school children aged 8 to 11 years in three regions and showed that nearly 60% of the children tested had one antibiotic in their urine and 25% had more than two antibiotics in their urine, highlighting the problem of antibiotic abuse.

In 2018, Li et al. reviewed the antibiotic contamination in major rivers and sea areas in China from 2005 to 2016, and the results showed that 12 antibiotics were widely present in river and sea water bodies and sediments with median concentrations of 100 ng L^{-1} and less than 100 ng g^{-1}, among which, antibiotic residues in Hai River water bodies and sediments posed an ecological risk to algae, invertebrate and fish. In 2020, Chen Guilin and others reviewed the distribution of antibiotic residues in groundwater in different regions of China, but the antibiotic contamination levels were mainly distributed around 200 ng L^{-1}, among which tetracyclines and quinolones were detected more frequently. Meanwhile, scholars in China have been

progressing in their research on the influencing factors of antibiotics in the environment.

In the Americas, the United States was the first country to investigate antibiotic contamination. In 1999, the United States Geological Survey (USGS) conducted a continuous monitoring study of 139 surface rivers in the country to investigate antibiotic contamination and found that the highest detection rate was for methicillin. After that, USGS also surveyed 47 groundwater and 74 drinking water sources in 2000 and 2001, respectively, and detected antibiotics such as SMX, TMP, ETM, AZM, and CIP at the highest concentration level of 1110 ng L^{-1} [78]. OFL, TC, and CIP were detected in Canadian wastewater plants with high concentrations and detection rates ranging from 18 to 977 ng L^{-1}.

In Brazil, Rafael [79] et al. and Keity [80] studied the sorption of sulfonamides such as SMM, SQX and SMX and quinolones such as CIP, NOR and ENO in Brazilian soils and found that some sulfonamides were poorly sorbed in sandy soils with low organic carbon and easily permeable to groundwater while quinolones were more readily sorbed in soils. In the European region, k-Hordern [81] et al. examined 56 drugs, personal care products and estrogenic substances in surface river waters within South Wales, UK, and only two substances were not detected, while among the antibiotics, AETM, TMP and AMX were detected at high rates in two rivers.

In Asia, Murata [82] et al. investigated the presence of 12 antibiotics in 37 major rivers in Japan and showed that the total antibiotic concentrations in major rivers in Japan is about 626 ng L^{-1} with a mean value of 7.3 ng L^{-1}. In Korea, Kim [83] et al. investigated the presence of 14 common drugs in Korean surface rivers and found that SMX was found to have a high detection rate. In Africa, K'oreje [84] investigated the presence of 24 common drugs in wastewater, surface water and groundwater in Nairobi and Kisumu, Kenya and found that SMX and TMP were detected at 100%.

1.3 Research structure and logical framework

1.3.1 Research purpose and core content

With the increasing use of antibiotics and the rising concentration of antibiotics in medical wastewater, the treatment of antibiotics in wastewater from medical buildings has become increasingly important. To enhance the efficiency of antibiotic removal in medical wastewater treatment, I proposed the design of a thicker membrane material with larger interconnected pores. Additionally, I attempted to synthesize a layer of adsorptive polymer on the membrane surface to enhance its affinity for antibiotic molecules. Through this approach, we successfully synthesized polymerization adsorption membranes (PAM) and tested their performance using Ciprofloxacin (CIP) as a model antibiotic. The results demonstrated the presence of adsorption capacity and permeation inhibition for CIP molecules on the PAM. Furthermore, to meet the demand for selective adsorption of specific types of antibiotic molecules, I introduced molecular imprinting technology onto the PAM membrane. This resulted in the synthesis of a Molecularly Imprinted Membrane (MIM) using CIP as a template. The MIM exhibited significantly improved absorption capacity and permeation inhibition for CIP molecules.

1.3.2 Chapter content overview and related instructions

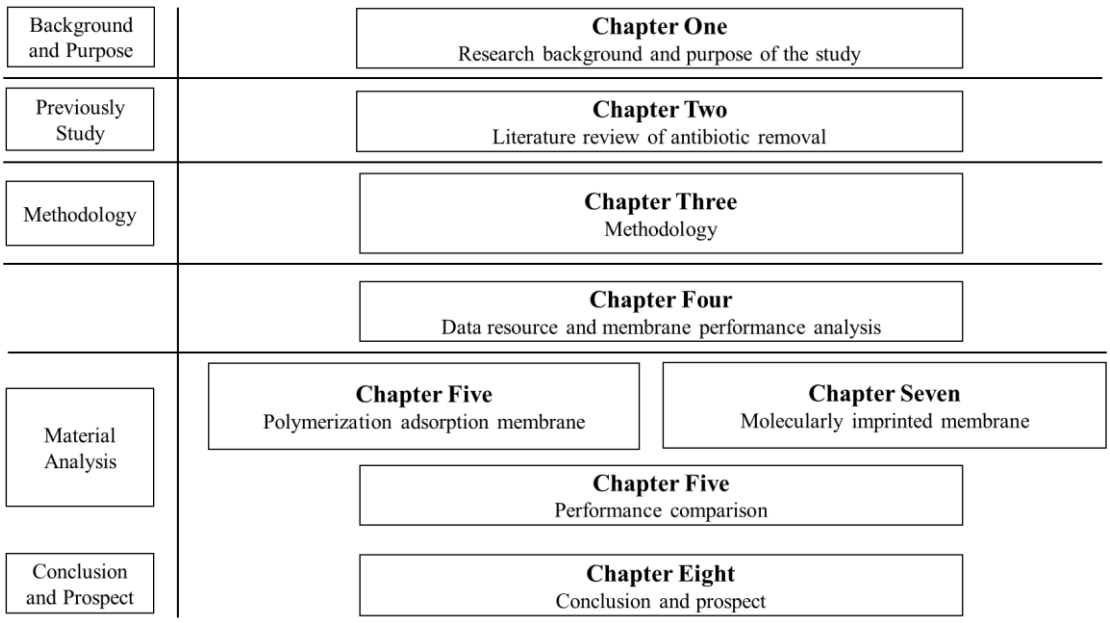

Fig 1-3 Chapter name and basic structure

The chapter names and basic structure of this paper are shown in Fig. 1-3. Besides, the brief

introduction of chapters schematic is shown in Fig. 1-4.

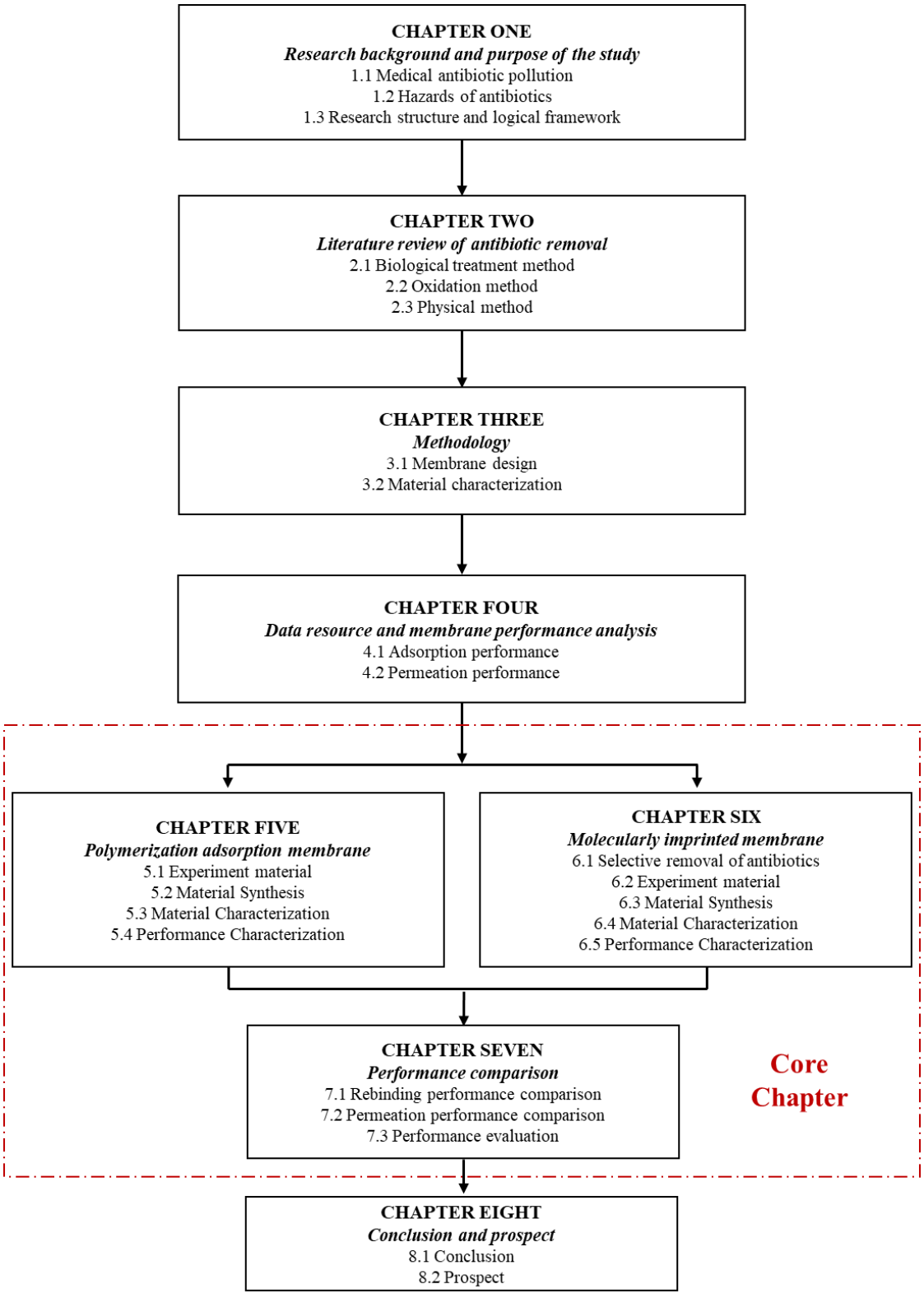

Fig 1-4 Brief chapter introduction

In Chapter 1, Research Background and Purpose of the Study:

The research backgrounds of the increasing use of antibiotics and the rising concentration of antibiotics in medical wastewater are introduced in chapter 1, including the sources and distribution of antibiotics in the environment. As well as the antibiotic pollution in water resources. Then the hazards of antibiotics pollution to the environment, creature and human beings is well introduced. Researching the treatment technologies for antibiotics in medical building wastewater is of great importance. At last, the research purpose and logical framework is shown in order to support reviewers understand the content of this paper.

In Chapter 2, Literature Review of Antibiotic Removal:

This chapter provides a comprehensive overview of past research on the removal of antibiotics from wastewater. The focus is on three primary treatment methods: biological treatment, oxidation methods, and physical methods. The biological treatment approach is cost-effective and can achieve high removal efficiencies but sensitive to environmental conditions, and have the potential for the development of antibiotic-resistant bacteria. The oxidation methods have high treatment efficiency but its energy and cost consumption are high, too. Physical methods, particularly membrane separation technology, offers high removal efficiencies, compatibility, and the potential for resource recovery. Therefore, the treatment of antibiotics by membrane technology is the focus of this study.

In chapter 3, Methodology:

In this chapter, the design of membrane synthesis methods was explored. The aim was to enhance both membrane flux and adsorption efficiency. To achieve this, the membrane thickness was increased, and a sacrificial template method was utilized to enhance the interconnected pore structure within the membrane. To address the issue of pore size affecting treatment efficiency, a plan was devised to synthesize a polymer layer on the inner and outer surfaces of the membrane to absorb antibiotic molecules. In order to ensure that the synthesized materials meet our requirements, a design for the characterization methods of the membrane materials was established. This involved conducting a series of material property characterizations, including scanning electron microscopy (SEM), X-ray photoelectron spectroscopy (XPS), Fourier-transform infrared spectroscopy (FTIR), in-situ diffuse reflectance infrared Fourier transform spectroscopy (In-situ DRIFT), and water contact angle

measurements.

In chapter 4, Data Resource and Membrane Performance Analysis:

This chapter focused on the planning and design of testing methods for membrane performance, with ciprofloxacin selected as the target molecule for testing. The testing methods were carefully planned to evaluate the efficacy of the membranes in adsorbing and permeating ciprofloxacin. The adsorption capacity would provide insights into the membrane's ability to remove the target molecule from the solution, while the permeation tests would assess the membrane's ability to allow or restrict the passage of the molecule through its structure. By conducting these tests and employing the provided calculation methods, the performance of the synthesized membranes could be quantitatively evaluated.

In Chapter 5, Polymerization Adsorption Membrane:

In this chapter, the synthesis of the Polymerization Adsorption Membrane (PAM) was performed. After determining the materials and characterization equipment, the PVDF-βCD-dopamine membrane (VCDM) was synthesized as a precursor, followed by ethylene modification and subsequent polymerization to obtain the desired PAM. The membrane was then subjected to material characterization, confirming the success of each reaction step. The performance testing began with isothermal adsorption tests, which revealed that the adsorption capacity of the PAM for ciprofloxacin (CIP) reached 22.04 mg g-1. Furthermore, the adsorption sites on the PAM exhibited a uniform and monolayer distribution, confirming its adsorption capability for CIP molecules. Subsequently, permeation adsorption experiments were conducted, and it was observed that the equilibrium of CIP molecules in solution was reached after 24 hours. This indicated that the PAM had an inhibitory effect on the permeation of CIP within 24 hours.

In Chapter 6, Molecularly Imprinted Membrane:

In this chapter, to maximize membrane utilization and address real antibiotic discharge scenarios, I enhanced the absorption capacity of the PAM membrane for a specific antibiotic molecule among various types. Through modification during synthesis, the final step incorporated molecular imprinting technology, using ciprofloxacin (CIP) as the template,

resulting in the creation of a Molecularly Imprinted Membrane (MIM). Material characterization confirmed the successful synthesis at each step. In adsorption performance tests, the MIM exhibited an impressive adsorption capacity of 121.12 mg g^{-1} for CIP molecules. The membrane surface demonstrated a uniform monolayer distribution of adsorption sites, with a coexistence of chemical adsorption and physical diffusion. Subsequently, selective adsorption and permeation experiments were conducted with four structurally similar but different types of antibiotics, including CIP. The results revealed that the MIM possessed significantly higher absorption capacity for CIP molecules compared to the other three types. The inhibitory effect on CIP permeation lasted for 36 hours, surpassing the 24-hour mark observed for the other types. These findings demonstrate the strong inhibitory and adsorption capabilities of the MIM specifically for CIP molecules.

In Chapter 7, Performance Comparison:

In this chapter, in order to evaluate the performance enhancement achieved by incorporating molecular imprinting technology, a comparison of the Molecularly Imprinted Membrane (MIM) and the Polyacrylamide (PAM) membrane was conducted. Additionally, the PAM membrane was subjected to adsorption and permeation experiments involving four structurally similar but different types of antibiotics. The results of the comparison indicated that the MIM is far superior to PAM in terms of adsorption capacity, permeation inhibition, adsorption selectivity and permeation selectivity, highlighting the role played by the imprinting sites on the membrane surface. Then regeneration performance and anti-fouling tests were performed on the MIM, demonstrating comparable regenerative properties and a wider range of resistance to fouling. Taking all the findings into consideration, the as-constructed MIM exhibited superior comprehensive properties compared to similar materials, thus presenting promising prospects for broader applications.

In Chapter 8, Conclusion:

The conclusion of each chapter is concluded.

Reference

[1] Eili Y. Klein, Thomas P. Van Boeckel, Elena M. Martinez, Suraj Pant, Sumanth Gandra, Simon A.

Levin, Herman Goossens, Ramanan Laxminarayan, Global increase and geographic convergence in antibiotic consumption between 2000 and 2015, Proceedings of the National Academy of Sciences 115(15) (2018) E3463-E3470.

[2] Xander Van Doorslaer, Jo Dewulf, Herman Van Langenhove, Kristof Demeestere, Fluoroquinolone antibiotics: An emerging class of environmental micropollutants, Science of The Total Environment 500-501 (2014) 250-269.

[3] G Wulff, AJAC Sarhan, Über die Anwendung von enzymanalog gebauten Polymeren zur Racemattrennung, Angewandte Chemie 84(8) (1972) 364-364.

[4] Ailette Prieto, Monika Möder, Rosario Rodil, Lorenz Adrian, Ernest Marco-Urrea, Degradation of the antibiotics norfloxacin and antibiotics by a white-rot fungus and identification of degradation products, Bioresource Technology 102(23) (2011) 10987-10995.

[5] Marie-Claire Danner, Anne Robertson, Volker Behrends, Julia Reiss, Antibiotic pollution in surface fresh waters: Occurrence and effects, Science of The Total Environment 664 (2019) 793-804.

[6] Qian-Qian Zhang, Guang-Guo Ying, Chang-Gui Pan, You-Sheng Liu, Jian-Liang Zhao, Comprehensive Evaluation of Antibiotics Emission and Fate in the River Basins of China: Source Analysis, Multimedia Modeling, and Linkage to Bacterial Resistance, Environmental Science & Technology 49(11) (2015) 6772-6782.

[7] Katie Tiseo, Laura Huber, Marius Gilbert, Timothy P. Robinson, Thomas P. Van Boeckel, Global Trends in Antimicrobial Use in Food Animals from 2017 to 2030, Antibiotics, 2020.

[8] Thomas P. Van Boeckel, Charles Brower, Marius Gilbert, Bryan T. Grenfell, Simon A. Levin, Timothy P. Robinson, Aude Teillant, Ramanan Laxminarayan, Global trends in antimicrobial use in food animals, Proceedings of the National Academy of Sciences 112(18) (2015) 5649-5654.

[9] Yiruhan, Qiao-Jun Wang, Ce-Hui Mo, Yan-Wen Li, Peng Gao, Yi-Ping Tai, Yan Zhang, Zhi-Li Ruan, Jia-Wei Xu, Determination of four fluoroquinolone antibiotics in tap water in Guangzhou and Macao, Environmental Pollution 158(7) (2010) 2350-2358.

[10] Hexing Wang, Bin Wang, Qi Zhao, Yanping Zhao, Chaowei Fu, Xin Feng, Na Wang, Meifang Su, Chuanxi Tang, Feng Jiang, Ying Zhou, Yue Chen, Qingwu Jiang, Antibiotic Body Burden of Chinese School Children: A Multisite Biomonitoring-based Study, Environmental Science & Technology 49(8) (2015) 5070-5079.

[11] QuocTuc Dinh, Elodie Moreau-Guigon, Pierre Labadie, Fabrice Alliot, Marie-Jeanne Teil, Martine

Blanchard, Joelle Eurin, Marc Chevreuil, Fate of antibiotics from hospital and domestic sources in a sewage network, Science of The Total Environment 575 (2017) 758-766.

[12] Hui Chen, Shan Liu, Xiang-Rong Xu, Guang-Jie Zhou, Shuang-Shuang Liu, Wei-Zhong Yue, Kai-Feng Sun, Guang-Guo Ying, Antibiotics in the coastal environment of the Hailing Bay region, South China Sea: Spatial distribution, source analysis and ecological risks, Marine Pollution Bulletin 95(1) (2015) 365-373.

[13] Yuxin Zhang, Haiyang Chen, Lijun Jing, Yanguo Teng, Ecotoxicological risk assessment and source apportionment of antibiotics in the waters and sediments of a peri-urban river, Science of The Total Environment 731 (2020) 139128.

[14] Pavla Kovalakova, Leslie Cizmas, Thomas J. McDonald, Blahoslav Marsalek, Mingbao Feng, Virender K. Sharma, Occurrence and toxicity of antibiotics in the aquatic environment: A review, Chemosphere 251 (2020) 126351.

[15] Th Heberer, K. Reddersen, A. Mechlinski, From municipal sewage to drinking water: fate and removal of pharmaceutical residues in the aquatic environment in urban areas, Water Science and Technology 46(3) (2002) 81-88.

[16] A. J. Watkinson, E. J. Murby, D. W. Kolpin, S. D. Costanzo, The occurrence of antibiotics in an urban watershed: From wastewater to drinking water, Science of The Total Environment 407(8) (2009) 2711-2723.

[17] Jin-Lin Liu, Ming-Hung Wong, Pharmaceuticals and personal care products (PPCPs): A review on environmental contamination in China, Environment International 59 (2013) 208-224.

[18] A. Gulkowska, H. W. Leung, M. K. So, S. Taniyasu, N. Yamashita, Leo W. Y. Yeung, Bruce J. Richardson, A. P. Lei, J. P. Giesy, Paul K. S. Lam, Removal of antibiotics from wastewater by sewage treatment facilities in Hong Kong and Shenzhen, China, Water Research 42(1) (2008) 395-403.

[19] Weiwei Ben, Bing Zhu, Xiangjuan Yuan, Yu Zhang, Min Yang, Zhimin Qiang, Occurrence, removal and risk of organic micropollutants in wastewater treatment plants across China: Comparison of wastewater treatment processes, Water Research 130 (2018) 38-46.

[20] Hou-Qi Liu, James C. W. Lam, Wen-Wei Li, Han-Qing Yu, Paul K. S. Lam, Spatial distribution and removal performance of pharmaceuticals in municipal wastewater treatment plants in China, Science of The Total Environment 586 (2017) 1162-1169.

[21] Christian G. Daughton, Pharmaceuticals and Personal Care Products in the Environment:

Overarching Issues and Overview, Pharmaceuticals and Care Products in the Environment, American Chemical Society2001, pp. 2-38. https://doi.org/doi:10.1021/bk-2001-0791.ch001 10.1021/bk-2001-0791.ch001.

[22] Qinglin Chen, Xinli An, Hu Li, Jianqiang Su, Yibing Ma, Yong-Guan Zhu, Long-term field application of sewage sludge increases the abundance of antibiotic resistance genes in soil, Environment International 92-93 (2016) 1-10.

[23] Anke Göbel, Angela Thomsen, Christa S. McArdell, Alfredo C. Alder, Walter Giger, Nicole Theiß, Dirk Löffler, Thomas A. Ternes, Extraction and determination of sulfonamides, macrolides, and trimethoprim in sewage sludge, Journal of Chromatography A 1085(2) (2005) 179-189.

[24] Chad A. Kinney, Edward T. Furlong, Steven D. Zaugg, Mark R. Burkhardt, Stephen L. Werner, Jeffery D. Cahill, Gretchen R. Jorgensen, Survey of Organic Wastewater Contaminants in Biosolids Destined for Land Application, Environmental Science & Technology 40(23) (2006) 7207-7215.

[25] Eva M. Golet, Irene Xifra, Hansruedi Siegrist, Alfredo C. Alder, Walter Giger, Environmental Exposure Assessment of Fluoroquinolone Antibacterial Agents from Sewage to Soil, Environmental Science & Technology 37(15) (2003) 3243-3249.

[26] Ruicheng Wei, Feng Ge, Siyu Huang, Ming Chen, Ran Wang, Occurrence of veterinary antibiotics in animal wastewater and surface water around farms in Jiangsu Province, China, Chemosphere 82(10) (2011) 1408-1414.

[27] P. Bound Jonathan, Nikolaos Voulvoulis, Household Disposal of Pharmaceuticals as a Pathway for Aquatic Contamination in the United Kingdom, Environmental Health Perspectives 113(12) (2005) 1705-1711.

[28] Qingwei Bu, Xiao Shi, Gang Yu, Jun Huang, Bin Wang, Jianbing Wang, Pay attention to non-wastewater emission pathways of pharmaceuticals into environments, Chemosphere 165 (2016) 515-518.

[29] Dong Li, Min Yang, Jianying Hu, Liren Ren, Yu Zhang, Kuiziao Li, Determination and fate of oxytetracycline and related compounds in oxytetracycline production wastewater and the receiving river, Environmental Toxicology and Chemistry 27(1) (2008) 80-86.

[30] Dongle Cheng, Huu Hao Ngo, Wenshan Guo, Soon Woong Chang, Dinh Duc Nguyen, Yiwen Liu, Qin Wei, Dong Wei, A critical review on antibiotics and hormones in swine wastewater: Water pollution problems and control approaches, Journal of Hazardous Materials 387 (2020) 121682.

[31] Hua Deng, Ren Wei, Wenya Luo, Lingling Hu, Bowen Li, Ya'nan Di, Huahong Shi, Microplastic

pollution in water and sediment in a textile industrial area, Environmental Pollution 258 (2020) 113658.

[32] Dongdong Zhang, Yaozong Cui, Hanghai Zhou, Cheng Jin, Xinwei Yu, Yongjiu Xu, Yanhong Li, Chunfang Zhang, Microplastic pollution in water, sediment, and fish from artificial reefs around the Ma'an Archipelago, Shengsi, China, Science of The Total Environment 703 (2020) 134768.

[33] Maya Ibrahim, Madona Labaki, Jean-Marc Giraudon, Jean-François Lamonier, Hydroxyapatite, a multifunctional material for air, water and soil pollution control: A review, Journal of Hazardous Materials 383 (2020) 121139.

[34] Vinod Kumar, Anket Sharma, Rakesh Kumar, Renu Bhardwaj, Ashwani Kumar Thukral, Jesús Rodrigo-Comino, Assessment of heavy-metal pollution in three different Indian water bodies by combination of multivariate analysis and water pollution indices, Human and Ecological Risk Assessment: An International Journal 26(1) (2020) 1-16.

[35] Klaus Kümmerer, Antibiotics in the aquatic environment – A review – Part I, Chemosphere 75(4) (2009) 417-434.

[36] Changwon Yang, Gwonhwa Song, Whasun Lim, A review of the toxicity in fish exposed to antibiotics, Comparative Biochemistry and Physiology Part C: Toxicology & Pharmacology 237 (2020) 108840.

[37] Mark Crane, Chris Watts, Tatiana Boucard, Chronic aquatic environmental risks from exposure to human pharmaceuticals, Science of The Total Environment 367(1) (2006) 23-41.

[38] Si Li, Wanzi Shi, Wei Liu, Huimin Li, Wei Zhang, Jingrun Hu, Yanchu Ke, Weiling Sun, Jinren Ni, A duodecennial national synthesis of antibiotics in China's major rivers and seas (2005–2016), Science of The Total Environment 615 (2018) 906-917.

[39] Si Li, Wanzi Shi, Mingtao You, Ruijie Zhang, Yuzhu Kuang, Chenyuan Dang, Weiling Sun, Yuhong Zhou, Wenjing Wang, Jinren Ni, Antibiotics in water and sediments of Danjiangkou Reservoir, China: Spatiotemporal distribution and indicator screening, Environmental Pollution 246 (2019) 435-442.

[40] Panwei Zhang, Huaidong Zhou, Kun Li, Xiaohui Zhao, Qiaona Liu, Dongjiao Li, Gaofeng Zhao, Liang Wang, Occurrence of pharmaceuticals and personal care products, and their associated environmental risks in Guanting Reservoir and its upstream rivers in north China, RSC Advances 8(9) (2018) 4703-4712.

[41] Thomas P. Van Boeckel, João Pires, Reshma Silvester, Cheng Zhao, Julia Song, Nicola G. Criscuolo, Marius Gilbert, Sebastian Bonhoeffer, Ramanan Laxminarayan, Global trends in antimicrobial resistance

in animals in low- and middle-income countries, Science 365(6459) (2019) eaaw1944.

[42] Xiangang Hu, Qixing Zhou, Yi Luo, Occurrence and source analysis of typical veterinary antibiotics in manure, soil, vegetables and groundwater from organic vegetable bases, northern China, Environmental Pollution 158(9) (2010) 2992-2998.

[43] Hexing Wang, Lingshuang Ren, Xin Yu, Jing Hu, Yue Chen, Gengsheng He, Qingwu Jiang, Antibiotic residues in meat, milk and aquatic products in Shanghai and human exposure assessment, Food Control 80 (2017) 217-225.

[44] Christine M. Velicer, Susan R. Heckbert, Johanna W. Lampe, John D. Potter, Carol A. Robertson, Stephen H. Taplin, Antibiotic Use in Relation to the Risk of Breast Cancer, JAMA 291(7) (2004) 827-835.

[45] Susanne A. Kraemer, Arthi Ramachandran, Gabriel G. Perron, Antibiotic Pollution in the Environment: From Microbial Ecology to Public Policy, Microorganisms, 2019.

[46] Boqiang Gao, Qianqian Chang, Hu Yang, Selective adsorption of ofloxacin and antibiotics from a binary system using lignin-based adsorbents: Quantitative analysis, adsorption mechanisms, and structure-activity relationship, Science of The Total Environment 765 (2021) 144427.

[47] Zhuoyao Chen, Weikang Lai, Yanbin Xu, Guangyan Xie, Waner Hou, Pan Zhanchang, Chaozhi Kuang, Yuxin Li, Anodic oxidation of antibiotics using different graphite felt anodes: Kinetics and degradation pathways, Journal of Hazardous Materials 405 (2021) 124262.

[48] Muhammad Babar Taj, Muneera D. F. Alkahtani, Ahmad Raheel, Saima Shabbir, Rida Fatima, Sadia Aroob, Rana yahya, Walla Alelwani, Nadiyah Alahmadi, Matokah Abualnaja, Sadia Noor, Raja Hammad Ahmad, Heba Alshater, Bioconjugate synthesis, phytochemical analysis, and optical activity of NiFe2O4 nanoparticles for the removal of antibiotics and Congo red from water, Scientific Reports 11(1) (2021) 5439.

[49] Kuldip Kumar, Satish C. Gupta, Yogesh Chander, Ashok K. Singh, Antibiotic Use in Agriculture and Its Impact on the Terrestrial Environment, Advances in Agronomy, Academic Press2005, pp. 1-54. https://doi.org/https://doi.org/10.1016/S0065-2113(05)87001-4.

[50] Premasis Sukul, Michael Spiteller, Fluoroquinolone Antibiotics in the Environment, Reviews of Environmental Contamination and Toxicology, Springer New York, New York, NY, 2007, pp. 131-162. https://doi.org/10.1007/978-0-387-69163-3_5.

[51] Gerd Hamscher, Silke Sczesny, Heinrich Höper, Heinz Nau, Determination of Persistent

Tetracycline Residues in Soil Fertilized with Liquid Manure by High-Performance Liquid Chromatography with Electrospray Ionization Tandem Mass Spectrometry, Analytical Chemistry 74(7) (2002) 1509-1518.

[52] Johannes Tolls, Sorption of Veterinary Pharmaceuticals in Soils: A Review, Environmental Science & Technology 35(17) (2001) 3397-3406.

[53] S. Morales-Muñoz, J. L. Luque-García, M. D. Luque de Castro, Continuous microwave-assisted extraction coupled with derivatization and fluorimetric monitoring for the determination of fluoroquinolone antibacterial agents from soil samples, Journal of Chromatography A 1059(1) (2004) 25-31.

[54] Richard Lindberg, Per-Åke Jarnheimer, Björn Olsen, Magnus Johansson, Mats Tysklind, Determination of antibiotic substances in hospital sewage water using solid phase extraction and liquid chromatography/mass spectrometry and group analogue internal standards, Chemosphere 57(10) (2004) 1479-1488.

[55] Sandra Babić, Martina Periša, Irena Škorić, Photolytic degradation of norfloxacin, enrofloxacin and antibiotics in various aqueous media, Chemosphere 91(11) (2013) 1635-1642.

[56] Roberto Rosal, Antonio Rodríguez, José Antonio Perdigón-Melón, Alice Petre, Eloy García-Calvo, María José Gómez, Ana Agüera, Amadeo R. Fernández-Alba, Occurrence of emerging pollutants in urban wastewater and their removal through biological treatment followed by ozonation, Water Research 44(2) (2010) 578-588.

[57] N. Vieno, T. Tuhkanen, L. Kronberg, Elimination of pharmaceuticals in sewage treatment plants in Finland, Water Research 41(5) (2007) 1001-1012.

[58] Timothy R. Walsh, Janis Weeks, David M. Livermore, Mark A. Toleman, Dissemination of NDM-1 positive bacteria in the New Delhi environment and its implications for human health: an environmental point prevalence study, The Lancet Infectious Diseases 11(5) (2011) 355-362.

[59] Min Qiao, Guang-Guo Ying, Andrew C. Singer, Yong-Guan Zhu, Review of antibiotic resistance in China and its environment, Environment International 110 (2018) 160-172.

[60] Hsin-Chi Tsai, Chi-Wei Tao, Bing-Mu Hsu, Yu-Ying Yang, Ying-Chin Tseng, Tung-Yi Huang, Shih-Wei Huang, Yi-Jie Kuo, Jung-Sheng Chen, Multidrug-resistance in methicillin-resistant Staphylococcus aureus (MRSA) isolated from a subtropical river contaminated by nearby livestock industries, Ecotoxicology and Environmental Safety 200 (2020) 110724.

[61] Tuan Xuan Le, Yukihiro Munekage, Shin-ichiro Kato, Antibiotic resistance in bacteria from shrimp farming in mangrove areas, Science of The Total Environment 349(1) (2005) 95-105.

[62] E. Vaccaro, M. Giorgi, V. Longo, G. Mengozzi, P. G. Gervasi, Inhibition of cytochrome P450 enzymes by enrofloxacin in the sea bass (Dicentrarchus labrax), Aquatic Toxicology 62(1) (2003) 27-33.

[63] Alistair B. A. Boxall, Paul Johnson, Edward J. Smith, Chris J. Sinclair, Edward Stutt, Len S. Levy, Uptake of Veterinary Medicines from Soils into Plants, Journal of Agricultural and Food Chemistry 54(6) (2006) 2288-2297.

[64] Huichun Zhang, Ching-Hua Huang, Adsorption and oxidation of fluoroquinolone antibacterial agents and structurally related amines with goethite, Chemosphere 66(8) (2007) 1502-1512.

[65] Ke Li, Yan Jin, Dasom Jung, Keunbae Park, Hireem Kim, Jeongmi Lee, In situ formation of thymol-based hydrophobic deep eutectic solvents: Application to antibiotics analysis in surface water based on liquid-liquid microextraction followed by liquid chromatography, Journal of Chromatography A 1614 (2020) 460730.

[66] Dragana Mutavdžić Pavlović, Tea Pinušić, Martina Periša, Sandra Babić, Optimization of matrix solid-phase dispersion for liquid chromatography tandem mass spectrometry analysis of 12 pharmaceuticals in sediments, Journal of Chromatography A 1258 (2012) 1-15.

[67] Ivan Senta, Ivona Krizman-Matasic, Senka Terzic, Marijan Ahel, Comprehensive determination of macrolide antibiotics, their synthesis intermediates and transformation products in wastewater effluents and ambient waters by liquid chromatography–tandem mass spectrometry, Journal of Chromatography A 1509 (2017) 60-68.

[68] Oya S. Okay, Kuixiao Li, Ayfer Yediler, Burak Karacik, Determination of selected antibiotics in the Istanbul strait sediments by solid-phase extraction and high performance liquid chromatography, Journal of Environmental Science and Health, Part A 47(10) (2012) 1372-1380.

[69] Si Li, Yuzhu Kuang, Jingrun Hu, Mingtao You, Xiaoyu Guo, Qiang Gao, Xi Yang, Qian Chen, Weiling Sun, Jinren Ni, Enrichment of antibiotics in an inland lake water, Environmental Research 190 (2020) 110029.

[70] R. Daghrir, P. Drogui, Tetracycline antibiotics in the environment: a review, Environmental Chemistry Letters 11(3) (2013) 209-227.

[71] Ngoc Han Tran, Martin Reinhard, Karina Yew-Hoong Gin, Occurrence and fate of emerging contaminants in municipal wastewater treatment plants from different geographical regions-a review,

Water Research 133 (2018) 182-207.

[72] Pinjing He, Jinghua Huang, Zhuofeng Yu, Xian Xu, Roberto Raga, Fan Lü, Antibiotic resistance contamination in four Italian municipal solid waste landfills sites spanning 34 years, Chemosphere 266 (2021) 129182.

[73] Ji-Feng Yang, Guang-Guo Ying, Jian-Liang Zhao, Ran Tao, Hao-Chang Su, Feng Chen, Simultaneous determination of four classes of antibiotics in sediments of the Pearl Rivers using RRLC–MS/MS, Science of The Total Environment 408(16) (2010) 3424-3432.

[74] Aolin Li, Lujun Chen, Yan Zhang, Yile Tao, Hui Xie, Si Li, Weiling Sun, Jianguo Pan, Zhidong He, Chaoan Mai, Yingying Fan, Huanchao Xian, Zebin Zhang, Donghui Wen, Occurrence and distribution of antibiotic resistance genes in the sediments of drinking water sources, urban rivers, and coastal areas in Zhuhai, China, Environmental Science and Pollution Research 25(26) (2018) 26209-26217.

[75] Si Li, Wanzi Shi, Huimin Li, Nan Xu, Ruijie Zhang, Xuejiao Chen, Weiling Sun, Donghui Wen, Shanliang He, Jianguo Pan, Zhidong He, Yingying Fan, Antibiotics in water and sediments of rivers and coastal area of Zhuhai City, Pearl River estuary, south China, Science of The Total Environment 636 (2018) 1009-1019.

[76] Sainan Sun, Yanan Chen, Yujin Lin, Dong An, Occurrence, spatial distribution, and seasonal variation of emerging trace organic pollutants in source water for Shanghai, China, Science of The Total Environment 639 (2018) 1-7.

[77] Lei Tong, Hui Liu, Cong Xie, Minjing Li, Quantitative analysis of antibiotics in aquifer sediments by liquid chromatography coupled to high resolution mass spectrometry, Journal of Chromatography A 1452 (2016) 58-66.

[78] Kimberlee K. Barnes, Dana W. Kolpin, Edward T. Furlong, Steven D. Zaugg, Michael T. Meyer, Larry B. Barber, A national reconnaissance of pharmaceuticals and other organic wastewater contaminants in the United States — I) Groundwater, Science of The Total Environment 402(2) (2008) 192-200.

[79] Rafael Marques Pereira Leal, Luis Reynaldo Ferracciú Alleoni, Valdemar Luiz Tornisielo, Jussara Borges Regitano, Sorption of fluoroquinolones and sulfonamides in 13 Brazilian soils, Chemosphere 92(8) (2013) 979-985.

[80] Keity Margareth Doretto, Livia Maniero Peruchi, Susanne Rath, Sorption and desorption of sulfadimethoxine, sulfaquinoxaline and sulfamethazine antimicrobials in Brazilian soils, Science of The

Total Environment 476-477 (2014) 406-414.

[81] Barbara Kasprzyk-Hordern, Richard M. Dinsdale, Alan J. Guwy, The occurrence of pharmaceuticals, personal care products, endocrine disruptors and illicit drugs in surface water in South Wales, UK, Water Research 42(13) (2008) 3498-3518.

[82] Ayako Murata, Hideshige Takada, Kunihiro Mutoh, Hiroshi Hosoda, Arata Harada, Norihide Nakada, Nationwide monitoring of selected antibiotics: Distribution and sources of sulfonamides, trimethoprim, and macrolides in Japanese rivers, Science of The Total Environment 409(24) (2011) 5305-5312.

[83] Sang D. Kim, Jaeweon Cho, In S. Kim, Brett J. Vanderford, Shane A. Snyder, Occurrence and removal of pharmaceuticals and endocrine disruptors in South Korean surface, drinking, and waste waters, Water Research 41(5) (2007) 1013-1021.

[84] K. O. K'Oreje, L. Vergeynst, D. Ombaka, P. De Wispelaere, M. Okoth, H. Van Langenhove, K. Demeestere, Occurrence patterns of pharmaceutical residues in wastewater, surface water and groundwater of Nairobi and Kisumu city, Kenya, Chemosphere 149 (2016) 238-244.

Chapter 2

LITERATURE REVIEW OF ANTIBIOTIC REMOVAL

2.1 Biological treatment method

Several biological treatment methods for antibiotics that are commonly used today include activated sludge method, single strain treatment with antibiotics, complex bacteriophage treatment of antibiotics, aerobic biological treatment technology, anaerobic biological treatment technology, anaerobic-aerobic combination treatment technology, and Physical and chemical method-biological method combination treatment technology.

2.1.1 Activated sludge method

The activated sludge method is widely employed as the predominant wastewater treatment technique in China. In the context of antibiotic wastewater treatment, this method utilizes activated sludge to adsorb and biodegrade antibiotics. The process primarily relies on the adsorptive capacity of activated sludge, while the biodegradation of antibiotics by activated sludge is comparatively less pronounced.

Li et al. [1] conducted a study on the adsorption and degradation behavior of 11 types of antibiotics, including β-lactams (ampicillin, cefadroxil), sulfonamides (sulfamethoxazole, sulfadiazine), quinolones (norfloxacin, ofloxacin, ciprofloxacin), tetracyclines (tetracycline), macrolides (roxithromycin, dehydrated erythromycin), and methomycin, in activated sludge. The findings revealed that the primary mode of pollutant removal was through adsorption degradation. Among the 11 antibiotics investigated, cefadroxil, sulfamethoxazole, and sulfadiazine primarily underwent biodegradation removal, while the remaining antibiotics were mainly removed through adsorption by the activated sludge. This study demonstrates the varying removal mechanisms of different antibiotics in activated sludge systems.

In the investigation conducted by Song et al. [2], the focus was on examining the adsorption and degradation behavior of tetracycline antibiotics in activated sludge. The results revealed that there was minimal degradation of tetracycline antibiotics observed in the activated sludge, leading to an insignificant biological oxygen demand (BOD5) reduction. In the case of untreated tetracycline wastewater, the activated sludge method primarily relied on adsorption as the dominant removal mechanism, with chemisorption playing a prominent role. These

findings emphasize the limited degradation potential of tetracycline antibiotics in activated sludge and highlight the significance of adsorption processes for their removal in wastewater treatment.

2.1.2 Single strain treatment with antibiotics

Several microorganisms, including photosynthetic bacteria, lactic acid bacteria, actinomycetes, yeasts, fermentative filamentous bacteria, Bacillus, and nitrifying bacteria, have been documented for their ability to reduce the levels of antibiotics [3].

Xu [4] et al. conducted a screening process to isolate tetracycline-degrading strains from soil containing long-term tetracycline residues. After domestication and enrichment, two strains, namely TD2 and TD3, were obtained, demonstrating efficient degradation capabilities towards tetracycline. Through phenotypic characteristics, physiological and biochemical properties, as well as 16S rDNA sequence homology analysis, TD2 was identified as Brevundimonas diminuta, while TD3 was identified as Ochrobactrum anthropi. Optimal degradation performance for TD2 was achieved with a carbon source absence, 0.5% peptone as the nitrogen source, and 0.015% CuSO4 as the mineral source. In contrast, TD3 exhibited the highest degradation efficiency in a medium containing 0.5% glucose as the carbon source, 1.5% beef paste as the nitrogen source, and 0.015% CuSO4 as the mineral source. Both strains shared similar optimal culture conditions, including a 5-day incubation time, a temperature of 30℃, a 1% inoculum, and a positive correlation between tetracycline degradation rate and aeration rate. Under these optimized conditions, both TD2 and TD3 achieved tetracycline degradation rates exceeding 90% [4].

To address the treatment of B-lactam cyclic antibiotic production wastewater, Wang Liqun and colleagues [5] employed a shake flask experiment using the wastewater as an isolation medium to isolate and screen potential strains from activated sludge. Their aim was to identify the strains, determine optimal action conditions, and verify their degradation effect on the wastewater's organic matter. Through their experiments, four strains (B4, B5, B2, and B7) were successfully isolated and screened. These strains exhibited high efficacy in degrading the organic matter of the wastewater and demonstrated tolerance to B-lactam ring antibiotics. They

were identified as Acinetobacter, Pseudomonas, Escherichia, and Bacillus, respectively.

Orthogonal tests were conducted to assess the factors influencing the degradation effect, revealing that temperature had the most significant impact, followed by shaker speed. Under the optimal simulated conditions (temperature: 35°C, speed: 150 r/min, initial pH: 7.0), the test group with the combination of effector strains exhibited an approximate 10% increase in organic matter degradation compared to the control group. Moreover, the entire system displayed enhanced resilience against fluctuations in organic matter, further solidifying the effectiveness of the treatment process.

To determine the optimal conditions for the degradation of tetracycline by Trichosporon mycotoxinivorans XPY-10 strain, Feng Fuxin and colleagues [6] conducted a comprehensive investigation on various factors including carbon source, organic nitrogen source, metal ions, initial substrate concentration, inoculum amount, pH, temperature, loading volume, shaking speed, and other physicochemical parameters that could affect the growth and degradation efficiency of tetracycline. Their findings revealed that sucrose and peptone were the optimum carbon and nitrogen sources, respectively, for the growth of strain XPY-10. Under these conditions, strain XPY-10 exhibited a degradation rate of 83.63% for tetracycline with an initial concentration of 600 mg/L within a 7-day period. This substantial degradation efficiency demonstrates the potential application of strain XPY-10 in treating water pollution caused by tetracycline.

Wen Xianghua and colleagues [7] focused on the degradation of tetracycline (TC) and oxytetracycline (OTC) using crude lignin peroxidase (LiP) derived from Chrysanthemum chrysogenum. Through in vitro experiments, they investigated the capability of LiP to degrade TC and OTC. The findings revealed that LiP exhibited a potent degradation ability towards both TC and OTC. The degradation process was found to be influenced by pH and temperature, with optimal conditions enhancing the degradation efficiency. Additionally, the addition of veratryl alcohol (VA) and initial hydrogen peroxide concentrations significantly enhanced the degradation of TC and OTC by LiP.

Prieto and colleagues [8] cultivated white rot bacteria in malt extracts and employed them

for the biodegradation of ciprofloxacin. The results demonstrated an impressive degradation rate exceeding 90%. This indicates the potential of white rot bacteria as effective agents for the degradation of ciprofloxacin.

2.1.3 Complex bacteriophage treatment antibiotics

In a study conducted by Shen Ying and colleagues [9], the effects of temperature, initial water content, and time on the biodegradation of oxytetracycline, tetracycline, and aureomycin in pig manure were investigated through L9(34) orthogonal batch experiments. Furthermore, changes in microbial communities during the degradation process were examined. The findings revealed that the maximum degradation rates of the three tetracycline antibiotics occurred at a temperature of 55.0°C and an initial water content of 60.0% over a period of 14 days. The degradation of all antibiotics followed the primary reaction kinetic model, and bacteria were identified as the dominant microorganisms. Statistical analysis indicated that temperature had a significant influence on the degradation of hygromycin and tetracycline, while the initial water content played a major role in the degradation of chrysomycin. However, none of the aforementioned factors had a significant impact on the degradation rates of the three tetracycline antibiotics or the relative abundance of fungi, actinomycetes, and bacteria.

In a study conducted by Shen Dongsheng and colleagues [10], the role of Staphylococcus sp. TJ-1 in the environmentally sound treatment of fresh pig manure was investigated using a combination of general physicochemical analysis and Biolog microplate technology. The findings demonstrated that the inoculation of Staphylococcus sp. TJ-1 significantly enhanced the degradation efficiency of hygromycin in pig manure ($p < 0.05$). By the end of the 21-day composting period, the degradation rate of hygromycin increased from 62.7% to 82.0%. In terms of compost composition, the levels of NH+4-N in the normal composting process without the inoculation of degrading bacteria and in the high-efficiency composting process with the inoculation of degrading bacteria were measured as 189.34 mg kg-1 and 42.36 mg kg-1, respectively. Similarly, the contents of NO3--N were recorded as 439.38 mg kg-1 and 238.06 mg kg-1, respectively. Furthermore, Biolog results indicated that the carbon source in the hygromycin-degrading bacteria TJ-1 facilitated the metabolism of hygromycin, thus aiding in

the degradation of nitrogen sources such as amino acids and aromatic compounds in the compost pile. This process helped mitigate the harmful effects of toxic substances on other microorganisms, ensuring the diversity and activity of the microbial community and contributing to the stability of the compost pile ecosystem.

In the study conducted by Zhang Shuqing and colleagues [11], the research aimed to explore technical approaches for degrading antibiotics and passivating heavy metals in livestock manure through experimental investigations. Using the high-temperature composting method, the degradation characteristics of different composting treatments on tetracycline antibiotics (TTC, OTC, and CTC) in livestock manure, as well as their effects on the water-soluble state of heavy metals (Cu, Zn, Cr, and As), were compared. The results revealed that the most effective removal of TTC, OTC, and CTC was achieved with the P+S and C+S treatments among the various composting approaches. Furthermore, the addition of specially selected BM bacterial agents facilitated the degradation of tetracycline antibiotics. The degradation and removal of TTC, OTC, and CTC were significantly improved by the addition of BM bacterial agents compared to the P+S + TCs and C+S + TCs treatments. However, the degradation and removal of OTC remained challenging in all treatments, with the lowest removal rate observed in the C+S+OTC treatment (40.23%). On the other hand, the addition of weathered coal as a passivator in the composting process showed remarkable efficacy in reducing the water-soluble contents of Cu, Zn, Cr, and As. In pig manure compost, the water-soluble contents of Cu, Zn, Cr, and As were reduced by 6.17%, 6.40%, 4.17%, and 1.83%, respectively, after composting compared to before composting when the weathered coal passivator was added. Similarly, in chicken manure compost, the corresponding reductions were 7.07%, 5.69%, 5.50%, and 2.07%. These findings highlight the potential of specific composting treatments and the use of BM bacterial agents and weathered coal passivators for the degradation of tetracycline antibiotics and the passivation of heavy metals in livestock manure.

Qin Li and colleagues [12] conducted a study using a field composting device to investigate the impact of inoculation treatment on enhancing composting efficiency and degrading antibiotic veterinary contaminants. They achieved this by introducing a domesticated composite bacterial system with dual functions of cellulose degradation and aureomycin

degradation into a high-temperature compost composed of chicken manure and straw. The findings of the study revealed that the bacterial system significantly facilitated cellulose degradation during the composting process. The cellulose content in the compost decreased by 62.5%, from an initial value of 22.00% to 8.25% at the end of composting. In comparison, the cellulose content in the uninoculated control treatments, CK and CK+ Aureomycin, decreased by 54.28% and 53.78%, respectively. Furthermore, the high-temperature composting process itself exhibited a certain degree of degradation effect on aureomycin. The degradation rates of aureomycin in the CK and CK+ Aureomycin treatments, which did not receive the inoculated bacterial system, were similar at approximately 60%. However, the treatment with the inoculated complex bacterial system demonstrated a significantly higher degradation rate of aureomycin at 82.23%, surpassing the degradation rates observed in the two uninoculated control treatments. These results suggest that the introduction of the domesticated composite bacterial system into the composting process effectively enhanced cellulose degradation and improved the degradation efficiency of aureomycin. The findings highlight the potential of using inoculation treatments with specialized bacterial systems to optimize composting processes and facilitate the degradation of antibiotic veterinary contaminants.

2.1.4 Aerobic biological treatment technology

In the study conducted by Li et al. [13], the effectiveness of activated sludge in treating 11 antibiotics from diverse classes was examined in both freshwater and saltwater systems. The findings revealed distinct degradation patterns for different antibiotics. Specifically, cephalothin and two sulfonamide antibiotics exhibited a predominant tendency towards biodegradation in both systems. On the other hand, three fluoroquinolone drugs, namely ampicillin, tetracycline, erythromycin, and metronidazole, primarily underwent adsorption, with tetracycline exhibiting remarkable adsorption capacity of up to 90% within a 15-minute timeframe. Notably, the adsorption capacity of activated sludge for the three fluoroquinolone drugs experienced a significant reduction in the presence of divalent cations within the saltwater system, although some level of biodegradation was still observed. It is worth mentioning that complete removal of erythromycin could not be achieved in both systems, indicating the challenges associated with its treatment using activated sludge.

In recent years, there has been a trend towards integrating aerobic biological treatment methods with other treatment approaches to address the limitations of the aerobic method when dealing with highly concentrated organic wastewater from the antibiotic industry. One of the main challenges of the aerobic biological method is the high concentration of organic pollutants in the wastewater. To effectively treat such wastewater, it often requires significant dilution of the original waste stream, sometimes by tenfold or even hundredfold. Moreover, the aerobic biological method is associated with high energy consumption and treatment costs, which can limit its widespread application. These drawbacks have prompted researchers and engineers to explore alternative approaches that can enhance the efficiency and cost-effectiveness of antibiotic wastewater treatment. By combining aerobic biological methods with other treatment techniques such as physicochemical processes, advanced oxidation, anaerobic digestion, or membrane filtration, it is possible to achieve better treatment outcomes and overcome the limitations of the aerobic method. These integrated approaches can help reduce energy consumption, enhance pollutant removal efficiency, and optimize the overall treatment process for antibiotic industrial wastewater. Overall, while the aerobic biological method has certain limitations in treating highly concentrated organic wastewater, the development of integrated treatment approaches offers promising solutions to improve the efficiency and cost-effectiveness of antibiotic wastewater treatment [14].

2.1.5 Anaerobic biological treatment technology

In the study conducted by Liu Feng et al. [15], a UASB (Upflow Anaerobic Sludge Blanket) anaerobic reactor was utilized to treat cephalosporin antibiotic pharmaceutical wastewater at medium temperature conditions. The researchers aimed to assess the reactor's performance and its potential for effective wastewater treatment. During stable operation of the UASB anaerobic reactor, the influent wastewater was characterized by a mass concentration of chemical oxygen demand (COD_{Cr}) of 14,300 mg/L. The reactor demonstrated efficient performance, with a volumetric load of 14.3 kg/(m^3 d), and a stable COD_{Cr} removal rate of approximately 85%. As a result, the effluent wastewater exhibited a reduced mass concentration of COD_{Cr}, which was below 2500 mg/L. The effluent volatile fatty acid (VFA) concentration was approximately 3 mmol/L. Additionally, the anaerobic reactor exhibited a gas production capacity of about 17

L/d. This gas production represents the anaerobic digestion process within the reactor. Overall, the experimental results indicated a favorable treatment effect for cephalosporin antibiotic wastewater, and the findings provided valuable insights for the design and application of anaerobic technology in treating such wastewater. By utilizing a UASB anaerobic reactor and achieving successful wastewater treatment, the study offers a foundation for the practical implementation of anaerobic technology for cephalosporin antibiotic wastewater treatment.

In the research conducted by Mai Wenning et al. [16], anaerobic composite bed technology was investigated for the treatment of antibiotic wastewater. The study consisted of a small pilot study with a reactor volume of 62 L, a pilot study with a reactor volume of 22 m^3, and a production application with a reactor volume of 600 m^3. The findings from the pilot study and production application demonstrated that the anaerobic composite bed technology is a practical and efficient anaerobic bioreactor. The technology exhibited several favorable characteristics, including good reaction-liquid mass transfer and separation, a large biomass, and a diverse range of biological species within the reactor. These factors contribute to the overall effectiveness of the treatment process. The anaerobic composite bed technology showed high treatment efficiency, meaning it achieved significant reductions in the concentration of antibiotics and other pollutants in the wastewater. Additionally, the technology exhibited a high level of operational stability, ensuring consistent and reliable performance over time. The results obtained from the small pilot study, pilot study, and production application collectively support the practicality and effectiveness of the anaerobic composite bed technology for the treatment of antibiotic wastewater. The research provides valuable insights for the implementation and utilization of this technology in real-world wastewater treatment scenarios.

2.1.6 Anaerobic aerobic combination treatment technology

The study conducted by Hu et al. [17] focused on the treatment of penicillin wastewater using intermittent aeration. The research investigated the effects of pH, treatment cycle, temperature, and shock load on the treatment efficiency of the wastewater. The method of intermittent aeration employed in the study utilized both facultative anaerobes and aerobic bacteria to effectively degrade the organic matter present in the penicillin wastewater. The notable aspect

of this method is that it does not require any physical or chemical pretreatment for the removal of sulfate ions and PPb (possibly referring to phenolic pollutants) in the penicillin wastewater. The results of the study demonstrated that the intermittent aeration method was highly effective in treating penicillin wastewater. The influent water with a COD concentration of up to 10,000 mg/L could be treated with a COD removal rate exceeding 85%. The feeding load in terms of COD reached 7 kg/m3·d, and the maximum impact load reached 14 kg/m3·d, indicating the robustness and capacity of the treatment process. Furthermore, the presence of foam generated by the substance "1231" in penicillin wastewater did not hinder the normal operation of the sequencing batch reactor (SBR) treatment plant. This suggests that the treatment method was able to accommodate and handle foam-related challenges effectively. Moreover, the study revealed that the intermittent aeration method achieved a PPb removal rate of over 97%, indicating its effectiveness in treating phenolic pollutants present in penicillin wastewater. Overall, the findings support the conclusion that intermittent aeration is an ideal and efficient method for the treatment of penicillin wastewater. The research provides valuable insights into the optimization of treatment parameters and underscores the potential of this approach for practical application in the treatment of penicillin-containing industrial wastewater.

The study conducted by Han Jianhong et al. [18] focused on the treatment of mixed wastewater from antibiotic production using a hydrolysis acidification membrane bioreactor (MBR) process. The research aimed to optimize the operation parameters and assess the treatment performance of various antibiotic mixed wastewater treatment processes. The results of the industrial experiments showed that the system achieved a high COD removal rate of 90% when the membrane bioreactor was operated with a feed water COD volume load ranging from 7 to 10 kg/m3·d-1. Additionally, the system exhibited significant removal efficiencies for ammonia nitrogen and total nitrogen, with removal rates of 80% and 65%, respectively. The hydrolysis acidification process employed in this study effectively reduced the concentration of non-ionic ammonia in the wastewater, thereby reducing its toxicity. The treated wastewater from the hydrolysis acidification reactor directly entered the aerobic membrane bio-oxidation zone. In this zone, organic nitrogen and ammonia ions were transformed into nitrite (NO2-) and nitrate (NO3-) under the action of nitrifying bacteria. To maintain the treatment process, a

portion of the membrane effluent was recirculated back to the hydrolysis acidification reactor through a reflux pump. This recycling process created a continuous cycle in which the wastewater treatment was carried out until the water quality reached the required standard. Once the water quality met the standard, it could be discharged. The comprehensive study demonstrated that the hydrolysis acidification membrane bioreactor process was effective in treating mixed wastewater from antibiotic production. It achieved a high removal rate for COD, ammonia nitrogen, and total nitrogen, ensuring significant reductions in the concentration of non-ionic ammonia and overall water toxicity. The combination of hydrolysis acidification and membrane bioreactor technology provides a promising approach for the treatment of complex wastewater streams generated in antibiotic production processes.

The study conducted by Shang Jiaji et al. [19] proposed a novel approach for treating antibiotic wastewater, which involved the combination of hydrolytic acidification and aerobic moving bed biofilm (MBBR) technology, along with the application of the Fenton process. The treatment process consisted of connecting a hydrolytic acidification reactor and an aerobic reactor in series. This method offers several advantages for the treatment of antibiotic wastewater. Firstly, it has a lower sludge treatment cost compared to traditional treatment methods. The hydrolytic acidification process promotes the breakdown of complex organic compounds, leading to reduced sludge production. Secondly, the system exhibits high treatment efficiency and stability. The combination of hydrolytic acidification and aerobic MBBR enables effective removal of organic pollutants, ensuring reliable and consistent treatment performance. Moreover, the system demonstrates good resistance to shock loads and high toxicity levels. Antibiotic wastewater can be highly variable in composition and toxicity, but this treatment approach can effectively handle such fluctuations. The hydrolytic acidification step helps to buffer and stabilize the system, allowing it to withstand sudden changes in wastewater characteristics. Compared to conventional activated sludge treatment, this method offers distinct advantages, particularly for the treatment of highly concentrated organic toxic wastewater. It provides better performance and efficiency in removing complex organic compounds, including antibiotic residues, from the wastewater. It is important to note that the pH conditions play a crucial role in this treatment method. Optimal pH control is necessary to

ensure the effectiveness of the Fenton process, which relies on the generation of hydroxyl radicals to degrade pollutants. Maintaining the appropriate pH range is vital for achieving efficient oxidation of organic compounds and ensuring the overall treatment performance.

The study conducted by Huang et al. [20] focused on treating high-quality concentrations of antibiotic wastewater using a composite aerobic biological treatment method. The goal was to achieve a high removal efficiency for COD (chemical oxygen demand) and BOD5 (biochemical oxygen demand), two important indicators of organic pollutant removal. The researchers found that a continuous flow treatment process was more suitable for wastewater containing high levels of difficult-to-biodegrade substances compared to an intermittent flow treatment process. In the composite aerobic treatment reactor, a complex microbial ecosystem was formed. This ecosystem had several benefits, including improved sludge settling performance and enhanced treatment capacity of the reactor. The complex aerobic biological method was primarily designed for treating antibiotic wastewater with high concentrations. One reason for favoring aerobic treatment over anaerobic treatment is the presence of high concentrations of sulfate ions (SO42-) in antibiotic wastewater. These sulfate ions can strongly inhibit the activity of methanogenic bacteria (MPB) and disrupt the normal operation of anaerobic digestion systems. Therefore, completed antibiotic wastewater treatment projects typically rely on aerobic biological treatment processes. However, it should be noted that there are still some challenges associated with this treatment method. To achieve the standard discharge of wastewater, further enhancements of the aerobic process are necessary. This may involve optimizing process parameters, such as aeration rate, hydraulic retention time, and nutrient supplementation, to ensure effective pollutant removal and compliance with regulatory requirements.

The study conducted by Jiang et al. [21] focused on the treatment of high levels of cephalosporin antibiotic wastewater using a combined process involving an upflow anaerobic sludge bed (UASB) reactor, flocculation treatment, and a sequential batch activated sludge reactor (SBR). In the UASB reactor stage, the influent COD concentration was 14.3 g/L, and the volumetric load was 14.3 kg/(m^3·d). The UASB reactor achieved a stable COD removal rate of approximately 85%. The effluent VFA (volatile fatty acid) concentration was around 3 mmol/L, and the gas production rate was about 17 L/d. To further enhance the treatment

efficiency, flocculation treatment was applied to the effluent from the UASB reactor. The flocculation process involved the addition of polyferric chloride (PFC) and polyacrylamide (PAM) at specific dosages. The COD of the effluent was reduced from 2.279 g/L to 1.133 g/L, resulting in a removal rate of 50.3%. The supernatant from the flocculation treatment was then treated in an SBR. At a reactor load of 1.2 kg/(m^3·d), the SBR achieved an effluent COD concentration below 200 mg/L, with a stable removal rate of approximately 80%. Overall, the combined UASB-flocculation-SBR process demonstrated effective removal of COD from high levels of cephalosporin antibiotic wastewater. The UASB reactor achieved significant COD removal, while the flocculation and SBR stages further enhanced the treatment efficiency, resulting in a final effluent with COD concentrations meeting the desired discharge standards.

The study conducted by Yang et al. [22] focused on the treatment of various antibiotic wastewater using a new process called hydrolysis acidification-AB biological method. This process is known for its shorter duration and higher energy efficiency compared to traditional treatment methods. In the hydrolysis acidification stage, specific anaerobic bacteria and parthenogenic anaerobic bacteria, which have a diverse range of species and fast metabolic rates, are employed. These bacteria facilitate the breakdown of complex organic compounds through hydrolysis, resulting in the conversion of insoluble organic matter into soluble organic matter. Following the hydrolysis acidification stage, the AB biological method is employed. In this method, two distinct microbial groups are formed. In the A level, the microbial group is predominantly composed of bacteria and mycobacteria, while in the B level, the microbial group is mainly composed of protozoa. This arrangement allows for the utilization of the unique characteristics of different microorganisms, leading to effective removal of contaminants in the antibiotic wastewater.

In the study conducted by Jia Renyong et al. [23], two different processes, namely activated sludge anoxic-aerobic membrane bioreactor (A/O-MBR) and immobilized anoxic-aerobic membrane bioreactor (I-A/O-MBR), were employed for treating antibiotic-containing wastewater. The researchers also analyzed the microbial community structure within the reactors to gain insights into the treatment process. The findings of the study revealed that as the sludge age decreased, the total number of microorganisms in the A/O-MBR reactor

decreased. Simultaneously, there was an increase in the proportion of antibiotic resistance genes, indicating the presence of microorganisms with antibiotic resistance in the reactor. This suggests that microorganisms with antibiotic resistance play a crucial role in the treatment of antibiotic-containing wastewater. The presence of these microorganisms can potentially contribute to the degradation of antibiotics and enhance the treatment efficiency. Furthermore, the study demonstrated that the hydraulic retention time (HRT) had little impact on the total number of bacteria in both the A/O-MBR and I-A/O-MBR reactors, when evaluated at the same sludge age. However, HRT influenced the contact time between the bacteria and the effluent, subsequently affecting the overall removal efficiency of the wastewater. This implies that optimizing the HRT can be an important factor in achieving desirable treatment outcomes.

2.1.7 Physical and chemical method-biological method combination treatment technology

Due to the intricate composition of antibiotic wastewater, which is comprised of various antibiotics, the biological toxicity of the wastewater is compounded. When solely relying on biological treatment methods, it becomes challenging to meet the required discharge standards for the treated wastewater. Consequently, it becomes necessary to implement pretreatment measures for antibiotic wastewater. The aim of pretreatment is twofold: firstly, to eliminate biotoxic substances present in the wastewater, and secondly, to reduce the overall wastewater concentration. Currently, both domestic and international practices for treating antibiotic wastewater typically employ a combination of physical-chemical and biological methods. Physical-chemical methods encompass techniques such as ionization and coagulation, while biological methods encompass anaerobic, aerobic, and anaerobic-aerobic approaches.

In the study conducted by Deng, Liangwei et al. [24], a flocculation-anaerobic-aerobic process was employed to treat various antibiotics including penicillin, tetracycline, rifampicin, and spiramycin. The application of this process successfully reduced the effluent COD to below 300 mg/L, meeting the discharge standard for the biopharmaceutical wastewater industry. These results demonstrate the feasibility of combining physical and biological methods for the treatment of antibiotic wastewater. However, it should be noted that the cost of implementing this treatment method is relatively high, and the process flow can be complex. As a result, many

antibiotic manufacturers may be discouraged from adopting this technology due to these factors. This has led to reluctance among several antibiotic manufacturers to adopt this technology, primarily due to the high treatment costs and intricate process flow involved.

While biological treatment has been widely utilized for the treatment of antibiotic wastewater, it is important to acknowledge several challenges that still need to be addressed. These include the requirement for a large treatment footprint, the emergence of resistant bacteria, the occurrence of foam, and difficulties in removing chromaticity. One of the primary concerns associated with biological treatment methods is the potential generation of drug-resistant bacteria and superbugs. Effectively managing and eliminating these bacteria is a critical aspect of future research. The biological treatment of antibiotic wastewater can lead to the proliferation of drug-resistant bacteria, and in some cases, the development of superbugs. If these bacteria are released into the natural environment without proper treatment, they can pose significant risks to human health. In milder cases, the efficacy of antibiotics that were once effective may be reduced or lost, thereby increasing the challenges and costs associated with patient treatment. In more severe scenarios, the consequences can be catastrophic, potentially leading to infections that cannot be cured due to the lack of effective antibiotics.

In summary, while biological treatment methods have proven effective in treating antibiotics in wastewater, they also have some limitations and disadvantages:

The first, slow degradation of certain antibiotics. Some antibiotics are highly persistent and resistant to biodegradation. Biological treatment methods may struggle to efficiently degrade these compounds, leading to incomplete removal and potential persistence in the treated effluent.

The second, development of antibiotic-resistant bacteria. The presence of antibiotics in wastewater can promote the development of antibiotic-resistant bacteria within the treatment system. This can pose a risk if these bacteria are released into the environment and contribute to the spread of antibiotic resistance.

The third, variable treatment efficiency. The performance of biological treatment methods can vary depending on the specific antibiotics present, their concentrations, and the wastewater

characteristics. Some antibiotics may be more challenging to remove, resulting in lower treatment efficiencies.

The fourth, high energy and operational costs. Biological treatment processes, particularly aerobic methods, require energy-intensive aeration and maintenance of optimal process conditions. These operational requirements can lead to higher energy consumption and associated costs.

The fifth, need for pre-treatment and post-treatment steps. In some cases, pre-treatment steps such as hydrolysis or chemical oxidation may be necessary to enhance the biodegradability of antibiotics. Similarly, post-treatment steps might be required to further polish the effluent and meet stringent discharge standards. These additional steps increase the complexity and cost of the overall treatment process.

Next, limited effectiveness against emerging contaminants. Biological treatment methods may struggle to effectively remove emerging contaminants, such as certain pharmaceutical metabolites or transformation products, which may exhibit higher persistence and resistance to biodegradation compared to parent compounds.

The last, potential formation of disinfection by-products. Some antibiotics and their degradation by-products can react with disinfectants, such as chlorine, during post-treatment disinfection processes. This can lead to the formation of disinfection by-products (DBPs), which may have their own adverse effects on human health and the environment.

2.2 Oxidation method

2.2.1 Fenton oxidation method

The Fenton oxidation method is a widely employed technique that utilizes Fenton's reagent to generate a significant quantity of highly reactive hydroxyl radicals, which serve as potent oxidizing agents for pollutant degradation. While this method has proven effective, it is important to acknowledge its drawbacks, such as high treatment costs and equipment susceptibility to corrosion. One of the limitations of the Fenton oxidation method is its relatively high treatment cost. The procurement and handling of Fenton's reagent, typically

composed of hydrogen peroxide (H_2O_2) and ferrous ions (Fe^{2+}), can contribute to the overall expenses of the treatment process. Additionally, the process requires careful control and monitoring to optimize the dosage of reagents, which further adds to the operational costs. Furthermore, the Fenton oxidation method is known to be associated with equipment corrosion issues. The strong oxidative nature of hydroxyl radicals can lead to the deterioration and damage of equipment components, including pipelines, reactors, and other infrastructure. The corrosive effects may require frequent maintenance, replacement of parts, and implementation of corrosion-resistant materials, leading to additional costs and operational challenges.

Li Zaixing et al. [25] conducted a study on the application of the Fenton oxidation method for the treatment of penicillin and oxytetracycline antibiotic wastewater. They investigated the efficiency of COD removal in the treated effluent under specific operating conditions. The results indicated that by applying a dosage of 5 mL/L of hydrogen peroxide (H_2O_2) with a concentration of 30%, maintaining a Fe^{2+}/H_2O_2 ratio of 1/20, initiating the process at an initial pH of 4, and allowing a reaction time of 60 minutes, the COD concentration in the treated effluent was reduced to less than 120 mg/L, with a removal rate exceeding 75%. This research demonstrates that the Fenton oxidation method can effectively reduce the COD content in penicillin and oxytetracycline antibiotic wastewater under the specified experimental conditions. The combination of appropriate H_2O_2 dosage, Fe^{2+}/H_2O_2 ratio, pH control, and reaction time plays a crucial role in achieving significant COD removal. It should be noted that the specific operating parameters and conditions may vary depending on the characteristics of the wastewater and the target pollutants.

Yan Xia [26] conducted a study focusing on the treatment of metronidazole wastewater using electro-Fenton and multiphase Fenton methods. The research aimed to address the challenges associated with real metronidazole wastewater, which exhibited specific water quality characteristics. The wastewater samples had a chemical oxygen demand (COD) concentration of 26,789 mg/L, a biochemical oxygen demand (BOD5) concentration of 4,554.1 mg/L, and a BOD5/COD ratio of 0.17. Furthermore, the total concentration of metronidazole and 2-methyl-5-nitroimidazole in the wastewater was 32.32 mg/L, with NH4+-N at 475 mg/L and Cl- at 688 mg/L. In the modified electro-Fenton method applied to the treatment of real metronidazole

wastewater, the initial concentration of metronidazole was set at 100 mg/L. Under these conditions, the removal efficiency of metronidazole reached 99.3%. Additionally, the study explored the use of an innovative multiphase Fenton oxidation catalyst consisting of FeOCl (iron oxychloride) and CNTs (carbon nanotubes). When this catalyst was employed, along with a catalyst addition of 1.2 g/L, an H2O2 input of 15 mmol/L, and a pH of 5, the removal efficiency of metronidazole was also 99.3%. Moreover, the removal efficiency of COD reached 68.3%.

Fenton oxidation is recognized for its notable advantages, including its rapid reaction time, high efficiency in pollutant degradation, and straightforward operation. However, it also possesses certain drawbacks that should be addressed when applying it to the treatment of antibiotic wastewater. One significant disadvantage is the high cost associated with the Fenton reagent and catalyst, which can impede its practical implementation. Therefore, finding strategies to reduce the overall cost of Fenton oxidation is of paramount importance. Exploring alternative reagents or catalysts that are more economical or developing methods to optimize the dosage and utilization of Fenton reagents can contribute to cost reduction in the process. Another concern is the high yield of sludge generated during Fenton oxidation treatment. The accumulation of sludge can pose challenges in terms of disposal and management. Therefore, it is crucial to explore methods to minimize sludge production, such as optimizing operating parameters or employing additional treatment steps to enhance sludge dewatering or reduce its volume. Furthermore, the corrosive nature of Fenton oxidation can lead to equipment degradation and require frequent maintenance or replacement. To improve the corrosion resistance of equipment, selecting appropriate materials that are resistant to Fenton oxidation conditions and ensuring proper coating or lining on equipment surfaces can help mitigate corrosion-related issues.

2.2.2 Photocatalytic oxidation method

Photocatalytic oxidation is an innovative advanced oxidation technique that harnesses light energy and employs a semiconductor as the catalyst. Through the absorption of specific photon energy, the electrons in the catalyst undergo an energy leap from their ground state, resulting in

the generation of electron-hole pairs. These photogenerated electron-hole pairs then migrate to the surface of the catalyst, creating highly active redox sites that facilitate the degradation of organic pollutants through various redox reactions. The implementation of photocatalytic oxidation technology for antibiotic wastewater treatment extensively utilizes photocatalysts, known for their exceptional stability and non-toxic nature.

Geng [27] and colleagues conducted a study to examine the impact of different factors on the photocatalytic degradation of sulfapyridine in simulated wastewater. The findings revealed that the optimal combination of conditions for UV/TiO_2 photocatalytic degradation of sulfapyridine in the simulated wastewater was achieved with 1 g/L of TiO_2 and 10 mg/L of sulfapyridine. Under these conditions, the degradation rate of sulfapyridine reached an impressive 99%. The primary mechanism responsible for this degradation was attributed to the direct oxidation occurring within the reaction sites.

Despite its numerous advantages, TiO_2 as a photocatalyst does have certain limitations, preventing its widespread application. These limitations include its wide bandgap, which restricts its utilization of visible light, and its low efficiency in recycling and reusing. As a result, the large-scale implementation of TiO_2 photocatalysis has been hindered.

In the study conducted by Liu and colleagues [28], a composite film catalyst called metal ion-doped phosphotungstic acid/TiO_2 ($M^+/H_3PW_{12}O_{40}/TiO_2$) was prepared using a sol-gel method combined with temperature-controlled and spin-coating techniques. The researchers utilized a parent heteropolyacid (HPA) and selected saturated Keggin-type phosphotungstic acid ($H_3PW_{12}O_{40}$) as the inorganic precursor, titanium tetraisopropoxide (TTIP) as the titanium source, and quartz flakes as the substrate. The aim of the study was to investigate the impact of different metal ions (Cu, Fe, Ag) and their dosages on the degradation rate of tetracycline solution when incorporated into the heteropolyacid/TiO_2 composite film catalysts. The results revealed that the addition of 5% mass of silver ions achieved a maximum degradation rate of 72.3% for tetracycline solution at a concentration of 40 mg/L. Similarly, the addition of 5% mass of copper ions resulted in a maximum degradation rate of 71.4%, while the addition of 2% mass of iron ions achieved a maximum degradation rate of 75% under the same conditions.

This research demonstrates the potential of metal ion-doped phosphotungstic acid/TiO_2 composite films as effective catalysts for the degradation of tetracycline solutions, with varying metal ions and their dosages influencing the degradation rates.

In the study conducted by Ai and colleagues [29], a β-In_2S_3 nanoparticle photocatalyst was prepared using a hydrothermal reaction method. The researchers focused on investigating the degradation effect of In_2S_3 on hygromycin, a compound used to simulate tetracycline antibiotic wastewater. The results revealed that β-In_2S_3 exhibited a cubic-phase nanoparticle structure, composed of nanosheets with a certain diameter. The degradation capacity of β-In_2S_3 for hygromycin was found to be significant, with a degradation rate exceeding 85%. To assess the recyclability of the catalyst, the degraded β-In_2S_3 was washed and dried using anhydrous ethanol. Remarkably, even after undergoing four cycles of recycling, the degradation capacity of β-In_2S_3 remained above 85%.

Currently, the application of photocatalytic oxidation method for treating antibiotic wastewater is primarily in the early stages of basic research and has limited industrial implementation. Research efforts are primarily directed towards the development of photocatalysts that possess narrow band gaps, exhibit high degradation rates, maximize sunlight utilization, and are cost-effective.

2.2.3 Electrochemical oxidation method

Electrochemical oxidation is an effective technique for water treatment that utilizes a specialized electrochemical reaction device to generate a significant quantity of -OH ions on the electrode surface in the presence of an electric field. This process facilitates the degradation of organic pollutants present in wastewater.

In their study, Guo, and colleagues [30] employed an electrochemical oxidation method to treat the secondary effluent of cephalosporin synthesis wastewater. They utilized Na2SO4 solution as the electrolyte, a titanium-coated ruthenium-iridium electrode as the anode, and a 2-ethylanthraquinone-modified graphite felt electrode as the cathode. The electrochemical oxidation process demonstrated effective reduction of the wastewater's chemical oxygen demand (COD) concentration. The initial COD concentration of 263.15 mg/L was significantly

reduced to 117.62 mg/L, resulting in a COD removal rate exceeding 55%. Moreover, the electrochemical system achieved a favorable current efficiency, surpassing 32%. Notably, the energy consumption associated with this treatment approach was measured at 51.54 kWh/kg COD. Despite the energy input, the resulting effluent met the required discharge standard. (4)

In the study conducted by Wang Huiqing et al. [31], electrocatalytic oxidation was employed to treat antibiotic sulfonamide wastewater. The research demonstrated that after 3 hours of electrocatalytic oxidation, the degradation rate of sulfonamide reached 89.2%. The experimental conditions consisted of an initial sulfonamide solution concentration of 0.12 mmol/L, a pH of 3, a current intensity of 20 mA/cm2, and a Na2SO4 electrolyte concentration of 50 mmol/L.

In the study conducted by Wu et al. [32], an electrocatalytic-persulfate system utilizing activated carbon was employed to treat sulfonamide antibiotic wastewater. The results showed that at a pH of 5 and a plate spacing of 9 cm, the degradation rate of sulfonamide reached 88.5%. Furthermore, even after the activated carbon was reused four times, the degradation rate of sulfonamide remained above 80%.

In the study conducted by Salazar et al. [33], boron-doped diamond film/stainless steel electrodes were utilized to degrade losartan wastewater. The results showed that under the reaction conditions of using chloride or sulfate ions as the conductive medium, pH 7.0, and a current density of 80 mA/cm2, the degradation rate of losartan reached 56% and 67% respectively. The treatment process took 180 minutes to completely remove losartan from the wastewater.

Electrochemical oxidation is an advantageous method for treating wastewater due to its high efficiency, operational feasibility, and absence of secondary pollution. It is particularly suitable for wastewater with high conductivity and moderate antibiotic concentrations. However, challenges such as the potential hazards, high voltage requirements, and significant energy consumption associated with electrochemical oxidation devices have yet to be fully addressed. These limitations have hindered the widespread application of electrochemical oxidation in antibiotic wastewater treatment, keeping it primarily in the laboratory research stage. The key

to the electrochemical oxidation method lies in the development and preparation of high-performance electrode materials. Future research efforts will focus on enhancing the performance of electrode materials to improve the efficiency and effectiveness of the electrochemical oxidation process in treating antibiotic wastewater. By addressing these material-related challenges, the application of electrochemical oxidation in large-scale antibiotic wastewater treatment can be further explored and optimized.

2.2.4 Catalytic wet oxidation method

Catalytic wet oxidation is a technique that facilitates the decomposition of organic substances into smaller molecules such as CO2, H2O, and other compounds in a liquid phase environment. This process occurs under high temperature and pressure conditions and requires the presence of a catalyst. The oxidizing agent used in catalytic wet oxidation can be air, oxygen, or other similar substances.

In the study conducted by Yan Li [34], FeCl3 and NaNO2 were employed as catalysts, while oxygen served as the oxidant for the catalytic wet oxidative degradation of enrofloxacin wastewater. The reaction was carried out at a temperature of 150°C and a pressure of 0.5 MPa for a duration of 120 minutes. The results showed that the enrofloxacin degradation rate reached nearly 100%. Furthermore, the removal rates of COD and TOC were 37% and 51%, respectively. The BOD_5/COD ratio of the degraded reaction solution increased from 0.01 to 0.12, indicating an improvement in biodegradability, and the toxicity decreased from 43% to 12%.

In the study conducted by Wang et al. [35], two pharmaceutical wastewaters, sodium fosfomycin and safranin, were combined. The wastewater had a chemical oxygen demand (COD) of 121,081 mg/L and a total organic carbon (TOC) of 5,823 mg/L. A Cu2+[PxWmOy]q- catalytic system was formed by adjusting the volume ratio of the mixed wastewaters, and catalytic wet oxidative degradation was performed at 250 °C and an initial oxygen partial pressure of 1.4 MPa. Under these conditions, the removal rates of the mixed wastewater components, sodium fosfomycin and safranin, were 41.1% and 43.0% respectively. Furthermore, approximately 95% of the organic phosphorus was converted into PO43- and 70%

of the organic nitrogen was converted into NH+4. The catalytic treatment significantly improved the biochemical properties of the effluent.

In the study conducted by Chen et al. [36], a nano-manganese cerium/γ-Al2O3 composite catalyst was prepared for the catalytic wet oxidative degradation of antibiotic wastewater generated during the production of cefoxitin, ceftizoxime sodium, and cefaclor. The wastewater had a chemical oxygen demand (COD) of 4350 mg/L and a total organic carbon (TOC) of 4586 mg/L. Under the experimental conditions of 170 °C, a partial pressure of oxygen of 0.75 MPa, a reaction time of 2 hours, and a catalyst dosage of 4 g/L, the COD and TOC removal rates were 82.03% and 88.03%, respectively. The nano-manganese cerium/γ-Al2O3 composite catalyst demonstrated effective degradation capabilities for the antibiotic wastewater.

Catalytic wet oxidation is a highly efficient and environmentally friendly technique for the treatment of antibiotic wastewater. While there are currently limited research and application examples of catalytic wet oxidation in antibiotic wastewater treatment, it is anticipated that as the technology becomes more mature and costs decrease, there will be a gradual increase in both research and practical applications of catalytic wet oxidation for treating antibiotic wastewater.

2.2.5 Chlorine oxidation method

Chlorine oxidation is a wastewater treatment method that involves the addition of chlorine-containing chemical reagents, such as chlorine gas, sodium hypochlorite, or chlorine dioxide, to the wastewater. By leveraging the strong oxidation capability of these chemical reagents, the pollutants or toxic substances present in the wastewater undergo redox reactions, leading to the conversion of these contaminants into non-toxic or less toxic substances.

In the study conducted by Gu et al. [37], antibiotic pharmaceutical wastewater was treated using bleaching powder concentrate ($Ca(ClO)_2$) with an effective chlorine concentration of 60%-65%. The initial chemical oxygen demand (COD) of the wastewater, which was 527 mg/L, was reduced to 184 mg/L under the experimental conditions of a 3.0 g/L effective chlorine dosage, pH 10, and 5 minutes of stirring. This resulted in a COD removal rate of 65%. Additionally, the turbidity of the wastewater decreased from 100 NTU to 20 NTU, with a

removal rate of 80%. The color of the wastewater also decreased from 320 to 10, achieving a removal rate of 97%. These findings demonstrate the effectiveness of using bleaching powder concentrate for the treatment of antibiotic pharmaceutical wastewater, as it effectively reduced COD, turbidity, and color levels.

In the study conducted by Zhang et al. [38], the researchers investigated the use of chlorine oxidation for removing the contaminant enrofloxacin from drinking water distribution systems. During the experiment, the chlorine concentration was increased from 4.23 μmol/L to 18.31 μmol/L over a reaction period of 180 minutes. As a result, the removal rate of enrofloxacin increased from 50.6% to 70.4%. This indicates that higher chlorine concentrations and longer reaction times lead to improved removal efficiency of enrofloxacin in the water distribution system.

2.2.6 Ozone oxidation method

Ozone is a potent oxidant, exhibiting a high oxidative capacity comparable to fluorine, hydroxyl radicals, and atomic oxygen (O), and surpassing monomeric chlorine by 1.52 times. In the context of antibiotic wastewater treatment, ozone oxidation operates through two main mechanisms: direct ozone oxidation and indirect oxidation via free radicals.

During direct ozone oxidation, ozone selectively targets aromatic rings, double bonds, and non-protonated amines within antibiotics. Several pathways are involved in direct ozone oxidation, including hydroxylation, demethylation, carbonylation, and methylene cleavage. Among these pathways, hydroxylation is the most prominent process in which hydroxyl groups are introduced into the antibiotic structure.

Indirect oxidation of antibiotics by free radicals occurs in two stages. Firstly, ozone undergoes self-decomposition to generate free radicals. Subsequently, the formation of hydroxyl substitution products initiates a free radical chain reaction, leading to the decomposition of antibiotics. Ozone oxidation is regarded as a highly efficient and practical advanced oxidation method for antibiotic wastewater treatment. It offers several advantages, including short reaction times, potent oxidation capability, absence of secondary pollution, and simple equipment requirements. Consequently, ozone oxidation is increasingly recognized and

valued in the treatment of antibiotic wastewater, particularly for β-lactam, sulfonamide, and tetracycline antibiotics. Notably, its removal effectiveness in these specific types of antibiotic wastewater is highly pronounced [39-40].

In the study conducted by Li et al. [41], ozone oxidation was employed to treat the biochemical effluent from an antibiotic pharmaceutical plant wastewater treatment station. The water sample exhibited the following characteristics: COD of 954.7 mg/L, BOD5 of 66.8 mg/L, ammonia nitrogen of 98 mg/L, pH of 8, and a BOD5/COD ratio of 0.07. The researchers investigated the impact of ozone oxidation on antibiotic wastewater treatment, both without a catalyst and with silica gel loaded with various metal catalysts. The findings revealed that the COD removal rate of antibiotic wastewater treated by ozone oxidation without a catalyst was less than 10%. However, when silica gel loaded with metal catalysts was employed, the COD removal rate significantly improved. Among the different catalysts tested, silica gel loaded with iron catalyst demonstrated the most cost-effective performance. The optimal catalyst dosage was determined to be 0.33 g/L in combination with ozone treatment for antibiotic wastewater. Under the conditions of a 1-hour reaction time, the ozone oxidation process with silica gel loaded iron catalyst achieved a COD removal rate of 54.9% and an ammonia nitrogen removal rate of 44.4%. The effluent COD concentration was below 300 mg/L, the effluent ammonia nitrogen concentration ranged from 40-50 mg/L, and the BOD5/COD ratio reached 0.2, indicating the improved quality of the treated wastewater.

In the study conducted by Gao Zixing et al. [42], a catalyst was prepared using NiO and CuO as active ingredients and γ-Al2O3 as the carrier through the impregnation method. The catalyst was then utilized in the ozone catalytic oxidation process to treat the effluent from an antibiotic industrial wastewater of a pharmaceutical group, which had a COD concentration of approximately 1024 mg/L. The experimental results demonstrated that the NiO-CuO-γ-Al2O3 catalyst, prepared under optimized conditions, exhibited excellent reusability. It could be reused multiple times while maintaining a COD removal rate of antibiotic wastewater above 45%. This indicates the effectiveness and durability of the catalyst in the ozone catalytic oxidation treatment of antibiotic wastewater.

Ozone oxidation has shown promising results in the degradation of antibiotic wastewater. It has been extensively utilized in water treatment processes in Western countries. However, the widespread application of ozone oxidation in engineering is limited by the high cost of ozone production technology and the technology's relative immaturity. Currently, in the field of antibiotic wastewater treatment, a combined approach of ozone oxidation pretreatment followed by biochemical treatment has proven to be effective in achieving enhanced degradation of antibiotic wastewater. This combined method takes advantage of the superior degradation capabilities of ozone oxidation, while also benefiting from the subsequent biological treatment processes. By integrating these two treatment methods, a more comprehensive and efficient degradation of antibiotic wastewater can be achieved.

2.2.7 Low temperature discharge plasma method

Plasma, as the fourth state of matter, is characterized by the presence of ions, electrons, excited atoms, free radicals, and other highly reactive particles. It differs from the traditional states of matter—gas, liquid, and solid. Plasma is typically generated through electrical discharge, and it can initiate a variety of chemical and physical effects. These effects include the production of oxidizing particles such as hydrogen peroxide, ozone, and hydroxyl radicals, as well as the release of ultraviolet radiation, shock waves, and liquid-electric cavitation.

The plasma method combines the advantageous features of various oxidation processes, including ozone oxidation, ultraviolet photolysis, pyrolysis, and free radical oxidation. This unique combination of effects enables plasma to effectively degrade almost any type of organic pollutants. By harnessing the reactive nature of plasma, organic compounds in wastewater can be efficiently broken down and eliminated, leading to significant pollutant removal and water purification [43].

In a study conducted by Kim et al [44], a medium-blocking discharge plasma method was employed to degrade three sulfonamide antibiotic wastewaters: sulfathiazole, sulfadimethoxine, and sulfamethoxazole. Under oxygen discharge conditions for a duration of 20 minutes, 100% degradation of 1 liter of each antibiotic solution with a concentration of 50 mg/L was achieved. The medium-blocking discharge plasma method effectively facilitated the breakdown and

elimination of these sulfonamide antibiotics, indicating its potential as a promising approach for the treatment of such wastewater contaminants.

In a study conducted by He et al [45], corona discharge plasma combined with nano-TiO2 was employed to treat simulated tetracycline wastewater. The treatment resulted in the degradation of 85.1% of the tetracycline and a 53.4% reduction in total organic carbon (TOC) for a volume of 250 mL of tetracycline solution with an initial concentration of 50 mg/L. The experimental conditions included a power of 36 W and a treatment duration of 20 minutes. The combination of corona discharge plasma and nano-TiO2 demonstrated promising effectiveness in the degradation and removal of tetracycline contaminants in wastewater.

The low-temperature discharge plasma method shows great promise for the degradation and treatment of antibiotic wastewater due to its advantages such as rapid reaction time, high efficiency, and versatility. However, despite its potential, this method is currently limited to laboratory research due to challenges such as high energy consumption, elevated discharge voltage, and safety hazards. Further advancements and optimizations are required to address these issues and enable the practical application of the low-temperature discharge plasma method for large-scale antibiotic wastewater treatment.

2.3 Physical method

2.3.1 Flocculation method

The flocculation method is a widely used technique for wastewater pretreatment. It involves the addition of flocculants, such as polymerized aluminum chloride (PAC), polymerized ferric sulfate (PFS), and polyacrylamide (PAM), to the wastewater. These flocculants help destabilize the colloidal particles present in the water. As a result of intermolecular forces, the destabilized colloids form small aggregates that subsequently coagulate with suspended matter in the water. These larger flocs then settle down due to gravity, facilitating their removal from the water. The flocculation method plays an important role in the initial treatment of wastewater, aiding in the removal of particulate matter and colloidal substances.

In the study conducted by Xing et al [46], polymerized ferric sulfate (PFS) was utilized as a

coagulant for the pretreatment of antibiotic fermentation wastewater originating from a pharmaceutical plant. The wastewater exhibited characteristics such as a brownish-brown color, an irritating odor, a COD concentration ranging from 14,700 to 17,600 mg/L, a BOD/COD ratio of 0.25-0.26, a pH range of 3-4, a suspended solids (SS) concentration between 94 and 150 mg/L, a total nitrogen (TN) concentration of 680-740 mg/L, a total organic carbon (TOC) concentration of 4,300-4,750 mg/L, an ammonium nitrogen (NH4+-N) concentration of 25-55 mg/L, and a chromaticity multiple of 7,000-8,000 times. The experimental findings indicated that by employing a PFS dosage of 135.26 mg/g COD, with an initial wastewater pH of 4, agitation at 300 r/min for 1 minute followed by 50 r/min for 12 minutes, and a sedimentation period of 60 minutes, the flocculation pretreatment achieved removal rates of 62.2% for COD, 62.5% for color, 88.2% for SS, and 49.6% for TOC.

In the study conducted by Qu et al [47], polymerized ferric sulfate (PFS) coagulant and polyacrylamide (PAM) coagulant were employed to flocculate and precipitate antibiotic wastewater from a pharmaceutical wastewater treatment plant following a hydrolysis acidification-SBR-secondary contact oxidation process. The water quality characteristics of the wastewater were as follows: turbidity ranging from 15 to 140 NTU, pH between 6.8 and 8.3, CODCr concentration ranging from 180 to 1,012 mg/L, conductivity of 1,700 to 3,800 μS/cm, chromaticity of 550 to 1,600 Pt/Co, sulfate concentration ranging from 532 to 980 mg/L, and total hardness of 426 to 536 mg/L. The experimental results revealed that through coagulation, the average removal rates of suspended matter, turbidity, and CODCr were 86.6%, 58.6%, and 32.9%, respectively.

In the study conducted by Wang et al [48], a new coagulant called poly(aluminium magnesium zinc) silicate (PSAMZ) was added to wastewater with an alkalinity of 25 mg/L and turbidity of 10 NTU. The effectiveness of this coagulant was evaluated in two different wastewater samples: one containing oxytetracycline (OTC) at a concentration of 0.02 mol/L, and the other containing tetracycline (TC) at a concentration of 0.03 mol/L. The results showed that the removal efficiency of the PSAMZ coagulant was 91.95% for the OTC wastewater and 90.03% for the TC wastewater.

The flocculation technique is effective in reducing the concentration of suspended particles and, to some extent, the COD levels in wastewater. However, it's important to note that the coagulant used in this method may occasionally lead to secondary pollution in water bodies. The choice and dosage of coagulants are influenced by the quality of the water being treated, and the process itself can be time-consuming and labor-intensive. In practical applications, the coagulation method is commonly combined with other treatment methods to effectively address antibiotic wastewater.

2.3.2 Adsorption method

The adsorption method encompasses physical adsorption and chemical adsorption. Physical adsorption occurs when a target substance is adsorbed onto an adsorbent surface through weak van der Waals forces. In contrast, chemical adsorption involves the adsorbent and target substance forming chemical bonds and undergoing electron transfer. Activated carbon is a commonly employed adsorbent for physical adsorption.

Manjunath et al [49] investigated the use of KOH-activated Krapevine activated carbon (KPAC) as an adsorbent for the removal of sulfadiazine, metronidazole, and tetracycline from single, binary, and ternary adsorption systems. The experimental findings demonstrated that the maximum adsorption capacities of sulfadiazine, metronidazole, and tetracycline in the single-component adsorption system were 18.48 g/L, 25.06 g/L, and 28.81 g/L, respectively. The total adsorption capacities in the single-component system were higher compared to the multi-component system. The maximum desorption rates for sulfadiazine, metronidazole, and tetracycline were 11.7%, 22.5%, and 13.9%, respectively. Apart from activated carbon, various novel adsorbents have been developed in recent years.

Xiao et al [50] developed a modified zeolite adsorption technique for the removal of trace antibiotics from livestock wastewater. Tetracycline present in the livestock wastewater was adsorbed using zeolites that were modified with nitric acid, hydrochloric acid, and sulfuric acid. The modified zeolites exhibited significant adsorption capacities, with removal rates of tetracycline reaching 61.1%, 90.7%, and 88.8% for nitric acid, hydrochloric acid, and sulfuric acid modifications, respectively.

In the study conducted by Yixin Zhang [51], four porous carbon adsorption materials were synthesized using different templates and carbon sources. Waste plastic polystyrene (PS), waste plastic polyethylene (PE), carbon nanotubes (CNT), and m-aminophenol resin were used as templates, while resorcinol/formaldehyde (RF) resin spheres were used as a carbon source for one of the materials. These adsorption materials exhibited excellent performance in the removal of cefadroxil, with maximum adsorption capacities of 241.2 mg/g, 304 mg/g, 328.3 mg/g, and 385 mg/g, respectively.

The adsorption method offers several advantages, including its simplicity in operation, low cost, high adsorption rate, and absence of toxic byproducts. However, it should be noted that the adsorption method does not provide a complete elimination of antibiotics but rather transfers them to the adsorbent material. Furthermore, the effectiveness of the adsorption process can be influenced by factors such as the specific surface area of the adsorbent, its porosity, and the presence of other competing substances in the wastewater.

2.3.3 Floatation method

The air flotation method is a water treatment technique that involves introducing gas into wastewater to create numerous small bubbles. These bubbles then capture and carry the small impurities present in the wastewater. As the bubbles rise to the surface, they bring the impurities with them, allowing the impurities to accumulate at the liquid surface. The collected impurities can then be removed from the liquid surface, effectively eliminating them from the wastewater.

Li [52] investigated the treatment of mixed fermentation and washing wastewater from the production of cephalosporin C sodium salt using a combined coagulation-air flotation-bio-ozone air flotation process. The wastewater had initial concentrations ranging from 7520 to 8500 mg/L for COD, 2658 to 3174 mg/L for BOD, 1785 to 2115 mg/L for SS, and pH levels between 5 and 7. The experimental results indicated that the coagulation-air flotation process achieved a consistent COD removal rate of 20% to 25%.

The air flotation method is highly effective in removing small impurities from wastewater, but it may not be as efficient in removing larger impurities. Additionally, the implementation of air flotation can be associated with high equipment costs and ongoing maintenance expenses.

2.3.4 Membrane separation technology

Membrane separation technology is a separation technology that emerged in a cross-disciplinary context, based on the difference in permeability of substances across membrane materials to achieve efficient separation. With the restriction of membrane pore size, small-sized substances can permeate to the other side of the membrane under driving forces (e.g., gravity, concentration difference, pressure, or electric potential), while large-sized substances cannot pass through the membrane pores and are intercepted [54-56], the principle of which is shown in Fig. 2-1.

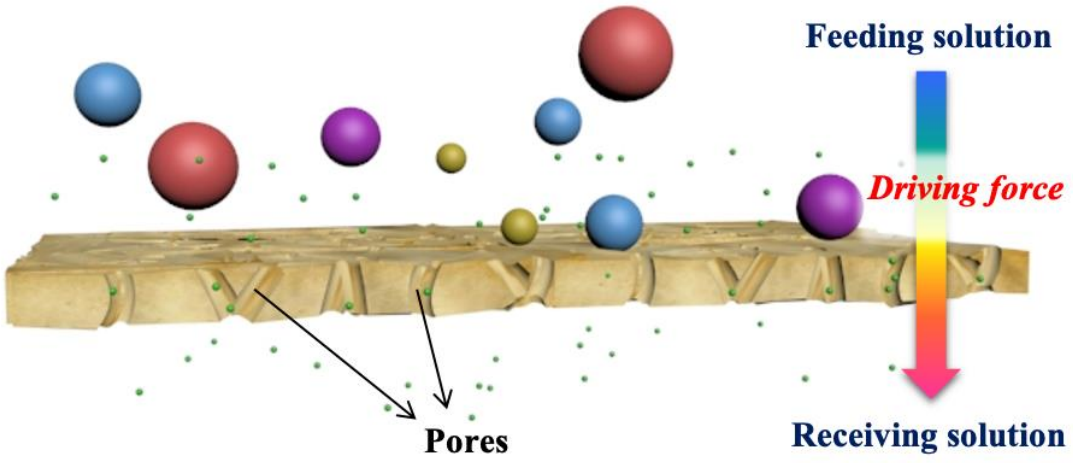

Fig 2-1 The schematic mechanism of MST

Depending on the size of the retained components, membrane separation processes can be classified as microfiltration, ultrafiltration, nanofiltration and reverse osmosis, etc., and their characteristics and common applications are shown in Table 2-1. MST is considered as one of the most promising separation technologies for traditional industrial production due to the advantages of low energy use, simple operation, and no secondary contamination. In the past decades, MST has shown great superiority in numerous processes such as water treatment, solid-phase extraction, petroleum refining, pharmaceutical purification, and gas separation in a wide range of chemical, biological, and environmental fields [57-59].

Regardless of the technology used, separation always requires some form of energy as a driving force. Traditional separation methods, such as distillation, create a driving force by

applying heat to harness the vapor pressure between two compounds. For membrane separation, the driving force can be one of the forms of energy such as pressure, concentration, electricity, etc.

Table 2-1 Types and characteristics of membrane separation

Membrane Separation Type	Membrane Material Pore Size	Permeable Components	Applications
Microfiltration (MF)	0.01-10 μm	Solvents, dissolved substances, etc.	Liquid clarification, sterilization, etc.
Ultrafiltration (UF)	1-100 nm	Solvents, small molecule components, ions, etc.	Enrichment or removal of macromolecular components, preliminary sieving of substances with different molecular weights, etc.
Nanofiltration (NF)	0.5-5 nm	Solvents, low-valent salt ions, etc.	Concentration and separation of small molecules, desalination, pure water preparation, etc.
Reverse Osmosis （RO）	0.1-1 nm	Solvents, etc.	Small molecule concentration, pure water preparation, etc.

The common driving force for membrane separation is pressure. When separating gases, a higher partial pressure is generally created on the feed side for the gas than on the permeate side, creating a pressure gradient that drives the gas through the membrane. The membrane preferentially allows one or more gases to pass through, thereby concentrating that gas on the permeate side. Pressure is the primary driving force in reverse osmosis, ultrafiltration, and microfiltration.

The concentration difference is also one of the driving forces of membrane separation technology. Some membranes operate in an environment where there is no significant pressure gradient, such as those used for renal dialysis. During dialysis, the concentration of impurities in the blood is higher than in the buffer, and a driving force is created by the concentration difference. This driving force plays only a small role in microfiltration applications.

Electricity in the form of voltage gradients can be used for membrane based electrodialysis. The separation process can be achieved by inducing charged molecules to pass through the membrane. Novel separation techniques combine pressure or concentration with charge/electricity-driven process conditions. By using ultrafiltration or microfiltration membranes with a limited pressure difference in an electric field, molecules and larger particles can be separated not only by their size but also by their electrical charge.

Membrane separation technologies can be divided into seven categories, namely microfiltration, ultrafiltration, reverse osmosis, nanofiltration, dialysis, gas membrane separation, and osmotic evaporation.

① Microfiltration

Microfiltration, also known as microporous filtration, is a modern precision filtration technology that can reach a filtration precision of 0.1 μm and can effectively filter out tiny particles and bacteria in solutions with particle sizes in the range of 0.1 to 50.0 μm.

In specific applications, its action with the help of the static pressure difference allows molecules and solvents smaller than the membrane pores to pass through and enter the low-pressure side of the membrane, while particles larger than the membrane pores such as sediment, algae, and bacteria in the solution are retained, and the general operating pressure is set in the range of 0.01 to 0.20 MPa.

At present, microfiltration technology is used in many fields. After microfiltration, water can be used in the pharmaceutical, food and beverage industries, as a pretreatment for ultrafiltration and reverse osmosis in the preparation of ultrafiltration water, and scientific research institutions and environmental protection departments can also use microfiltration technology

to test the water and air environment.

② Ultrafiltration

Ultra-filtration (UF) is a type of membrane separation technology that allows solutions to flow through porous membranes under pressure, allowing solvents and small molecules to pass smoothly, while large molecules are retained to separate different substances. Under pressure, the filtered solution passes through the surface of the membrane at a certain flow rate, so that solvents and small molecules can reach the lower pressure side of the membrane, while large molecules and particles larger than the membrane pores cannot pass through. The use of ultrafiltration technology can effectively remove most of the colloidal substances and many organic substances contained in the water. Therefore, ultrafiltration membranes can achieve deep treatment of drinking water, and ultrafiltration membranes in ultrafiltration water purifiers used in households are generally made of hollow fiber materials.

At present, ultrafiltration technology is also widely used in many fields, such as industrial ultrapure water and solution concentration and separation, with the characteristics of easy operation, low energy consumption and short production cycle. The use of ultrafiltration technology not only can effectively reduce the production cost of enterprises, but also does not require the addition of chemical reagents, and does not need to change the original temperature of the solution. Therefore, the pH and temperature of the solution will not change, and the biological macromolecules in the solution will not be denatured, inactivated and autolyzed. In the preparation of biomolecules, the main function is desalination, dehydration and concentration. However, ultrafiltration technology also has certain limitations, as its production process determines that it cannot be used for the preparation of dry powder preparations, in the concentration of protein concentrated solutions was only up to 50% in the test.

③ Reverse osmosis

Reverse-osmosis (RO), also known as reverse osmosis, is the separation of substances in solution by means of pressure. Currently, in RO process, there are two main types of semi-permeable membranes in common use: asymmetric membrane and composite membrane, and

the production equipment uses hollow fiber or rolled membrane separation equipment to separate one or more substances in a mixed solution under pressure by using the selectivity of the semi-permeable membrane. Reverse osmosis technology is also used to separate substances in mixed solutions by pressure, and the general operating pressure range is set at 1.5 to 10.5 MPa. reverse osmosis technology can retain various inorganic ions, colloidal substances, and small molecules in solutions, which can be used in water treatment to obtain purer water. In addition, the use of reverse osmosis technology can remove suspended, dissolved, and colloidal substances from mixed solutions, and achieve the purpose of separation and purification through the filtration effect of semi-permeable membranes.

In the process of application, the same volume of dilute solution and concentrated solution are placed on both sides of the semipermeable membrane. Under normal circumstances, the solvent in the dilute solution will flow to the concentrated solution side by itself, so the liquid level on the concentrated solution side will be partly higher, and eventually a pressure difference, i.e., osmotic pressure, will be generated between the two sides. The osmotic pressure is different in different concentrations, different temperatures, and different kinds of solutions. At this time, if the pressure value of the concentrated solution side is raised, when the pressure value exceeds the osmotic pressure, the solvent in the concentrated solution side will reverse to the dilute solution side, and since the direction of osmosis is opposite to that of osmosis in the natural state, it is called reverse osmosis.

At present, reverse osmosis membranes have been gradually promoted and applied in China, in many pure water preparation scenarios and domestic water treatment. Ultra pressure reverse osmosis technology can complete the desalination of concentrated salt solutions within 1 MPa pressure, which is effective in seawater and brackish water desalination, industrial wastewater treatment, heavy metal wastewater treatment, and can also be used for the concentration of fruit juice, sugar, coffee and milk products in the food and beverage industry.

④ Nanofiltration Technology

Nanofiltration (NF), also under the action of pressure difference, is the separation of substances in solution. Compared with other membrane separation technologies that use

pressure difference as the force, nanofiltration technology emerged later and is a new membrane filtration technology that emerged in the process of developing reverse osmosis technology to meet the needs of industrial water softening and reducing enterprise costs, and the filtration precision is also between ultrafiltration and reverse osmosis technology. Nanofiltration technology has two distinctive features: firstly, it can separate organic matter with small molecular mass in solution; secondly, the charged membrane is prone to the Dornan effect during the desalination process. Nanofiltration membranes are mostly charged membranes, and the ion valence and concentration will have a greater impact on the separation effect of nanofiltration membranes.

Nanofiltration and permeate membranes are both nonporous membranes, and many scholars believe that the mass transfer mechanism in their separation process is accomplished by dissolution-diffusion. However, since nanofiltration membranes are mostly charged membranes, when used for inorganic salt separation, in addition to the control of chemical potential gradient, the electric potential gradient is also the main influencing factor, thus it can be determined that the separation effect of nanofiltration membranes is related to the charging performance and the charging state of the solute.

At this stage, nanofiltration technology is commonly used in the purification of drinking water and industrial water, the treatment of industrial wastewater and the concentration of substances in the industrial field, etc. The operating pressure range is controlled from 0.5 to 2.0 MPa, and small molecules with molecular weights of 200 to 1000 can be effectively retained. Compared with reverse osmosis technology, it requires lower differential pressure and is often called “low-pressure reverse osmosis” in the industry. In practice, nanofiltration membranes are less effective in retaining monovalent ions such as Na+ and Cl-, but are more effective in retaining divalent ions such as Ca2+, Mg2+, SO42-, and other small molecular weight substances such as pesticides, pigments, dyes, antibiotics, peptides, and amino acids. In addition, nanofiltration technology is significantly better than reverse osmosis technology in terms of the retention efficiency of low concentration of divalent ions and small molecular weight substances, and can effectively reduce production costs.

⑤ Dialysis

Dialysis, also known as dialysis, is a new technology for membrane separation by means of concentration differences. In dialysis, a semi-permeable membrane is applied with selective permeability to solutes, so that small molecules and ions can pass through the semi-permeable membrane smoothly, while colloidal particles in the solution are retained, thus quickly removing useless impurities from the solution. When using membrane dialysis technology, the solution needs to be placed in a dialysis with a built-in semi-permeable membrane, and the outside of the dialyzer is a dispersion medium (usually water), which is used to disperse the colloidal solution, and the time to change the dispersion medium can be determined according to the dialysis situation. The time to change the dispersion medium is determined by the dialysis condition.

The purification of colloidal substances can be achieved using specialized dialyzers. To improve the diffusion effect, a DC electric field can also be applied externally. Under the action of the electric field, the charged particles in the solution will accelerate their migration, and this dialysis technique after the application of DC electric field is also called electrodialysis.

The driving force in the dialysis process comes from the depth gradient in the solution, where the solvent and small molecules pass through the semi-permeable membrane to the other side. The membrane dialysis effect is influenced by several factors such as flux, membrane area and thickness, concentration gradient and diffusion coefficient, while the temperature and viscosity of the solution and the pore size of the semi-permeable membrane are the keys to determine the diffusion coefficient, and the size of the semi-permeable membrane pore size is also an important indicator of the flux.

At this stage, the application of electrodialysis technology has been relatively mature, mainly used in the desalination process of seawater and brackish water, and is an important method for producing fresh water in many freshwater-scarce regions around the world.

With the rapid development of membrane technology, newly developed charge membranes have become more selective, thermally stable, and mechanically strong, and have lower

membrane resistance, making them useful in food, medical, chemical, and industrial wastewater treatment, in addition to desalination processes. In practice, one electrodialysis machine consists of hundreds of pairs of anion and cation exchange membranes, which improves the efficiency and effectiveness of dialysis, but also increases the cost of use.

⑥ Gas membrane separation

Gas membrane separation is also based on the effect of pressure difference and the selectivity of separation membranes. The permeation rates of different gases in a gas mixture differ greatly in the separation membrane, thus enabling the separation of different components of the gas mixture. In recent years, gas membrane separation technology has developed rapidly, and asymmetric membranes and polymer composite membranes are commonly used in industry, which have higher permeating flux and higher mechanical strength.

The separation of a certain gas from a gas mixture can be done quickly by using the gap between the selectivity of polymer membranes for different kinds of gas molecules and their permeability.

In the process of applying gas membrane separation technology, a highly concentrated gas mixture containing multiple gas components enters the membrane separation module after pretreatment. Due to the different speed of permeation through the membrane, the faster permeating gases quickly reach the other side of the membrane, while the slower permeating gases are retained, thus achieving the purpose of gas separation.

Polymer membranes are highly selective, with different gas permeation rates, so the polymer membrane can be selected for the specific gas to be separated. For example, gas membrane separation technology can be used to separate oxygen from air, and it can also be used to recover hydrogen from ammonia tail gas, etc. The requirements for polymer membranes vary in different application scenarios.

At present, gas membrane separation technology is widely used in industrial fields, such as ammonia synthesis, natural gas purification and dehumidification, nitrogen preparation, oxygen enrichment, waste gas pollutant treatment, etc. It has the advantages of low investment, low

energy consumption and simple operation, creating good economic and social benefits.

⑦ Osmotic evaporation

Permeate evaporation (PV), also known as permeate gasification, is a type of membrane separation technology, mainly used for the separation of liquid-phase and gas-phase mixtures. Compared with microfiltration, ultrafiltration, nanofiltration, reverse osmosis and other technologies, pervaporation technology is very different.

The first point is that a phase change occurs during the membrane separation process, with the membrane as the boundary presenting a liquid state on the feed side and a gaseous state after the material reaches the permeate side through permeation.

Secondly, the separation is not based on molecular weight, but on selective adsorption of the membrane. The permeate membrane has a two-layer structure, the first layer is a porous and stable support layer, and the second layer is a polymer with a strong permeation selectivity, preferentially selecting the close material to pass through and evaporate off the adsorption after reaching the permeate side of the membrane.

Thirdly, the process of evaporation by permeation is accomplished with the help of the partial pressure of the vapor on the feed side and the partial pressure difference on the permeate side, where the pressure on the feed side is kept normal, while the pressure on the permeate side can be generated by using high vacuum, inert gas purging, and condensation.

At present, permeation evaporation technology is widely used in petrochemical, pharmaceutical, food and environmental protection. For example, it has great advantages in the treatment of VOCs. It is an economic, efficient, and environmentally friendly green separation technology, which is in line with the sustainable development strategy advocated by the current society.

In their study, Li et al. [60] employed a polyvinylidene fluoride ultrafiltration membrane and developed a novel approach combining ultrafiltration with extraction to directly crystallize benzylpenicillin sodium from the fermentation broth. The process was conducted at a temperature of 14°C and a pressure of 0.1 MPa. The results demonstrated that the obtained

penicillin met the standards outlined in the pharmacopeia, and the yield was found to be 6.76% higher compared to the conventional indirect method.

Li et al. [61] investigated the extraction of penicillin utilizing a mesoporous fiber ultrafiltration membrane under an operating pressure ranging from 0.1 to 0.15 MPa. The results indicated that the ultrafiltration membrane exhibited effective removal of proteins from the penicillin fermentation broth, completely replacing the need for an emulsion breaker such as PPB. Moreover, it successfully eliminated impurities from the raw material solution and resulted in significant decolorization, leading to a reduction in the color grade of the final product. Overall, this membrane-based approach enhanced the quality of penicillin.

Shi et al. [62] suggested that ultrafiltration can effectively address the emulsification issue encountered in penicillin extraction, providing a viable alternative to rotary vacuum filtration. By utilizing an ultrafiltration membrane, all soluble proteins can be retained while maintaining the same product yield as the original process. This method offers the advantage of reduced solvent loss and cost, as there is no need for the addition of an emulsion breaker. Ultrafiltration proves to be an efficient and cost-effective solution for penicillin extraction.

Ding Jiaqi et al. [63] conducted forward osmosis experiments using bionic forward osmosis membranes with aqueous channel proteins. They used NaCl solution and seawater as the draw solutions, and three antibiotic wastewaters containing methomyl (TMP), tetracycline (TC), and sulfamethoxazole (SMZ) as the feed solutions. The results demonstrated that the permeate membranes retained approximately 100%, 99%, and 90% of these antibiotics, respectively.

Fan [64] employed nanofiltration membrane technology to treat spiramycin wastewater. The experimental water used was spiramycin preparation water sourced from Daqing River. NF90 nanofiltration membrane was utilized, and under the operating conditions of 0.6 MPa, 30°C, and a flow rate of 3 L/min, the desalination rate remained stable at approximately 82%. Moreover, after 6 hours of operation, the retention rate of spiramycin achieved an impressive 98.9%.

Membrane separation technology has several advantages in the treatment of antibiotic wastewater as the follows:

Efficient separation: Membrane separation technology effectively removes antibiotics from water. By selecting suitable membrane pore sizes and materials, it achieves efficient separation and reduction of antibiotic concentrations.

High selectivity: Membrane separation technology selectively separates antibiotics based on their molecular size, charge, solubility, and other properties. This means that target antibiotics can be removed while preserving other useful substances.

Low energy consumption: Compared to traditional physicochemical treatment methods, membrane separation technology generally achieves efficient antibiotic removal with lower energy consumption. The pressure or electric field driving forces involved in the membrane separation process are relatively low.

Sustainability: Membrane separation technology enables continuous operation and automated control, with longer lifespan and minimal maintenance requirements. Additionally, concentrated antibiotic waste generated during membrane separation can be further treated or recycled, enhancing resource utilization.

Flexibility: Membrane separation technology can be adjusted and optimized according to specific needs. Different types of membranes (such as microfiltration, ultrafiltration, and nanofiltration membranes) and membrane combinations can be utilized to meet the requirements of different antibiotic wastewater treatment scenarios.

Therefore, this study chose to utilize membrane separation technology to remove antibiotics from medical wastewater.

Reference

[1] LI B, ZHANG T. Biodegradation and absorption of antibiotics in the activated sludge process ［J］. Environmental Science & Technology, 2010, 44(9):3468-3473.

[2] Song, X. C. (2014). Adsorption behavior and mechanism of tetracycline antibiotics on activated sludge. (Doctoral dissertation). Tianjin: Nankai University. (pp. 103-106).

[3] He, D. C., Xu, Z. C., Wu, G. Y., et al. (2011). Research progress on environmental behavior

of tetracycline antibiotics. Animal Medical Advances, 32(4), 98-102.

[4] Xu, X. L., Li, W. F., Lei, J., et al. (2011). Screening, identification, and degradation characteristics of tetracycline-degrading bacteria. Journal of Agricultural Biotechnology, 19(3), 549-556.

[5] Wang, L. Q., Sun, W., Zhang, G. D., et al. (2008). Isolation and screening of typical antibiotic wastewater purification strains and their effectiveness study. Journal of China Agricultural University, 13(4), 97-101.

[6] Feng, F. X., Xu, X. P., Cheng, Q. X., et al. (2013). Degradation characteristics of tetracycline by the efficient degrading yeast Trichosporon mycotoxinivorans XPY-10. Journal of Environmental Engineering, 7(12), 4779-4785.

[7] Wen, X., Jia, Y., Li, J. (2009). Degradation of tetracycline and oxytetracycline by crude lignin peroxidase prepared from Phanerochaete chrysosporium - A white rot fungus. Chemosphere, 75(8), 1003-1007.

[8] Prieto, A., Moder, M., Rodil, R., et al. (2011). Degradation of the antibiotics norfloxacin and ciprofloxacin by a white-rot fungus and identification of degradation products. Bioresource Technology, 102(23), 10987-10995.

[9] Shen, Y., Wei, Y. S., Zheng, J. X., et al. (2009). Biodegradation of tetracycline residues in pig manure. Journal of Process Engineering, 9(5), 962-968.

[10] Shen, D. S., He, H. Z., Wang, M. Z., et al. (2013). Role of streptomycin-degrading bacterium TJ-1 in the harmless treatment of pig manure. Acta Scientiae Circumstantiae, 33(1), 147-153.

[11] Zhang, S. Q., Zhang, F. D., Liu, X. M., et al. (2006). Effects of high-temperature composting on the degradation of antibiotics and immobilization of heavy metals in livestock and poultry manure. Scientia Agricultura Sinica, 39(2), 337-343.

[12] Qin, L., Gao, R. Y., Li, G. X., et al. (2009). Study on the degradation effect of exogenous mixed bacterial system on cellulose and chlortetracycline in compost. Journal of Agro-

Environment Science, 28(4), 820-823.

[13] Li, B., & Zhang, T. (2010). Biodegradation and adsorption of antibiotics in the activated sludge process. Environmental Science & Technology, 44(9), 3468-3473.

[14] Gong, Y. K., Zhang, L. S. (2006). Research progress on the treatment of antibiotic wastewater. Industrial Water Treatment, 25(12), 1-5.

[15] Liu, F., Jiang, Y. L., Xiong, F. F., et al. (2012). Experimental study on UASB treatment of cephalosporin antibiotic pharmaceutical wastewater. Industrial Water and Wastewater, 43(5), 28-31.

[16] Mai, W. N., Zhou, R. M. (2002). Anaerobic hybrid bed treatment technology for antibiotic wastewater. Environmental Pollution Control Technology and Equipment, 3(5), 23-27.

[17] Hu, X. D., Zheng, Q. H., Xu, S. (2009). Experimental study on intermittent aeration method for the treatment of penicillin wastewater. Environmental Science and Management, 34(3), 92-95, 135.

[18] Han, J. H., Sun, J. M., Ren, L. R. (2007). Treatment of antibiotic wastewater by hydrolysis-acidification-membrane bioreactor. Journal of Beijing University of Science and Technology, 29(6), 30-33.

[19] Shang, J. J., Xing, Z. P., Sun, D. Z. (2008). Treatment of antibiotic wastewater by hydrolysis-acidification coupled with aerobic MBBR and Fenton process. Industrial Water Treatment, 28(12), 13-17.

[20] Huang, H. S., Qi, P. S., Liu, Y. Z., et al. (2008). Treatment of high-quality concentrated antibiotic wastewater by a combined aerobic biological method. Journal of Harbin University of Commerce: Natural Sciences Edition, 24(1), 21-25.

[21] Jiang, Y. L., Jiang, D., Song, Y. J., et al. (2012). UASB-coagulation-SBR treatment of high-concentration cephalosporin antibiotic wastewater. Water Treatment Technology, 38(10), 65-69.

[22] Yang, J. S., Li, X. D., Li, Y. J., et al. (2000). Experimental study on hydrolysis-acidification-AB biological method for the treatment of antibiotic wastewater. Journal of

Environmental Sciences, 22(6), 50-53.

[23] Jia, R. Y., Xia, S. Q., Zhang, S. F. (2011). Treatment effectiveness and microbial community structure in two MBR processes for antibiotic-containing wastewater. Water Purification Technology, 30(5), 28-33.

[24] Deng, L. W., Peng, Z. B., et al. (1998). Experimental study on coagulation-anaerobic-aerobic treatment of antibiotic wastewater. Environmental Science, 19(6), 66-69.

[25] Li, Z. X., Zuo, J. E., Ju, P. P., et al. (2013). Deep treatment of antibiotic wastewater secondary effluent using Fenton oxidation. Journal of Environmental Engineering, 7(1), 132-136.

[26] Xia, Y. (2019). Study on the treatment of metronidazole wastewater using electro-Fenton and heterogeneous Fenton processes. (Doctoral dissertation). Wuhan: Wuhan University. (pp. 59-128).

[27] Geng, F. H., Jia, T. T., Zhang, S. W., et al. (2018). Photocatalytic degradation of sulfadiazine by TiO2 under UV light. Water Treatment Technology, 37(1), 89-96.

[28] Liu, H., Zou, J. Y., Wu, W., et al. (2016). Study on the degradation of antibiotic wastewater using metal ion-doped TiO2 composite membranes. New Chemical Materials, 44(12), 79-81.

[29] Ai, C. L., Zhou, D. D., Zhang, R. R., et al. (2015). Preparation of β-In2S3 and its degradation of tetracycline under solar light. Environmental Science, 36(8), 2911-2917.

[30] Guo, Y. B. (2014). Experimental study on the deep treatment of secondary effluent from cephalosporin synthesis wastewater using electrochemical oxidation. (Doctoral dissertation). Shijiazhuang: Hebei University of Science and Technology. (pp. 53-54).

[31] Wang, H. Q., Li, Y., Si, Y. B., et al. (2018). Electrochemical oxidation degradation of sulfonamide antibiotics in water. Journal of Environmental Engineering, 12(3), 779-787.

[32] Wu, N., Tan, Y. C., Qian, H., et al. (2018). Removal of sulfonamides in water using an electro/peroxydisulfate system catalyzed with activated carbon. Polish Journal of Environmental Studies, 28(3), 1957-1965.

[33] Salazar, C., Contreras, N., Mansilla, H. D., et al. (2016). Electrochemical degradation of the antihypertensive losartan in aqueous medium by electro-oxidation with boron-doped diamond electrode. Journal of Hazardous Materials, 319, 84-92.

[34] Li, Y. (2011). Study on wet oxidation degradation methods for antibiotic wastewater. (Master's thesis). Shanghai: East China University of Science and Technology. (pp. 32-41).

[35] Wang, G. W. (2012). Study on catalytic wet oxidation-aerobic granular sludge treatment of high-concentration pharmaceutical wastewater. (Doctoral dissertation). Dalian: Dalian University of Technology. (pp. 31-52).

[36] Chen, C., Zhao, J. D., Cheng, T., et al. (2018). Preparation of nano-manganese cerium/γ-Al2O3 composite catalyst and its catalytic wet oxidation treatment of antibiotic production wastewater. Journal of Synthetic Crystals, 47(11), 2288-2294.

[37] Gu, J. J. (2006). Study on the treatment of antibiotic pharmaceutical wastewater using chemical oxidation and membrane separation technologies. (Master's thesis). Tianjin: Tianjin University. (pp. 35-38).

[38] Zhang, T. Q., He, G. L., Dong, F. L., et al. (2019). Chlorination of enoxacin (ENO) in the drinking water distribution system: Degradation, byproducts, and toxicity. The Science of the Total Environment, 676, 31-39.

[39] Xu, W. J., Zhang, G. C., Zheng, M. X., et al. (2010). Treatment of antibiotic wastewater using ozone oxidation technology. Chemical Progress, 22(5), 1002-1009.

[40] Huang, J., Tang, J., Lin, C. Y., et al. (2019). Research progress on the application of ozone oxidation technology for the deep treatment of antibiotic wastewater. Applied Chemical Industry, 48(8), 1974-1979.

[41] Li, C., Yang, C. J., Wei, H. M., et al. (2017). Treatment of antibiotic wastewater by catalytic ozone oxidation process for biological effluent. Chemical Engineering and Environmental Protection, 37(1), 79-82.

[42] Gao, Z. X., Yao, L. X., Yang, W. L., et al. (2017). Preparation of catalysts for ozone

catalytic oxidation treatment of antibiotic wastewater. Industrial Water Treatment, 37(3), 52-55.

[43] Tong, B., Wang, B. W., Chi, C. M., et al. (2017). Influence of additives on plasma degradation of methylene blue. Chemical Progress, 36(2), 705-711.

[44] Kim, K., Kam, S. K., Mok, Y. S. (2015). Elucidation of the degradation pathways of sulfonamide antibiotics in a dielectric barrier discharge plasma system. Chemical Engineering Journal, 271, 31-42.

[45] He, D., Sun, Y. B., Xin, L., et al. (2014). Aqueous tetracycline degradation by non-thermal plasma combined with nano-TiO2. Chemical Engineering Journal, 258, 18-25.

[46] Xing, Z. P. (2008). Study on the treatment of antibiotic fermentation wastewater by coagulation-hydrolysis/aerobic MBBR-Fenton process. (Master's thesis). Harbin: Harbin Institute of Technology. (pp. 35-52).

[47] Qu, G., Wang, Z., Fan, Z. F., et al. (2008). Deep treatment of antibiotic pharmaceutical wastewater by coagulation-sand filtration-microfiltration-reverse osmosis integrated technology. Membrane Science and Technology, 28(3), 72-78.

[48] Wang, Y. H., Wei, Q. S., Ji, Y. Z., et al. (2017). Preparation of polyaluminum magnesium zinc coagulant and preliminary exploration of its performance and mechanism in antibiotic removal. Journal of Safety and Environment, 17(3), 1057-1063.

[49] Manjunath, S. V., Singh Baghel, R., Kumar, M. (2020). Antagonistic and synergistic analysis of antibiotic adsorption on Prosopis juliflora activated carbon in multicomponent systems. Chemical Engineering Journal, 381, 122713.

[50] Xiao, H., Yu, M., Xu, Y. X., et al. (2012). Method for removing trace antibiotics from livestock and poultry wastewater using modified zeolite: Patent No. 102583893A [Patent]. July 18, 2012.

[51] Zhang, Y. X. (2019). Preparation of porous carbon materials and their adsorption of antibiotics in wastewater. (Master's thesis). Shijiazhuang: Hebei University of Science and Technology. (pp. 11-49).

[52] Li, Y. (2011). Treatment of antibiotic production wastewater by coagulation-air flotation-bio-ozone flotation. Journal of North China Institute of Water Conservancy and Hydroelectric Power, 32(6), 148-150.

[53] Thanigaivelan Arumugham, Reshika Gnanamoorthi Amimodu, Noel Jacob Kaleekkal, Dipak Rana, Nano CuO/g-C3N4 sheets-based ultrafiltration membrane with enhanced interfacial affinity, antifouling and protein separation performances for water treatment application, Journal of Environmental Sciences 82 (2019) 57-69.

[54] Abdul Hai, Ali Ahmed Durrani, Munirasu Selvaraj, Fawzi Banat, Mohammad Abu Haija, Oil-water emulsion separation using intrinsically superoleophilic and superhydrophobic PVDF membrane, Separation and Purification Technology 212 (2019) 388-395.

[55] Nasibeh Hajilary, Mashallah Rezakazemi, Saeed Shirazian, Biofuel types and membrane separation, Environmental Chemistry Letters 17(1) (2019) 1-18.

[56] Azqa Khalid, Muhammad Aslam, Muhammad Abdul Qyyum, Abrar Faisal, Asim Laeeq Khan, Faisal Ahmed, Moonyong Lee, Jeonghwan Kim, Nulee Jang, In Seop Chang, Aqeel Ahmed Bazmi, Muhammad Yasin, Membrane separation processes for dehydration of bioethanol from fermentation broths: Recent developments, challenges, and prospects, Renewable and Sustainable Energy Reviews 105 (2019) 427-443.

[57] Ryan P. Lively, David S. Sholl, From water to organics in membrane separations, Nature Materials 16(3) (2017) 276-279.

[58] Shobha Muthukumaran, Sandra E. Kentish, Geoff W. Stevens, Muthupandian Ashokkumar, APPLICATION OF ULTRASOUND IN MEMBRANE SEPARATION PROCESSES: A REVIEW, 22(3) (2006) 155-194.

[59] Maryam Takht Ravanchi, Tahereh Kaghazchi, Ali Kargari, Application of membrane separation processes in petrochemical industry: a review, Desalination 235(1) (2009) 199-244.

[60] Li, S. Z., Hu, Y. P., Wang, D. Z. (2000). A new method for direct crystallization of sodium benzylpenicillin. Chinese Journal of Antibiotics, 25(3), 175-177.

[61] Li, X. Y., Luan, B. L., Han, G. A. (1996). Application of ultrafiltration in antibiotic extraction. Water Treatment Technology, 22(4), 213-216.

[62] Shi, R. M., Xu, Q. M. (1997). Ultrafiltration and solvent extraction of antibiotic fermentation broth. Foreign Medicine (Special Issue of Antibiotics Journal), 18(1), 33-39.

[63] Ding, J. Q., Cai, T., Huang, M. H. (2018). Retention characteristics of different antibiotics in reclaimed water by reverse osmosis membrane. Membrane Science and Technology, 38(6), 97-103.

[64] Fan, W. H. (2012). Study on nanofiltration for the treatment of antibiotics in water. (Master's thesis). Beijing: Beijing University of Chemical Technology. (p. 43).

Chapter 3

METHODOLOGY

3.1 Membrane design

3.1.1 Membrane fluxes and sacrificial template method

Low membrane fluxes are often a prominent challenge when it comes to bottlenecks in conventional membrane treatment technologies. Membrane flux limitations have a number of negative impacts on the fields of water treatment, separation and filtration. First, low membrane flux limits the capacity of the treatment system, resulting in a reduction in the efficiency of the process. In addition, low membrane fluxes also mean that longer treatment times are required to achieve the required water yield, thereby reducing the process yield. This is particularly important for application scenarios that require large volumes of treated water, especially in the treatment of medical building's wastewater.

In order to achieve greater flux, the construction of membrane materials with three-dimensional macropore structures is an important strategy. Among them, the sacrificial template method is widely used in the preparation of membrane materials. This method utilizes a soluble template substance that acts as a temporary support structure during the formation of membrane materials, and subsequently leaves a hollow pore structure by selectively removing or destroying the template substance.

The sacrificial template method can be used to enhance the flux of the membrane. The advantage of the sacrificial template method is its ability to introduce a highly ordered three-dimensional pore structure in the membrane material, which provides a larger flux and higher permeation performance. This structure increases the effective surface area of the membrane, providing more channels and spaces for water or solute molecules to pass through. Membrane materials with three-dimensional macroporous structures have higher permeation rates and lower resistance to permeation than conventional planar or microporous membranes, resulting in higher fluxes[1].

In the sacrificial template method, the selection of a suitable template substance is crucial. The template substance should have good solubility and controlled degradability to ensure that the desired pore structure can be formed during the preparation of the membrane material.

Commonly used template substances include organic small molecules, polymers or nanoparticles. Depending on the need, these template substances can be removed by dissolution, pyrolysis, hydrolysis, etc., leaving hollow pore channels.

While increasing membrane flux can improve bottlenecks in traditional membrane treatment technologies, it can also lead to a new problem, namely, a decrease in membrane treatment effectiveness. This problem requires us to find a balance between increasing flux and ensuring that the treatment still meets the requirements.

3.1.2 Synthetic polymers on membrane surfaces

As the membrane flux increases, the retained material on the membrane surface may not have enough time to fully contact and interact with the membrane, resulting in a portion of the target material escaping without being removed. This may lead to a decrease in retention rate during water treatment and the effectiveness of the treated water quality is affected.

However, I can counter this problem with an approach that constructs effective adsorption sites on the three-dimensional macroporous structure of the membrane to block antibiotic molecules and improve their removal efficiency.

To achieve this goal, I have adopted a strategy of synthesizing polymers on the membrane surface. By introducing a specific polymer structure on the membrane surface, I was able to form a series of highly selective adsorption sites. These sites are precisely positioned inside the pore channels of the membrane and at the pore entrances, allowing for specific interactions with antibiotic molecules. This interaction enhances the adsorption of antibiotics on the membrane surface and effectively blocks their transport through the channels, thus improving the removal efficiency [2].

Notably, the construction of adsorption sites by synthesizing polymers on the membrane surface not only improves the antibiotic treatment efficiency, but also maintains a relatively high membrane flux. This is because this approach does not significantly affect the overall flux characteristics of the membrane, while achieving more efficient antibiotic removal by increasing the number and selectivity of adsorption sites.

Thus the method of constructing effective adsorption sites based on synthetic polymers on the surface of membranes with three-dimensional macroporous structure provides an innovative solution to the problem of decreasing the treatment efficiency of antibiotic molecules due to the increase of membrane flux. By this method, I can improve both membrane flux and antibiotic removal efficiency, opening new possibilities for the effective removal of harmful substances such as antibiotics from water bodies.

3.1.3 Components of the polymerization reaction

The process of synthesizing polymers on membrane surfaces for the adsorption of antibiotic molecules requires the consideration of multiple key components, each of which plays an important role in achieving efficient adsorption.

① First, the selection of functional monomers is crucial. Functional monomers should have properties that interact with the target antibiotic molecule, such as specific chemical structures, affinity groups or functional groups. These interactions can be achieved through hydrogen bonds, ionic interactions, van der Waals forces, etc., which enhance the adsorption of antibiotics on the membrane surface. The selection of appropriate functional monomers is a key step to achieve highly selective adsorption.

Depending on the structure of the antibiotic molecule, methacrylic acid (MAA), methyl methacrylate (MMA), and acrylic acid (AA) are a common class of choices when selecting functional monomers for polymers with adsorption properties, specifically because they all have acidic functional groups that can form hydrogen bonds or ionic interactions with basic functional groups (e.g., amine groups) in the antibiotic molecule. Such interactions can provide strong adsorption capabilities, making the polymers highly selective and affinity for antibiotic molecules.

② Second, crosslinkers play an important role in the formation of polymers. The role of cross-linking agents is to introduce cross-linked structures, thus increasing the stability and mechanical strength of the polymer. The selection of the appropriate crosslinker requires consideration of its compatibility, reactivity, and crosslinking ability with the functional

monomer. The right crosslinker ensures good crosslinking of the polymer, enhances its structural stability, and provides more reliable support for the adsorption of antibiotic molecules.

In terms of crosslinker selection, Pentaerythritol tetra(3-mercaptopropionate) (PT3M) as a crosslinker crosslinking structure can provide multiple sites for the adsorption of target molecules, such as antibiotic molecules. These sites can interact with the target molecules through selective adsorption, enabling efficient molecular recognition and adsorption. Therefore, the selection of PT3M as a cross-linking agent helps to form effective adsorption sites on the membrane surface and enhances the selective adsorption of antibiotic molecules.

In addition, PT3M is a sulfhydryl functional group cross-linker, while MAA is a monomer containing carboxyl functional group, and they have good chemical reactivity and affinity for each other, and can be cross-linked effectively by the sulfhydrylene click reaction. This match makes PT3M a suitable choice to react with MAA monomers to form stable cross-linked structures.

③ In addition, co-crosslinkers are also one of the important components. The main role of co-crosslinkers is to promote the crosslinking reaction and to regulate the reactivity and rate of crosslinkers. The degree of crosslinking and the structure of the polymer can be influenced by the appropriate choice of co-crosslinkers. This modulation can affect the pore structure, pore size and porosity of the polymer, which in turn can adjust its adsorption properties. Therefore, the proper use of co-crosslinkers in the polymer synthesis process is a key part in achieving the desired pore structure and optimizing the adsorption properties.

Dipentaerythritol penta-/hexa-acrylate (DPHA), is a polyacrylate compound with multiple acrylic groups. These acrylic groups can react with the carboxyl groups in the MAA monomer to form a cross-linked structure, which increases the stability and mechanical strength of the polymer layer.

DPHA has multiple acrylic groups that enable it to click react with a variety of functional groups. This versatility allows it to react with different monomers and crosslinkers in polymerization reactions to form complex polymer network structures, thereby enhancing the

performance and stability of the polymer layer.

The polyacrylic acid groups of DPHA provide longer side chain lengths, which contribute to the formation of larger pores and spatial structures during the polymerization reaction. This spatial cross-linking effect helps to increase the pore size and flux of the membrane and improve the availability of antibiotic adsorption sites.

Therefore, DPHA was chosen as a co-crosslinker for this study.

3.1.4 Types of reactions for polymerization

Polymerization reactions are chemical processes in which monomer molecules are linked together by covalent bonds to form polymers. The polymerization reaction is one of the central steps in the synthesis of polymers.

① Conventional polymerization process

The conventional polymer synthesis process has a number of shortcomings, including:

Multi-step reactions: Conventional polymer synthesis usually requires multi-step reactions, including the synthesis of prepolymers, the use of activators, and the control of reaction conditions, resulting in a complex and time-consuming synthesis process.

By-product generation: Traditional polymer synthesis often generates by-products that need to be separated and purified, increasing process complexity and waste generation.

Low reaction selectivity: Some traditional polymerization reactions may be reactive to multiple functional groups, resulting in side reactions that reduce product purity and quality.

② Click chemistry

Click chemistry is an efficient and highly selective chemical reaction that has attracted a lot of attention and applications in the last decades. The reactions are based on rapid and controlled reactions between stable reactants, usually under mild conditions, and do not require complex catalysts or high energy input. The characteristics of click chemistry reactions make it an important tool in the fields of synthetic chemistry, medicinal chemistry, materials science and

biotechnology.

The success of click chemistry reactions lies in the low strain energy and high stability of the reactants, which drives the reactions. This stability allows click chemistry reactions to be carried out in living organisms, leading to a wide range of applications in biochemistry and biomedicine. For example, click chemistry reactions can be used to label and tag biomolecules, construct drug molecules, modify biological materials, and study the interactions of biological systems.

The emerging click chemistry reaction, as an efficient and highly selective synthetic method, can compensate for the shortcomings of traditional polymer synthesis and offers the following advantages:

Fast reaction: Click chemistry reactions are usually highly efficient and fast-running reactions with fast reaction rates and short reaction times, enabling the polymerization process to be completed in a relatively short period of time.

High selectivity: Click chemistry reactions are highly selective among reactants, and usually only the desired click reaction occurs, reducing the occurrence of side reactions and facilitating the purification and separation of products.

No by-product generation: Click chemistry reactions usually do not generate by-products, avoiding the steps of by-product separation and purification in traditional polymerization processes and reducing waste generation.

Mild reaction conditions: Most click chemistry reactions are carried out under mild conditions, eliminating the need for complex reaction conditions and catalysts, reducing the energy consumption and cost of the synthesis process.

Wide range of applications: Click chemistry reactions are applicable to different types of functional groups and chemicals, and can be used to synthesize a wide range of polymer structures and functions, which are widely used in materials science, medicinal chemistry, biotechnology, and other fields.

Thus, click chemistry reactions have higher efficiency, selectivity and environmental

friendliness compared to conventional polymer synthesis, making them ideal polymerization reactions for our present study.

3.1.5 Thiol-ene click reaction

Thiol-ene click reaction is an important click chemistry reaction, also known as thiol-ene cycloaddition reaction or thiol-ene cycloaddition reaction [3]. The reaction has the following advantages:

First, the thiol-ene click reaction is highly selective. This reaction occurs only between reactive functional groups with sulfhydryl groups (-SH) and olefins (e.g., acryloyl), and almost no side reactions occur. Therefore, the thiol-ene click reaction can achieve high purity polymer products, avoiding the formation of by-products and the complexity of purification.

Secondly, the reaction rate of the thiol-ene click reaction is fast and the reaction conditions are mild. This means that the polymerization process can be completed in a relatively short time and without high temperature or high-pressure conditions. This helps to improve the efficiency and productivity of the synthesis, and saves energy and time.

In addition, the thiol-ene click reaction has a high reactant stability. The sulfhydryl group (-SH) and the olefin (e.g., acryloyl) have good stability under common experimental conditions and are less prone to spontaneous reaction or deactivation. This stability facilitates the control and reproducibility of the reaction, resulting in more reliable and consistent polymer synthesis.

In addition, the thiol-ene click reaction can be carried out under mild conditions, such as in biological systems or biomedical applications. This gives it potential in areas such as biomaterials, drug delivery systems, and biosensors. For example, polymer modifiers can be specifically linked to biomolecules (e.g., proteins or peptides) through the thiol-ene click reaction, resulting in functionalized polymers for biomedical research and applications.

Finally, the thiol-ene click reaction is highly tractable and adaptable. The thiol-ene click reaction is applicable to different types of functional groups and compounds, including thiol-ene, thiol ether and thiol ester. This gives it flexibility and versatility in polymer design and functionalization for different applications.

3.1.6 Vinyl Modified Membrane Surface

Considering the respective functional groups and double bonds of MAA, PT3M and DPHA, they are all able to undergo addition polymerization reactions with vinyl. Therefore, the modification of vinyl functional groups on the membrane surface can be considered, which can promote the adhesion and fixation of polymers on the membrane surface and the inner wall of the pores [4].

When it comes to ethylene modification of the membrane surface, a commonly used choice is to utilize KH570 (γ-aminopropyltrimethoxysilane) as a coupling agent. KH570 possesses certain characteristics that make it an ideal option for ethylene modification.

KH570 is a silane coupling agent that contains amino-propyl and methoxy functional groups. This enables KH570 to react with functional groups on the substrate surface, forming strong chemical bonds and facilitating the adhesion of polymers to the substrate surface. This coupling effect enhances the adhesion and stability of the modification layer.

Furthermore, the methoxy functional groups of KH570 play a crucial role in the ethylene modification process. The methoxy groups can react with ambient moisture, forming silanol groups. These silanol groups can undergo copolymerization with the ethylene functional groups, further strengthening the stability and adhesion of the modification layer. Therefore, KH570 initiates copolymerization during the formation of the modification layer, contributing to the formation of robust chemical bonds.

Another important advantage is the coexistence of hydrophobic and hydrophilic functional groups in KH570, allowing it to form a well-wetting modification layer on the membrane surface. This modification layer improves the hydrophilicity of the membrane, enhancing the adsorption efficiency of antibiotics from water.

Additionally, KH570 exhibits antimicrobial properties, inhibiting the attachment and growth of bacteria and microorganisms on the membrane surface. This helps to reduce membrane fouling and contamination. It is crucial for maintaining the flux and stability of the membrane.

In summary, as a coupling agent in the ethylene modification process, KH570 offers a stable

and highly functional modification layer through its chemical bonding, copolymerization, surface wetting properties, and antimicrobial characteristics. Choosing KH570 enhances the performance and application effects of the membrane, ensuring a strong bond between the modification layer and the membrane surface, and improving the stability and durability of the modification layer.

3.1.7 Increase membrane thickness

Increasing the thickness of the membrane helps increase the opportunity for antibiotic molecules to meet the polymer within the membrane, with the following benefits:

Increased adsorption capacity: thicker membranes provide more surface area and adsorption volume to accommodate more antibiotic molecules. This increases the loading of the adsorbent, increasing the capacity to adsorb antibiotics, improving adsorption efficiency and capturing higher concentrations of antibiotic molecules.

Extended contact time: thicker membranes provide a longer diffusion path, allowing more time for antibiotic molecules to come into contact with the polymer within the membrane. This extended contact time increases the opportunity for antibiotic-polymer interactions, promoting a more efficient adsorption process and reducing possible breakthrough or incomplete adsorption.

Improved mass transfer: thicker membranes improve the mass transfer of antibiotic molecules within the membrane structure. Due to the slower diffusion rate, the interaction between the antibiotic molecules and the adsorbent is more adequate, achieving a more complete and effective adsorption process.

Improved mechanical stability: Increasing the thickness of the membrane improves the mechanical stability of the membrane, making it more able to withstand pressure and external environmental influences. This helps to increase the durability and stability of the membrane, allowing it to operate over time and continue the adsorption process.

3.2 Material characterization

3.2.1 Scanning Electron Microscope (SEM)

Scanning Electron Microscope (SEM) is a commonly used microscopy technique that employs a high-energy electron beam to scan the surface of a sample and detect the resulting signals to obtain high-resolution surface morphology and compositional information. The working principle of SEM is based on electron optics and signal detection technology.

SEM utilizes a thermionic or field emission electron gun as the electron source. These electron sources generate high-energy electron beams, typically ranging from several kilovolts to tens of kilovolts. The electron beams are accelerated and focused to form a fine beam spot.

Lens System: The lens system in SEM consists of electron lenses and scanning coils. Electron lenses are used to focus the electron beam, ensuring it is as small as possible and focused on the surface of the sample. Scanning coils are employed to control the scanning of the electron beam on the sample surface.

Sample Stage: The sample stage is a platform that supports the sample and provides a stable position. The sample is placed on the sample stage and often requires metal coating to enhance conductivity. The sample stage also has a micromotion device that allows precise stepping movement of the sample under the scanning electron beam.

Signal Detection: SEM obtains images and information by detecting various signals generated from the sample surface. Commonly detected signals include secondary electrons (SE) and backscattered electrons (BSE). Secondary electrons are generated by the excitation of surface atoms and molecules by the electron beam, while backscattered electrons are produced by the interaction of the electron beam with atomic nuclei in the sample. These signals are captured by detectors and converted into electrical signals.

Image Formation: Detectors in SEM convert the collected signals into images. These images can be displayed on a monitor and digitally saved. The brightness and contrast of the images can be adjusted to enhance the details and contrast of the sample.

Scanning: Scanning coils in SEM control the scanning of the electron beam on the sample surface. The position of the electron beam on the sample surface changes with the control of

the scanning coils, forming a pixel array and ultimately composing a complete image. By adjusting scanning parameters such as scanning speed and coil shape, SEM images with different resolutions and sizes can be obtained.

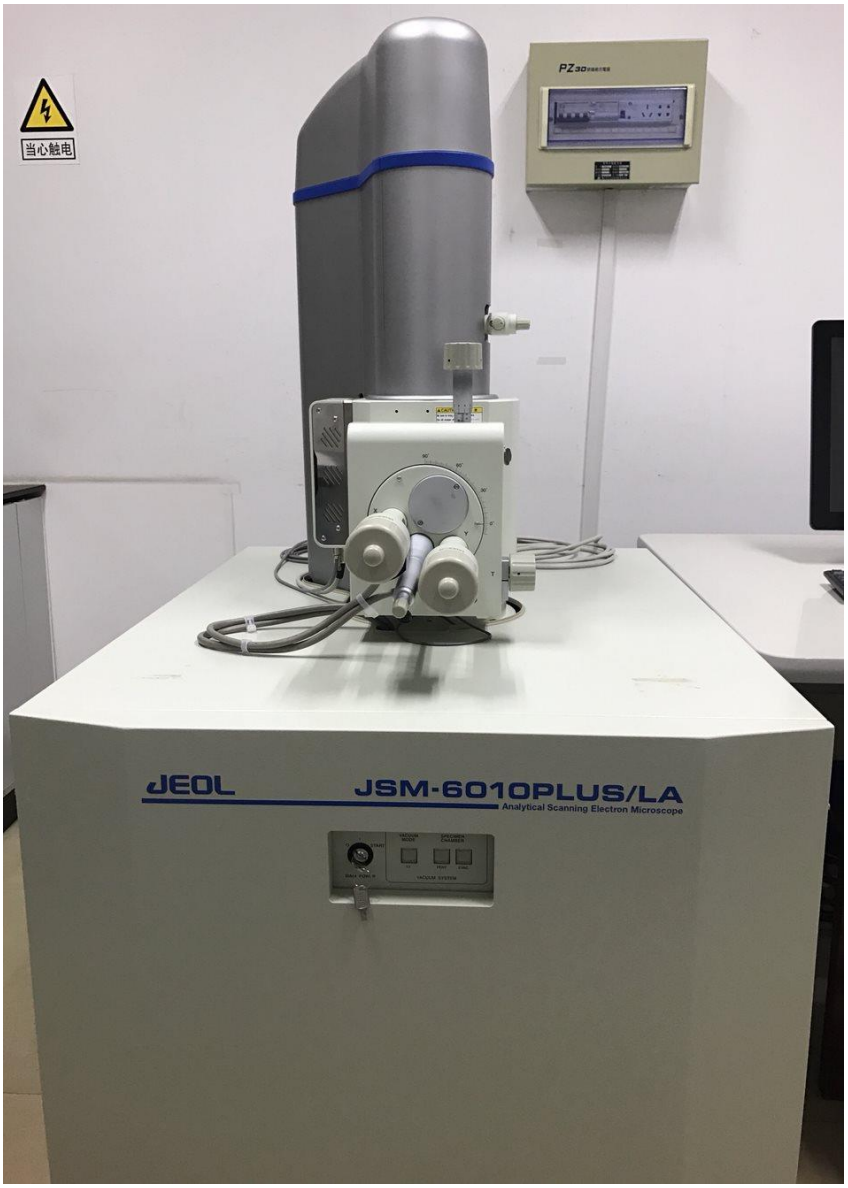

Fig. 3-1 The photo of SEM

The purpose of performing SEM characterization on the synthesized membrane containing adsorptive polymer capable of adsorbing antibiotic molecules is to gain a comprehensive understanding of the membrane's surface morphology and microstructure, as well as to verify the distribution and coverage of the polymer. The specific objectives include the below purposes.

Surface morphology analysis, by observing the surface morphology of the membrane using SEM, information such as roughness, pore structure, and texture can be obtained. This helps evaluate the surface characteristics of the membrane and the coverage of the polymer.

Polymer distribution detection, SEM provides high-resolution imaging to detect the distribution of the polymer on the membrane surface. The dispersion and uniformity of the polymer can be observed, determining its coverage and distribution on the membrane surface.

Pore structure analysis, SEM reveals the pore structure and pore size distribution of the membrane, allowing assessment of the membrane's permeability and adsorption capacity for antibiotics. By observing the size, shape, and distribution of the pores, insights can be gained into the porosity of the polymer membrane and its capacity to accommodate antibiotic molecules.

3.2.2 X-ray Photoelectron Spectroscopy (XPS)

X-ray Photoelectron Spectroscopy (XPS), also known as Electron Spectroscopy for Chemical Analysis (ESCA), is a widely used surface analysis technique that provides information about the surface chemistry, elemental oxidation states, and electronic structure of materials. XPS involves irradiating the sample surface with X-rays and measuring the emitted photoelectrons to study the surface properties of the material.

The working principle of XPS is based on the photoelectric effect. When the sample surface is irradiated with high-energy X-rays, photoelectrons are emitted from the surface. The energy of these photoelectrons is related to the energy difference required to remove them from the atoms or molecules, thereby providing information about the surface chemical composition of the sample.

An XPS experimental setup consists of several main components: an X-ray source, an analysis chamber, a photoelectron spectrometer, and a data acquisition system. X-ray sources typically use monochromatic X-rays with high energy and narrow line widths, such as magnesium Kα line (1253.6 eV) or aluminum Kα line (1486.6 eV). After the sample surface is irradiated with X-rays, the emitted photoelectrons are focused and collected into the

photoelectron spectrometer for energy analysis. The spectrometer, which can be a hemispherical or cylindrical analyzer, separates and detects the photoelectrons based on their energy. Finally, the data acquisition system records and analyzes the intensity and energy distribution of the photoelectron spectrum to obtain information about the sample surface.

XPS analysis provides valuable information. Firstly, XPS can determine the chemical composition of the sample surface, including the presence of elements and their relative abundances. Secondly, XPS provides information about the oxidation states of elements. By analyzing the peak positions and shapes of the photoelectron spectrum, the oxidation states or chemical bonding states of elements can be determined. Additionally, XPS can probe the electronic structure characteristics of the sample surface, including band structures and valence band energy levels.

XPS finds wide applications in various fields. In materials science, it is commonly used to study thin films, coatings, nanomaterials, and surface-modified materials. In chemistry and catalysis, XPS provides information about surface-active sites of catalysts, reaction mechanisms, and surface reactants. In the field of bioscience, XPS is used to investigate bio-interfaces, protein structures, and cell surfaces.

In this study, XPS analysis of the synthesized membrane material allows the determination of the chemical composition of the membrane surface, including adsorbent polymers and other chemicals that may be present. It can provide quantitative information about the presence of elements and their relative abundance, and help to assess the distribution and content of adsorbent polymers.

XPS analysis can also provide information about the oxidation state of elements in adsorbent polymers. By analyzing the peak position and shape of the photoelectron spectra, the oxidation state or chemical bonding state of the element can be determined. This is important for understanding the interactions and chemical reactions between adsorbent polymers and antibiotic molecules.

3.2.3 Fourier Transform Infrared Spectroscopy (FTIR)

Fourier Transform Infrared Spectroscopy (FTIR) is a commonly used analytical technique for studying the structure, chemical composition, and molecular vibrations of materials. It provides detailed information about a sample by measuring its absorption and scattering of infrared radiation.

Fig. 3-2 The photo of FTIR

The working principle of FTIR is based on the vibrational absorption of molecules. When infrared radiation passes through a sample, the chemical bonds within the molecules absorb specific energy from the infrared spectrum, causing vibrations. These vibrations are closely related to the chemical structure and functionality of the molecules. By measuring the intensity and wavenumber of the absorbed light, different chemical groups, functional groups, and their interactions in the sample can be understood.

The FTIR experimental setup consists of several main components: a light source, sample chamber, interferometer, and detector. The light source is typically an infrared source, such as a tungsten lamp or an infrared laser, producing a spectrum covering the infrared region. The

sample is placed in the sample chamber, where it interacts with the light. The interferometer separates the light into different wavenumbers, generating an interferogram. Finally, the detector measures the intensity of the interferogram, resulting in an infrared spectrum that is analyzed and interpreted.

FTIR provides rich information about the sample. Firstly, it can identify the chemical groups and functional groups present in the sample. Each chemical group has its unique vibrational frequency and absorption peaks. By analyzing the position and intensity of these peaks, the chemical composition and structural features of the sample can be determined. Secondly, FTIR can detect the presence of functional groups, determine the types of chemical bonds, and evaluate the interactions between different chemical groups in the sample.

Furthermore, FTIR can be used for quantitative analysis. By measuring the intensity of absorption peaks in relation to the concentration of compounds in the sample, quantitative measurements can be achieved. This technique finds widespread applications in various fields, including materials science, chemistry, biomedical research, and environmental science. In materials science, FTIR is commonly used to analyze polymer materials, coatings, nanomaterials, and composite materials. In chemistry, FTIR is employed for characterizing the structure and reaction mechanisms of organic compounds. In the biomedical field, FTIR is utilized to study the structure and functionality of proteins, nucleic acids, and cells.

The purpose of conducting Fourier Transform Infrared (FTIR) spectroscopy characterization on the surface membrane containing adsorptive polymers synthesized for the adsorption of antibiotic molecules encompasses several important aspects. Firstly, FTIR analysis serves to validate the successful synthesis and surface modification of the membrane. By comparing the infrared spectra of unmodified membranes and those modified with adsorptive polymers, it becomes possible to ascertain the effective adsorption and fixation of the polymer onto the membrane surface.

Secondly, FTIR spectroscopy provides valuable insights into the nature of interactions between the adsorptive polymers and the antibiotic molecules. By examining the characteristic peaks and intensity changes in the infrared spectrum, it becomes feasible to unravel the intricate

details of chemical bonding, intermolecular forces, and adsorption mechanisms that underpin the polymer-antibiotic interactions. This information contributes to a deeper understanding of the molecular-level interactions and the formation of complex functional groups within the membrane matrix.

Moreover, FTIR analysis offers a comprehensive understanding of the surface chemical composition of the membrane. It facilitates the identification and quantification of specific functional groups and chemical bonds present within the polymer-modified membrane. By carefully analyzing the intensity and position of distinctive peaks in the infrared spectrum, crucial details regarding the presence, distribution, and relative abundance of the adsorptive polymers and antibiotic molecules can be deduced.

FTIR characterization of the surface membrane containing adsorptive polymers plays a vital role in elucidating the intricate interplay between the polymer modification layer and the adsorbed antibiotic molecules. Furthermore, it provides a thorough assessment of the surface chemical properties, including the identification of functional groups, chemical bonding patterns, and the spatial distribution of the adsorptive polymers. This comprehensive understanding, obtained through FTIR analysis, contributes significantly to the optimization, refinement, and further advancement of membrane design for enhanced adsorption of antibiotic molecules, thereby supporting the development of novel and effective strategies in the field of antimicrobial applications.

3.2.4 In-situ Diffuse Reflectance Infrared Fourier Transform Spectroscopy (DRIFTS)

In-situ Diffuse Reflectance Infrared Fourier Transform Spectroscopy (DRIFTS) is a powerful and widely used surface analysis technique when it comes to studying real-time reactions and adsorption processes occurring on solid surfaces. It provides us with an opportunity to gain a deeper understanding of surface chemical changes, functional groups, and chemical reactions.

The working principle of In-situ DRIFTS involves directing infrared radiation onto the sample surface and measuring the reflected or scattered light. This technique transforms the spectral signals into high-resolution infrared spectra through Fourier transformation, enabling us to accurately analyze the absorption characteristics of the sample surface. By observing the

infrared absorption spectra of the sample surface, I can identify the types, quantities, and structures of the adsorbates.

One of the advantages of In-situ DRIFTS is its capability for real-time and in-situ observations. This means that I can monitor surface reactions and adsorption processes in the actual reaction environment, such as catalytic reactions, gas adsorption, and solvent adsorption. By continuously monitoring the changes in the infrared spectra during the reaction process, I can obtain important information about reaction rates, intermediate product formation, adsorption dissociation, and more, thereby uncovering the mechanisms and kinetics of the reactions.

Furthermore, In-situ DRIFTS can be combined with other characterization techniques to provide more comprehensive information. For example, coupling it with mass spectrometry can provide information about the mass of reactants and collision dynamics, while using it in conjunction with atomic force microscopy (AFM) allows the observation of surface morphology and nanoscale structural changes. This integrated approach offers us a more comprehensive surface analysis, facilitating a better understanding and interpretation of the structure-performance relationship in surface reactions.

In-situ DRIFTS is a versatile surface analysis technique with a wide range of applications in catalysis research, materials science, environmental science, and more. Its real-time and in-situ capabilities make it an essential tool for researchers to delve into and explore solid surface reactions and adsorption processes. By combining different analytical methods and techniques, I can reveal the mechanisms of surface reactions more comprehensively and provide strong support for material design and optimization of catalytic processes.

When a surface membrane containing adsorbent polymers that can effectively adsorb antibiotic molecules is successfully synthesized, conducting in-situ DRIFTS (in-situ Diffuse Reflectance Infrared Fourier Transform Spectroscopy) characterization of the membrane serves several purposes.

Firstly, in-situ DRIFTS provides a real-time and dynamic analysis approach, allowing us to accurately observe and record the adsorption process of antibiotic molecules on the surface of

the polymer membrane. By monitoring changes in the infrared spectra, I can explore the chemical reactions and interactions occurring during adsorption, understanding the bonding, adsorption mechanisms, and possible reaction pathways between the antibiotic molecules and the polymer membrane. This aids in a deeper understanding of the adsorption behavior, kinetics, and adsorption capacity of antibiotics on the membrane surface.

Secondly, in-situ DRIFTS offers unique advantages for characterizing the adsorbed state of antibiotic molecules on the polymer membrane. By analyzing characteristic peak positions and intensities in the infrared spectra, I can determine the structure and mode of existence of the adsorbed molecules, further confirming the selective adsorption and adsorption capacity of the polymer membrane for antibiotics. Moreover, quantitative analysis of the infrared spectra enables the determination of key parameters such as coverage, number of adsorption sites, and thickness of the adsorbed layer, providing a comprehensive assessment of adsorption performance.

Thirdly, in-situ DRIFTS allows real-time monitoring and tracking of the reaction processes of antibiotic molecules on the surface of the polymer membrane. If chemical reactions occur during the adsorption process, changes in the infrared spectra will provide information on the formation of reaction intermediates, changes in bonding states, and possible degradation reactions. This helps reveal the transformation pathways, reaction mechanisms, and the catalytic or inhibitory effects of the polymer membrane on the reactions of antibiotic molecules. Through real-time monitoring with in-situ DRIFTS, critical dynamic information can be obtained, providing important clues for understanding and controlling the adsorption and reaction processes of antibiotic molecules.

Furthermore, in-situ DRIFTS can be used for detailed characterization of the chemical composition and structure of membranes with adsorbent polymers. By analyzing peak positions, shapes, and intensity distributions in the infrared spectra, I can determine the functional groups, polymer structure, and chemical bonding states of the membrane. This contributes to the evaluation of the chemical stability, interactions with substrates, and structural features of the polymer membrane. This information is crucial for the design, synthesis, and performance

tuning of membrane materials.

Through in-situ DRIFTS characterization of a surface membrane containing adsorbent polymers for the adsorption of antibiotic molecules, comprehensive information regarding the adsorption process, adsorbed state, reaction processes, and chemical composition of the membrane can be obtained. This will provide strong support for a deeper understanding of the interaction mechanisms between antibiotics and the polymer membrane, optimization of adsorption performance and reaction properties of the membrane, and important scientific basis and guidance for the research and application of novel antibiotic adsorbent materials.

3.2.5 Ultraviolet-Visible Spectroscopy (UV-Vis)

Ultraviolet-Visible Spectroscopy (UV-Vis) is a commonly used analytical technique for measuring the absorption and transmission characteristics of substances in the ultraviolet (UV) and visible (Vis) light range. It is an important and widely applied spectroscopic method that provides valuable information about molecular electronic structure, energy level transitions, solution concentrations, chemical reaction kinetics, and material characterization.

Fig. 3-3 The Photo of UV-Vis

The working principle of UV-Vis spectroscopy is based on molecular absorption spectroscopy. When a sample is exposed to UV and visible light sources, the molecules in the

sample interact with the light, causing changes in the energy of absorbed or transmitted photons. This energy change is related to the molecular energy levels, electronic transitions, and chemical bonds within the molecules. Specifically, as light passes through the sample, molecules absorb energy from the light, exciting electrons from the ground state to an excited state, resulting in absorption peaks. By measuring the intensity and energy of the light absorbed or transmitted by the sample at different wavelengths, I can obtain the absorption spectrum of the sample.

A typical UV-Vis spectroscopy setup consists of a light source, optical path, sample chamber, grating, detector, and data acquisition system. The light source typically uses deuterium and tungsten lamps to provide light in the UV and visible ranges, respectively. The optical path includes optical elements such as lenses, mirrors, and gratings that guide and disperse the light beam. The sample chamber is used to hold the sample and maintain its stability. The grating disperses the light beam to focus different wavelengths onto the detector. The detector records the intensity of light absorbed or transmitted by the sample and converts it into electrical signals. Finally, the data acquisition system converts the electrical signals into a spectral graph for further analysis and interpretation.

UV-Vis spectroscopy provides valuable information through spectral analysis. Firstly, by detecting the positions and intensities of absorption peaks in the sample's absorption spectrum, I can identify the presence of absorption bands and their corresponding wavelength ranges. This helps determine the chemical composition, purity, and substance concentrations in the sample. Secondly, by analyzing the shape, bandwidth, and intensity of the absorption spectrum, I can gain insights into energy level transitions and electronic structure features within the molecules. Additionally, UV-Vis spectroscopy is employed in the study of molecular structural changes, determination of reaction kinetics, and characterization of photosensitive materials.

UV-Vis spectroscopy finds wide applications in various fields. In chemistry and biochemistry, it is commonly used for quantitative analysis, compound identification, investigation of photochemical reactions, and kinetic processes. In environmental science, UV-Vis spectroscopy is employed to monitor and assess pollutants in water, atmospheric pollutants, and soil

contaminants. In materials science and surface/interface science, UV-Vis spectroscopy is utilized for characterizing optical properties of materials, studying photocatalytic activities, and exploring the applications of photosensitive materials.

UV-Vis spectroscopy is a valuable and extensively used spectroscopic technique that provides important information about molecular structure, energy level transitions, chemical reactions, and solution concentrations by measuring the absorption and transmission characteristics of samples in the UV and visible light ranges. It offers significant support and guidance to scientific research and practical applications in various fields.

When successfully synthesizing a surface membrane containing an adsorptive polymer capable of adsorbing antibiotic molecules, the application of Ultraviolet-Visible Spectroscopy (UV-Vis) for characterization serves several purposes and holds significant importance:

Firstly, UV-Vis allows for an in-depth study of the membrane material's absorption properties. UV-Vis measurements cover a range of wavelengths from ultraviolet to visible light, enabling us to observe the interaction between the membrane material and light. By analyzing the absorption spectra, I can explore the extent and intensity of the membrane material's absorption of different wavelength light, thereby revealing the interaction modes between the membrane material and light during the adsorption of antibiotic molecules.

Secondly, UV-Vis analysis can be used to assess the adsorption performance of the membrane material. By monitoring changes in the UV-Vis absorption spectra, I can evaluate the membrane's adsorption capacity and selectivity towards antibiotic molecules. This quantitative assessment of adsorption performance helps us understand the efficiency, capacity, and provides guidance for optimizing the membrane material.

UV-Vis allows for real-time monitoring of the reaction kinetics between the membrane and antibiotic molecules. By tracking changes in the UV-Vis absorption spectra, I can observe the dynamic variations during the adsorption process, such as reaction rates, equilibrium states, and reaction mechanisms. This aids in gaining a deeper understanding of the interaction and adsorption kinetics between the membrane material and antibiotic molecules.

UV-Vis analysis enables the investigation of structural changes in the membrane material. By analyzing the peak positions and shapes in the UV-Vis absorption spectra, I can infer structural characteristics such as conformational changes, polymerization degree, and cross-linking in the membrane. This helps us understand the potential structural changes that may occur after adsorbing antibiotic molecules and provides insights for the design and improvement of the membrane material.

UV-Vis can be employed to evaluate the stability of the membrane material. By analyzing changes in the absorption spectra, I can assess whether degradation, dissolution, or morphological changes occur during the adsorption of antibiotic molecules. This aids in determining the durability, lifespan, and long-term stability of the membrane material.

The utilization of UV-Vis for analyzing a surface membrane containing an adsorptive polymer provides comprehensive information, encompassing absorption properties, adsorption performance, reaction kinetics, structural changes, and material stability. This information is crucial for optimizing membrane material design, enhancing adsorption performance, gaining insights into adsorption kinetics and structural characteristics, and ensuring the long-term stability of the membrane material.

3.2.6 Contact angle measurement

Contact angle measurement is a widely used technique in surface science and material characterization to assess the wetting behavior of a liquid droplet on a solid surface. The contact angle is the angle formed between the tangent line at the droplet's three-phase contact point and the solid surface. This angle provides valuable information about the interfacial interactions and surface properties of the material.

The measurement of contact angle involves placing a liquid droplet of interest, typically water or a specific test liquid, onto the surface of the solid material. The droplet is carefully dispensed onto the surface, and an image is captured using a high-resolution camera or microscope. The shape of the droplet is analyzed to determine the contact angle.

There are different methods for measuring contact angles, including the sessile drop method,

captive bubble method, and Wilhelmy plate method. The most commonly used technique is the sessile drop method, where a droplet is placed on the surface, and the contact angle is measured from the image of the droplet.

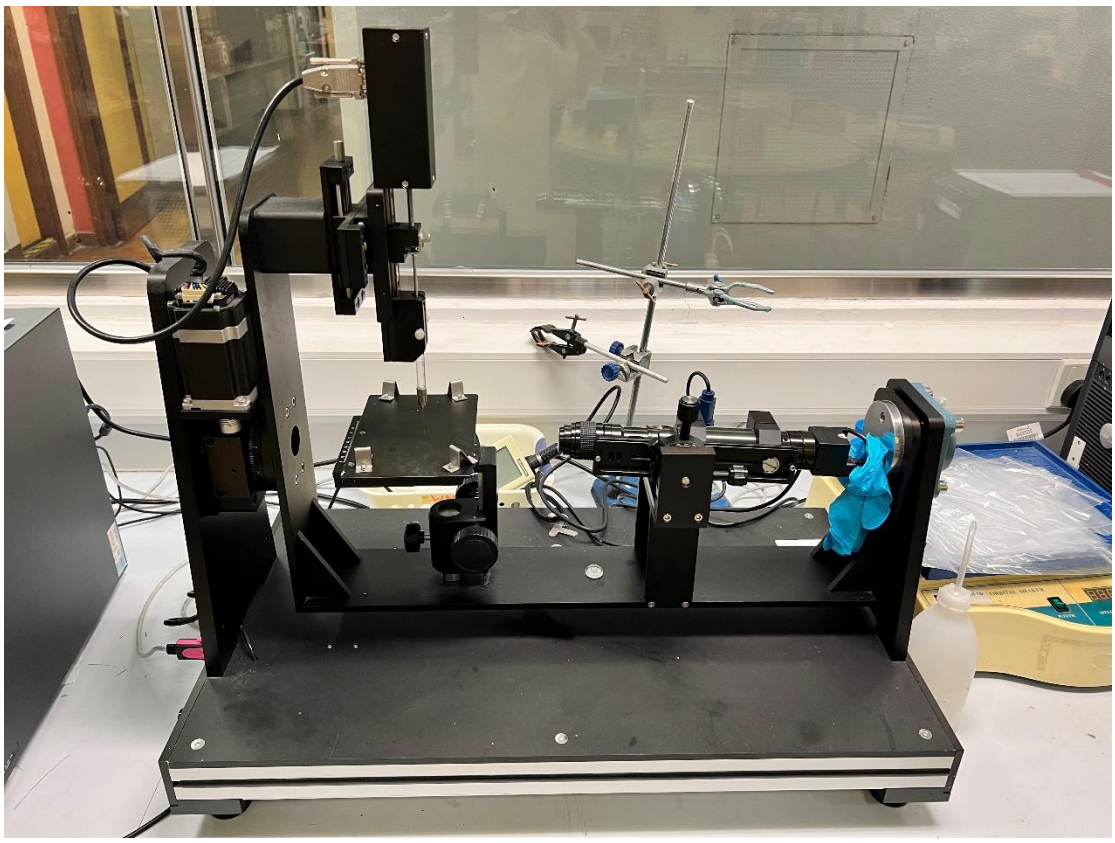

Fig. 3-4 The photo of contact angle measurement

The contact angle measurement provides several important insights into the surface properties of the material:

Wetting behavior: The contact angle reflects the wetting characteristics of the liquid on the surface. A low contact angle (close to 0°) indicates complete wetting, where the liquid spreads out extensively on the surface, indicating good surface wettability. Conversely, a high contact angle (close to 180°) suggests poor wetting, with the liquid forming a nearly spherical shape and showing limited interaction with the surface.

Surface energy: The contact angle measurement can be used to estimate the surface energy of the solid material. By applying suitable mathematical models such as Young's equation, the contact angle can be correlated to the interfacial tensions between the liquid, solid, and

surrounding gas phase. This information helps in understanding the surface properties, such as hydrophilicity or hydrophobicity, of the material.

Surface roughness and topography: Contact angle measurements can provide insights into the surface roughness and topography of the material. Irregular or rough surfaces tend to have higher contact angles due to increased surface area and reduced wetting. By analyzing the contact angle variation with different droplet sizes, surface roughness parameters such as the apparent contact angle hysteresis can be determined, providing information about the surface texture.

Surface modification and coating evaluation: Contact angle measurements are useful for evaluating the effectiveness of surface modifications or coatings. By comparing contact angles before and after surface treatments, such as chemical modifications or functional coatings, the impact of these modifications on the surface properties and wettability can be assessed. This is particularly relevant in applications such as self-cleaning surfaces, anti-fog coatings, and adhesion studies.

Quality control and material characterization: Contact angle measurements are employed in quality control processes to ensure consistent surface properties and wettability of materials. They are also used for material characterization, particularly in fields such as materials science, chemistry, biology, and nanotechnology. Contact angle measurements can aid in understanding the behavior of liquids on various surfaces and assist in the design and development of functional materials.

Contact angle measurement is a versatile technique that provides valuable information about the wetting behavior, surface energy, roughness, and surface modifications of materials. It is widely used in scientific research, industrial applications, and quality control processes to optimize material properties, evaluate surface treatments, and develop innovative surface technologies.

Conducting contact angle measurements on surfaces of polymer films containing adsorptive properties, which can adsorb antibiotic molecules, serves the following purposes:

Assessing wetting performance: Contact angle measurements evaluate the wetting properties of the film surface. By measuring the contact angle formed by a liquid droplet on the film, information about the degree of wetting can be obtained. A smaller contact angle indicates better wetting.

Characterizing interface properties: Contact angles provide insights into the interfacial properties between the film surface and the liquid droplet. By measuring changes in the contact angle, interactions between the film surface and adsorbed molecules can be understood, thereby inferring adsorption performance and interfacial energy.

Surface energy evaluation: Contact angle measurements can be used to assess the surface energy of the film. By measuring the contact angles on different liquids, the polar and non-polar components of the film surface can be calculated, revealing the chemical characteristics and hydrophilicity/hydrophobicity of the film surface.

Evaluating interfacial activity: Contact angle measurements can evaluate the interfacial activity of the film surface. For polymer films with adsorptive properties, changes in the contact angle can reflect the diffusion and aggregation of adsorbed molecules on the film surface, providing insights into adsorption performance and interfacial activity.

Optimizing film performance: Contact angle measurements enable the optimization of surface properties for polymer films with adsorptive properties. This includes adjusting the chemical composition and structure of the film surface, altering the content and arrangement of polymers, etc., to enhance adsorption performance and membrane stability.

In summary, conducting contact angle measurements on polymer films containing adsorptive properties allows for the assessment of wetting performance, interface properties, and interfacial activity. It aids in optimizing the surface characteristics of the film, thereby improving the efficiency and performance of adsorbing antibiotic molecules.

Reference

[1] Mingming Wu, Weimin Liu, Peng Mu, Qingtao Wang, Jian Li, Sacrifice template strategy to the fabrication of a self-cleaning nanofibrous membrane for efficient crude oil-in-water

emulsion separation with high flux, ACS Applied Materials & Interfaces 12(47) (2020) 53484-53493.

[2] KC Khulbe, C Feng, T Matsuura, The art of surface modification of synthetic polymeric membranes, Journal of Applied Polymer Science 115(2) (2010) 855-895.

[3] Charles E Hoyle, Christopher N Bowman, Thiol–ene click chemistry, Angewandte Chemie International Edition 49(9) (2010) 1540-1573.

[4] Ran Xu, Min Jia, Yalei Zhang, Fengting Li, Sorption of malachite green on vinyl-modified mesoporous poly (acrylic acid)/SiO2 composite nanofiber membranes, Microporous and Mesoporous Materials 149(1) (2012) 111-118.

Chapter 4

DATA RESOURCE AND MEMBRANE PERFORMANCE ANALYSIS

4.1 Adsorption performance

In terms of membrane performance, I first need to test the adsorption performance of the membrane.

The first aim is to evaluate the adsorption properties. The membranes in this study were designed to achieve adsorption of antibiotic molecules. The adsorption performance test allows the membrane to be evaluated for adsorption of the target molecule. This helps to determine the suitability of the membrane for the separation, detection, or removal of antibiotic molecules.

The next step is to understand the adsorption capacity. Adsorption performance testing can help determine the adsorption capacity of a membrane for a target antibiotic molecule. This is the maximum amount of target molecules that can be adsorbed per unit area or unit volume of membrane. Understanding adsorption capacity helps determine the capacity and efficiency of a membrane for practical applications.

Membrane interactions with target antibiotic molecules: Adsorption performance testing also assesses the interactions of membrane materials with target antibiotic molecules. This refers to the degree of adsorption of the membrane to the target antibiotic molecule. Understanding membrane interactions with target antibiotic molecules can help evaluate membrane selectivity and removal efficiency in complex mixtures.

Finally, it is also possible to optimize membrane structure and performance: adsorption performance testing can be used to optimize membrane structure and performance. By testing the adsorption performance of membranes under different conditions, optimization strategies in terms of optimal operating parameters, material ratios and membrane structures can be determined. This helps to improve the adsorption efficiency and selectivity of the membranes.

4.1.1 Selection of Ciprofloxacin (CIP)

CIP, also known as ciprofloxacin, has a molecular formula of $C_{17}H_{18}FN_3O_3$ and a relative molecular weight of 331.35. It is a odorless, slightly yellow or off-white crystalline powder with a bitter taste. CIP is soluble in water, slightly soluble in methanol, and insoluble in ethanol. It is a typical synthetic fluoroquinolone antibiotic drug, known for its broad spectrum of

antibacterial activity and strong bactericidal properties [1-4]. It is widely used in the treatment of various infections, including skeletal infections, joint infections, abdominal infections, infectious gastroenteritis, respiratory tract infections, skin infections, typhoid fever, and urinary tract infections. It exhibits strong activity against Escherichia coli, Pseudomonas aeruginosa, Haemophilus influenzae, Neisseria gonorrhoeae, Streptococcus spp., Legionella pneumophila, Staphylococcus aureus, and others [5-7]. Compared to other fluoroquinolone antibiotics such as norfloxacin and enrofloxacin, CIP has approximately 2-4 times higher antibacterial activity, making it widely used in the clinical treatment of bacterial infections in humans and other animals.

Studies have shown that over 85% of CIP, in its original form and as metabolites, is transferred to the environment through wastewater [8]. Currently, the detected concentration of CIP in wastewater has evolved from the ng L^{-1} and μg L^{-1} levels to the mg L^{-1} level worldwide. For example, the detected concentration of CIP in medical wastewater can reach 21 μg L^{-1} [9], while the detected concentration of CIP in related industrial wastewater can be as high as 4.9 mg L^{-1} [10]. The highest detected concentration of CIP in effluent from wastewater treatment plants in China is 1323 ng L^{-1}, in Brazil it can reach 2378 ng L^{-1} [11], and in Finland, the highest detected concentration of CIP in wastewater treatment plant effluent is as high as 4230 ng L^{-1} [12].

CIP, present in domestic wastewater, medical wastewater, aquaculture wastewater, and industrial wastewater, enters wastewater treatment plants without effective removal (currently, there are no specific environmental quality and emission standards for antibiotics in China) [13]. As a result, the majority of CIP ultimately enters surface water and causes contamination of groundwater through water cycling [14]. Upon entering water bodies, either directly or indirectly, CIP, even at trace levels, remains biologically active and poses hazards to the ecological environment and human health. The specific impacts can be summarized as follows [15-18]: (i) Unmetabolized CIP excreted as random isomers enters the natural environment, leading to long-term exposure of organisms to CIP, inducing the generation of antibiotic resistance genes, and facilitating the acquisition of drug resistance by pathogenic bacteria through water cycling and food chains, potentially giving rise to the emergence of superbugs.

(ii) CIP exhibits toxicity to various aquatic organisms, inhibiting their metabolic processes when exposed to CIP-polluted water for prolonged periods. Moreover, different organisms have varying sensitivities to CIP, which can lead to ecological imbalances. (iii) CIP accumulates in higher trophic-level organisms through the food chain, resulting in concentrations higher than those in the environment. Long-term consumption of CIP-contaminated water or food by humans may lead to intestinal disorders, allergic reactions, and even affect the human immune system, posing potential hazards to human health.

The widespread use and release of ciprofloxacin may result in high concentrations of ciprofloxacin in the environment. Prolonged exposure to high concentrations of ciprofloxacin may increase the risk of human exposure to it, thus posing a potential health risk.

Therefore, I selected the antibiotic molecule for this adsorption performance experiment as the ciprofloxacin molecule.

4.1.2 Isothermal adsorption experiments

Isothermal adsorption is a comprehensive experimental and theoretical approach used to describe the adsorption process of substances on the surface of solids when they come into meet gases or liquids. In isothermal adsorption, substances are adsorbed onto the solid surface, forming an adsorption layer or film, which is influenced by the interaction forces between the adsorbate and the solid surface.

Isothermal adsorption experiments are typically conducted at a constant temperature to control the temperature effect on the adsorption process. The adsorbent used in the experiments is often a material with a large surface area and adsorption activity, such as porous materials, nanoparticles, or activated carbon. The adsorbate can be gas molecules or substances dissolved in liquids.

During isothermal adsorption experiments, the adsorption amount is typically measured as a function of the adsorbate concentration. By plotting adsorption isotherms, the relationship between adsorption amount and adsorbate concentration can be determined. The results from isothermal adsorption experiments provide insights into the kinetics and equilibrium properties

of the adsorption process.

Theoretically, the isothermal adsorption process can be described by adsorption isotherms, which include parameters such as adsorption capacity and adsorption equilibrium constant. Various models, such as the Langmuir model, Freundlich model, and Tempkin model, can be used to fit the adsorption isotherms. These models are based on assumptions regarding adsorption site saturation and the interaction forces between the adsorbate and the adsorbent, and they help explain various phenomena and properties of the adsorption process.

Isothermal adsorption finds widespread applications in various fields. In environmental science, it is used to study the adsorption behavior of pollutants in soils and water bodies and evaluate their migration and removal efficiency. In chemical processes, isothermal adsorption is employed for separation and purification of components in mixtures, such as gas separation and liquid-phase chromatography. In materials science, isothermal adsorption is utilized to assess the adsorption capacity and selectivity of adsorbents, facilitating the development of novel adsorbent materials.

Langmuir model

The Langmuir model is a classical isothermal model of adsorption, which is often used to describe the adsorption process between a substance in a gas or solution and a solid surface. The model was proposed by Irving Langmuir in 1918 and is widely used to characterize the behavior and properties of various adsorption systems based on the assumption that adsorbed molecules form a monolayer on a surface.

The Langmuir model assumes that the adsorption process between the adsorbed molecule and the solid surface is reversible and that there is no interaction between the adsorption sites. The model is based on the key assumptions that (1) adsorption sites are uniformly distributed and remain constant in number during the adsorption process, and (2) adsorbed molecules form a monolayer adsorption on the adsorption sites and there is no multilayer adsorption.

The parameters of the Langmuir model can be obtained by fitting experimental data to obtain information on adsorption properties such as the adsorption equilibrium constant K and the

adsorption capacity. The model can be used to explain the saturation behavior and equilibrium state of the adsorption process and to provide a theoretical basis and quantitative description of the adsorption system.

It is important to note that the Langmuir model is applicable to simple systems without multilayer adsorption and interactions in the adsorption process. For complex adsorption systems, such as multilayer adsorption, interactions, or inhomogeneous surface distribution, the Langmuir model may not be applicable and a more complex adsorption isotherm model is required for the description.

Langmuir model is expressed as

$$Q_e=(Q_mK_LC_e)/(1+K_LC_e),$$

where C_e (mg L^{-1}) and Q_e (mg g^{-1}) are concentration and rebinding capacity at equilibrium, Qm (mg g^{-1}) is the theoretical maximum rebinding capacity, and K_L (L mg^{-1}) is the Langmuir constant.

Freundlich model

The Freundlich model is an empirical equation used to describe the adsorption behavior of solutes onto solid surfaces. It is widely applied in various fields, including environmental science, chemistry, and engineering. The model is named after the German chemist Fritz Freundlich, who introduced it in 1906.

The Freundlich model assumes that the adsorption process occurs on a heterogeneous surface with non-uniform energy distribution. It suggests that as the concentration of the solute increases, the adsorption capacity also increases, but at a decreasing rate. The Freundlich model provides insights into the adsorption mechanisms, surface properties, and potential applications of adsorbents in water treatment, pollutant removal, and separation processes.

It is important to note that while the Freundlich model is widely used and provides valuable information, it is an empirical model and may not accurately describe all adsorption systems. Other models, such as the Langmuir model and BET model, are also commonly employed to characterize adsorption phenomena, and the choice of model depends on the specific system

and objectives of the study.

Freundlich model is expressed as

$$Q_e = K_F C_e^{1/n}$$

where C_e (mg L^{-1}) and Q_e (mg g^{-1}) are concentration and rebinding capacity at equilibrium, as well as K_F ($mg^{1-1/n}$ $L^{1/n}$ g^{-1}) and n are Freundlich constants.

4.1.3 Kinetic adsorption experiments

Kinetic adsorption is a comprehensive and detailed experimental method used extensively in scientific research and engineering applications to understand the time evolution and dynamic behavior of adsorbates during the adsorption process. It provides insights into the adsorption mechanism, optimization of adsorption processes, and design of efficient adsorbent materials.

The design and execution of kinetic adsorption experiments involve considerations from various aspects. Firstly, appropriate adsorbents and adsorbate media need to be selected to ensure effective interactions with the target adsorbate. Experimental conditions such as temperature, pressure, and solution pH should be carefully controlled to ensure accuracy and reproducibility of the results.

In kinetic adsorption experiments, various techniques are typically employed to monitor the concentration of the adsorbate in the adsorbent media over time. These include spectrophotometry, electrochemical methods, mass spectrometry, and others. By measuring the concentration of the adsorbate at different time points, information about the adsorption rate can be obtained, and the kinetics of the adsorption process can be inferred.

The results of kinetic adsorption experiments provide valuable information and insights. They help determine the rate-controlling steps in the adsorption process, i.e., whether chemical or physical adsorption dominates the adsorption rate. Furthermore, careful analysis of the experimental data allows for the extraction of key parameters such as adsorption rate constants, reaction orders, and apparent activation energies, which are crucial for establishing adsorption kinetic models and predicting adsorption behavior.

Kinetic adsorption experiments have significant implications in various fields. In environmental science, they can be used to study the adsorption behavior of pollutants in soil or water systems and evaluate the removal efficiency of adsorbent materials. In chemical engineering processes, kinetic adsorption experiments can optimize the conditions and operating parameters of adsorption processes to enhance the performance and efficiency of adsorption equipment. In the field of biomedicine, kinetic adsorption experiments can elucidate the adsorption and release behavior of drugs in biological systems, facilitating the design and optimization of drug therapies.

Kinetic adsorption experiments are essential tools for in-depth understanding of adsorption processes. They find wide-ranging applications in scientific research and engineering, playing a vital role in environmental protection, chemical process optimization, and biomedical advancements.

The data obtained from the Kinetic adsorption experiments will be attempted to be fitted to Pseudo-first-order model and Pseudo-second-order model.

Pseudo-first-order model

Pseudo-first-order is a commonly used kinetic model that describes the rate behavior of certain reaction steps in chemical reactions. The pseudo-first-order model assumes that the concentration of one component in the reactants is much larger than the others, making the consumption rate of this component the rate-determining step of the overall reaction.

The mathematical expression of the pseudo-first-order model is usually represented as that the pseudo-first-order model has a wide range of applications, particularly in describing the kinetics of first-order reactions and fast reactions. It is commonly used to evaluate the degradation rate of chemicals in solution, the pharmacokinetics of drugs, and the kinetics of catalytic reactions.

In practical applications, the pseudo-first-order model is often employed in kinetic adsorption experiments to assess the rate of adsorption reactions. By measuring the concentration of the adsorbate on the adsorbent as a function of time, the pseudo-first-order rate constant k can be

determined. This parameter can be used to compare the adsorption rates of different systems and optimize adsorption process conditions.

It is important to note that the pseudo-first-order model is applicable only under specific conditions where the concentration changes of the reactant conform to the kinetics of a pseudo-first-order reaction. In certain cases, reactions may involve multiple steps or the concentration changes of reactants may not adhere to the assumptions of pseudo-first-order kinetics. In such cases, alternative kinetic models may be more appropriate.

The pseudo-first-order model is a commonly used kinetic model for describing the rate behavior of certain chemical reactions. It finds valuable applications in kinetic adsorption experiments and other studies of reaction kinetics. However, it is important to select the appropriate kinetic model based on the specific circumstances and validate and analyze the experimental data accordingly.

Pseudo-first-order model is expressed by

$$Q_t = Q_e - Q_e e^{-k't}$$

where Q_e and Q_t (mg g^{-1}) are rebinding capacities at the equilibrium and time t (min), and k' (min^{-1}) is the equilibrium rate constants of the pseudo-first-order model.

Pseudo-second-order model

The pseudo-second-order model is a commonly used kinetic model that describes the rate behavior of certain reaction steps in chemical reactions. The model assumes that the concentration of one component in the reactants is much larger than the others, making the consumption rate of that component the rate-determining step of the overall reaction.

The main characteristic of the pseudo-second-order model is that in the initial stages of the adsorption reaction, the relationship between adsorption amount and time approximates linearity, unlike the exponential growth observed in the pseudo-first-order model. This model is suitable for describing the chemical adsorption process between the adsorbent and the adsorbate in an adsorption system.

The pseudo-second-order model has numerous applications, particularly in the study of adsorption reaction kinetics. It can be used to evaluate adsorption rates, adsorption capacities, and equilibrium adsorption amounts, among other parameters. Additionally, the pseudo-second-order model can be employed to predict the kinetic behavior of adsorption processes, optimize experimental conditions, and assess the performance of adsorbent materials.

In practical applications, the pseudo-second-order model is commonly used in adsorption performance testing and adsorption kinetics research. By measuring the change in adsorbate concentration on the adsorbent over time, the pseudo-second-order rate constant, k, can be determined. This parameter can be used to compare adsorption rates in different systems, evaluate the adsorption performance of adsorbents, and provide insights for the design of adsorption processes in industrial applications.

It is important to note that the pseudo-second-order model is applicable only under specific conditions that satisfy the assumptions of pseudo-second-order reaction kinetics. In certain cases, reactions may involve multiple steps or the concentration changes of reactants may not follow the assumptions of pseudo-second-order kinetics. In such situations, careful selection of appropriate kinetic models and data analysis methods is crucial.

The pseudo-second-order model is a commonly used kinetic model that describes the rate behavior of certain reaction steps in chemical reactions. It holds significant value in adsorption performance testing and adsorption kinetics research. However, it is essential to choose the appropriate kinetic model based on the specific circumstances and to verify and analyze experimental data accordingly.

Pseudo-second-order model is expressed as

$$Q_t=(k''Q_e^2t)/\ (1+\ k''Q_et)$$

where Q_e and Q_t (mg g^{-1}) are rebinding capacities at the equilibrium and time t (min), as well as k'' (g mg^{-1} min^{-1}) is the equilibrium rate constants of the pseudo-second-order model.

4.2 Permeation performance

Conducting permeation experiments on membranes holds significant importance and benefits:

Evaluating permeation selectivity, permeation experiments are crucial for assessing the selectivity of molecularly non-imprinted membranes towards different molecules. By measuring the permeation of molecules through the membrane, the membrane's selectivity for specific molecules can be determined. This is vital for screening target molecules, separating valuable substances from mixed solutions, and purifying target compounds. Comparing the permeation rates of different molecules allows for evaluating the affinity and selectivity of the membrane material towards various molecules, thereby optimizing membrane design and application.

Studying permeation kinetics, permeation experiments provide an essential means to study the kinetics of molecule transport through molecularly non-imprinted membranes. By monitoring the changes in parameters such as time, permeation rate, and mass transfer flux during the permeation process, a deeper understanding of the membrane's permeation mechanism and transport behavior can be obtained. This is crucial for comprehending the membrane's structural characteristics, solute-membrane interactions, and mass transfer mechanisms during permeation. Additionally, studying permeation kinetics aids in predicting the membrane material's permeation performance and stability in practical applications.

Optimizing membrane material design, permeation experiments enable the evaluation and comparison of different membrane materials' permeation performance. This helps in selecting the most suitable membrane material for specific applications and guiding membrane design and fabrication processes. By adjusting the material composition, structural features, and surface properties of the membrane, higher permeation selectivity, increased permeation flux, and improved membrane stability can be achieved. The results from permeation experiments provide valuable references and guidance for the improvement and optimization of membrane materials.

Validating separation efficiency, permeation experiments can validate the actual separation efficiency of molecularly non-imprinted membranes. By measuring the concentration changes

of target molecules in the permeate, the membrane's separation efficiency for the target molecules can be evaluated and compared to the expected separation performance. This is crucial for verifying the membrane's performance and application feasibility. Through the validation of experimental results, further optimization and improvement of membrane material design and fabrication can be carried out to achieve more efficient, stable, and sustainable separation processes.

Conducting permeation experiments on molecularly non-imprinted membranes holds significant importance. It allows for the evaluation of permeation selectivity, study of permeation kinetics, optimization of membrane material design, and validation of separation efficiency. This information provides guidance and drives advancements in the performance and practical application of molecularly non-imprinted membranes in separation science, environmental protection, pharmaceuticals, and other fields.

Permeation performance was investigated by the static permeation, which was performed based on a self-designed device shown in Fig. 4-1 and 4-2. In brief descriptions, a piece of membrane was tailored and placed between two flanges of the H-shaped tube. Two compartments separated by the membrane were filled with 100 mL of mixed solution (10 mg L–1 of CIP) and pure solvent (deionized water), respectively. Samples were taken from each chamber at a pre-determined time (0-48 h), where the concentration of solutes was measured by UV-Vis at 275 nm (CIP). Thus, permeation flux (J, mg min^{-1} cm^{-2}) and permeability coefficient (P, L min^{-1} cm^{-1}) can be calculated using the following equations (Eq. 7-8):

$$J = \frac{\Delta C_D V_D}{\Delta t A} \tag{7}$$

$$P = \frac{Jd}{C_P - C_D} \tag{8}$$

where $\Delta C_D/\Delta t$ (mg L^{-1} min^{-1}), V_D (L), A (cm^2) and d (cm) are the change of concentrations in dialysate, the volume of dialysate, effective area, and thickness of the membrane, as well as (C_P-C_D) (mg L^{-1}) is the difference of concentrations between permeate and dialysate.

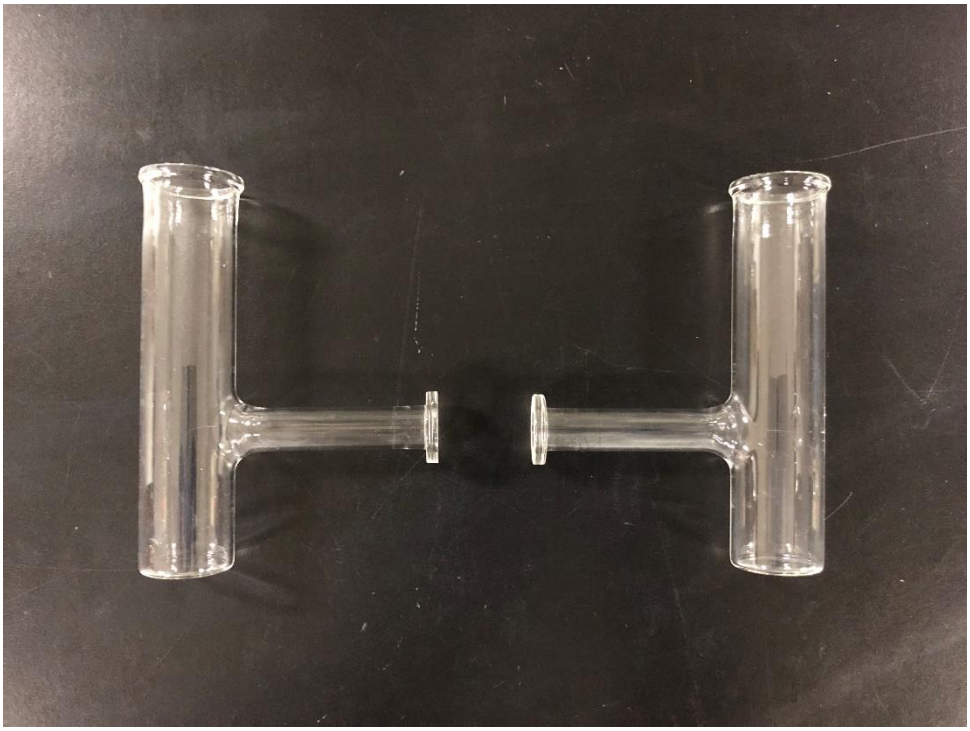

Fig. 4-1 The H-type device for permeation before the experiment

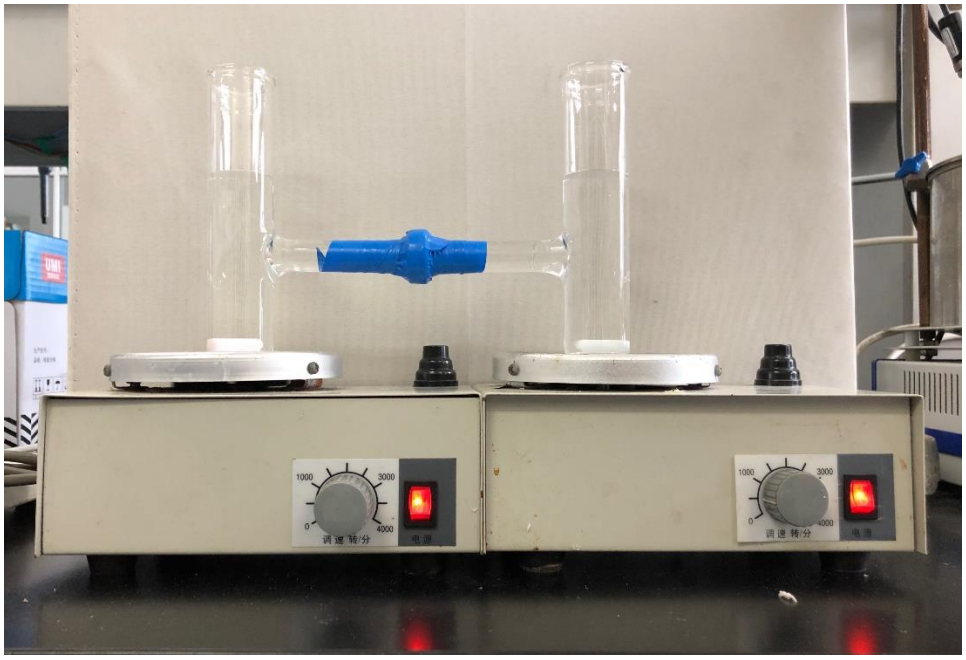

Fig. 4-2 The H-type device for permeation after the experiment

Reference

[1] Leal RMP, Figueira RF, Tornisielo VL, et al. Occurrence and sorption of fluoroquinolones in poultry litters and soils from São Paulo State, Brazil[J]. Sci. Total Environ., 2012, 432: 344-

349.

[2] Hu X, Hu X, Peng Q, et al. Mechanisms underlying the photocatalytic degradation pathway of ciprofloxacin with heterogeneous TiO2[J]. Chem. Eng. J., 2020, 380: 122366.

[3] Movasaghi Z, Yan B, Niu C. Adsorption of ciprofloxacin from water by pretreated oat hulls: Equilibrium, kinetic, and thermodynamic studies[J]. Ind. Crop. Prod., 2019, 127: 237-250.

[4] Zhang G-F, Liu X, Zhang S, et al. Ciprofloxacin derivatives and their antibacterial activities[J]. Eur. J. Med. Chem., 2018, 146: 599-612.

[5] Herold C, Ocker M, Ganslmayer M, et al. Ciprofloxacin induces apoptosis and inhibits proliferation of human colorectal carcinoma cells[J]. Brit. J. Cancer, 2002, 86(3): 443-448.

[6] Zhang C-Z, Ren S-Q, Chang M-X, et al. Resistance mechanisms and fitness of Salmonella Typhimurium and Salmonella Enteritidis mutants evolved under selection with ciprofloxacin in vitro[J]. Sci. Rep.-UK, 2017, 7(1): 9113.

[7] Breda SA, Guzmán ML, Confalonieri A, et al. Systemic exposure, tissue distribution, and disease evolution of a high solubility ciprofloxacin-aluminum complex in a murine model of septicemia induced by salmonella enterica serotype enteritidis[J]. Mol. Pharmaceut., 2013, 10(2): 598-605.

[8] Wang, J., Xu, Y., Li, X., et al. (2017). Residual antibiotics in livestock and poultry manure and their impact on the environment. Animal Husbandry and Veterinary Medicine, 49(10), 140-144.

[9] Van Doorslaer X, Dewulf J, Van Langenhove H, et al. Fluoroquinolone antibiotics: An emerging class of environmental micropollutants[J]. Sci. Total Environ., 2014, 500-501: 250-269.

[10] Babić S, Periša M, Škorić I. Photolytic degradation of norfloxacin, enrofloxacin and ciprofloxacin in various aqueous media[J]. Chemosphere, 2013, 91(11): 1635-1642.

[11] Rosal R, Rodríguez A, Perdigón-Melón JA, et al. Occurrence of emerging pollutants in urban wastewater and their removal through biological treatment followed by ozonation[J].

Water Res., 2010, 44(2): 578-588.

[12] Vieno N, Tuhkanen T, Kronberg L. Elimination of pharmaceuticals in sewage treatment plants in Finland[J]. Water Res., 2007, 41(5): 1001-1012.

[13] Li, H., & Chen, X. (2018). Pollution status and hazards of antibiotics in the environment. China Resources Comprehensive Utilization, 36(5), 82-84+95.

[14] Shao, Y., Xi, B., Cao, J., et al. (2013). Distribution and removal of antibiotics in urban wastewater treatment systems. Environmental Science & Technology, 36(7), 85-92+182.

[15] Wen, H., Shi, J., Xun, H., et al. (2015). Research progress on the distribution, dissemination, and removal of antibiotic resistance genes in aquatic environments. Chinese Journal of Applied Ecology, 26(2), 625-635.

[16] Walsh TR, Weeks J, Livermore DM, et al. Dissemination of NDM-1 positive bacteria in the New Delhi environment and its implications for human health: An environmental point prevalence study[J]. Lancet Infect. Dis., 2011, 11(5): 355-362.

[17] Deng, Y., & Ni, F. (2011). Residual antibiotics in aquatic environments and their hazards. South-to-North Water Diversion and Water Science & Technology, 9(3), 96-100.

[18] Wang, R., Liu, T., & Wang, T. (2006). Fate of antibiotics in the environment and their ecological toxicity. Acta Ecologica Sinica, 26(1), 265-270.

Chapter 5

POLYMERIZATION ADSORPTION MEMBRANE

5.1 Experiment material

5.1.1 Experimental drugs

① Polyvinylidene fluoride (PVDF) was supplied by a local supplier.

Fig. 5-1 The photo of PVDF

② β-Cyclodextrin (β-CD) as shown in the Fig. 5-1.

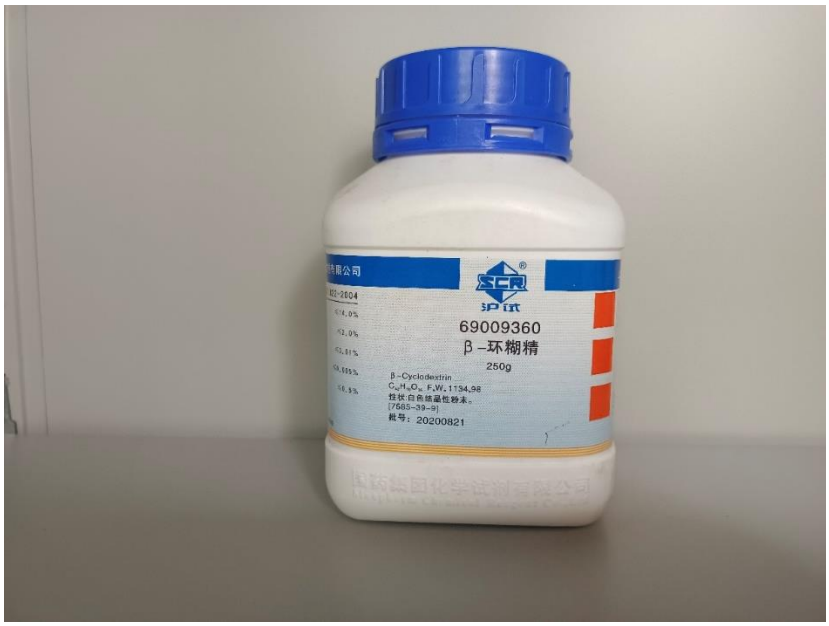

Fig.5-2 The photo of β-CD

③ Dopamine hydrochloride (DA) as shown in the Fig. 5-2.

Fig. 5-3 The photo of DA

④ 3-(trimethoxy silyl) propyl methacrylate (KH570)

Fig. 5-4 The photo of KH570

⑤ Ciprofloxacin hydrochloride (CIP)

⑥ Methyl acrylic acid (MAA) as shown in the Fig. 5-5.

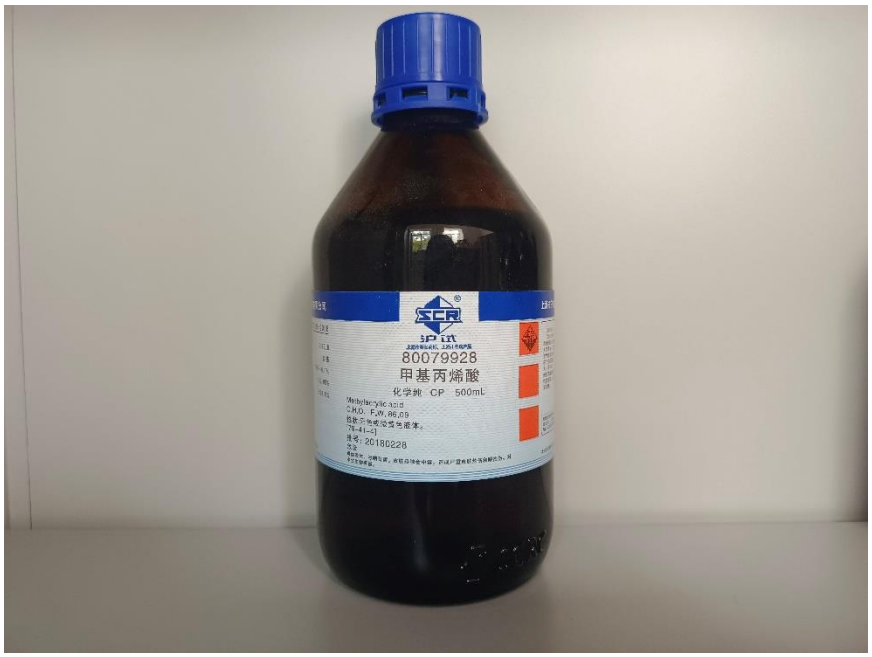

Fig. 5-5 The photo of MAA

⑦ Pentaerythritol tetra(3-mercaptopropionate) (PT3M)

Fig. 5-6 The photo of PT3M

⑧ Di pentaerythritol penta-/hexa-acrylate (DPHA)

Fig. 5-7 The photo of DPHA

⑨ 2,2-dimethoxy-2-phenylacetophenone (DMPA)

⑩ Sodium chloride (NaCl) from Sinopharm Chemical Reagent as shown in the Fig. 5-8.

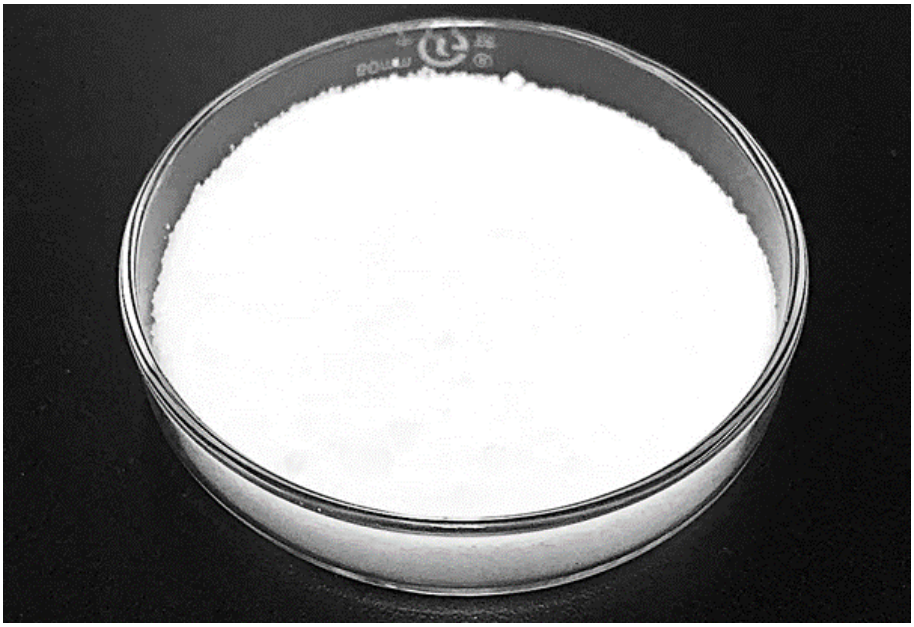

Fig. 5-8 The photo of NaCl

⑪ Ethanol as shown in the Fig. 5-9.

Fig. 5-9 The photo of ethanol

⑫ Acetonitrile as shown in the Fig. 5-10.

Fig. 5-10 The photo of acetonitrile

⑬ Methanol as shown in the Fig. 5-11.

Fig. 5-11 The photo of methanol

⑭ Acetic acid (MAA) as shown in the Fig. 5-12.

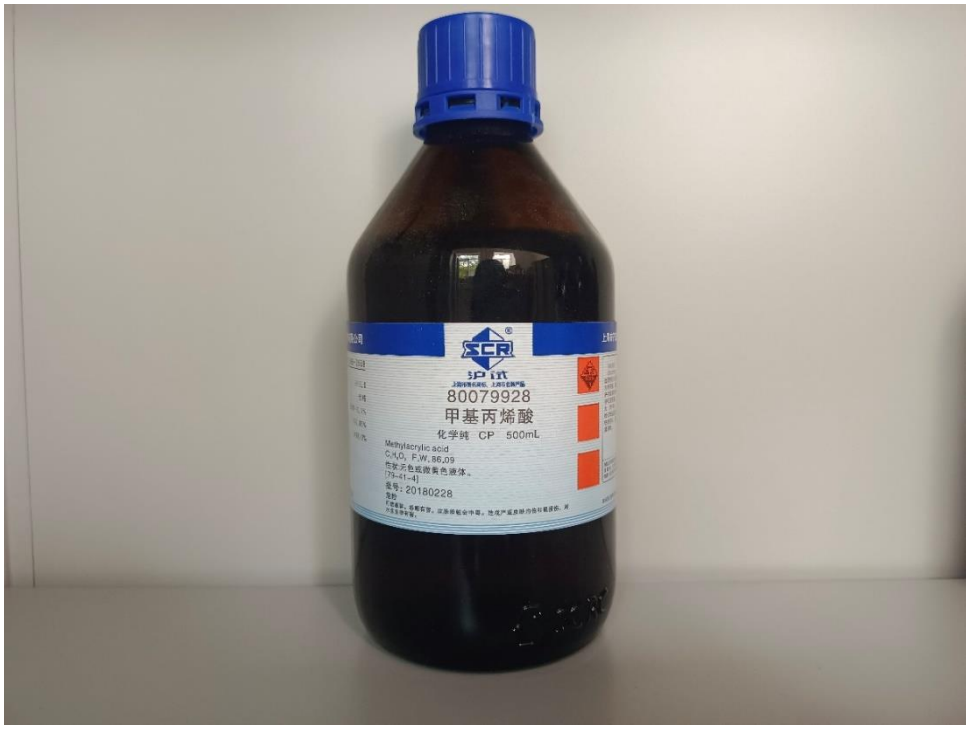

Fig. 5-12 MAA

⑮ Phosphate buffered saline (PBS, pH = 7.4)

5.1.2 Characterization instruments

① The evolution of morphology was investigated by Scanning Electron Microscopy (SEM)

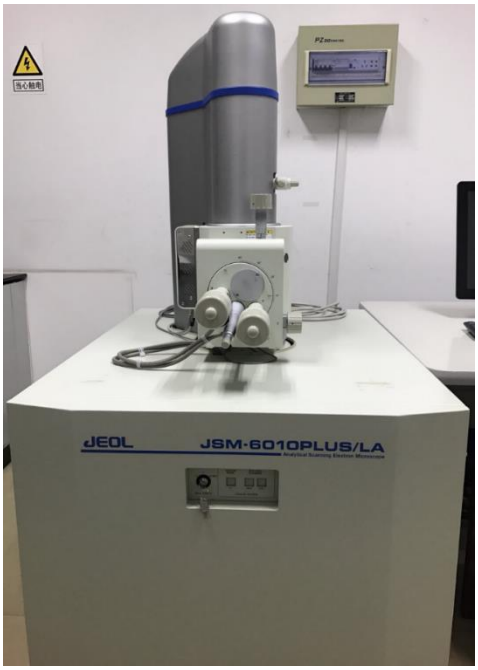

Fig. 5-13 The photo of SEM

② Synthesis of intermediates and products was demonstrated by Fourier-Transform Infrared Spectroscopy (FTIR)

Fig. 5-14 The photo of FTIR

③ Insight on Click-chemistry reaction between functional monomer and crosslinker was explored by in-situ Diffuse Reflection Infrared Fourier Transform Spectroscopy (in-situ DRIFTS)

④ Contact angle meter: Comparison of PDA modified PVDF/β-CD porous membranes based on thermally induced embedding and traditional surface grafting by water contact angles via contact angle meter.

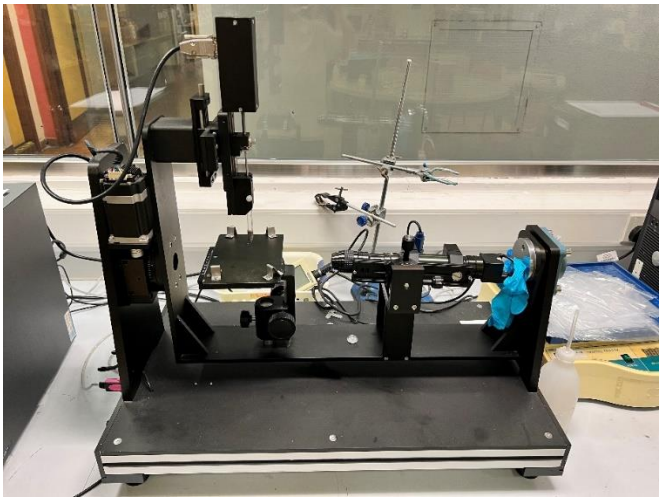

Fig. 5-15 The photo of contact angle meter

⑤ UV-Vis: The concentrations of individual solutes in the solution are determined by UV-Vis detection.

Fig. 5-16 The photo of UV-Vis

5.2 Material Synthesis

5.2.1 VCDM

To conduct the preparation of the membrane, a series of carefully controlled steps were followed.

Firstly, a mixture was prepared by combining 2.0 grams of polyvinylidene fluoride (PVDF), 0.1 grams of β-cyclodextrin (β-CD), and 8.0 grams of sodium chloride (NaCl) particles.

Digital photos of sacrificed templates (NaCl nanoparticles) are shown as blow.

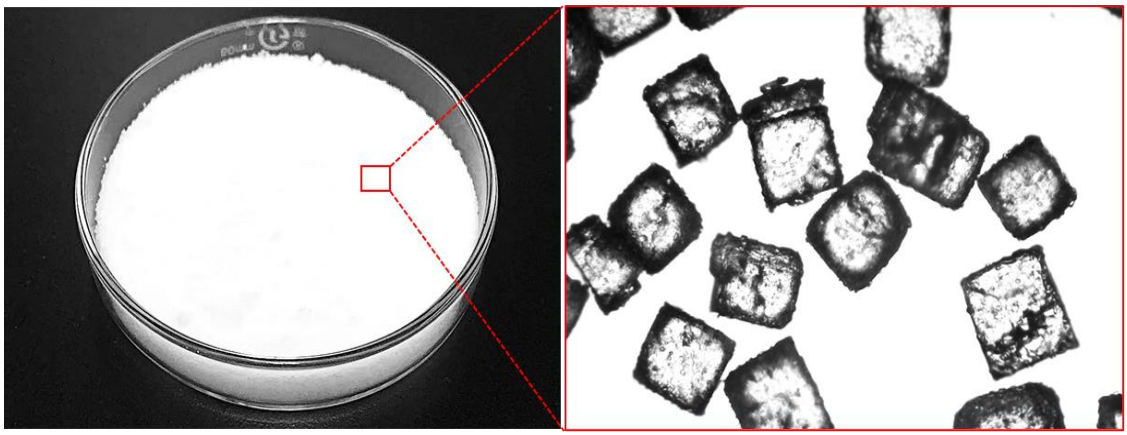

Fig. 5-17 Digital photos of sacrificed templates (NaCl nanoparticles)

The components were meticulously measured to ensure precise ratios and accurate composition. The mixture was then transferred to a Teflon container, which provided a suitable environment for the subsequent steps.

In order to enhance the membrane's properties, 0.05 grams of dopamine hydrochloride (DA) were added to the mixture. The addition of DA served a crucial role in the modification process, as it promoted the formation of functional groups on the surface of the membrane. These functional groups played a vital role in enhancing the adsorption and separation capabilities of the membrane.

Fig. 5-18 Containers for synthetic reactions

The next step involved thorough blending of the mixture to ensure homogeneity and proper distribution of the components. This step required careful attention to detail, as any inconsistencies in blending could result in variations in the membrane's structure and performance. The mixture was blended for a specific duration, allowing for adequate interaction and integration of the different components.

Fig. 5-19 The photo of the oven.

To initiate the transformation of the mixture into a membrane, a carefully controlled heating process was employed. The mixture, meticulously prepared with 2.0 grams of polyvinylidene fluoride (PVDF), 0.1 grams of β-cyclodextrin (β-CD), and 8.0 grams of sodium chloride (NaCl) particles, was subjected to a specific temperature and duration. This crucial step involved heating the mixture to a molten state, precisely maintaining a temperature of 200℃ for a duration of 1.0 hour in the oven shown in Fig. 5-19.

After the heating process, the molten mixture was allowed to cool down gradually, leading to solidification. Once solidified, the next step entailed purifying the membrane to remove the residual NaCl particles. This purification was achieved by subjecting the solidified mixture to a thorough treatment with hot deionized (DI) water. The hot DI water effectively dissolved and washed away the NaCl particles, leaving behind a purified membrane matrix.

Upon completion of the purification process, a visually distinct transformation occurred. The fluffy and porous PVDF/β-CD/PDA membrane (referred to as VCDM) emerged, showcasing its unique structural characteristics. The membrane displayed a well-defined porosity, with interconnected pores providing pathways for efficient mass transfer and filtration.

Fig. 5-20 The photo of the VCDM

To ensure the stability and durability of the VCDM membrane, a meticulous drying process was employed. The membrane was carefully separated from the purification solution and subjected to controlled drying conditions. This drying phase aimed to remove any remaining moisture from the membrane, leading to the attainment of a fully dry and stable VCDM membrane ready for subsequent characterization and performance evaluation.

The comprehensive fabrication process described above involved precise heating, cooling,

purification, and drying steps. Each step played a crucial role in achieving the desired structure, porosity, and performance of the PVDF/β-CD/PDA membrane.

5.2.2 Vinylated VCDM

To introduce vinyl groups onto the VCDM membrane surface, a vinylated modification process was carried out utilizing the hydrolysis of siloxane. The procedure involved a series of meticulously controlled steps, enabling the incorporation of vinyl functionality onto the membrane.

The initial step involved preparing a suitable mixture for the infiltration process. An ethanol solution (80 mL) was combined with deionized (DI) water (20 mL) to create a homogeneous solvent environment. Into this solution, a carefully selected piece of VCDM membrane was immersed, ensuring thorough coverage of the membrane surface.

To initiate the vinylated modification, 3-(trimethoxy silyl) propyl methacrylate (KH570), a key reagent, was introduced into the mixture. Precisely 3.0 mL of KH570 was added, and the entire system was subjected to reflux conditions, employing a controlled temperature of 80℃ for a duration of 16 hours. This reflux process facilitated the hydrolysis of siloxane groups present in KH570, allowing the vinyl moieties to bind to the surface of the VCDM membrane.

Following the vinylation reaction, the resulting vinylated VCDM membrane required purification to eliminate any residual chemical compounds. This purification step involved rinsing the membrane with ethanol and subsequent washing with DI water. These rinsing and washing processes effectively removed any remnants of unreacted reagents, by-products, or impurities, ensuring the integrity and purity of the modified membrane.

To achieve the desired moisture content and stability, the purified vinylated VCDM membrane underwent a carefully controlled drying process. The membrane was subjected to ambient conditions at room temperature (25°C) with a controlled relative humidity of 60%. This drying phase allowed for the gradual evaporation of residual moisture, ensuring a fully dry and stable vinylated VCDM membrane for further characterization and subsequent utilization.

The comprehensive vinylated modification process described above involved meticulous

selection of reagents, controlled reaction conditions, and thorough purification and drying steps. Each step played a vital role in the successful incorporation of vinyl groups onto the VCDM membrane surface. The vinylated VCDM was shown in Fig. 5-21.

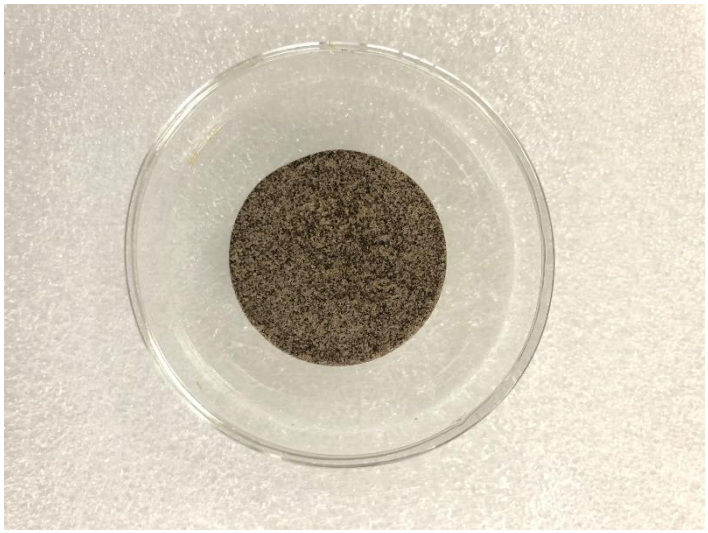

Fig. 5-21 The photo of the Vinylated VCDM

5.2.3 PAM

To initiate the synthesis process, 0.4 mmol of methylacrylic acid (MAA) was dissolved in 75 mL of acetonitrile, creating a homogeneous solution. The solution was subjected to continuous stirring for a period of 60 minutes to ensure complete dissolution and uniformity. This step facilitated the formation of a suitable reaction medium for subsequent reactions.

Following the dissolution of MAA, a carefully selected piece of vinylated VCDM membrane was introduced into the solution. The membrane was added to promote the incorporation of functional groups and enhance the overall reactivity of the system. Additionally, 1.2 mmol of pentaerythritol tetra(3-mercaptopropionate) (PT3M) and 0.4 mmol of dipentaerythritol penta-/hexa-acrylate (DPHA) were sequentially added to the mixed solution. These reagents played critical roles in the subsequent polymerization reaction, contributing to the cross-linking and structural stability of the resulting polymer.

To initiate the polymerization process, 20 mg of 2,2-dimethoxy-2-phenylacetophenone (DMPA) was introduced into the system under a nitrogen atmosphere and in dark conditions. This photoinitiator served as a catalyst, facilitating the generation of reactive species upon

exposure to ultraviolet (UV) light.

The polymerization reaction was initiated by subjecting the reaction mixture to continuous stirring under UV light with a wavelength of 365 nm. This UV irradiation promoted the activation of the photoinitiator and the subsequent cross-linking of the monomers, leading to the formation of the desired polymer network. The reaction proceeded for a duration of 4.0 hours to ensure complete conversion and polymerization of the monomers. The reaction process under ultraviolet (UV) irradiation is conducted in the apparatus shown in Fig. 5-22.

Fig. 5-22 UV irradiation chamber

Upon completion of the polymerization reaction, the resulting polymeric material, known as polymerization adsorption membrane (PAM), required purification to remove any residual reagents or impurities. This purification step involved rinsing the membrane with ethanol, a solvent known for its ability to dissolve organic compounds, followed by washing with deionized (DI) water to ensure the removal of any remaining contaminants.

Finally, the purified polymerization adsorption membrane (PAM) was subjected to a drying process to remove residual moisture and solvents, resulting in a dry and stable polymeric membrane. The dried polymerization adsorption membrane (PAM) exhibited enhanced properties, including improved mechanical strength, chemical stability, and potential applications in various fields such as membrane separations, water treatment, and biomedical applications.

The synthesis of PAM involved a series of carefully controlled steps, including the dissolution of MAA, addition of vinylated VCDM membrane, incorporation of PT3M and

DPHA, introduction of the photoinitiator DMPA, UV-induced polymerization, purification, and drying. Each step played a crucial role in the successful formation of the PAM, with desired properties and potential applications in diverse fields.

5.3 Material Characterization

5.3.1 Synthesis of PAM

A thermally induced approach is proposed for the formation of PAM, which can be described as a three-step synthesis.

① The PDA-embedded interpenetrating-bicontinuous porous membrane was thermally synthesized using a blending and fusing strategy. As a result, an interpenetrating-bicontinuous morphology, consisting of continuous pores and matrix, was achieved on the surface of VCDM (Fig. 5-23).

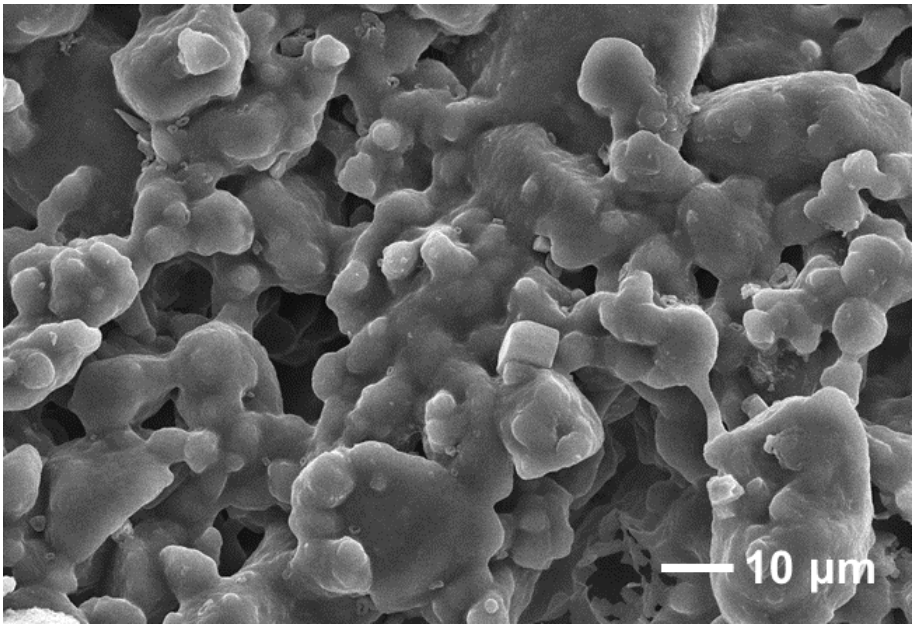

Fig. 5-23 SEM images of VCDM

This synthesis approach allowed for precise control over the structure and morphology of the material, providing a solid foundation for subsequent performance optimization and applications. The interpenetrating-bicontinuous porous structure offers a high surface area and porosity, leading to improved performance and efficiency in applications such as adsorption

and separation.

It profits from the fluxible polymers in a molten state to fill the gaps of sacrificial templates. It is worth noting that although obvious edges exist on sacrificed templates, the obtained continuous matrix is mellow.

For the purpose of demonstration, a comparison was made between the microtopography of the interpenetrating-bicontinuous porous membrane with and without the addition of dopamine (DA) at the same magnification. When the membrane was formed without DA, clear boundaries that were complementary to the NaCl nanoparticles appeared in the microstructure of the matrix (Fig. 5-24).

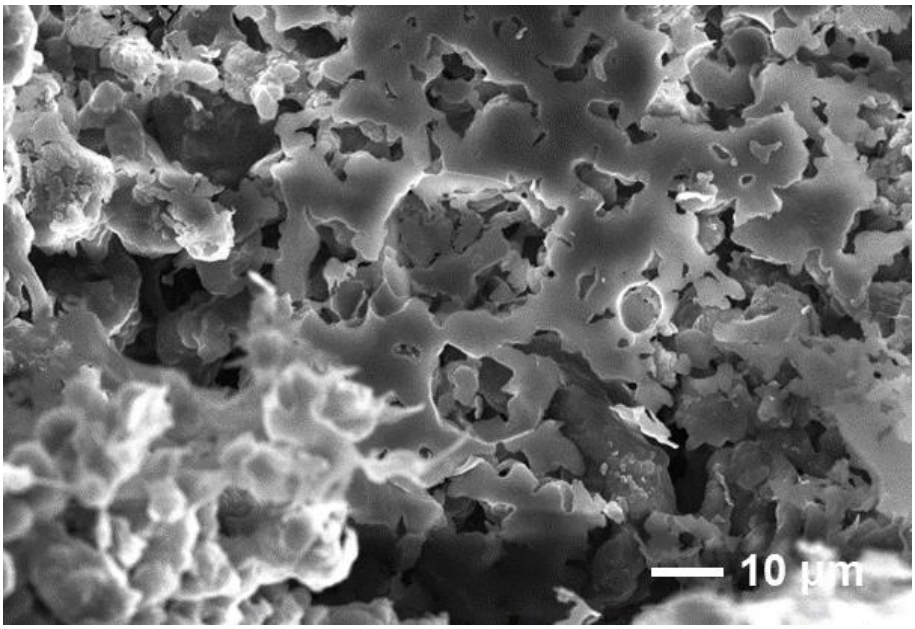

Fig. 5-24 SEM of PVDF/β-CD membrane

However, when DA was added, these boundaries were replaced by smooth radians (Fig. 5-23).

This significant differentiation can be attributed to the unique adhesion of embedded DA, which increases the interaction between PVDF chains and enhances the surface tension of the molten polymers. Consequently, the presence of DA leads to a smoother microtopography. This observation highlights the influence of DA on the morphological characteristics of the membrane, offering insights into the role of DA in the synthesis process and its impact on the

overall structure and properties of the material.

② Subsequently, a vinylated modification process was performed on the VCDM to create a secondary platform for imprinting polymerization. In comparison to the microtopography of the VCDM, there were no noticeable differences observed in the overall microstructure, except for the emergence of new tiny nanoparticles on the surface (Fig. 5-25).

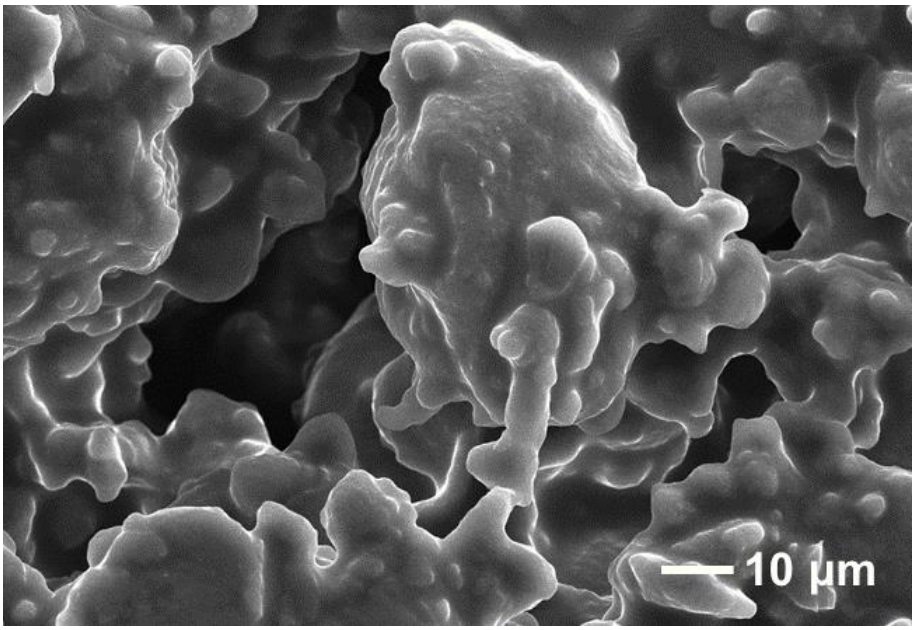

Fig. 5-25 SEM images of vinylated VCDM

This phenomenon suggests that the vinylated modification applied to the VCDM does not induce significant alterations in the interpenetrating-bicontinuous morphology. Despite the presence of the vinylated groups, the overall structure and arrangement of the matrix and pores remained largely unaffected. This observation highlights the compatibility of the vinylated modification approach with the existing morphology of the VCDM, thereby serving as a suitable foundation for subsequent polymerization. The introduction of the tiny nanoparticles on the surface further suggests the successful incorporation of vinyl groups, which may play a crucial role in the subsequent molecular imprinting process.

③ The polymerization process was subsequently conducted utilizing an efficient thiol-ene Click reaction. The resulting microstructure revealed the presence of distinctive irregular nanoparticles dispersed throughout the continuous matrix. These observations serve as

compelling evidence for the formation of polymers through the utilization of Click chemistry, further indicating the successful accomplishment of g polymerization on the vinylated VCDM substrate. The irregularity and distribution of the nanoparticles within the continuous matrix highlight the effectiveness of the polymerization process, as the polymerization reaction occurred selectively within the desired regions of the membrane, resulting in the creation of specific adsorption that are capable of adsorbing antibiotic molecule.

5.3.2 Chemical characterizations

① FTIR

The synthetic route was supplementally analyzed by Fourier Transform Infrared (FTIR) spectra, which provided valuable insights into the chemical composition. The resulting FTIR spectra exhibited distinctive absorption signals at specific wavenumbers, namely 1648, 1457, 1182, and 1064 cm^{-1} (as illustrated in Fig. 5-26).

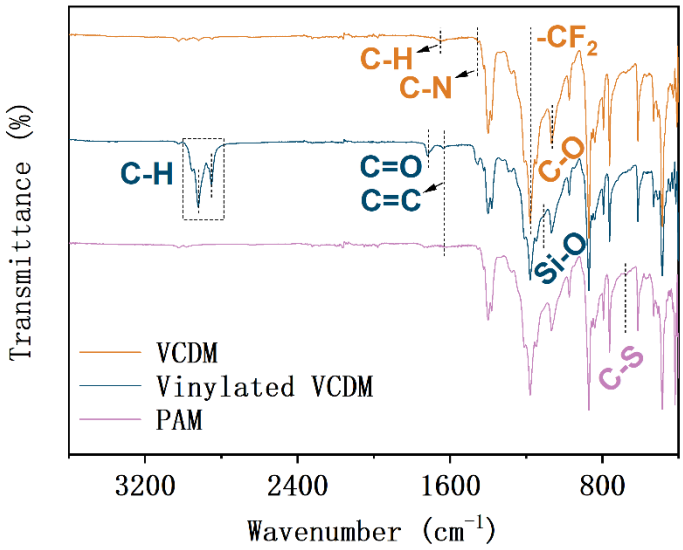

Fig. 5-26 FTIR spectra of obtained membranes

These absorption peaks can be unequivocally attributed to the characteristic vibrations of various chemical components present in the synthesized VCDM. Specifically, the absorption peak at 1648 cm^{-1} corresponds to the C–H vibrations originating from the PVDF component,

while the peak at 1457 cm^{-1} is indicative of C–N vibrations associated with the β-CD component. Furthermore, the absorption peak at 1182 cm^{-1} can be attributed to the $–CF_2$ vibrations stemming from the PVDF component, and the peak at 1064 cm^{-1} represents the C=O vibrations derived from the PDA component. These distinct absorption signals not only confirm the successful synthesis of VCDM but also provide valuable evidence regarding the presence and contribution of PVDF, β-CD, and PDA within the composite material. [1-4]

Comparative analysis of the O-H signal redshift observed on the VCDM substrate, in contrast to pure PVDF, β-CD, and PDA, provides compelling evidence for the stable association and intermolecular interactions among the three components within the mixed matrix (Fig. 5-27) [5].

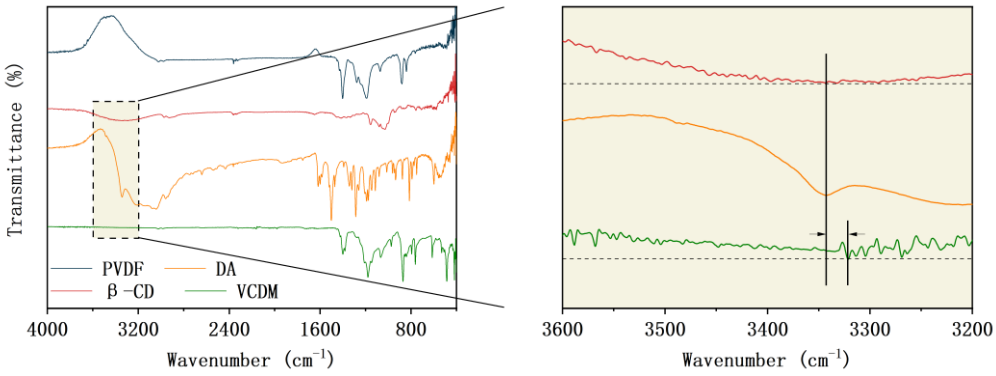

Fig. 5-27 FTIR spectra of PVDF, β-CD, PDA and VCDM

The significant redshift in the O-H signal indicates the formation of robust hydrogen bonds between PVDF, β-CD, and PDA molecules, leading to a cohesive and interconnected network. These intermolecular hydrogen bonds play a vital role in the structural integrity and stability of the VCDM, facilitating enhanced material properties and desirable functionalities. The presence of intermolecular hydrogen bonding not only reinforces the physical interlocking of the components but also contributes to the overall strength and durability of the VCDM, making it a promising candidate for a wide range of applications in various fields. The detailed characterization and analysis of the O-H signal provide valuable insights into the molecular interactions and bonding mechanisms within the VCDM, further supporting its potential for advanced material design and tailored applications.

After the vinylated modification, several new signals are observed in the FTIR spectrum of the VCDM. The appearance of peaks at 2921, 2854, 1718, 1633, and 1109 cm^{-1} signifies the presence of functional groups such as $–CH_3$, $–CH_2$, C=O, C=C, and Si–O, which are consistent with the chemical composition of KH570 [6, 7]. This observation confirms that compounds containing these groups have been successfully grafted onto the VCDM surface.

Furthermore, the presence of these functional groups suggests that the employed functional monomers and crosslinkers have introduced thiol and vinyl groups onto the PAM substrate. The absence of the thiol and vinyl signals in the FTIR spectrum, along with the persistence of the S–C signal at 679 cm^{-1}, strongly indicates the successful polymerization through the thiol-ene Click reaction. The grafted vinyl groups play a crucial role as chemical bridges, facilitating the formation of polymerization onto the interpenetrating-bicontinuous porous membrane.

Another noteworthy observation is the decline of the original vinyl signal on the vinylated VCDM, further confirming the successful formation of the polymerization. This decline can be attributed to the consumption of vinyl groups during the reaction, as they react with the thiol groups to form covalent bonds, resulting in the formation of the desired polymer network.

The comprehensive analysis of the FTIR spectrum provides valuable insights into the chemical modifications and polymerization processes occurring on the VCDM surface. The presence of specific functional groups and the disappearance of certain signals substantiate the successful grafting and polymerization reactions, validating the synthesis of the desired interpenetrating-bicontinuous porous membrane. This detailed understanding of the chemical changes and structural transformations contributes to the characterization and optimization of the VCDM for various applications in fields such as membrane technology, catalysis, and separation science.

To gain deeper insights into the internal mechanism, the polymerization process based on the thiol-ene Click reaction was further investigated using time-dependent in-situ DRIFTS (Diffuse Reflectance Infrared Fourier Transform Spectroscopy) spectra, as shown in Fig. 5-28.

During the progression of the reaction, notable changes in the spectra are observed. Specifically, the S–H (sulfhydryl) and C=C (carbon-carbon double bond) signals display a

negative growth, indicating their consumption over time. Conversely, the S–C (sulfur-carbon) and C–H (carbon-hydrogen) signals exhibit positive growth, suggesting their increasing presence.

These spectroscopic changes provide valuable insights into the underlying mechanisms of the thiol-ene Click reaction. The observed decrease in the S–H and C=C signals suggests the continuous consumption of thiol and vinyl groups, respectively. Simultaneously, the increase in the S–C signal signifies the formation of new S–C groups, which result from the chemical bonding between the thiol and vinyl groups. Furthermore, the rise in the C–H signal can be attributed to the breakage of vinyl groups, leading to the generation of additional carbon-hydrogen bonds.

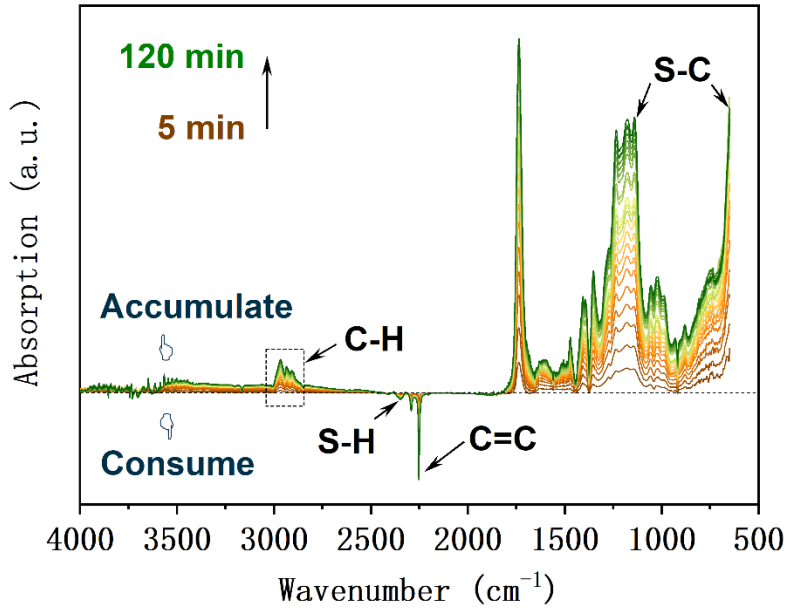

Fig. 5-28 In-situ DRIFTS spectra of the imprinting polymerization based on thiol-ene Click reaction

The observed trends in the time-dependent in-situ DRIFTS spectra align well with the well-established mechanism of the thiol-ene Click reaction. This mechanism involves the reaction between thiol and vinyl groups, leading to the formation of covalent sulfur-carbon bonds (S–C) while consuming thiol and vinyl functionalities. The increase in the C–H signal is consistent with the expected changes in the carbon-hydrogen bonds due to the reaction.

These detailed spectroscopic observations provide valuable insights into the dynamic changes occurring during the thiol-ene Click reaction. The time-dependent in-situ DRIFTS analysis enhances our understanding of the polymerization process, allowing for the optimization of reaction conditions and the control of the resulting polymer structure.

5.3.3 Hydrophilicity

In order to further elucidate the superiority of the PDA-embedded strategy, a detailed comparison was conducted between PDA-modified PVDF/β-CD membranes prepared through thermally induced embedding and traditional surface grafting methods. The focus of the comparison was on investigating the effect on hydrophilicity.

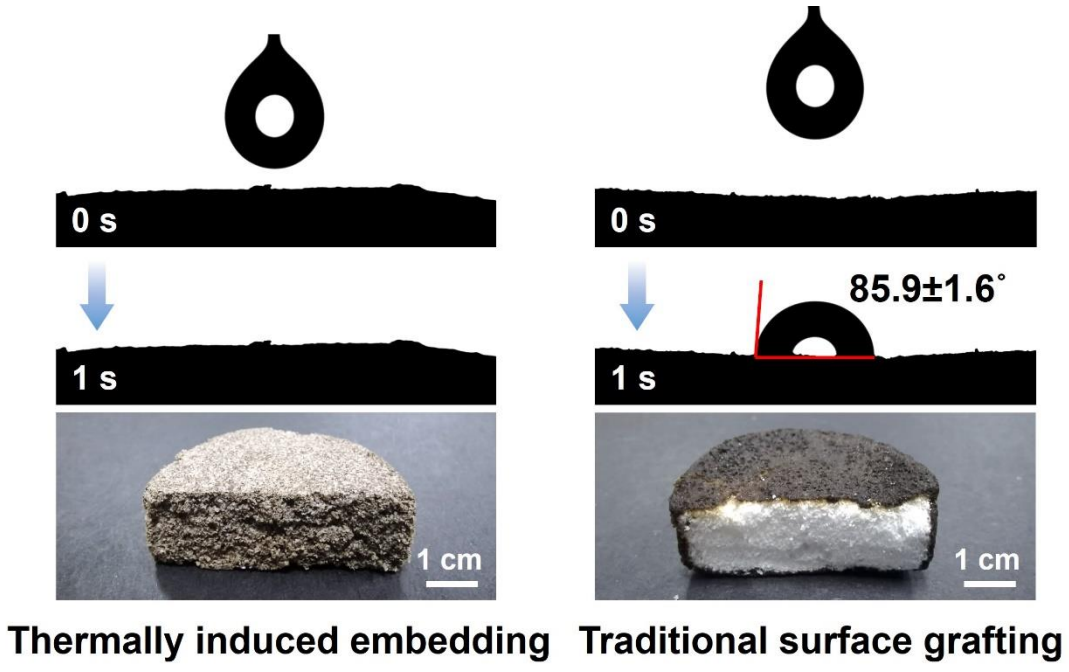

Fig. 5-29 Comparison of PDA modified PVDF/β-CD porous membranes based on thermally induced embedding and traditional surface grafting: water contact angles

To evaluate the hydrophilicity, water contact angles were measured and compared between the two membrane types. As shown in Fig. 5-29, the membrane prepared using the thermally induced embedding strategy exhibited significantly improved hydrophilicity. Upon contact with the membrane, the water droplet was completely absorbed in less than 1 second. In contrast, the membrane prepared through traditional surface grafting retained a water contact angle of

85.9 degrees even after 1 second.

This notable difference can be attributed to the distinct characteristics of the two strategies. The thermally induced embedding strategy ensures the homogeneous distribution of PDA throughout the interpenetrating-bicontinuous porous matrix. Consequently, water molecules can readily enter the pores, leading to rapid absorption. On the other hand, the traditional surface grafting strategy only allows PDA to be grafted onto the shallow surface of the membrane. While this approach does impart some hydrophilicity, it falls short compared to the membrane prepared through thermally induced embedding.

These findings highlight the advantages of the PDA-embedded strategy in achieving enhanced hydrophilicity. The homogeneous distribution of PDA within the membrane matrix enables efficient water absorption, resulting in a significantly reduced water contact angle. In contrast, the traditional surface grafting approach, limited to the membrane surface, is less effective in promoting hydrophilicity. The comparison underscores the superiority of the thermally induced embedding strategy for achieving improved hydrophilicity in PDA-modified PVDF/β-CD membranes.

5.4 Performance Characterization

Isothermal and kinetic absorbing performance was respectively explored for the investigation of absorbing performance.

5.4.1 Isothermal adsorption performance

In the whole range of tested conditions, PAM all exhibited a significant adsorption capacity for CIP molecules. Since PAM is synthesized as a polymer on the membrane surface, its affinity for CIP is based on the interaction between the functional monomer and the target antibiotic molecule.

For the concentration-dependent mode (Fig. 5-30), As the concentration of ciprofloxacin solution increased, the uptake of CIP by PAM was accompanied by an increase. As the concentration of ciprofloxacin solution increased, the uptake of CIP by PAM was accompanied by an increase. This elevation tended to stagnate after the concentration exceeded to 150 mg L^{-}

[1]. This indicates that the polymers synthesized on the membranes do play a role in the adsorption of ciprofloxacin molecules.

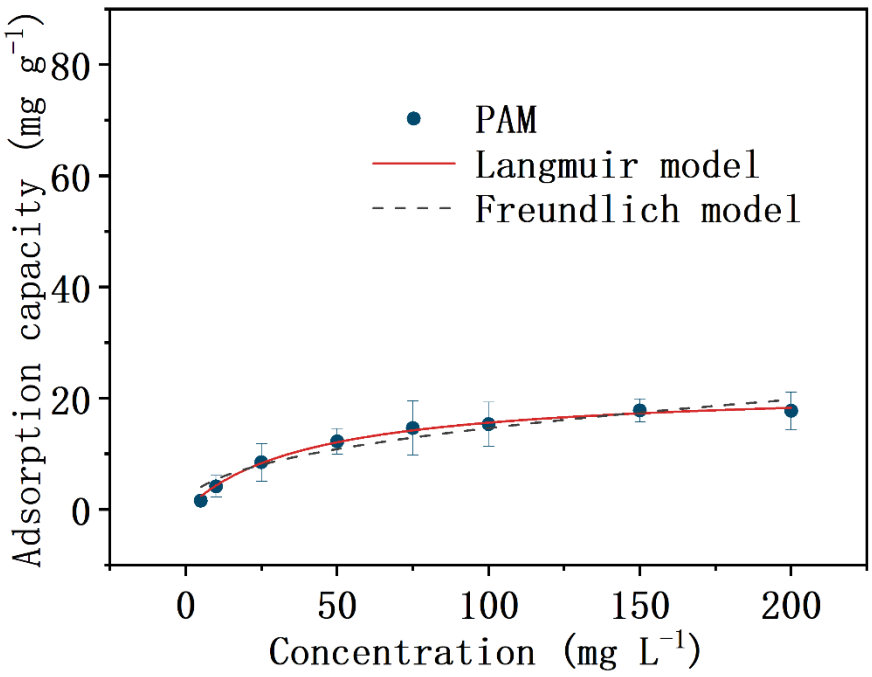

Fig. 5-30 Adsorption capacities of PAM with fitted isothermal models

Adsorption data are then fitted with Langmuir [8] (Fig. 5-31) and Freundlich (Fig. 5-32) isothermal models, respectively.

Table 5-1. Constants of isothermal adsorption onto PAM

Membrane	Langmuir[a]			Freundlich[b]		
	Q_m	K_L	R^2	K_F	$1/n$	R^2
PAM	22.04	0.0243	0.9952	2.0097	0.4311	0.9390

[a] Langmuir model is expressed as $Q_e=(Q_mK_LC_e)/(1+K_LC_e)$, where C_e (mg L^{-1}) and Q_e (mg g^{-1}) are concentration and rebinding capacity at equilibrium, Q_m (mg g^{-1}) is the theoretical maximum rebinding capacity, and K_L (L mg^{-1}) is the Langmuir constant.

[b] Freundlich model is expressed as $Q_e=K_FC_e^{1/n}$, where C_e (mg L^{-1}) and Q_e (mg g^{-1}) are concentration and rebinding capacity at equilibrium, as well as K_F (mg$^{1-1/n}$ L$^{1/n}$ g^{-1}) and n are

Freundlich constants.

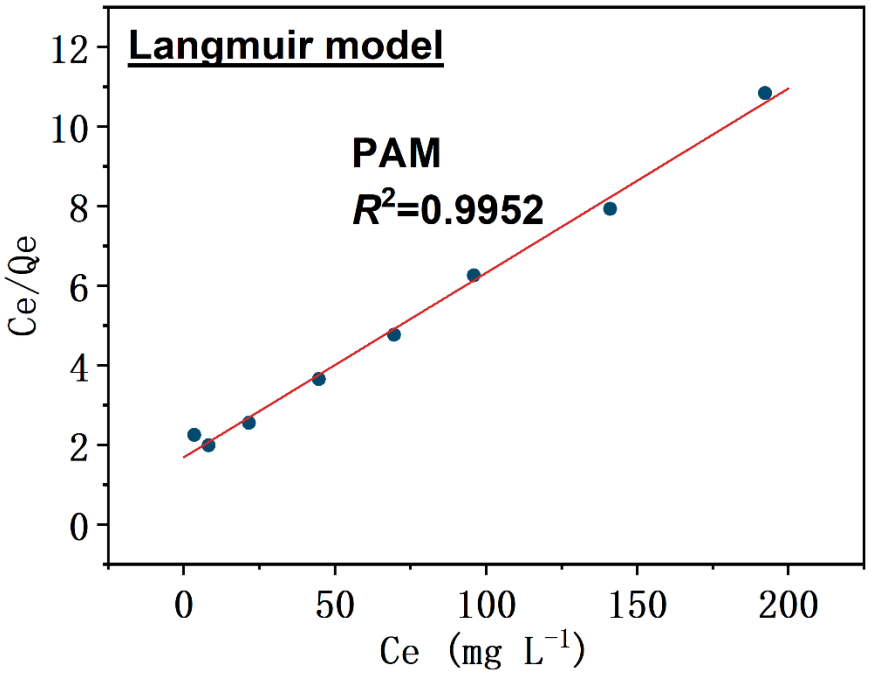

Fig. 5-31 Linear fitting of Langmuir models

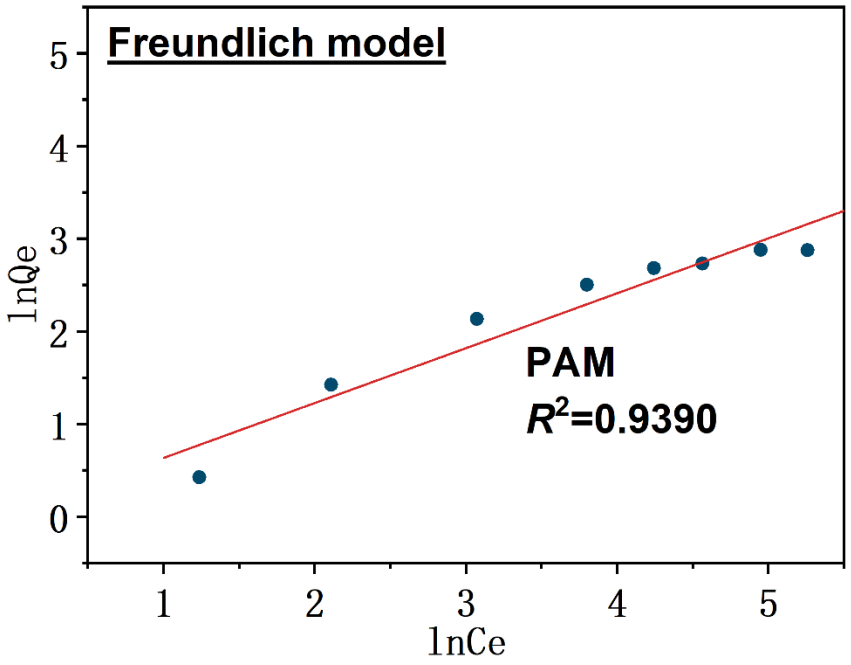

Fig. 5-32 Linear fitting of Freundlich models

According to constants in Table 5-1, adsorption data of PAM fit better with the Langmuir model ($R^2 = 0.9952$) than the Freundlich model ($R^2 = 0.9390$). This indicates that the adsorption sites on the PAM exhibit a uniform and monolayer distribution [9].

5.4.2 Kinetic absorbing performance

For the time-dependent model (Fig. 5-33), a similar trend from the concentration-dependent model appears on PAM.

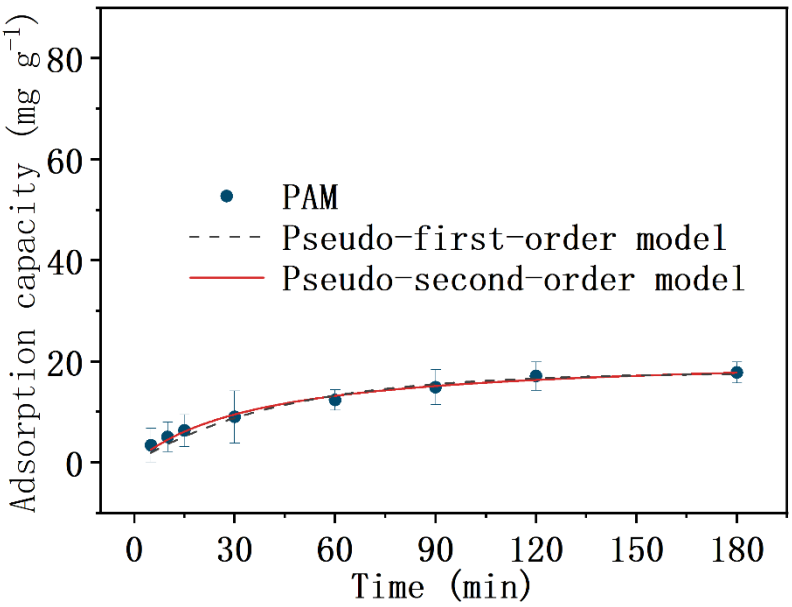

Fig. 5-33 Adsorption capacities of PAM with fitted kinetic models

Its adsorption capacity has been steadily increasing from the beginning, with the upward trend slowing down at 120 minutes of adsorption time, and the growth of adsorption capacity tending to plateau at 180 minutes of adsorption time. This phenomenon proves that the polymer layer on the membrane surface acts as an adsorption agent for the absorption of CIP molecules.

Adsorption data are, then, fitted with Pseudo-first-order [10] (Fig. 5-34) and Pseudo-second-order [11] (Fig. 5-35) model, respectively.

From fitting results in Table 5-2, adsorption data of PAM show better relevancy with the Pseudo-second-order model (R^2=0.9897) than the pseudo-first-order model (R^2=0.9642), suggesting that the adsorption onto PAM is determined by both chemisorption and physical

diffusion [12]. This further corroborates the specific adsorption of ciprofloxacin molecules by the polymer layer on the membrane surface.

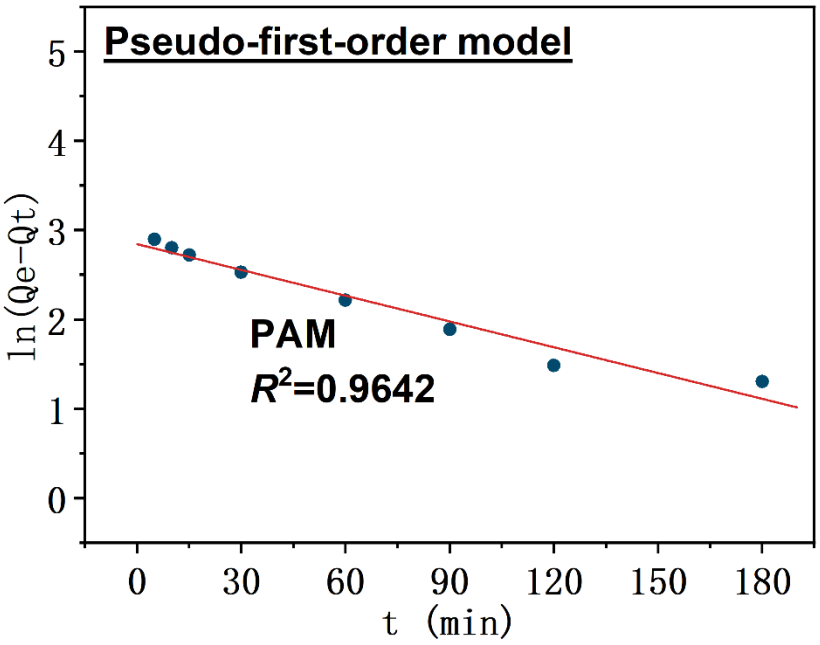

Fig. 5-34 Linear fitting of Pseudo-first-order models

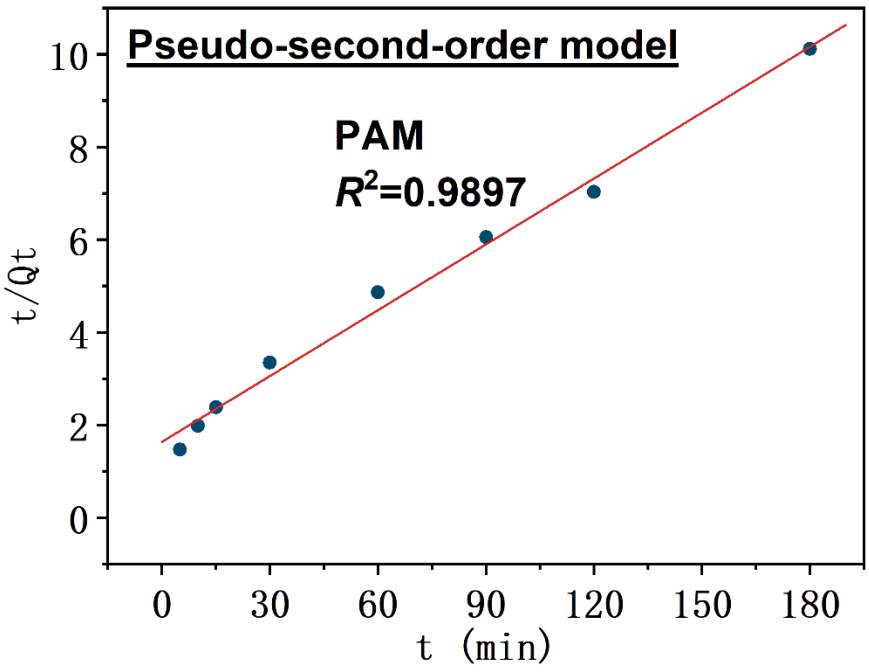

Fig. 5-35 Linear fitting of Pseudo-second-order models

Table 5-2. Constants of kinetic adsorption onto PAM.

Membrane	Pseudo-first-order[a]			Pseudo-second-order[b]		
	Q_e	k'	R^2	Q_e	k''	R^2
PAM	17.80	0.0227	0.9642	21.48	0.0012	0.9897

[a] Pseudo-first-order model is expressed by $Q_t=Q_e-Q_e e^{-k't}$, where Q_e and Q_t (mg g^{-1}) are rebinding capacities at the equilibrium and time t (min), and k' (min^{-1}) is the equilibrium rate constants of the pseudo-first-order model.

[b] Pseudo-second-order model is expressed as $Q_t=(k''Q_e^2t)/(1+k''Q_et)$, where Q_e and Q_t (mg g^{-1}) are rebinding capacities at the equilibrium and time t (min), as well as k'' (g mg^{-1} min^{-1}) is the equilibrium rate constants of the pseudo-second-order model.

5.4.3 Permeation performance

A solution with 10mg L^{-1} of CIP was employed for the permeation investigations. The typical static permeation was performed on PAM. The experimental setup and the experimental procedure are shown in Fig. 5-36 and Fig. 5-37.

A piece of PAM was tailored and placed between two flanges of the H-shaped tube. Two compartments separated by the membrane were filled with 100 mL of mixed solution (10 mg L–1 of CIP) and pure solvent (deionized water), respectively. Samples were taken from each chamber at a pre-determined time (0-48 h), where the concentration of solutes was measured by UV-Vis at 275 nm (CIP).

Fig. 5-38 shows the evolution of concentration in permeate and dialysate of PAM.

The time of permeation equilibrium appeared in the 24th hour after the start of permeation, and the concentration of permeation equilibrium was less than 5 mg L^{-1}, which proved that there was adsorption of PAM to CIP during the permeation process, indicating that the polymer layer on the surface of PAM did have adsorption function for CIP molecules.

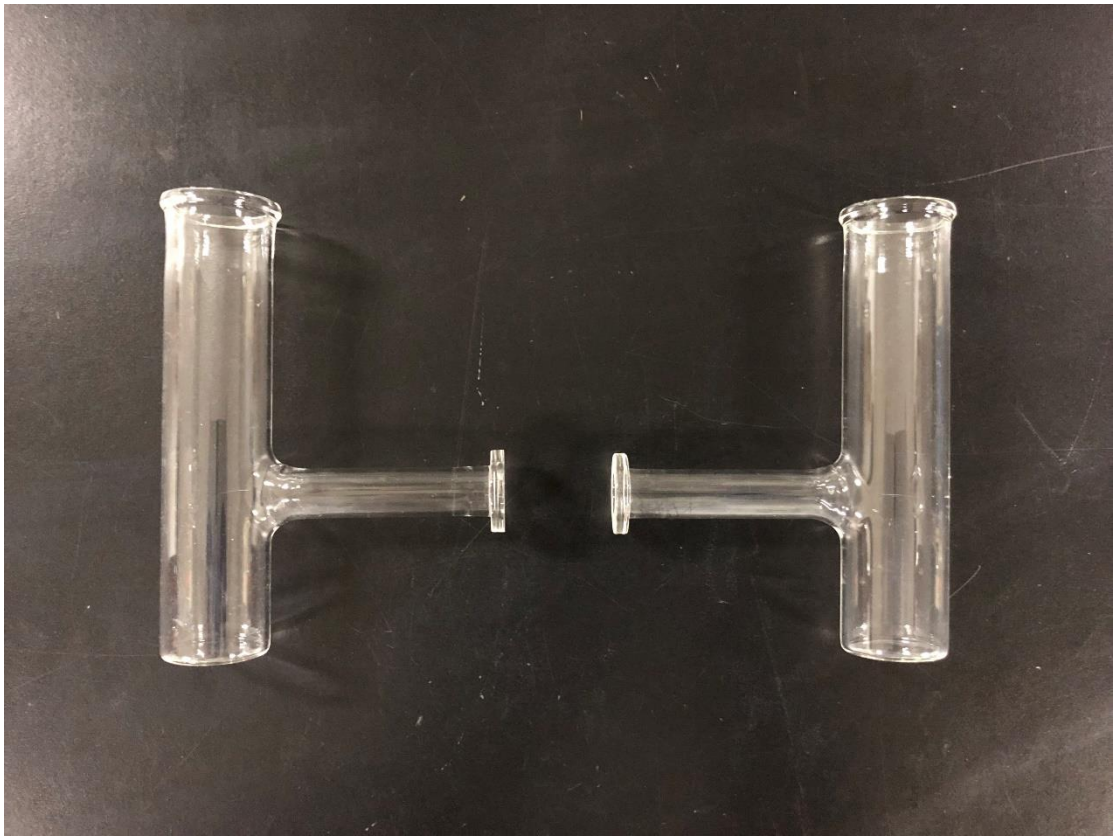

Fig. 5-36 Schematics illustrating the device for permeation before experiments

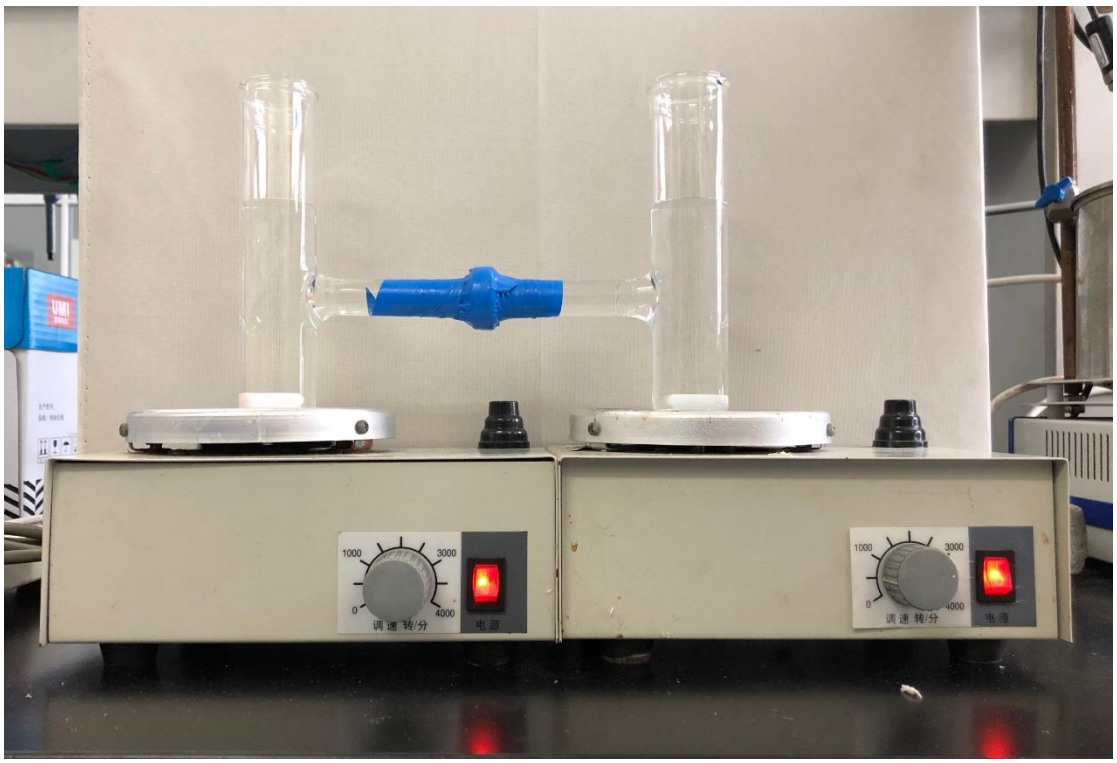

Fig. 5-37 Schematics illustrating the device for permeation during experiments

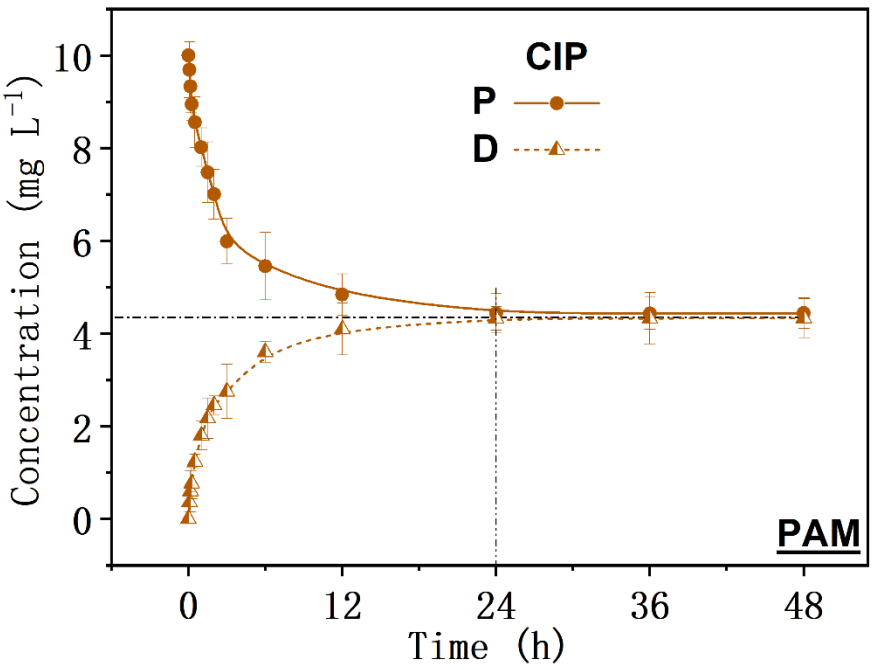

Fig. 5-38 Permeation performance of PAM

Reference

[1] C. Deng, C. Cao, Y. Zhang, J. Hu, Y. Gong, M. Zheng, Y. Zhou, Formation and stabilization mechanism of β-cyclodextrin inclusion complex with C10 aroma molecules, Food Hydrocolloid. 123 (2022) 107013.

[2] J. Lu, Y.-Y. Qin, Y.-L. Wu, M.-N. Chen, C. Sun, Z.-X. Han, Y.-S. Yan, C.-X. Li, Y. Yan, Mimetic-core-shell design on molecularly imprinted membranes providing an antifouling and high-selective surface, Chem. Eng. J. 417 (2021) 128085.

[3] S. Türk, E. Yılmaz, An innovative layer-by-layer coated titanium hydroxide-(gentamicin-polydopamine) as a hybrid drug delivery platform, J. Drug. Deliv. Sci. Tec. 67 (2022) 102943.

[4] H. Yin, C. Wang, J. Yue, Y. Deng, S. Jiao, Y. Zhao, J. Zhou, T. Cao, Optimization and characterization of 1,8-cineole/hydroxypropyl-β-cyclodextrin inclusion complex and study of its release kinetics, Food Hydrocolloid. 110 (2021) 106159.

[5] J. Zhao, W. Wang, P. Fu, J. Wang, F. Gao, Evaluation of the spontaneous combustion of

soaked coal based on a temperature-programmed test system and in-situ FTIR, Fuel 294 (2021) 120583.

[6] Y. Hao, F. Liu, H. Shi, E. Han, Z. Wang, The influence of ultra-fine glass fibers on the mechanical and anticorrosion properties of epoxy coatings, Prog. Org. Coat. 71 (2011) 188-197.

[7] B.L. Zhu, H. Zheng, J. Wang, J. Ma, J. Wu, R. Wu, Tailoring of thermal and dielectric properties of LDPE-matrix composites by the volume fraction, density, and surface modification of hollow glass microsphere filler, Compos. Part. B-Eng. 58 (2014) 91-102.

[8] B. Park, S.H. Yun, C.Y. Cho, Y.C. Kim, J.C. Shin, H.G. Jeon, Y.H. Huh, I. Hwang, K.Y. Baik, Y.I. Lee, H.S. Uhm, G.S. Cho, E.H. Choi, Surface plasmon excitation in semitransparent inverted polymer photovoltaic devices and their applications as label-free optical sensors, Light: Sci. Appl. 3 (2014) e222-e222.

[9] J. Lu, Y. Wu, X. Lin, J. Gao, H. Dong, L. Chen, Y. Qin, L. Wang, Y. Yan, Anti-fouling and thermosensitive ion-imprinted nanocomposite membranes based on grapheme oxide and silicon dioxide for selectively separating europium ions, J. Hazard. Mater. 353 (2018) 244-253.

[10] F. Pincella, K. Isozaki, K. Miki, A visible light-driven plasmonic photocatalyst, Light: Sci. Appl. 3 (2014) e133-e133.

[11] Y. Qin, H. Li, J. Lu, Y. Yan, Z. Lu, X. Liu, Enhanced photocatalytic performance of MoS2 modified by AgVO3 from improved generation of reactive oxygen species, Chinese J. Catal. 39 (2018) 1470-1483.

[12] J. Lu, Y. Qin, C. Yu, X. Lin, M. Meng, Y. Yan, H. Fan, Y. Wu, C. Li, Stable, regenerable and 3D macroporous Pd (II)-imprinted membranes for efficient treatment of electroplating wastewater, Sep. Purif. Technol. 235 (2020) 116220.

Chapter 6

MOLECULARLY IMPRINTED MEMBRANE

6.1 Selective removal of antibiotics

Although the performance characterization of the constructed PAM in the previous chapter has demonstrated its surface polymer layer's adsorption capability towards antibiotic molecules, this removal process lacks specificity. Considering that the predominant types of antibiotic contamination may vary during different seasons and periods, actual medical facility wastewater often contains multiple antibiotics simultaneously, with one or several types being the major constituents, present at significantly higher concentrations compared to other antibiotic species. Moreover, those antibiotics present at low concentrations are already at relatively safe levels and do not require specific treatment.

Therefore, in the indiscriminate treatment process, these low-concentration antibiotics, which do not require treatment, compete for adsorption sites with the high-concentration antibiotics that actually need to be treated. This competition hinders the effective removal of high-concentration antibiotics, resulting in the inefficient utilization of treatment resources. Hence, considering the actual scenario, it becomes crucial to design and construct membranes with specific adsorption properties tailored for a particular antibiotic species.

Consequently, I propose incorporating molecular imprinting technology onto the PAM, to synthesize molecularly imprinted membranes with selective adsorption properties towards specific antibiotic molecules. This approach would enable targeted and efficient removal of the desired high-concentration antibiotics during the treatment process of medical facility wastewater.

6.1.1 Molecular Imprinting Technology (MIT)

Molecular Imprinting Technology (MIT) is a technology that simulates the recognition of molecules in nature, such as “antibody” and “antigen”, “enzyme” and “substrate”. Molecularly imprinted polymers (MIPs) with specific recognition properties at the binding site and spatial structure that exactly match the target molecule. MIPs are a novel technique to produce molecularly imprinted polymers (MIPs) with specific recognition properties at binding sites and spatial structures that exactly match the target molecules. These recognition sites are highly

compatible with the template molecules in terms of size, spatial structure, and binding sites, and can selectively recognize and bind the template molecules at the molecular level. The most important features of this technology are conformational predetermination, specific recognition, and wide practicality, and the MIPs prepared from it have been widely used in chromatographic analysis, adsorption separation, selective catalysis, and targeted release. The intersection and coupling between multiple disciplines can generate novel technologies based on creativity and high efficiency, therefore, combining MIT and PAM to prepare specific selective separation membranes is one of the new development directions of molecular imprinting. As a novel separation technique that couples the advantages of MIT and PAM, Molecularly Imprinted Membranes (MIMs) have been developed and applied significantly in recent years.

In this context, the coupling of Molecularly Imprinting Technology (MIT) and PAM offers the possibility to achieve selective separation at the molecular scale.

MIT has attracted a lot of attention in the past half century because of its natural “receptor-ligand” interaction mechanism and relatively simple preparation process.

The process mechanism of MIT can be summarized as follows [1, 2]: the template molecule first self-assembles with the functional monomer by non-covalent or reversible covalent bonding, and the resulting complex is copolymerized with a suitable cross-linker to form a polymer, and the template molecule is subsequently removed from the cross-linked polymer using physicochemical methods to obtain specific binding sites with shapes, sizes, and interactions matching those of the target molecule (Fig. 6-1).

Since 1972, when Wulff and Sarhan [3] first synthesized artificial receptors based on MIT, MIT has been considered one of the most effective methods for integrating specific molecular recognition sites into polymer networks or other substrate surfaces.

Since molecularly imprinted materials tend to have good mechanical, thermodynamic and chemical stability properties, they have been widely introduced into numerous research areas such as separations (including chromatographic separations, capillary electrophoresis separations, solid phase extraction separations and membrane separations), immunoassays, antibody mimics, artificial enzymes, biosensors, catalysis, organic synthesis, drug delivery and

drug development [4, 5].

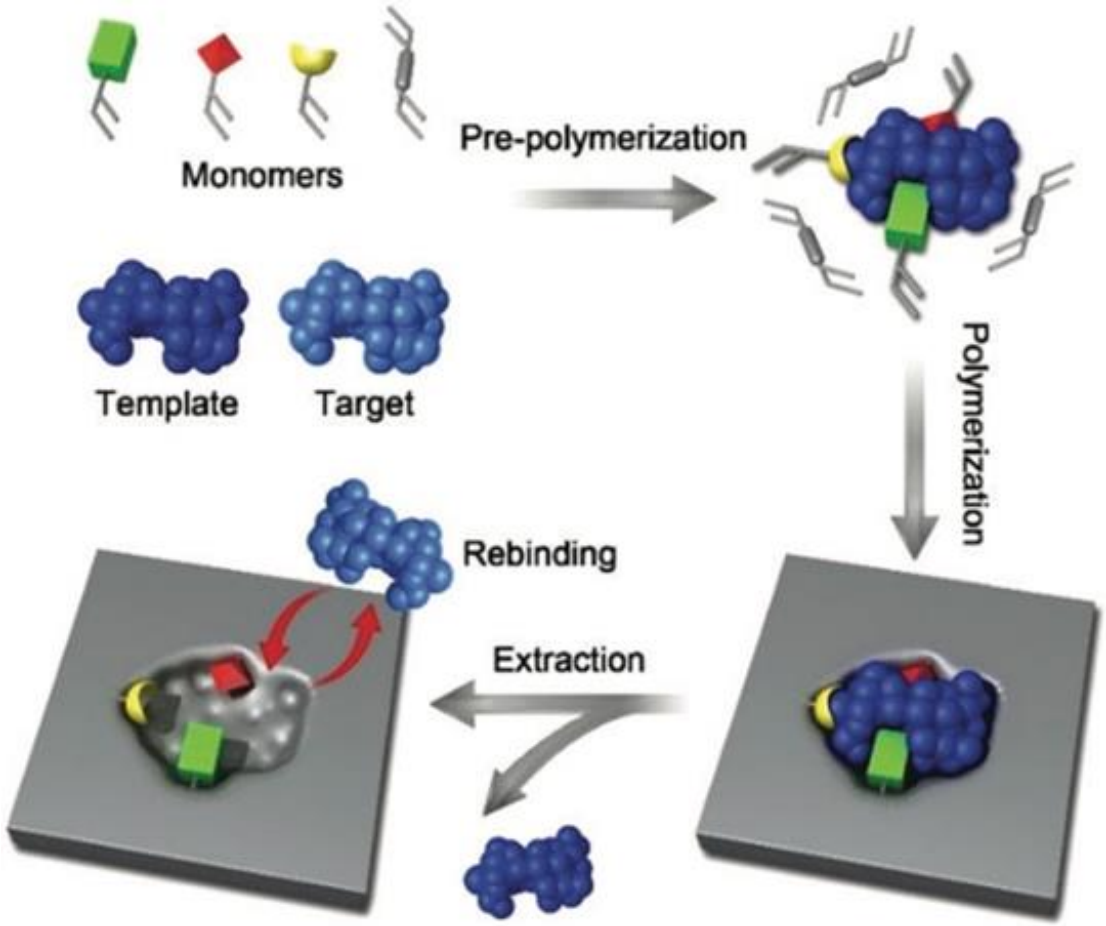

Fig. 6-1 The schematic mechanism of molecular imprinting technology.

6.1.2 Molecularly imprinted membranes (MIMs)

Molecules are the basic units of matter, and molecular interactions are everywhere, and the study of these interactions is an important direction of scientific research at this stage, and this type of research is receiving more and more attention as technology advances. Molecular blotting is one such technique that mimics the specific binding mechanism of antigens and antibodies based on intermolecular forces. It is a cutting-edge technology that can be used to prepare polymers that perfectly match the spatial structure and binding sites of a specified target template molecule, and has attracted much attention due to its ability to selectively separate certain compounds, especially in complex biological samples in recent years. Polymers with specific recognition and selective adsorption to a specific target (template molecule) and its structural analogues, prepared by molecular imprinting, are called molecularly imprinted

polymers.

The origin of molecular blotting date back to the middle of the twentieth century, when Pauling proposed the "antigen formation theory" in his book, in which he argued that during the formation of an antibody, its three-dimensional structure tries to form as many binding sites as possible with the antigen, and in this process the antigen is “mosaicked” into the antibody like a template [6]. In this process, the antigen is “embedded” in the antibody like a template. Although Pauling's “antigen formation theory” was eventually rejected by the theory of “clonal selection”, it became the theoretical basis for the molecular blotting technique. Based on the “antigen formation theory”, Dickey proposed the concept of “specific adsorption” in 1949 and prepared blotting silica that could specifically adsorb dye molecules [7, 8].

This research was an important marker for the emergence of molecular imprinted technology, and this imprinted silica is the first synthetic molecular imprinted material. With the introduction of the concept of “specific adsorption”, molecular blotting entered a phase of rapid development two decades later. The most influential of these was the preparation of molecularly imprinted polymers specific for the chiral isomers of glycolic acid by covalent polymerization in 1972 by a team led by Wulff. In covalent polymerization, the molecularly imprinted polymers are covalently bonded to the template molecules, and the molecularly imprinted polymers are structurally stable after adsorption of the template molecules, which makes the elution of these molecularly imprinted polymers very difficult and does not facilitate the diffusion of molecular imprinted technology.

Starting in the 1980s, Mosbash's team successfully prepared molecularly imprinted polymers using theophylline molecules as templates by a non-covalent method, and this research was published in the journal Nature, and the widespread use of non-covalent methods in molecular imprinting technology led to a tremendous development. After that, molecular imprinting technology entered a phase of rapid development and the Society of Molecularly Imprinting (SMI) was established in Sweden in 1997.

At present, the research on molecular imprinting is not only limited to small molecules as templates, but also reports on molecularly imprinted polymers prepared from biomolecules

such as peptides and proteins. The application of molecular blotting technology has also evolved from the original application to the separation and purification of samples to the crossover with different disciplines and fields of technology, and has been applied to more research directions such as membrane separation and sensors [9-11].

Molecularly imprinted membranes are generally constructed by filling or synthesizing molecularly imprinted polymers with molecular recognition sites on the surface and in the pores of membranes.

Depending on the preparation strategies, molecularly imprinted membranes can be classified as filling type molecularly imprinted membranes, free-standing type molecularly imprinted membranes, hybrid type molecularly imprinted membranes and composite type molecularly imprinted membranes.

① Filling type molecularly imprinted membranes

Filling type molecularly imprinted membranes are the simplest form of molecularly imprinted membranes, consisting of end membranes (filter plates) and packing (molecularly imprinted polymers) and are prototyped as filled columns.

Due to the diversity of fillers, filling type molecularly imprinted membranes can achieve simultaneous adsorption separation of multiple target molecules by the strategy of filling with multiple molecularly imprinted polymers.

In addition, due to the simple preparation method of filled MIMs, they are theoretically very favorable for industrial applications. The first filling type molecularly imprinted membranes were successfully obtained as early as 2002 by filling molecularly imprinted polymers between two filter plates [12, 13].

Filling type molecularly imprinted membranes, despite their early beginnings, have been rarely reported in recent years and their development has come to a near standstill. The main reason for this is that the morphology and structure of molecularly imprinted recognition sites are easily damaged during the grinding and crushing of molecularly imprinted polymers, which drastically affects their actual performance [14, 15]. Therefore, filling type molecularly

imprinted membranes are now rarely used in practical industrial separations.

② Free-standing type molecularly imprinted membranes

Free-standing type molecularly imprinted membranes, in contrast to filling type molecularly imprinted membranes, have no additional support structure and directly form membrane-like structures with cross-linked molecularly imprinted polymers.

The usual preparation process is: firstly, the molecularly imprinted polymer is added to the dispersed phase, and the highly cross-linked molecularly imprinted polymer is obtained by precipitation polymerization and in situ polymerization, and then the solvent is removed in combination with filtration to obtain the molecularly imprinted polymer layer with a membrane-like structure [16-18].

Although free-standing molecularly imprinted membranes compensate for the shortcomings of filling type molecularly imprinted membranes, the construction of such molecularly imprinted membranes usually requires a high degree of cross-linking of molecularly imprinted polymers to ensure the selectivity of the resulting MIMs, which makes self-supporting MIMs tend to have poor stability, low porosity, and permeation flux.

In order to remedy the above shortcomings, some research works have improved the construction strategy of free-standing molecularly imprinted membranes by introducing micro- and nanomaterials to assist in the synthesis of free-standing molecularly imprinted membranes: firstly, molecularly imprinted polymer layers are synthesized on the surface of micro- and nanomaterials (such as carbon nanotubes, metal oxide nanowires, graphene oxide, carbon nitride and biofibers), so that the resulting micro and nanocomposites form spatial three-dimensional channels when cross-linked into a membrane, and then molecularly imprinted polymers can be distributed on the inner walls of the spatial three-dimensional channels to improve the number of effective sites and membrane flux of conventional free-standing molecularly imprinted membranes.

③ Hybrid molecularly imprinted membranes

Hybrid molecularly imprinted membranes are a kind of molecularly imprinted membranes obtained by hybrid membrane matrix and molecularly imprinted polymers to make membranes and are a derivative type of filled molecularly imprinted membranes.

The hybrid of membrane matrix and molecularly imprinted polymers helps to improve the structural stability of the resulting molecularly imprinted membranes, while combining the simplicity of the preparation process.

The preparation process can be summarized as follows: firstly, synthetic molecularly imprinted polymers are prepared or molecularly imprinted polymers are loaded on the surface of other micro- and nanocarrier materials and added to the cast membrane solution composed of membrane matrix materials, and after modeling, the co-mingled molecularly imprinted membranes are obtained by volatile solvent and phase conversion operations [19].

During the hybrid membrane formation process, the molecularly imprinted polymers have uniform and stable structural properties with the membrane matrix due to the presence of bonding, coordination, van der Waals forces, and confinement, which effectively compensate for the shortcomings of self-supporting molecular imprinted membrane.

Although these MIMs have strong stability as well as uniform site dispersion, site encapsulation is always a challenge for co-mingled MIMs, and the relatively few exposed sites greatly limit the overall adsorption capacity and selectivity of the membrane compared to the large number of sites encapsulated within the membrane matrix.

Despite the above-mentioned shortcomings, the simple preparation process and stable overall structure still show irreplaceable advantages. Therefore, up to now, hybrid MIMs are still the most widely studied and applied kind of MIMs.

6.1.3 Mechanism of mass transfer in molecularly imprinted membranes

So far, the selectivity principle based on MIMs can be summarized in two models with opposing modes of action [20]: the solution-diffusion model (inhibition of target penetration model) and the “Gate” model (facilitation of target penetration model), whose mechanisms of action are shown in Fig. 6-2.

① Solution-diffusion model

The solution diffusion model is the mainstream model describing the selectivity principle of MIMs, which specifies that when the target and non-target molecules diffuse near the molecular imprinting site, the strong affinity between the site and the target molecules enables the target molecules to be rapidly adsorbed by the site, while the non-target molecules interact with the site weakly and are not easily captured by the site, and this difference is used to inhibit the penetration of the target molecules in the mixed solution to the other side of the membrane to achieve selective separation, purification, concentration, etc.

In this theoretical model, saturation adsorption is the main determinant of the performance of MIMs, and therefore, the regeneration of MIMs is mainly dependent on the effective elution of the adsorbed target molecules.

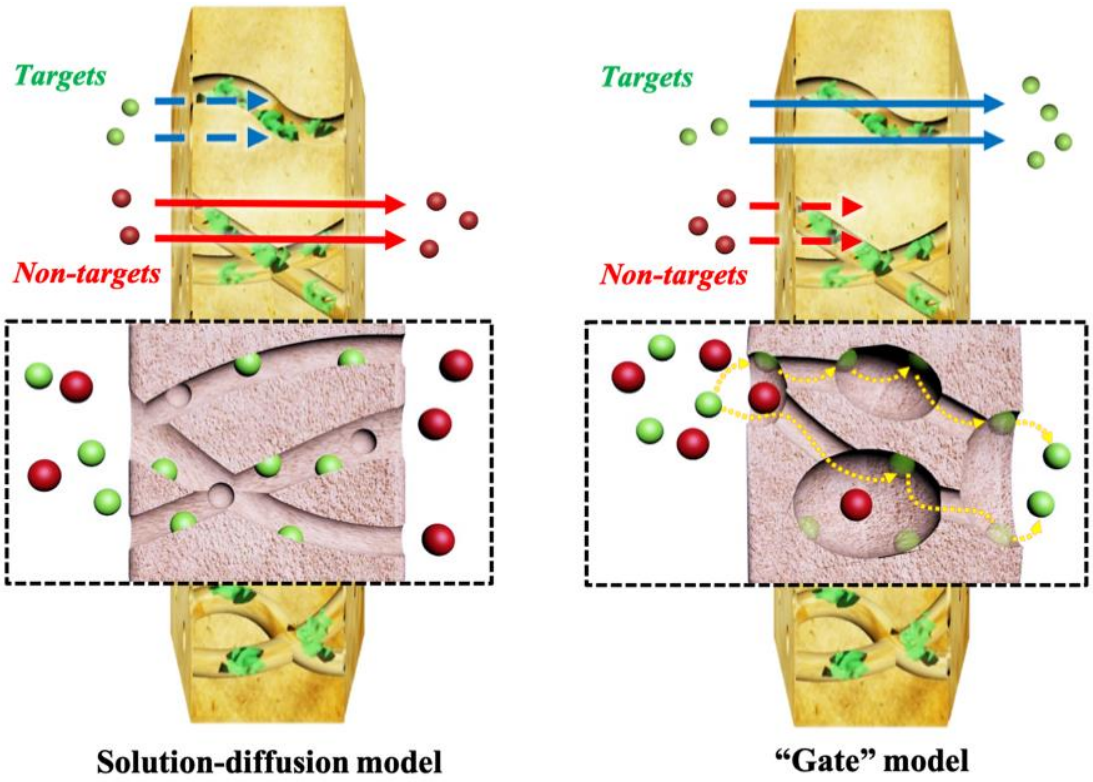

Fig. 6-2 The schematic mechanisms of selective separation onto MIMs.

② “Gate” model

The "gate" model is a descriptive model as opposed to the solvent diffusion model and was

first proposed by Piletsky et al. [21]. It is specified as follows: due to the specific interaction between the target molecule and the molecularly imprinted site, the site prefers to bind to the target molecule and is less likely to bind to the non-target molecule. This strong interaction becomes the driving force that induces the rapid transfer of the target molecule from one site to another and thus behaves as a facilitator of penetration for it.

For non-target molecules, their permeation is driven by diffusion only, and thus, target molecules will pass through the membrane in preference to non-target molecules for the purpose of separation. In this model, although MIMs are not subject to site-adsorption saturation, concentration polarization becomes a key factor affecting the performance of MIMs. Therefore, effective anti-fouling modification and immediate flushing of MIMs are effective methods to achieve their sustainable applications.

6.2 Experiment material

6.2.1 Experimental drugs

① Polyvinylidene fluoride (PVDF) as shown in Fig. 6-3.

Fig. 6-3 The photo of PVDF

② β-Cyclodextrin (β-CD) as shown in Fig. 6-4.

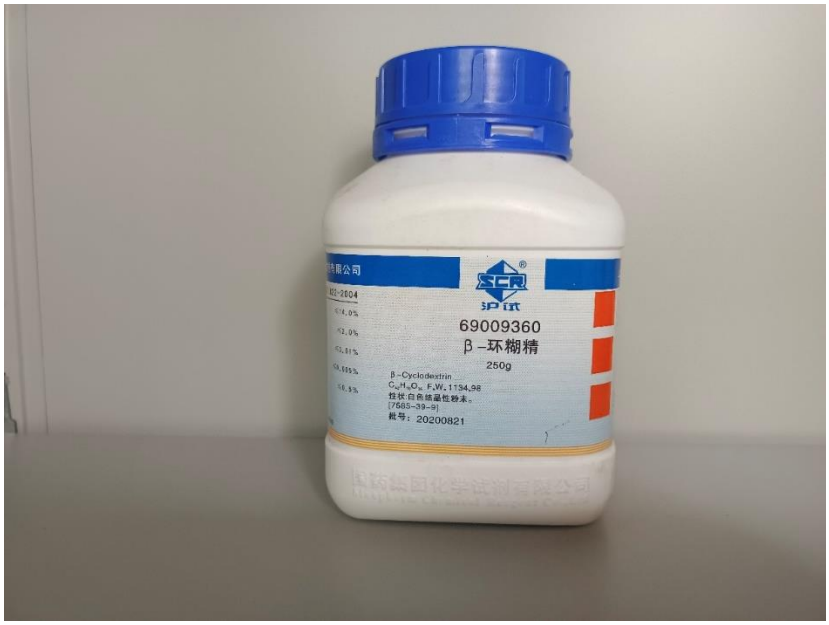

Fig.6-4 The photo of β-CD

③ Dopamine hydrochloride (DA) as shown in the Fig. 6-5.

Fig. 6-5 The photo of DA

④ 3-(trimethoxy silyl) propyl methacrylate (KH570)

Fig. 6-6 The photo of KH570

⑤ Ciprofloxacin hydrochloride (CIP)

⑥ Methyl acrylic acid (MAA) as shown in Fig. 6-7.

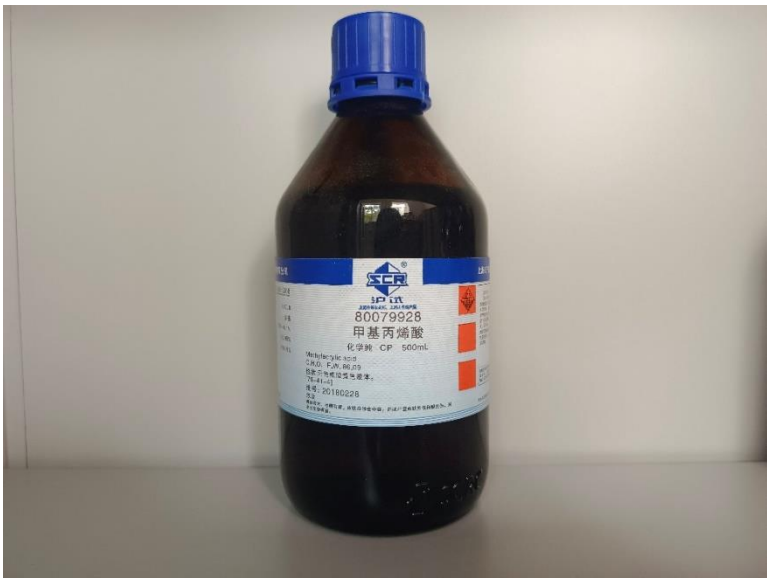

Fig. 6-7 The photo of MAA

⑦ Pentaerythritol tetra(3-mercaptopropionate) (PT3M) as shown in Fig. 6-8.

Fig. 6-8 The photo of PT3M

⑧ Di pentaerythritol penta-/hexa-acrylate (DPHA)

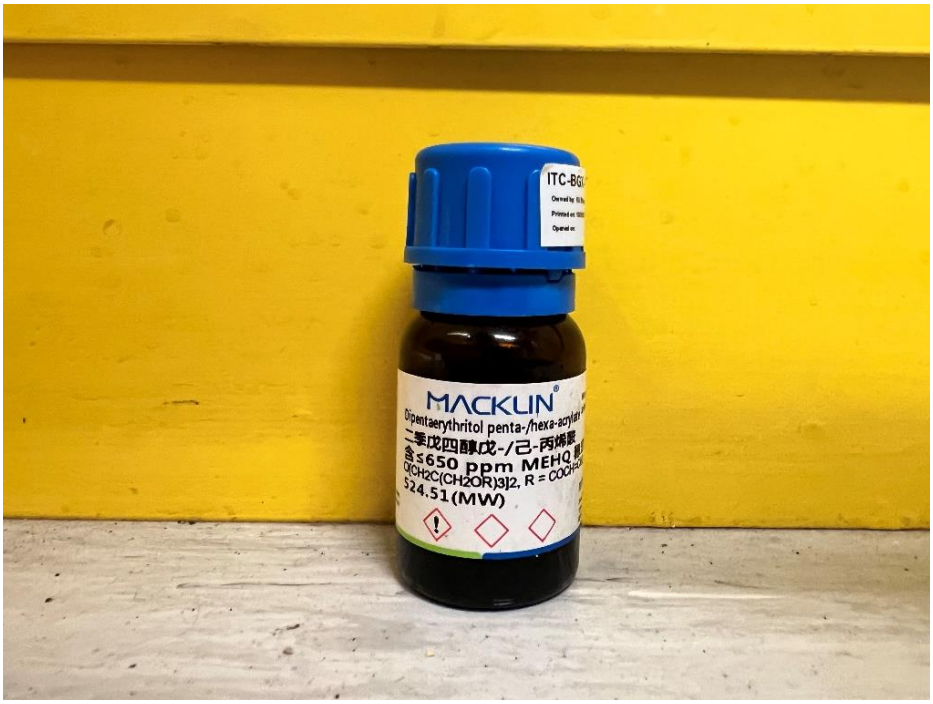

Fig. 6-9 The photo of DPHA

⑨ 2,2-dimethoxy-2-phenylacetophenone (DMPA)

⑩ Sodium chloride (NaCl).

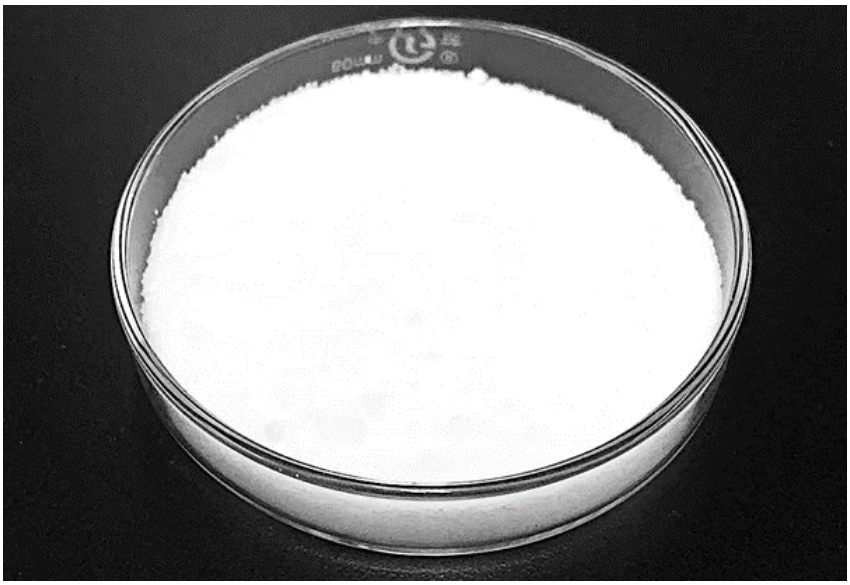

Fig. 6-10 The photo of NaCl

⑪ Ethanol (95%) as shown in the Fig. 6-11.

Fig. 6-11 The photo of ethanol

⑫ Acetonitrile as shown in the Fig. 6-12.

Fig. 6-12 The photo of acetonitrile

⑬ Methanol as shown in the Fig. 6-13.

Fig. 6-13 The photo of methanol

⑭ Acetic acid (MAA) as shown in the Fig. 6-14.

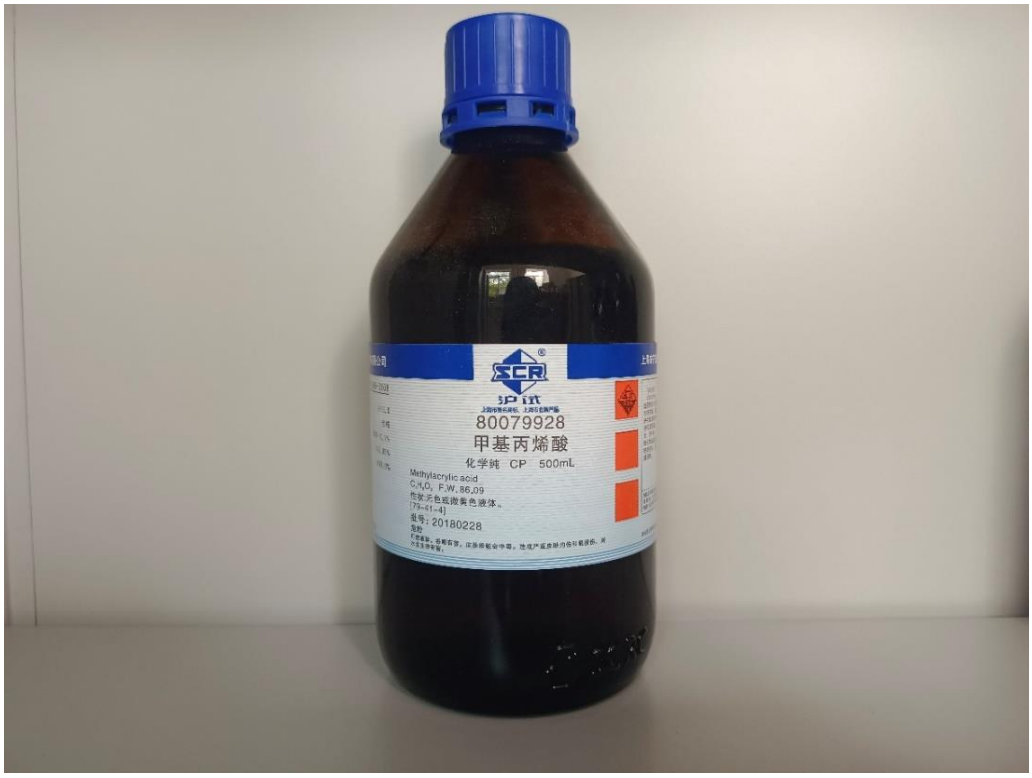

Fig. 6-14 The photo of MAA

⑮ Phosphate buffered saline (PBS, pH=7.4)

6.2.2 Characterization instruments

① The evolution of morphology and elemental mapping images was investigated by Scanning Electron Microscopy (SEM)

② Synthesis of intermediates and products was demonstrated by X-Ray Photoelectron Spectroscopy (XPS)

③ UV-Vis and 1H NMR: The interactions between templates and functional monomers was analyzed based on UV-Vis spectrophotometer (UV-Vis) and 1H Nuclear Magnetic Resonance Spectrometer (1H NMR). The concentration of each component in the performance test was measured by UV-Vis.

Fig. 6-15 The photo of UV-Vis

6.3 Material Synthesis

6.3.1 VCDM

To initiate the synthesis, meticulous measurements were carried out by combining 2.0 grams of polyvinylidene fluoride (PVDF), 0.1 grams of β-cyclodextrin (β-CD), and 8.0 grams of sodium chloride (NaCl) particles within a Teflon container. To enhance the membrane's properties, 0.05 grams of dopamine hydrochloride (DA) were introduced to the mixture, followed by a thorough blending process. The resultant mixture underwent a carefully controlled heating procedure, employing a Muffle furnace set at 200℃ for a duration of 1.0 hour, ensuring the formation of a molten state.

Subsequently, with a gradual cooling process, the molten mixture solidified, forming a cohesive mass. To remove the sodium chloride (NaCl) particles from the solidified mixture, a purification step was performed, involving the use of hot deionized (DI) water. This purification process efficiently eliminated the NaCl particles, resulting in a purified mixture.

Upon completion of the purification step, the mixture transformed into a fluffy and porous membrane, known as the PVDF/β-CD/polydopamine (PDA) membrane or VCDM. To finalize the synthesis process, the VCDM membrane underwent a carefully controlled drying process, facilitating the removal of any remaining solvents or moisture. Finally, after the drying

procedure, the resulting membrane, characterized by its fluffy and porous nature, was successfully obtained, ready to be utilized in various applications.

6.3.2 Vinylated process

The next step involved the implementation of vinylated modification on the VCDM membrane, utilizing the hydrolysis of siloxane as the basis. To initiate this process, a carefully prepared mixture consisting of 80 mL of ethanol and 20 mL of deionized (DI) water was utilized. Within this mixture, a piece of the VCDM membrane was carefully infiltrated, ensuring proper contact and distribution.

To facilitate the vinylated modification, 3.0 mL of 3-(trimethoxysilyl)propyl methacrylate (KH570) was added to the mixture. The resulting mixture was then subjected to reflux, employing a heating temperature of 80℃ for a duration of 16 hours. This reflux process promoted the hydrolysis of siloxane and the subsequent incorporation of vinyl groups onto the surface of the VCDM membrane, resulting in the formation of vinylated VCDM.

Following the vinylation process, the vinylated VCDM membrane underwent a purification step to eliminate any chemical residues. This purification involved the use of ethanol and DI water, ensuring the removal of any unwanted impurities or by-products.

To complete the synthesis process, the purified vinylated VCDM membrane underwent a drying process at room temperature (25°C) with a relative humidity of 60%. This controlled drying process allowed for the removal of residual solvents and moisture, resulting in a stable and dry membrane ready for further characterization and application.

6.3.3 Molecular imprinting process

In a typical synthesis procedure, the first step involved the dissolution of 0.1 mmol of CIP (template molecule) and 0.4 mmol of methylacrylic acid (MAA) in 75 mL of acetonitrile. This solvent facilitated the mixing and solubilization of the components, creating a homogeneous solution. The resulting mixture was then subjected to stirring for a duration of 60 minutes to ensure proper interaction and distribution of the dissolved species.

Following the stirring step, a vinylated VCDM membrane, prepared in advance, was

carefully immersed into the mixed solution. The addition of 1.2 mmol of pentaerythritol tetra(3-mercaptopropionate) (PT3M) and 0.4 mmol of dipentaerythritol penta-/hexa-acrylate (DPHA) followed in a sequential and orderly manner. This precise addition of components aimed to establish a controlled environment for subsequent reactions.

To initiate the molecular imprinting process, 20 mg of 2,2-dimethoxy-2-phenylacetophenone (DMPA), a photosensitive compound, was introduced to the solution under the protection of nitrogen and in dark conditions. This step ensured the initiation of the polymerization reaction under specific conditions.

Once the components were assembled, stirring under ultraviolet light (365 nm) was carried out for a period of 4.0 hours. The ultraviolet light served as the activating agent, promoting the polymerization and cross-linking of the monomers, resulting in the formation of a molecularly imprinted membrane (MIM).

After completion of the polymerization process, the obtained membrane was subjected to purification to remove impurities. This purification step involved successive treatments with ethanol and deionized (DI) water, effectively eliminating any residual substances that may affect the membrane's properties.

To remove the template molecules, the purified membrane was further treated with an eluant consisting of a mixture of methanol and acetic acid in a specific ratio (Vmethanol/Vacetic acid = 95/5). This eluant selectively washed away the template molecules, leaving behind the imprinted sites on the membrane, which retained their recognition capabilities.

Finally, the MIM membrane underwent a drying process, allowing for the complete removal of moisture. This drying step was performed under controlled conditions, such as ambient temperature, and resulted in the final product, a fully functional molecularly imprinted membrane (MIM), ready for further applications and evaluations.

6.4 Material Characterization

6.4.1 Material synthesis

The overall reaction process is like that of PAM, a thermally induced approach is proposed for the formation of MIM, which can be described as a three-step synthesis:

① The PDA-embedded interpenetrating-bicontinuous porous membrane was synthesized using a blending and fusing approach, utilizing thermal methods. This synthesis strategy resulted in the successful formation of an interpenetrating-bicontinuous morphology, characterized by a continuous pore and matrix structure on the VCDM substrate. This achievement was made possible by leveraging the flexibility of the polymers in their molten state, allowing them to fill the voids left by sacrificial templates.

It is noteworthy that despite the presence of noticeable edges on the sacrificed templates, the resulting continuous matrix exhibited a smooth and uniform appearance. To illustrate this, a comparison was made between the microtopography of the interpenetrating-bicontinuous porous membrane with and without the addition of DA, using the same magnification. In the microstructure of the matrix formed without DA, distinct boundaries were observed, which aligned with the NaCl nanoparticles. However, with the incorporation of DA, these boundaries were replaced by smooth curves.

This significant difference can be attributed to the unique adhesion properties of the embedded DA, which increases the interaction between PVDF chains and enhances the surface tension of the molten polymers. Consequently, this interaction leads to a smoother microtopography, as evidenced by the absence of clear boundaries and the presence of smooth curves.

Overall, the thermal synthesis approach involving the blending and fusing strategy, along with the incorporation of DA, resulted in the successful formation of a PDA-embedded interpenetrating-bicontinuous porous membrane, exhibiting a uniform and smooth microtopography.

② Afterward, a vinylated modification was carefully conducted on the VCDM substrate to establish a secondary platform that facilitates imprinting polymerization. When examining the microtopography of the modified VCDM, noticeable differentiations were not observed, except

for the emergence of minuscule nanoparticles on the surface. This intriguing phenomenon suggests that the vinylated modification applied to the VCDM does not induce any significant alterations in its interpenetrating-bicontinuous morphology. Hence, it can be inferred that the introduction of the vinylated modification does not disrupt the overall structure and integrity of the interpenetrating-bicontinuous porous membrane.

③ The imprinting polymerization process was carried out utilizing the highly efficient thiol-ene Click reaction. As depicted in Fig. 6-16, the presence of irregular nanoparticles scattered across the continuous matrix provides clear evidence of polymer formation through Click chemistry. This observation strongly supports the successful implementation of imprinting polymerization on the vinylated VCDM substrate. Further analysis, as shown in Fig. 6-17, Fig. 6-18, Fig. 6-19 reveals the elemental mapping images of the resulting MIM. The uniform distribution of elements such as C, F, N, and O signifies the excellent dispersity and compatibility of β-CD and PDA within the PVDF matrix. Similarly, the presence of Si and S elements indicates the uniform vinylated modification and imprinting polymerization achieved on the VCDM substrate. The comparable coverage of Si and S elements further verifies the effective role of KH570 as a chemical bridge, exerting precise control over the molecularly imprinted polymers (MIPs). This comprehensive elemental mapping supports the overall success and reliability of the imprinting process.

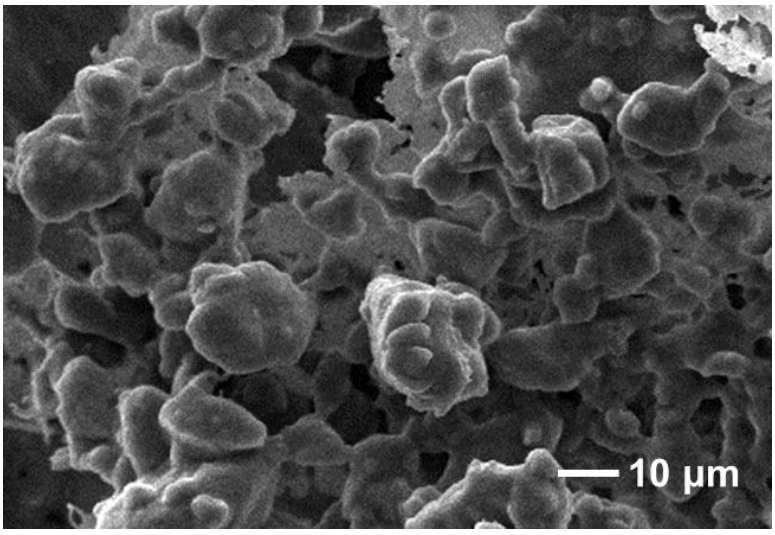

Fig. 6-16 The SEM image of MIM

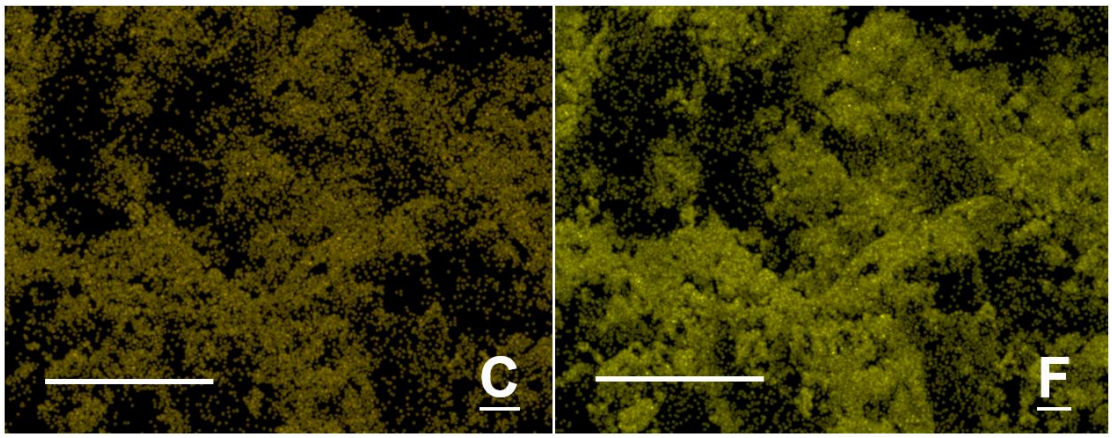

Fig. 6-17 C and F elemental mapping images of MIM

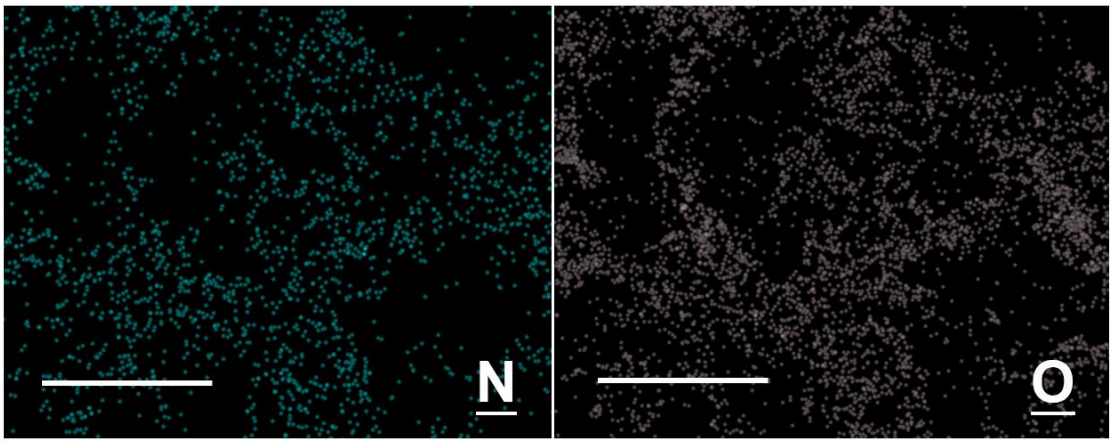

Fig. 6-18 N and O elemental mapping images of MIM

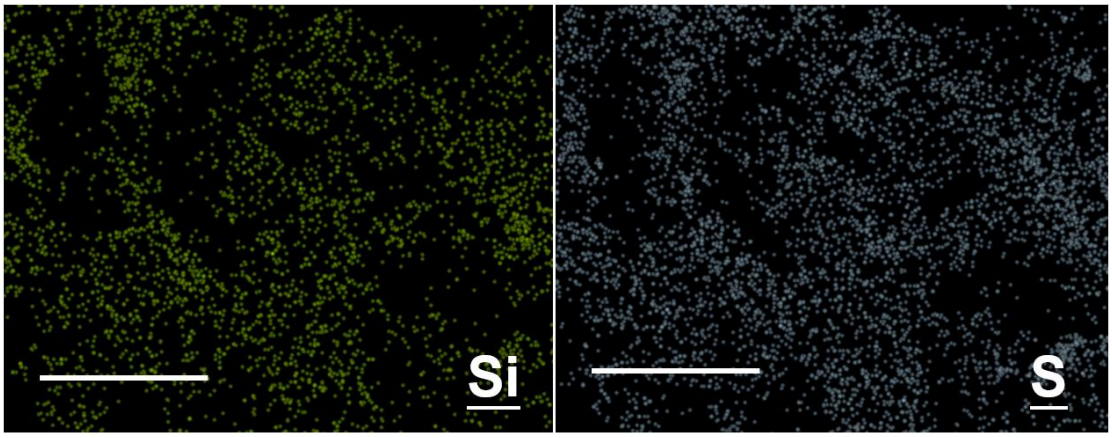

Fig. 6-19 Si and S elemental mapping images of MIM

6.4.2 Chemical characterizations

① XPS

To gain a more comprehensive understanding, an in-depth investigation of the chemical evolution of the prepared membranes was conducted using X-ray photoelectron spectroscopy (XPS). The C 1s signal of the VCDM membrane (Fig. 6-20) exhibited distinct peaks at 292.0, 287.0, 285.6, and 284.8 eV, corresponding to C–F, H–C–H, C–O/C–N, and C–C, respectively [22-24]. These peaks provide conclusive evidence regarding the chemical composition of VCDM, which comprises PVDF, β-CD, and PDA. Following the vinylated modification, the emergence of the Si 2p signal (Fig. 6-21) featuring Si–O–Si (102.5 eV) and Si–O–C (101.9 eV) further confirms the successful grafting of KH570 onto VCDM [25, 26]. As the S element is exclusively present in the crosslinker (PT3M), the detection of the S signal (Fig. 6-22) indicates the stable grafting of the crosslinker onto the membrane. Notably, it is important to highlight that the raw PT3M contains an equal amount of S–H and S–C groups. The notably weaker S–H (164.2 eV) signal, in comparison to S–C (163.0 eV), suggests that some S–H groups are consumed during the formation of the molecularly imprinted polymers (MIPs).

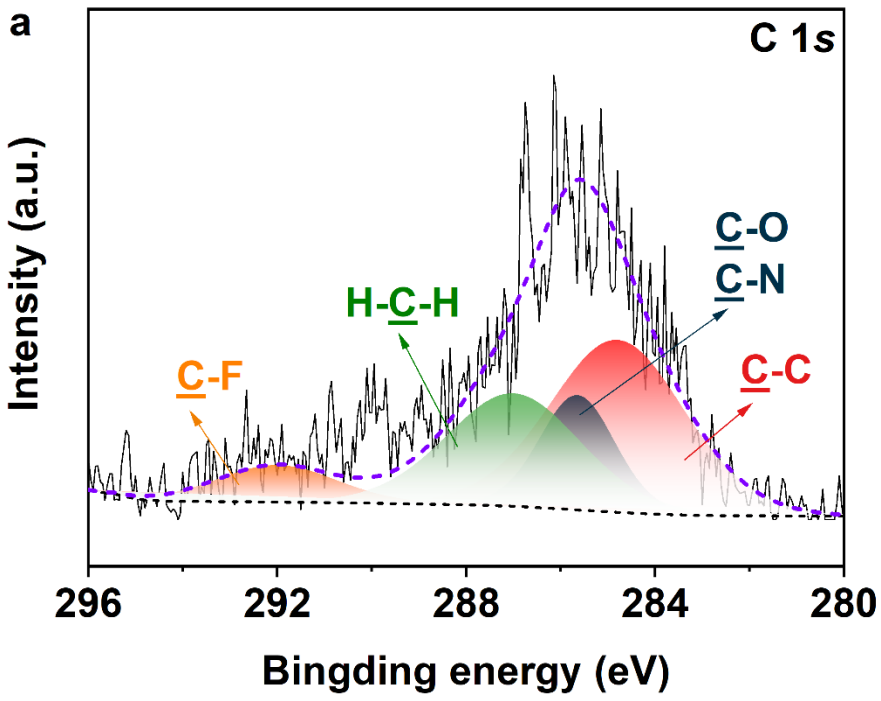

Fig. 6-20 XPS spectra of a) VCDM (C 1s)

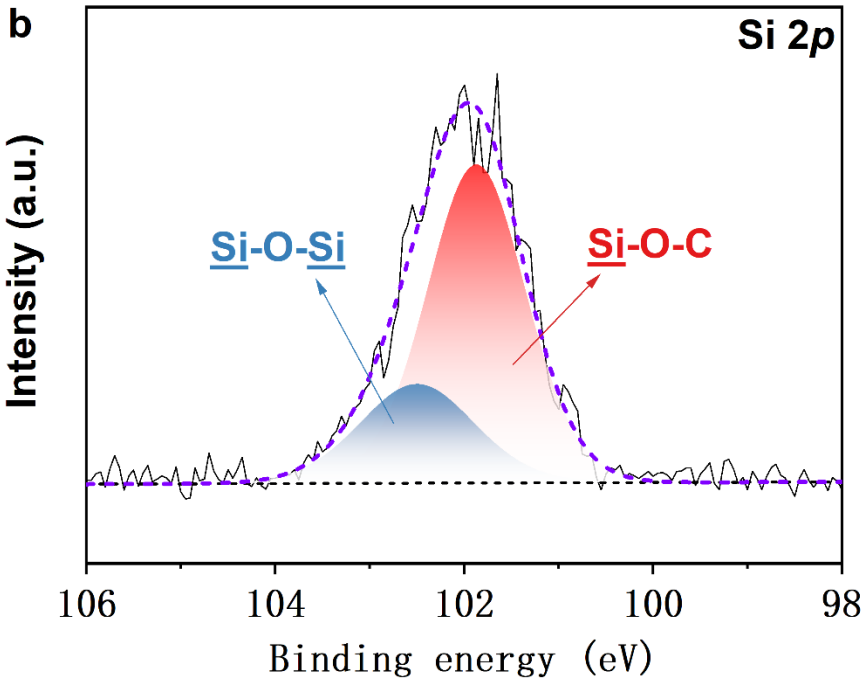

Fig. 6-21 XPS spectra of vinylated VCDM (Si 2p)

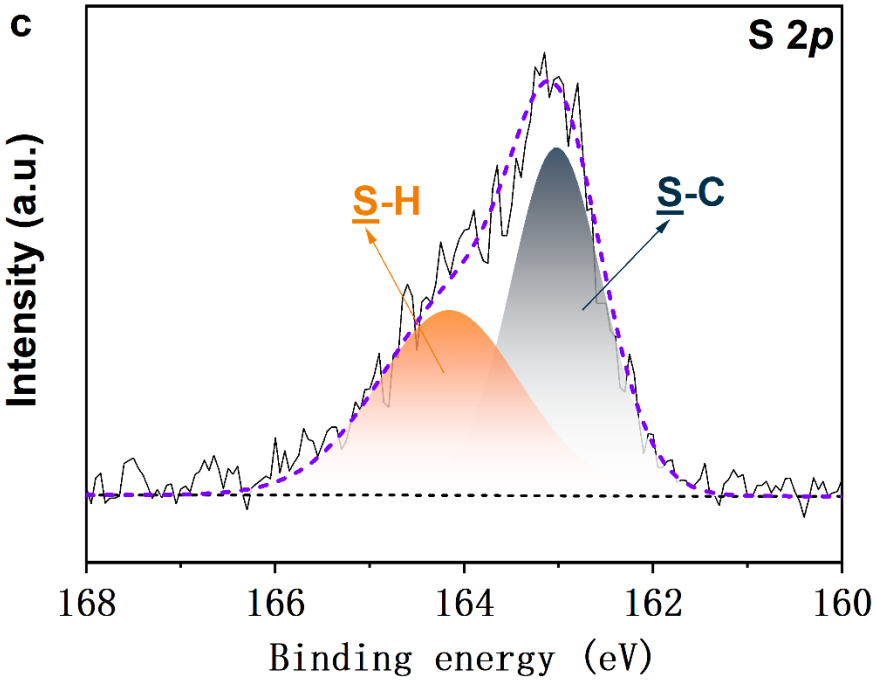

Fig. 6-22 XPS spectra of MIM (S 2p)

② Bovine serum albumin (BSA) binding experiments

BSA binding experiments were meticulously performed to evaluate the binding capability of the MIM membrane. A single piece of MIM was carefully submerged in a precisely measured 10 mL solution of BSA with varying concentrations (5, 25, 50, 100, and 200 mg L−1), ensuring comprehensive coverage of the membrane surface. The immersion process lasted for a specific duration of 24 hours, maintaining a constant temperature of 4.0℃ to ensure controlled conditions. To stabilize the conformation of BSA and preserve its native structure, the solvent used was phosphate buffered saline (PBS) with a pH value of 7.4, which provided an optimal environment for the binding interaction. Subsequently, the concentration of BSA present in the solution was accurately determined using a state-of-the-art UV-Vis spectrophotometer, specifically calibrated to measure absorbance at the wavelength of 278 nm. This precise analytical technique allowed for precise quantification and characterization of the BSA concentration, enabling a comprehensive assessment of the binding efficiency and performance of the MIM membrane in capturing and retaining BSA molecules. The binding capacity of BSA (QB, mg g^{-1}) can be calculated according to the following equation:

$$Q_B = (C_{B0} - C_B) \times \frac{V_B}{m_B} \quad (1)$$

where C_{B0} (mg L^{-1}) and C_B (mg L^{-1}) represent concentrations of BSA in the solution before and after binding, V_B (L) means the volume of BSA solution, and m_B (g) is the weight of the membrane.

For mitigating the presence of potential pollutants in MIMs, an array of pre-treatment methods can be employed, targeting both inorganic and organic pollutants. These pre-treatments, such as precipitation and adsorption, have proven to be highly effective in reducing or entirely eliminating these pollutants from the system. However, when it comes to microorganisms, while the removal rate can reach an impressive 99%, it is crucial to note that the abundant metabolites, particularly proteins, may still persist even after treatment.

To assess the anti-fouling performance of MIMs, BSA, a well-known fouling agent, was

chosen as a representative model pollutant. BSA possesses a propensity for non-specific interactions, allowing it to adsorb onto the surface of substrates. Consequently, BSA serves as an ideal model for investigating the anti-fouling properties of the membranes.

Notably, Fig. 6-23 illustrates that the membrane prepared using the thermally induced embedding strategy exhibits a weaker binding capacity compared to the membrane prepared using traditional surface grafting methods. This finding suggests that the thermally induced embedding strategy yields a superior anti-protein (anti-fouling) characteristic on the membrane surface. A plausible explanation for this observation is that the presence of PDA throughout the porous matrix facilitates the rapid formation of a water layer on the membrane surface, leveraging its robust water invasiveness. This dynamic water layer effectively impedes the approach of BSA molecules, thereby improving the anti-fouling performance of the membrane.

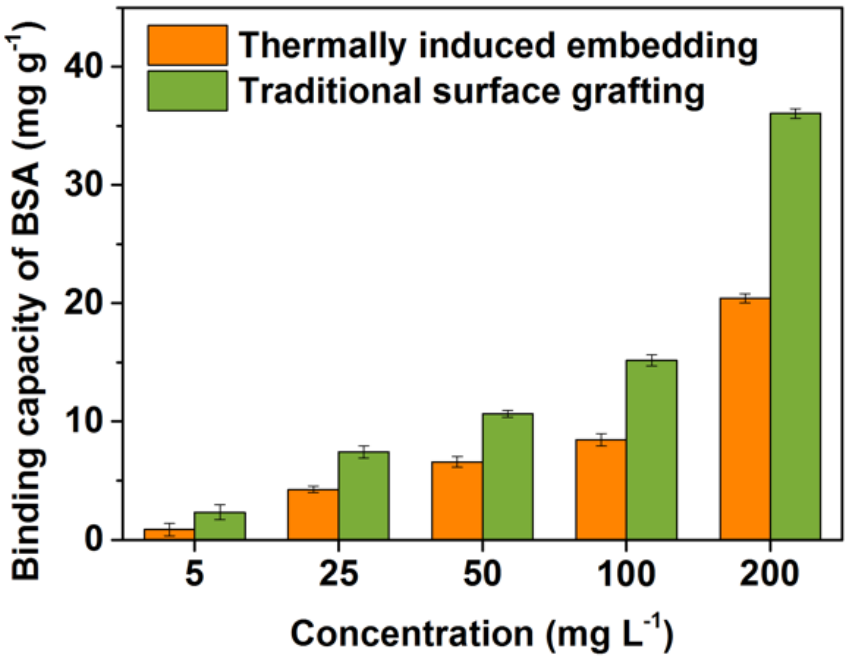

Fig. 6-23 Comparison of MIM's binding capacity of BSA based on thermally induced embedding and traditional surface grafting

③ Optimization of imprinting polymerization

As the key step in the formation of MIM, the imprinting polymerization needs to be optimized in detail. It is of great significance that the functional monomers will strongly interact with the template before polymerization [27]. Since the intensity of interactions will directly

affect the formation of host-guest complexes and then affect the imprinting effect, the optimal proportion of functional monomers and templates was primarily investigated based on the UV-Vis spectra.

Fig. 6-24 (a) shows that the maximum absorbance of CIP appears at 275 nm, which exhibits the change of redshift with the addition of MAA. The changes suggest that the stable host-guest complexes are formed between templates (CIP) and functional monomers (MAA) through the chemical interactions in the mixture. When the ratio of CIP to MAA reaches 1: 4, the change of redshift achieves the largest. At this point, the interactions are the strongest, and the constructed imprinted sites could exhibit the strongest affinity to CIP. It should be noted that the further increase of MAA will lead to the decline of the redshift. A possible reason is that too large amount of the functional monomers may lead to their own association and weaken the interactions with the targets. Then, the interactions between CIP and MAA at the optimum ratio were further investigated by 1H NMR. It is of great significance that the downfield shift of H suggests the formation of hydrogen bonds, while the upfield shift suggests the formation of ionic bonds.

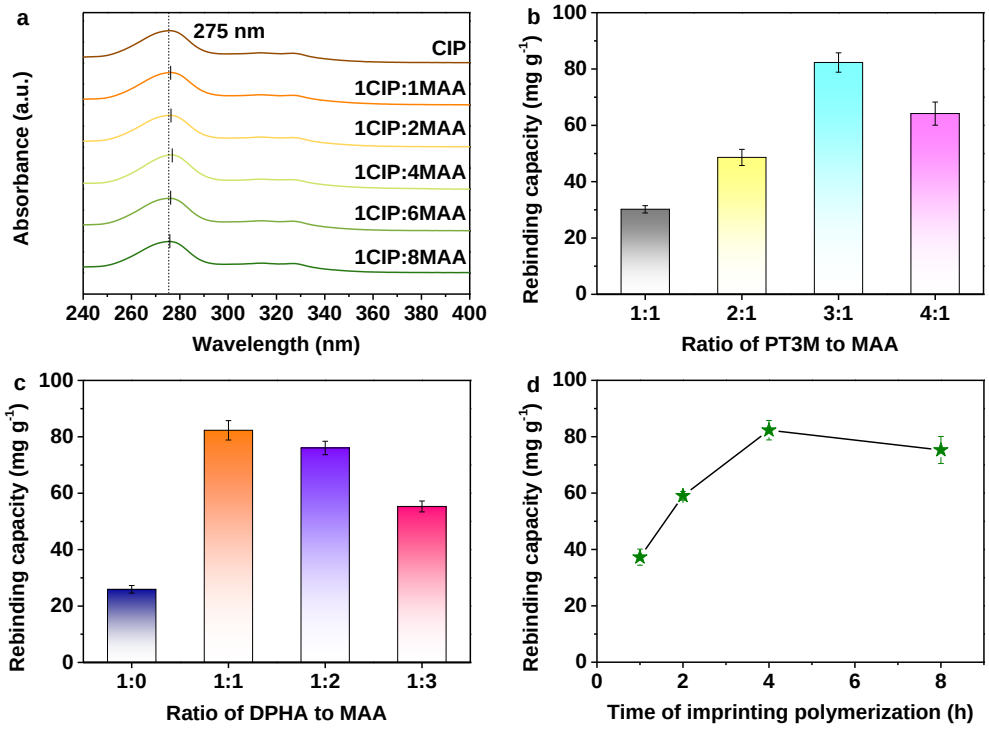

Fig. 6-24. a) UV-Vis spectra of CIP and complexes composed of CIP and MAA. Effect of

b) ratio of PT3M to MAA, c) ratio of DPHA to MAA and, d) time of imprinting polymerization on the rebinding capacity of MIM. (Error bars are standard deviations from three experiments with independently prepared membranes.)

Spectra in Fig. 6-25 show that the possible donors of hydrogen bonds in both CIP and MAA exhibit the obvious downfield shift after forming the CIP-MAA complex, suggesting that the interactions between CIP and MAA are attributed to the formation of hydrogen bonds.

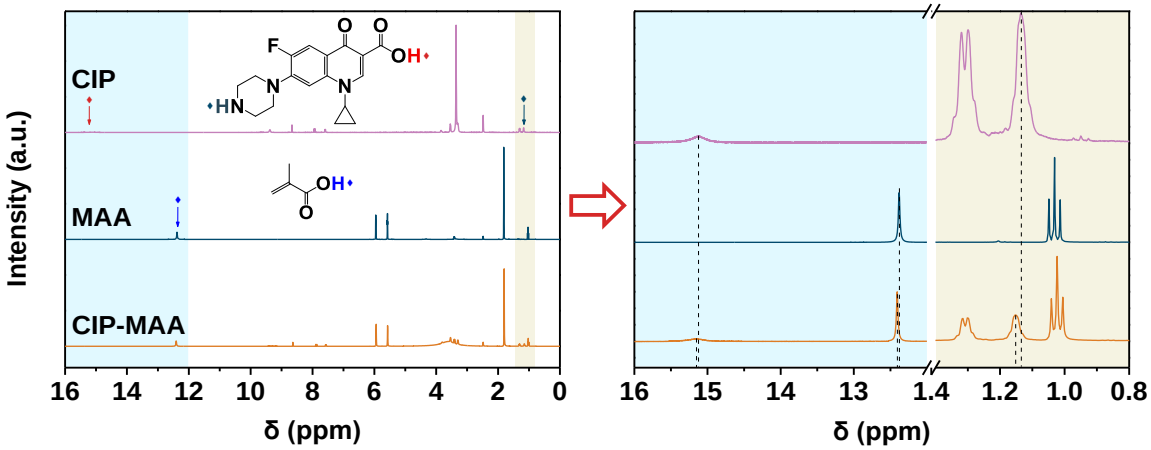

Fig. 6-25. 1H NMR spectra of CIP, MAA and EIP-MAA complex.

Subsequently, MAA was used as a reference to further optimize the amount of crosslinker (PT3M) and assistant crosslinker (DPHA). The rebinding capacity (200 mg L^{-1}, 24 h) of MIM prepared with variable conditions was employed as the measure.

Fig. 6-24 (b) shows that the rebinding capacity is availably enhanced with the increasing amount of crosslinker, which reaches the maximum when the ratio of PT3M to MAA is 3: 1. This should result in a large number of crosslinkers that will promote the formation of more effective imprinted sites. Especially, the further increase of the crosslinker does not further improve the rebinding capacity but leads to an obvious decline. The possible reason is that the excessive crosslinker leads to the excessive polymerization of monomers, which destroys the originally formed host-guest complexes and results in the reduction of effective imprinted sites. Then, the content of DPHA was further optimized with the ratio of PT3M to MAA for 3: 1.

Fig. 6-24 (c) displays that the MIM with the addition of an assistant crosslinker shows a

much higher rebinding capacity than that without the assistant crosslinker. The thiol-ene Click reaction between MAA and PT3M is not enough to form a polymer network with a high crosslinking degree. Although the imprinted sites can be formed, it is difficult for the sites to be effectively loaded on the membrane matrix. The addition of the assistant crosslinker just makes up for this deficiency, which effectively assists the formation of a polymer network by the vinyl-based polymerization and promotes the loading of sites on the membrane. However, when the ratio of DPHA to MAA exceeds 1: 1, the rebinding capacity interestingly decreases. The reason for this phenomenon should be that the over-cross-linked polymers embed the numerous imprinted sites, which leads to the decrease of the selective rebinding onto the MIM. Therefore, the optimal ratio of MAA/PT3M/DPHA is selected as 1: 3: 1.

Then, the imprinting polymerization time was further optimized with the optimal ratio of template, monomer, crosslinker and assistant crosslinker. As can be observed from Fig. 6-24 (d), the rebinding capacity of MIM continuously enhances with the increase of polymerization time and reaches the maximum at 4 h. It suggests that the increasing time of imprinting polymerization enables the effective formation of more imprinted sites. When the polymerization time exceeds 4 h, however, the rebinding capacity of as-obtained MIM decreases obviously. It should be ascribed that the long period of polymerization will lead to the agglomeration of the polymers. The reduced effective sites ultimately lead to the decline of the specific rebinding.

④ Quantum chemistry simulations

As the key step in molecular imprinting, the thiol-ene Click reaction was further explored by investigating transition states. All the calculations of structural optimizations were performed at B3LYP/6-311G** of DFT. The SMD solvation model was used and the solvent is acetonitrile [28, 29]. Frequency calculations were performed at the same level of theory as for geometry optimization to characterize the stationary points as minima (no imaginary frequencies) and the imaginary frequencies of two transition states are given in the part of Cartesian Coordinates. All the calculations were performed with Gaussian 09 software package.

The molecular imprinting reaction path was further investigated for insight into the

mechanism by DFT calculations.

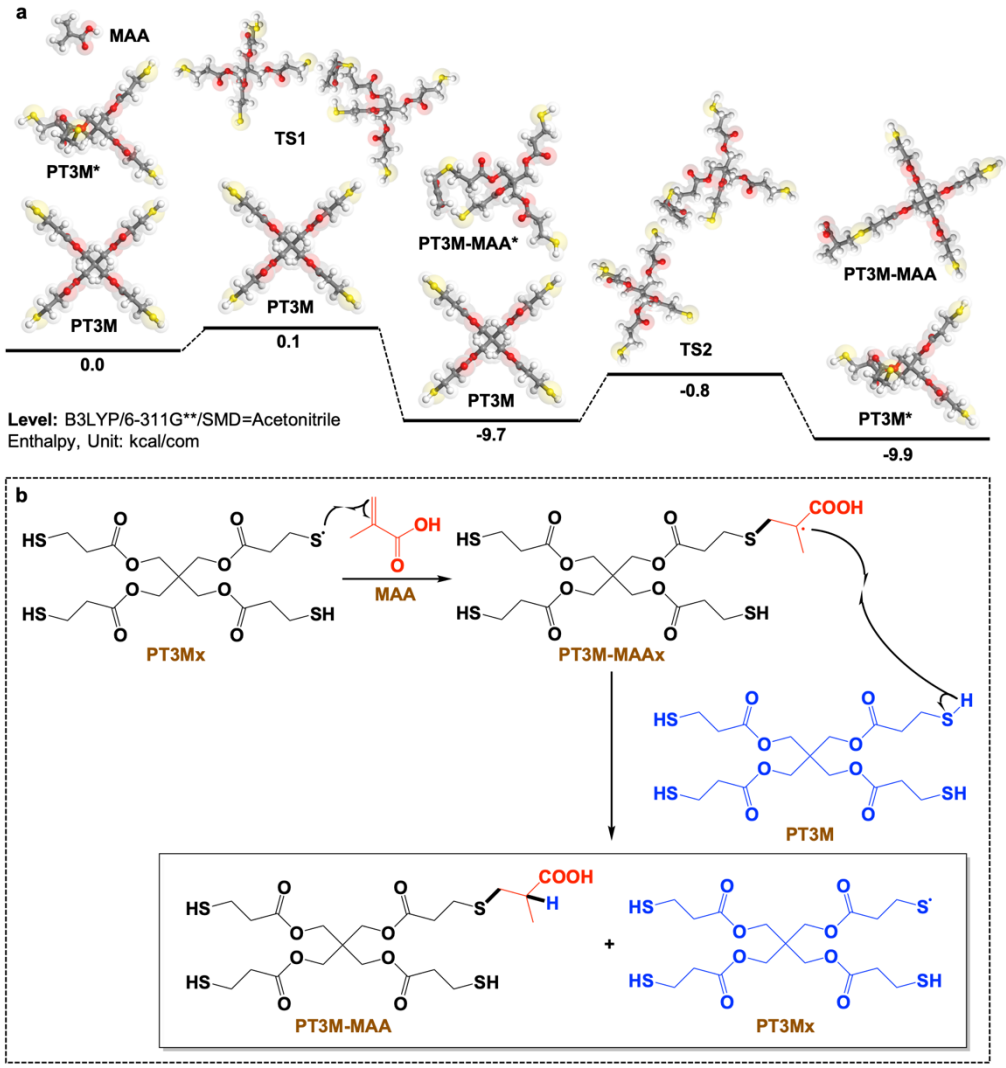

Fig. 6-26 a) Step-growth mechanism of thiol-ene Click reaction during molecular imprinting. b) Mechanism of thiol-ene Click reaction based on MAA and PT3M.

Fig. 6-26 (a) displays the step-growth mechanism of the thiol-ene Click reaction based on MAA and PT3M, from which the reaction can be described as two steps. For the first step (MAA + PT3M* + PT3M → PT3M-MAA* + PT3M), a thiol radical of PT3M first attacks the vinyl of MAA and goes through the first transition state (TS1). The propagation of charge, therefore, can be achieved in the radical species by forming the complex PT3M-MAA*. For the second step (PT3M-MAA* + PT3M → PT3M-MAA + PT3M*), the proton from another PT3M is extracted by the free radical of PT3M-MAA*, which leads to the second transition state (TS2) and results in the chain transfer. As a result, the product PT3M-MAA and a new

thiol radical are obtained. According to the above analysis, the reaction mechanisms are summarized in Fig. 6-26 (b). According to enthalpies, the activation enthalpies of the transition states are calculated as 0.1 kcal mol-1 and -0.8 kcal mol-1, respectively. The low barriers of the transition states suggest the feasibility of the reaction at room temperature, while the reduction of the total energy confirms the spontaneous reaction on the thermodynamics. The results further complement the mechanism of the molecular imprinting based on the thiol-ene Click reaction.

6.5 Performance Characterization

6.5.1 rebinding characteriization

Isothermal and kinetic rebinding performance was respectively explored for the investigation of selective recognition. In the whole range of tested conditions, MIM exhibits a high adsorption capacity. For the concentration-dependent mode (Fig. 6-27), a non-uniform trend of increase appears in the rebinding capacity of MIM. Specifically, the rebinding capacity increases rapidly with a low concentration of CIP, while the trend becomes slow when the concentration is over 150 mg L^{-1}. It is reasonable to assume that the imprinted sites have made a crucial contribution to the improvement of rebinding rates, which further demonstrates the enhanced effect of imprinted sites.

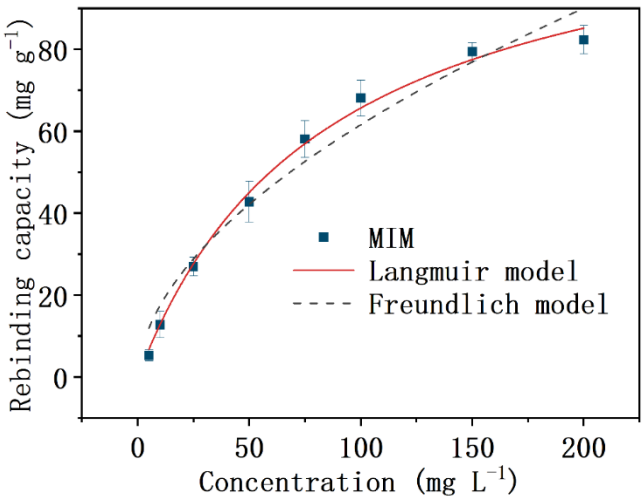

Fig. 6-27 Rebinding capacities of MIM with fitted isothermal models.

Rebinding data are then fitted with Langmuir [30] (Fig. 6-28) and Freundlich(Fig. 6-29) isothermal models, respectively. According to constants in Table S1, rebinding data of MIM fit better with the Langmuir model (R^2 = 0.9980) than the Freundlich model (R^2 = 0.9694).

Table 6-1. Constants of isothermal rebinding onto MIM.

Membrane	Langmuir[a]			Freundlich[b]		
	Q_m	K_L	R^2	K_F	$1/n$	R^2
MIM	121.12	0.0118	0.9980	4.9468	0.5476	0.9694

[a] Langmuir model is expressed as $Q_e=(Q_mK_LC_e)/(1+K_LC_e)$, where C_e (mg L^{-1}) and Q_e (mg g^{-1}) are concentration and rebinding capacity at equilibrium, Q_m (mg g^{-1}) is the theoretical maximum rebinding capacity, and K_L (L mg^{-1}) is the Langmuir constant.

[b] Freundlich model is expressed as $Q_e=K_FC_e^{1/n}$, where C_e (mg L^{-1}) and Q_e (mg g^{-1}) are concentration and rebinding capacity at equilibrium, as well as K_F ($mg^{1-1/n}$ $L^{1/n}$ g^{-1}) and n are Freundlich constants.

It indicates that the imprinted sites on MIM exhibit a uniform and monolayer distribution [31].

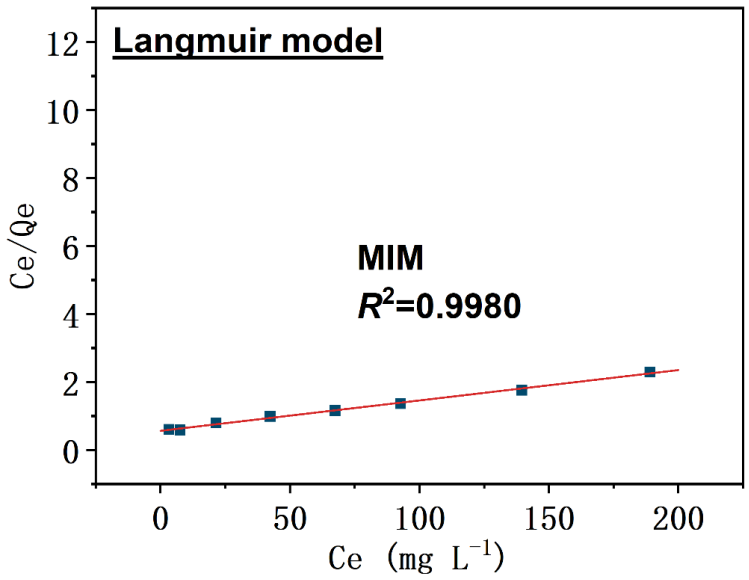

Fig. 6-28 Linear fitting Langmuir models

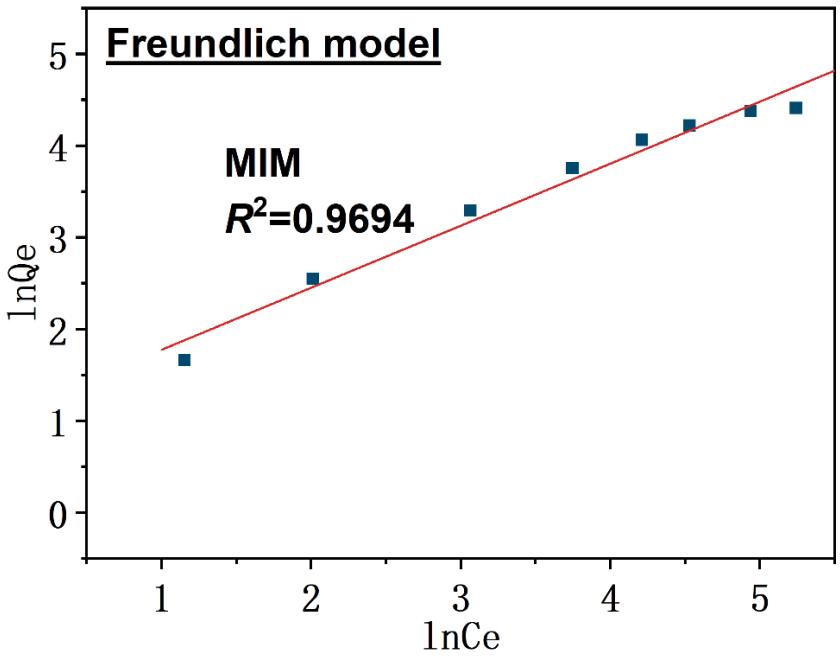

Fig. 6-29 Linear fitting Langmuir models

For the time-dependent model (Fig. 6-30), a distinct trend from the concentration-dependent model appears on MIM.

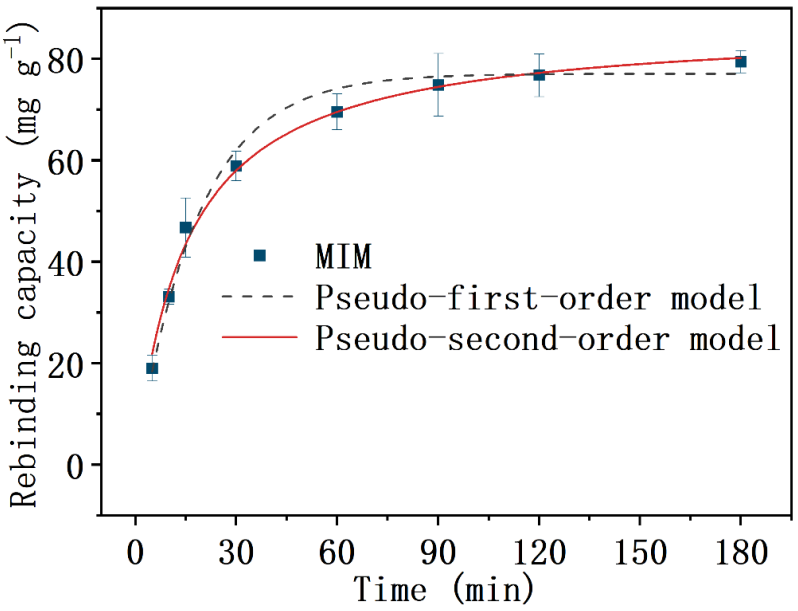

Fig. 6-30 Rebinding capacities of MIM with fitted kinetic models.

The rebinding capacity increases rapidly at first and reaches the platform in about 60 min. Rebinding data are, then, fitted with Pseudo-first-order [32] (Fig. 6-31) and Pseudo-second-order [33] (Figure 7f) model, respectively.

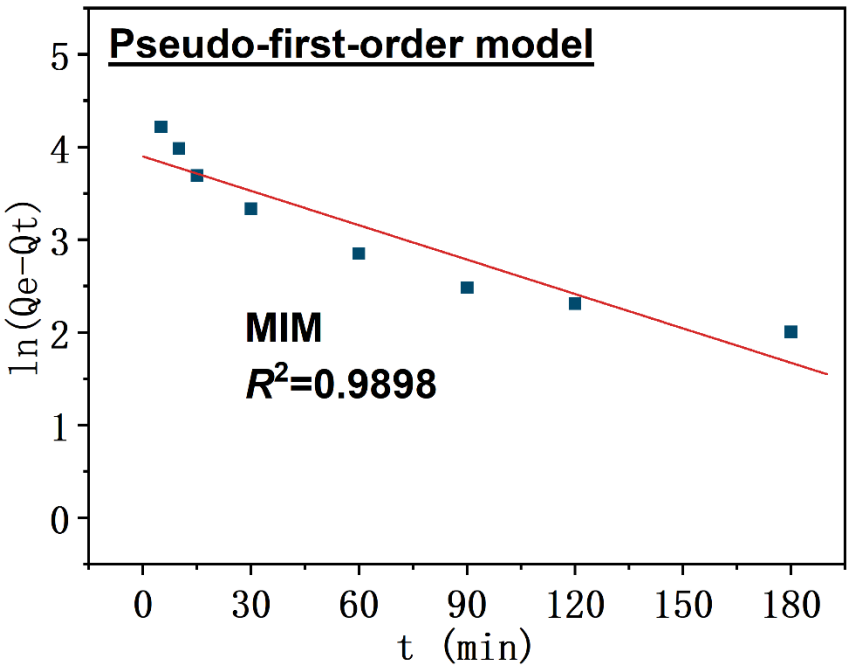

Fig. 6-31 Linear fitting of Pseudo-first-order models

Table 6-2. Constants of kinetic rebinding onto MIM

Membrane	Pseudo-first-order[a]			Pseudo-second-order[b]		
	Q_e	k'	R^2	Q_e	k''	R^2
MIM	77.06	0.0543	0.9898	86.83	0.0008	0.9940

[a] Pseudo-first-order model is expressed by $Q_t=Q_e-Q_e e^{-k't}$, where Q_e and Q_t (mg g^{-1}) are rebinding capacities at the equilibrium and time t (min), and k' (min^{-1}) is the equilibrium rate constants of the pseudo-first-order model.

[b] Pseudo-second-order model is expressed as $Q_t=(k''Q_e^2t)/(1+k''Q_et)$, where Q_e and Q_t (mg g^{-1}) are rebinding capacities at the equilibrium and time t (min), as well as k'' (g mg^{-1} min^{-1}) is the equilibrium rate constants of the pseudo-second-order model.

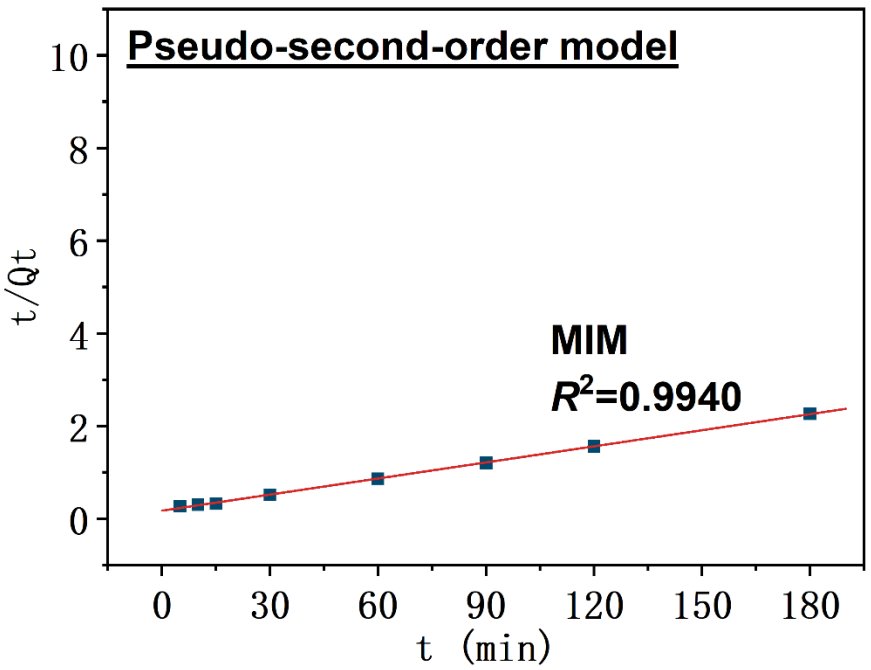

Fig. 6-32 Linear fitting of Pseudo-second-order models

From fitting results in Table 6-2, rebinding data of MIM show better relevancy with the Pseudo-second-order model (R^2 = 0.9940) than the pseudo-first-order model (R^2 = 0.9898), suggesting that the rebinding onto MIM is determined by both chemisorption and physical diffusion.

6.5.2 Selectivity characterization

For investigating the selective of the imprinted sites, concentration-dependent (Fig. 6-33) and time-dependent (Fig. 6-34) selective rebinding operations were performed on MIM using ENR, NOR and OFL as non-targets. MIM shows high rebinding capacity towards the targets than the non-targets.

Besides the effectiveness, the significantly distinguishing rebinding capacities also indicate the selectivity of the imprinted sites towards CIP, which is determined by the imprinting polymerization using CIP as the template. It should be noted that, onto MIM, the rebinding towards CIP in the mixed system is weaker than that in a single target system. The phenomenon is especially remarkable at a high concentration (> 50 mg L^{-1}). It results from that the non-

specific interaction between sites and non-targets leads to competition between targets and non-targets. Since more non-targets own the chance to occupy imprinted sites with a high concentration, the decline will be more obvious.

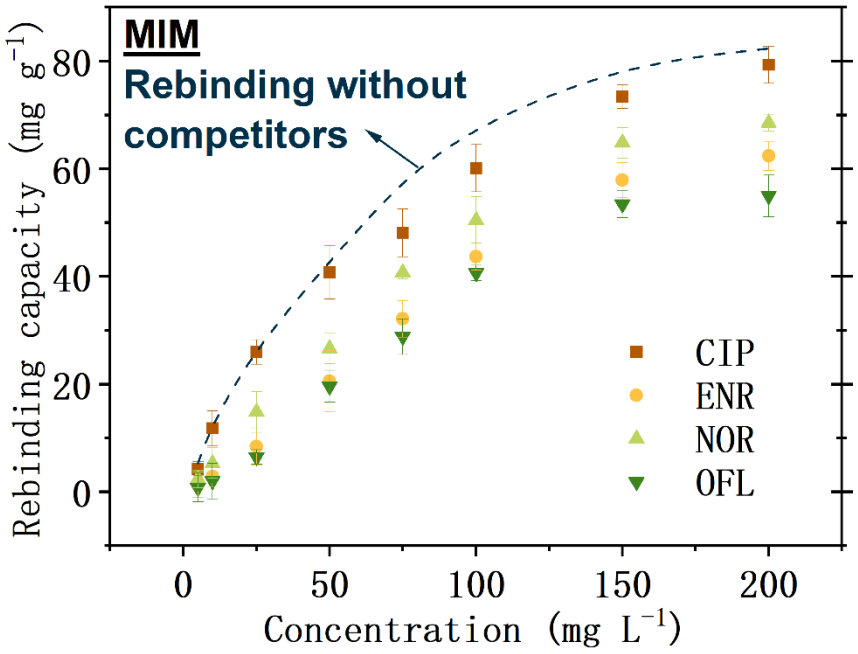

Fig. 6-33 Concentration-dependent selective rebinding performance onto MIM

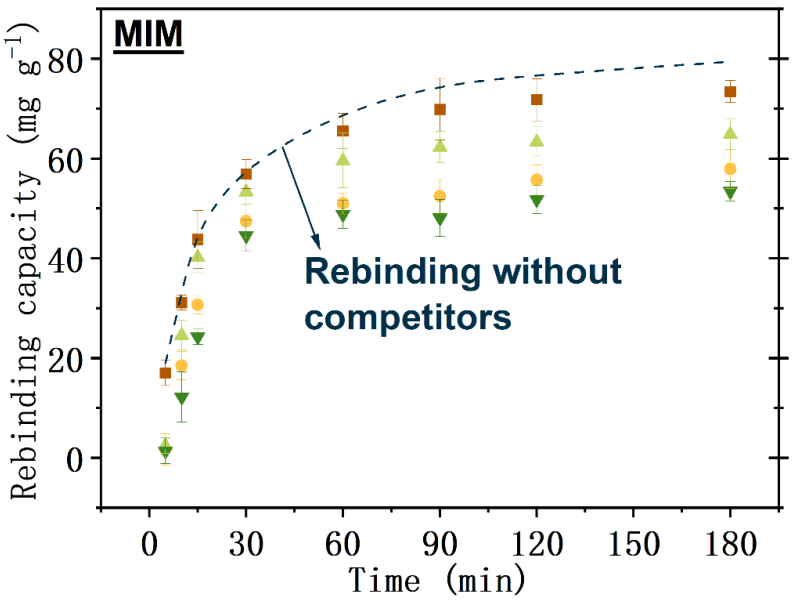

Fig. 6-34 Time-dependent selective rebinding performance onto MIM

Then, the separation factors are calculated according to selective rebinding data, as displayed in Fig. 6-35.

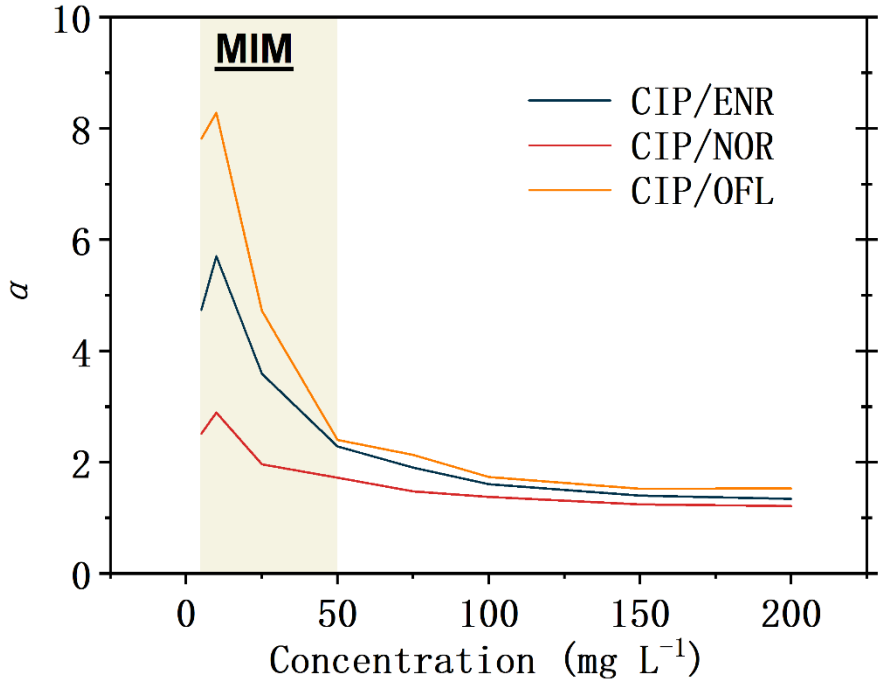

Fig. 6-35 Separation factors (α) onto MIM

The remarkable selectivity of MIM is approached with a low concentration (< 50 mg L^{-1}), where the optimal one (αCIP/ENR = 5.70, αCIP/NOR = 2.89 and αCIP/OFL = 8.28) is achieved at 10 mg L^{-1}. It indicates that the low concentration is more conducive to demonstrating the capability of imprinted sites on selective recognition and rebinding of CIP. The phenomenon is consistent with the apparent interference caused by competitors at the high concentration (> 50 mg L^{-1}). The intrinsic reason should be that the high concentration promotes a shift of the equilibrium towards saturation. Considering the limited number of imprinted sites on MIM, the non-specific rebinding will, therefore, be enhanced at the high concentration, thus weakening the specificity dominated by specific rebinding.

6.5.3 Permeation performance

A mixed solution with 10 mg L^{-1} of CIP, ENR, NOR and OFL was employed for the permeation investigations. The typical static permeation was performed on MIM. Fig. 6-36 shows the

evolution of concentration in permeate and dialysate of MIM. The obvious difference appears in the equilibrium time of CIP (36 h) and non-targets (24 h), where the hysteretic equilibrium onto MIM indicates a significant retarding effect on the CIP permeation. At the same time, the equilibrium concentration of CIP was much lower than that of the non-targets, indicating that MIM exhibits a strong rebinding effect on CIP in the mixed system. The deduction is consistent with that of selective rebinding experiments. Therefore, it can be inferred that MIM will effectively retard the permeation of CIP by causing selective recognition and rebinding toward CIP.

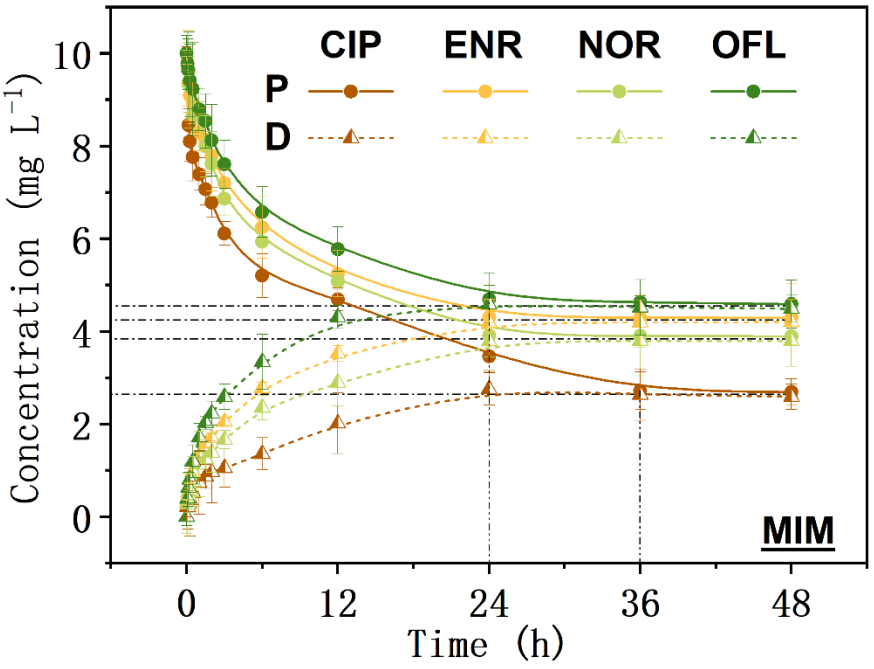

Fig. 6-36 Permeation performance of target and non-targets onto MIM

Then, the permeation fluxes (J) of CIP and non-targets are compared for in-depth understanding. Due to the differential in permeability, the evolution curves of CIP and non-targets onto MIM display an immense variability, especially within 24 h (Fig. 6-37). As a result, it leads to the conclusive feasibility of selective separation by the specially designed MIM.

For investigating the effective operation condition, the evolution of the permeability coefficient (P) is further analyzed. As to MIM (Fig. 6-38), both CIP and non-targets show a

decreasing trend in the permeability coefficient in the first 3 hours.

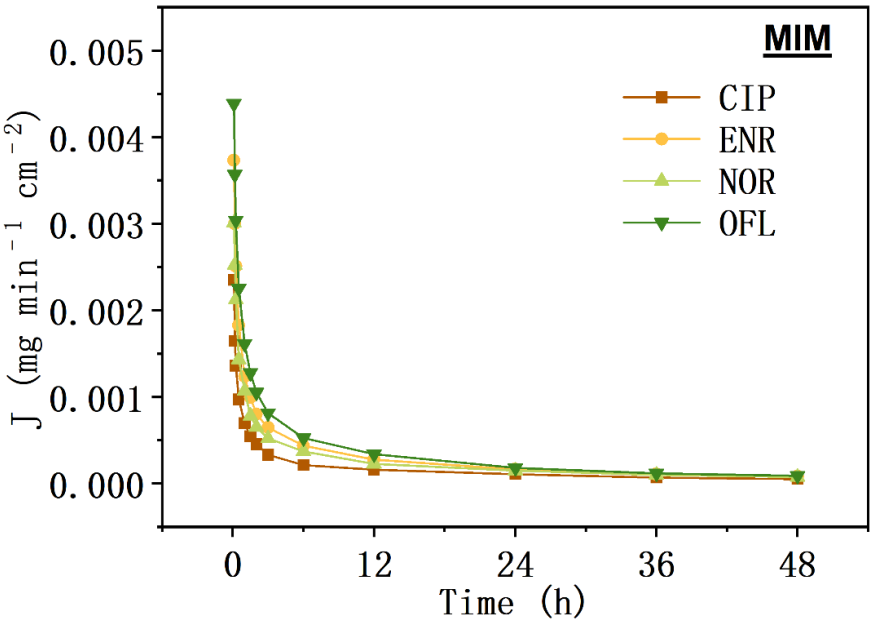

Fig. 6-37 Permeation flux of target and non-targets onto MIM

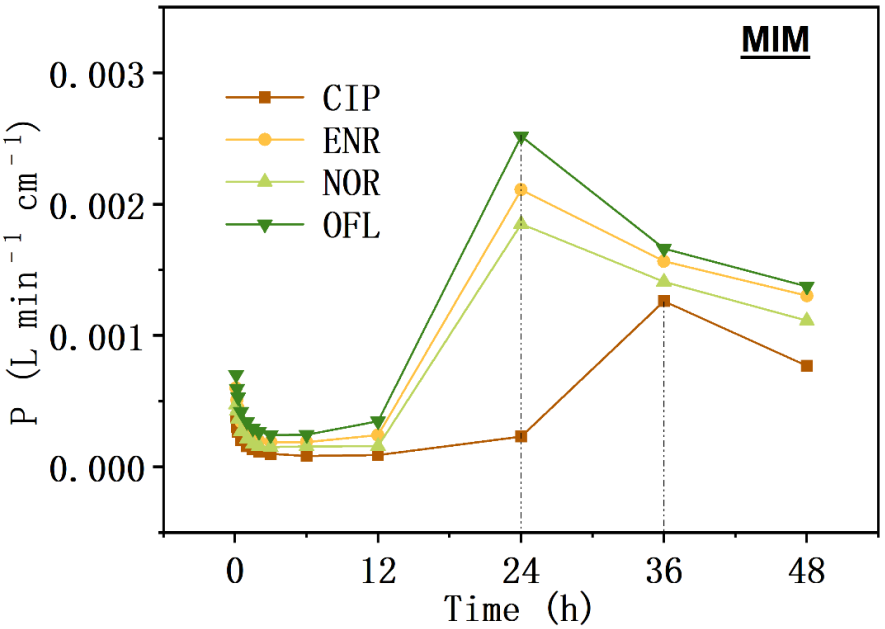

Fig. 6-38 Permeability coefficient of target and non-targets onto MIM

It can be interpreted as the rapid diffusion of molecules appearing under the concentration

gradient at the beginning of permeation, while the specific rebinding of CIP and the non-specific rebinding of non-target provided by imprinted sites inhibit their permeability. The decreased concentration difference between permeate and dialysate, together with the enhanced retarding ability, leads to the decline of the permeability coefficients. Subsequently, the permeability coefficients raise with the system approaches the equilibrium rebinding. During this process, the retarding effect on CIP is more lasting than on non-targets due to the stronger interaction between the imprinted site and CIP. It, therefore, leads to the sluggish arrival of the maximum on CIP (36 h), compared with the non-targets (24 h).

6.5.4 Regeneration performance

Since the porous sleeve is proposed for enhanced recycling and reusability, investigation of regeneration performance is necessary for the evaluation of MIM. The regeneration cycles were performed by extraction (Vmethanol/Vacetic acid = 95/5) after a typical permeation. The permselectivity coefficients of MIM during 10 regeneration cycles are summarized in Fig. 6-39 (a), which only exhibit tiny fluctuations (8.4%~10.8%). For the further investigation of this decreasing tendency, the change of MIM occurred in the surface structure and chemical composition were characterized by SEM and XPS. Fig. 6-39 (b) shows that the microtopography in the 1st and 10th cycles does not change significantly. It indicates that there is no obvious exfoliation of the imprinted polymers during long-term successive employment. The phenomenon is attributed to the protective effect of the interpenetrating-bicontinuous porous sleeve, which prevents the imprinted polymers from being destroyed by the external forces. Then, when comparing the chemical composition, the differentiation between the 1st and 10th cycles catches our attention. As shown in Fig. 6-39 (c) and Fig. 6-39 (d), an obvious shift emerges in the binding energy of C=O, while a significant decline appears on O–C. It indicates that the provider of carboxyl groups (MAA) is rebound with other molecules, suggesting that a few rebound CIP molecules on the MIM were not effectively removed from the imprinted sites during the regeneration cycles. It also provides a guide for the future research on further improvement of the regeneration performance.

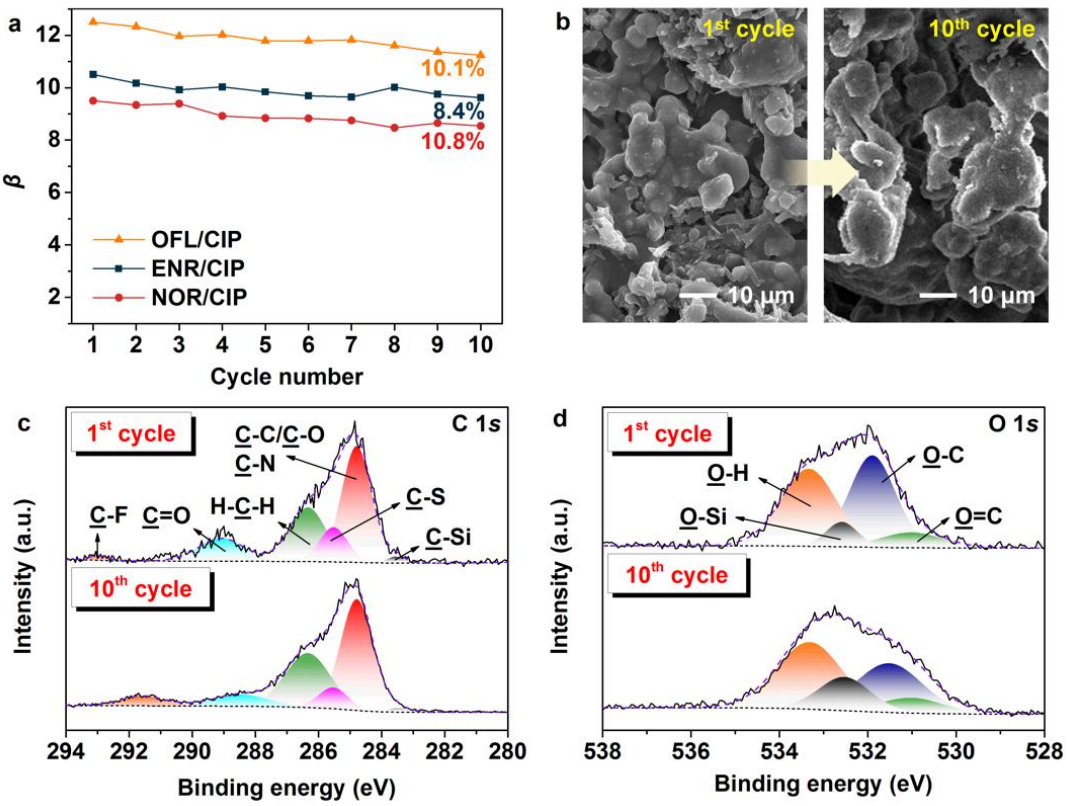

Fig. 6-39. a) Regenerated permselectivity, b) surface structure and c) chemical composition of MIM in permeation/extraction cycles.

Reference

[1] Manuela Gast, Harald Sobek, Boris Mizaikoff, Advances in imprinting strategies for selective virus recognition a review, TrAC Trends in Analytical Chemistry 114 (2019) 218-232.

[2] Jianming Pan, Wei Chen, Yue Ma, Guoqing Pan, Molecularly imprinted polymers as receptor mimics for selective cell recognition, Chemical Society Reviews 47(15) (2018) 5574-5587.

[3] G Wulff, AJAC Sarhan, Über die Anwendung von enzymanalog gebauten Polymeren zur Racemattrennung, Angewandte Chemie 84(8) (1972) 364-364.

[4] Anna Kubiak, Magdalena Biesaga, Application of Molecularly Imprinted Polymers for Bisphenols Extraction from Food Samples – A Review, Critical Reviews in Analytical Chemistry 50(4) (2020) 311-321.

[5] S. A. Piletsky, E. V. Piletskaya, K. Yano, A. Kugimiya, A. V. Elgersma, R. Levi, U. Kahlow, T. Takeuchi, I. Karube, T. I. Panasyuk, A. V. El'skaya, A Biomimetic Receptor System for Sialic Acid Based on Molecular Imprinting, Analytical Letters 29(2) (1996) 157-170.

[6] Linus Pauling, A Theory of the Structure and Process of Formation of Antibodies*, Journal of the American Chemical Society 62(10) (1940) 2643-2657.

[7] Frank H. Dickey, The Preparation of Specific Adsorbents, Proceedings of the National Academy of Sciences 35(5) (1949) 227-229.

[8] Frank H. Dickey, Specific Adsorption, The Journal of Physical Chemistry 59(8) (1955) 695-707.

[9] Sharon Marx, Zvi Liron, Molecular Imprinting in Thin Films of Organic−Inorganic Hybrid Sol−Gel and Acrylic Polymers, Chemistry of Materials 13(10) (2001) 3624-3630.

[10] Sharon Fireman-Shoresh, David Avnir, Sharon Marx, General Method for Chiral Imprinting of Sol−Gel Thin Films Exhibiting Enantioselectivity, Chemistry of Materials 15(19) (2003) 3607-3613.

[11] K. Lee, R. R. Itharaju, D. A. Puleo, Protein-imprinted polysiloxane scaffolds, Acta Biomaterialia 3(4) (2007) 515-522.

[12] M. Lehmann, H. Brunner, G. E. M. Tovar, Selective separations and hydrodynamic studies: a new approach using molecularly imprinted nanosphere composite membranes, Desalination 149(1) (2002) 315-321.

[13] Masakazu Yoshikawa, Kalsang Tharpa, Ştefan-Ovidiu Dima, Molecularly Imprinted Membranes: Past, Present, and Future, Chemical Reviews 116(19) (2016) 11500-11528.

[14] M Lehmann, H Brunner, GEM Tovar, Molecularly imprinted nanoparticles as selective phase in composite membranes: Hydrodynamics and separation in nanoscale beds, Chemie Ingenieur Technik 75(1-2) (2003) 149-153.

[15] Mathias Ulbricht, Membrane separations using molecularly imprinted polymers, Journal of Chromatography B 804(1) (2004) 113-125.

[16] R. Kiełczyński, M. Bryjak, Molecularly imprinted membranes for cinchona alkaloids separation, Separation and Purification Technology 41(3) (2005) 231-235.

[17] Hong Ying Wang, Takaomi Kobayashi, Nobuyuki Fujii, Molecular Imprint Membranes Prepared by the Phase Inversion Precipitation Technique, Langmuir 12(20) (1996) 4850-4856.

[18] Hong Ying Wang, Takaomi Kobayashi, Takahiro Fukaya, Nobuyuki Fujii, Molecular Imprint Membranes Prepared by the Phase Inversion Precipitation Technique. 2. Influence of Coagulation Temperature in the Phase Inversion Process on the Encoding in Polymeric Membranes, Langmuir 13(20) (1997) 5396-5400.

[19] Adnan Mujahid, Amina Maryam, Adeel Afzal, Sadia Zafar Bajwa, Tajamal Hussain, Muhammad Imran Din, Usman Latif, Muhammad Irshad, Molecularly imprinted poly(methyl methacrylate)-nickel sulfide hybrid membranes for adsorptive desulfurization of dibenzothiophene, Separation and Purification Technology 237 (2020) 116453.

[20] Yilin Wu, Ming Yan, Xinlin Liu, Peng Lv, Jiuyun Cui, Minjia Meng, Jiangdong Dai, Yongsheng Yan, Chunxiang Li, Accelerating the design of multi-component nanocomposite imprinted membranes by integrating a versatile metal–organic methodology with a mussel-inspired secondary reaction platform, Green Chemistry 17(6) (2015) 3338-3349.

[21] S. A. Piletsky, E. V. Piletskaya, K. Yano, A. Kugimiya, A. V. Elgersma, R. Levi, U. Kahlow, T. Takeuchi, I. Karube, T. I. Panasyuk, A. V. El'skaya, A Biomimetic Receptor System for Sialic Acid Based on Molecular Imprinting, Analytical Letters 29(2) (1996) 157-170.

[22] P. Kaspar, D. Sobola, K. Částková, A. Knápek, D. Burda, F. Orudzhev, R. Dallaev, P. Tofel, T. Trčka, L. Grmela, Z. Hadaš, Characterization of polyvinylidene fluoride (pvdf) electrospun fibers doped by carbon flakes, Polymers 12 (2020) 2766.

[23] N. Gao, J. Yang, Y. Wu, J. Yue, G. Cao, A. Zhang, L. Ye, Z. Feng, β-Cyclodextrin functionalized coaxially electrospun poly(vinylidene fluoride)@polystyrene membranes with higher mechanical performance for efficient removal of phenolphthalein, React. Funct. Polym. 141 (2019) 100-111.

[24] X. Gong, Y. Liu, Y. Wang, Z. Xie, Q. Dong, M. Dong, H. Liu, Q. Shao, N. Lu, V.

Murugadoss, T. Ding, Z. Guo, Amino graphene oxide/dopamine modified aramid fibers: Preparation, epoxy nanocomposites and property analysis, Polymer 168 (2019) 131-137.

[25] J. Lu, Y. Qin, C. Li, Y. Wu, M. Meng, Z. Dong, C. Sun, M. Chen, Y. Yan, Irregular dot array nanocomposite molecularly imprinted membranes with enhanced antibacterial property: Synergistic promotion of selectivity, rebinding capacity and flux, Chem. Eng. J. 405 (2021) 126716.

[26] B. Li, X. Liu, X. Zhang, J. Zou, W. Chai, J. Xu, Oil-absorbent polyurethane sponge coated with KH-570-modified graphene, J. Appl. Polym. Sci. 132 (2015) 41821.

[27] M. Meng, Y. Feng, M. Zhang, Y. Ji, J. Dai, Y. Liu, P. Yu, Y. Yan, Optimization of surface imprinted layer attached poly(vinylidene fluoride) membrane for selective separation of salicylic acid from acetylsalicylic acid using central composite design, Chem. Eng. J. 231 (2013) 132-145.

[28] A.D. Becke, Density-functional thermochemistry. III. The role of exact exchange, J. Chem. Phys. 98 (1993) 5648-5652. https://doi.org/10.1063/1.464913.

[29] A.V. Marenich, C.J. Cramer, D.G. Truhlar, Universal solvation model based on solute electron density and on a continuum model of the solvent defined by the bulk dielectric constant and atomic surface tensions, J. Phys. Chem. B 113 (2009) 6378-6396.

[30] B. Park, S.H. Yun, C.Y. Cho, Y.C. Kim, J.C. Shin, H.G. Jeon, Y.H. Huh, I. Hwang, K.Y. Baik, Y.I. Lee, H.S. Uhm, G.S. Cho, E.H. Choi, Surface plasmon excitation in semitransparent inverted polymer photovoltaic devices and their applications as label-free optical sensors, Light: Sci. Appl. 3 (2014) e222-e222.

[31] J. Lu, Y. Wu, X. Lin, J. Gao, H. Dong, L. Chen, Y. Qin, L. Wang, Y. Yan, Anti-fouling and thermosensitive ion-imprinted nanocomposite membranes based on grapheme oxide and silicon dioxide for selectively separating europium ions, J. Hazard. Mater. 353 (2018) 244-253.

[32] F. Pincella, K. Isozaki, K. Miki, A visible light-driven plasmonic photocatalyst, Light: Sci. Appl. 3 (2014) e133-e133. https://doi.org/10.1038/lsa.2014.14.

[33] Y. Qin, H. Li, J. Lu, Y. Yan, Z. Lu, X. Liu, Enhanced photocatalytic performance of MoS2 modified by AgVO3 from improved generation of reactive oxygen species, Chinese J. Catal. 39 (2018) 1470-1483. https://doi.org/10.1016/S1872-2067(18)63111-0.

Chapter 7

PERFORMANCE COMPARISON AND DISCUSSION

7.1 Rebinding performance comparison

7.1.1 Isothermal and kinetic rebinding performance

Isothermal and kinetic rebinding performance was respectively compared for the investigation of selective recognition. In the whole range of tested conditions, MIM exhibits a much higher rebinding capacity than PAM. The differentiation primarily confirms the enhanced effect of imprinted sites (recognition sites) on rebinding CIP. Since the PAM was synthesized by the same route as MIM just without template, its affinity towards CIP is achieved only based on the interactions between monomers and targets, but no shape effect of the site. It can be, therefore, inferred that the shape effect plays the leading role in the differentiation of the rebinding capacity.

For the concentration-dependent mode (Fig. 7-1), a non-uniform trend of increase appears in the rebinding capacity of MIM.

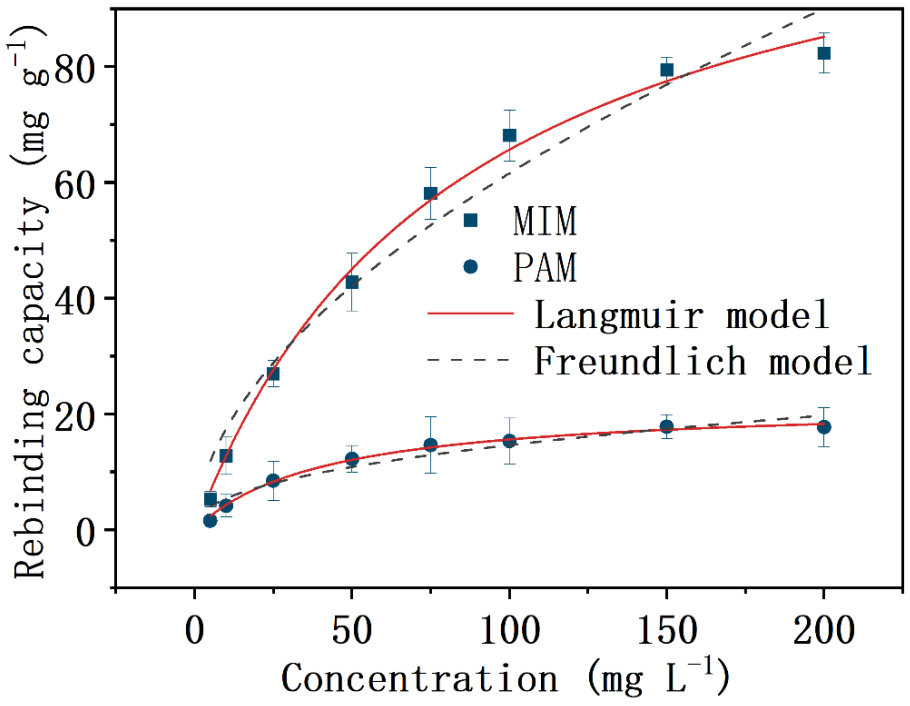

Fig. 7-1 Rebinding capacities of MIM and PAM with fitted isothermal models.

Specifically, the rebinding capacity increases rapidly with a low concentration of CIP, while

the trend is similar to that of PAM when the concentration is over 150 mg L^{-1}. In contrast to the consistently sluggish growth of PAM, it is reasonable to assume that the imprinted sites have made a crucial contribution to the improvement of rebinding rates, which further demonstrates the enhanced effect of imprinted sites.

Rebinding data are then fitted with Langmuir [1] (Fig. 7-2) and Freundlich [2] (Fig. 7-3) isothermal models, respectively.

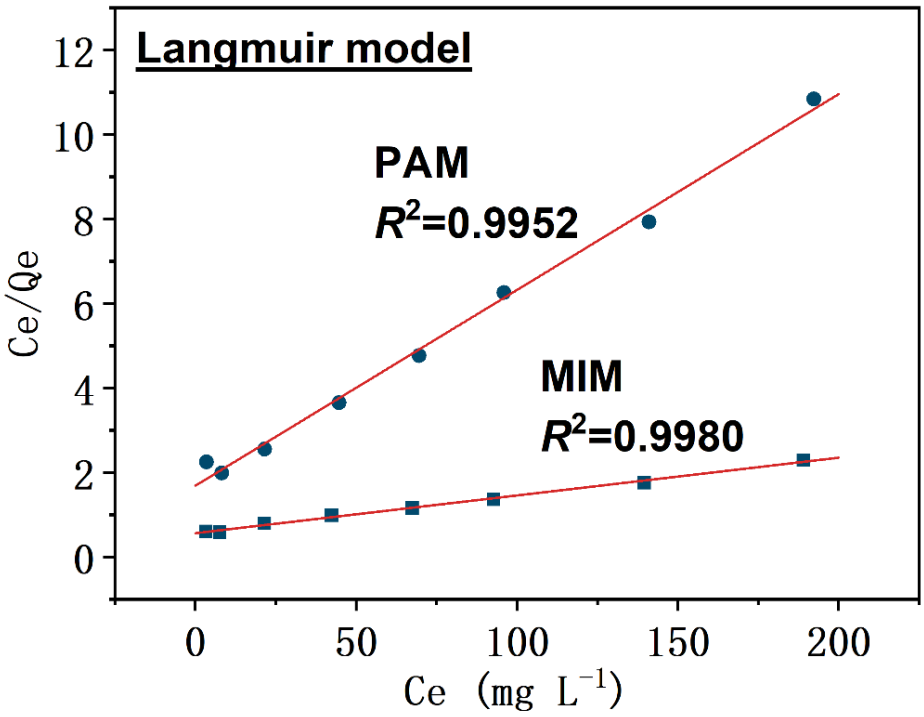

Fig. 7-2 Linear fitting of Langmuir models onto MIM and PAM

According to constants, rebinding data of MIM fit better with the Langmuir model (R^2 = 0.9980) than the Freundlich model (R^2 = 0.9694). It indicates that the imprinted sites on MIM exhibit a uniform and monolayer distribution [3]. Although no imprinted site has been synthesized on PAM, its rebinding data are more consistent with the Langmuir model (R^2 = 0.9952), compared with the Freundlich model (R^2 = 0.9390). The reason should result from that, despite the non-specificity, the uniformly distributional non-imprinted polymers on PAM are still the core contributors for the CIP binding, which therefore leads to a similar isotherm with MIM.

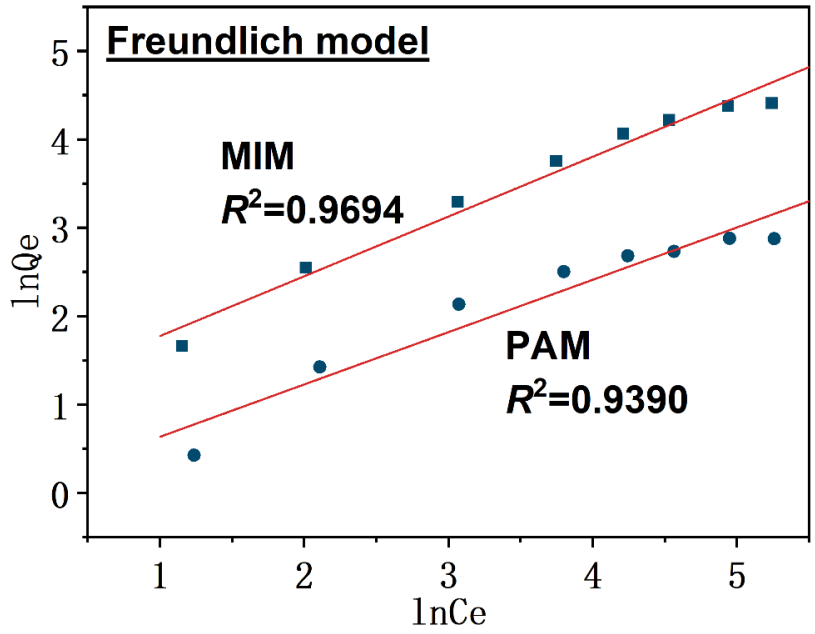

Fig. 7-3 Linear fitting of Freundlich models

For the time-dependent model (Fig. 7-4), a distinct trend from the concentration-dependent model appears on MIM comparing with PAM.

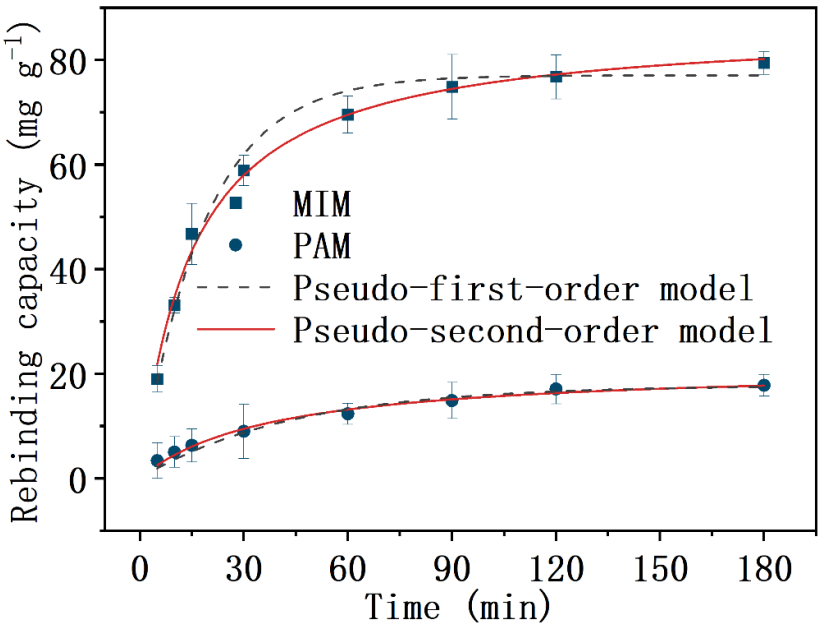

Fig. 7-4 Rebinding capacities of MIM and PAM with fitted kinetic models

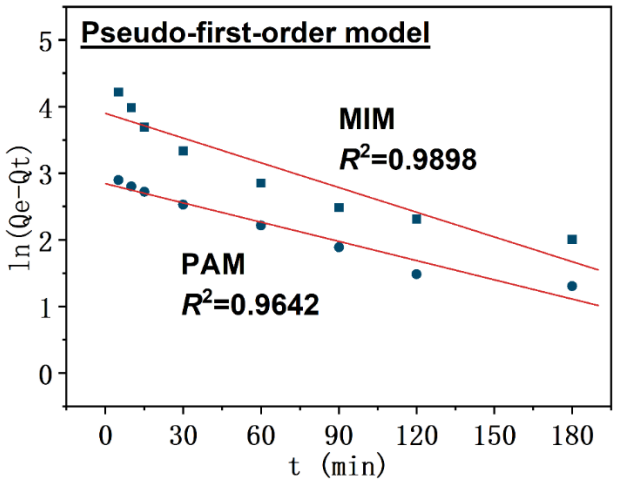

Fig. 7-5 Linear fitting of Pseudo-first-order models onto MIM and PAM

The rebinding capacity increases rapidly at first and reaches the platform in about 60 min. Compared with the consistent stationary trend of PAM under the same conditions, the phenomenon suggests the significant enhancement of imprinted sites on the rebinding rate. Rebinding data are, then, fitted with Pseudo-first-order [4] (Fig. 7-5) and Pseudo-second-order [5] (Fig. 7-6) model, respectively. Due to the nonnegligible contribution of non-imprinted polymers, the rebinding data of PAM are also more consistent with the pseudo-second-order (R^2 = 0.9897) model than the pseudo-first-order model (R^2 = 0.9642).

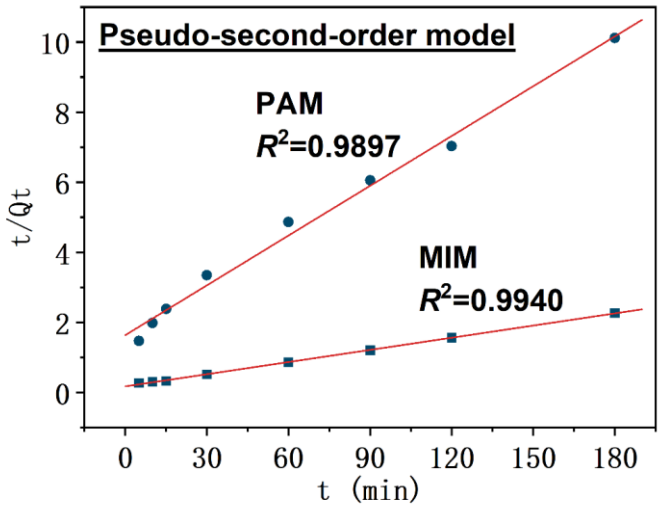

Fig. 7-6 Linear fitting of Pseudo-second-order models onto MIM and PAM

7.1.2 Adsorption performance with non-targets

For investigating the selective of the imprinted sites, concentration-dependent (Fig. 7-7 left) and time-dependent (Fig.7-7 right) selective rebinding operations were performed on MIM and PAM using ENR, NOR and OFL as non-targets.

Compared with the indistinctive differential onto PAM, MIM shows higher rebinding capacity towards the targets than the non-targets. Besides the effectiveness, the significantly distinguishing rebinding capacities also indicate the selectivity of the imprinted sites towards CIP, which is determined by the imprinting polymerization using CIP as the template.

It should be noted that, onto MIM, the rebinding towards CIP in the mixed system is weaker than that in a single target system. The phenomenon is especially remarkable at a high concentration (> 50 mg L^{-1}). It results from that the non-specific interaction between sites and non-targets leads to competition between targets and non-targets.

Since more non-targets own the chance to occupy imprinted sites with a high concentration, the decline will be more obvious. In contrast, the shape-matched recognition site for CIP does not exist on PAM, so the influence of competitors on the rebinding capacity of CIP is negligible.

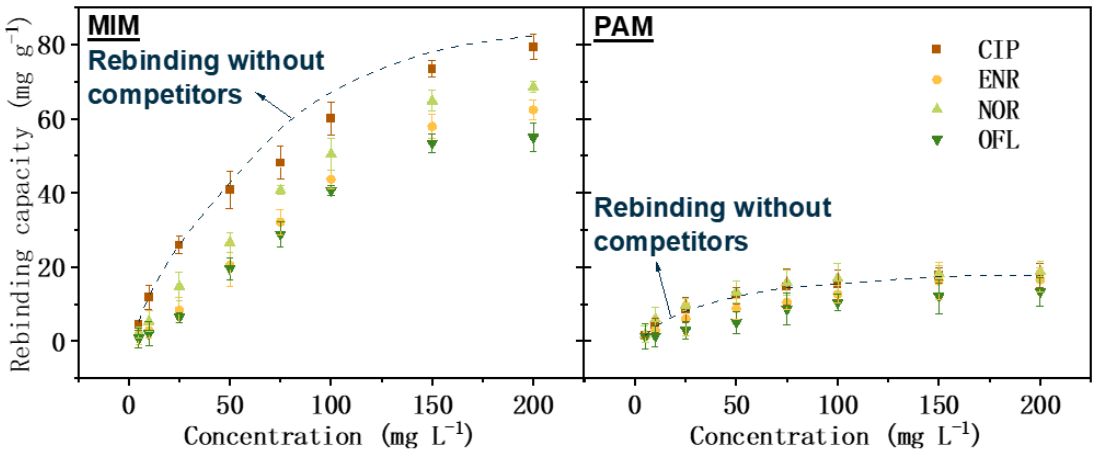

Fig. 7-7 Comparison of concentration-dependent selective rebinding performance onto MIM and PAM

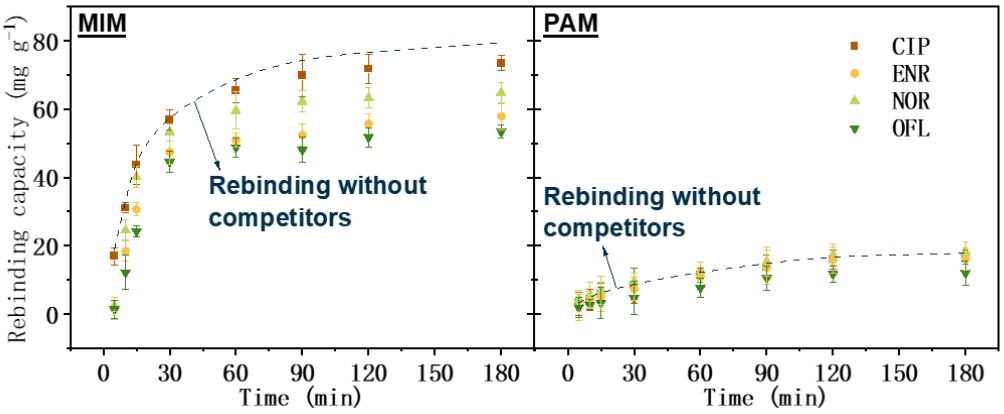

Fig. 7-8 Comparison of time-dependent selective rebinding performance onto MIM and PAM

Then, the separation factors are calculated according to selective rebinding data, as displayed in Fig. 7-9.

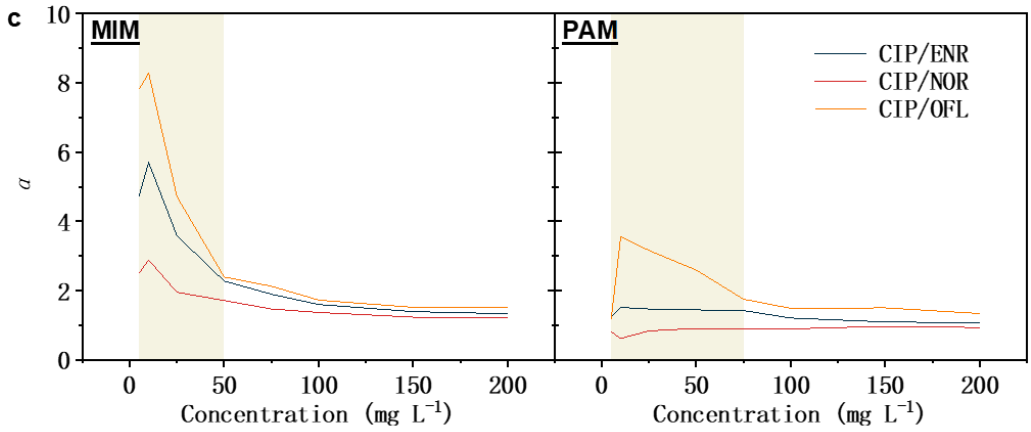

Fig. 7-9 Separation factors (α) onto MIM and PAM

The remarkable selectivity of MIM is approached with a low concentration (< 50 mg L^{-1}), where the optimal one (αCIP/ENR = 5.70, αCIP/NOR = 2.89 and αCIP/OFL = 8.28) is achieved at 10 mg L^{-1}. It indicates that the low concentration is more conducive to demonstrating the capability of imprinted sites on selective recognition and rebinding of CIP. The phenomenon is consistent with the apparent interference caused by competitors at the high concentration (> 50 mg L^{-1}). The intrinsic reason should be that the high concentration promotes a shift of the equilibrium towards saturation. Considering the limited number of imprinted sites on MIM, the

non-specific rebinding will, therefore, be enhanced at the high concentration, thus weakening the specificity dominated by specific rebinding. Compared with MIM, the as-obtained PAM, as expected, shows no obvious specificity towards CIP because of the absence of a template during the polymerization.

The remarkable selectivity of MIM is approached with a low concentration (< 50 mg L^{-1}), where the optimal one (αCIP/ENR = 5.70, αCIP/NOR = 2.89 and αCIP/OFL = 8.28) is achieved at 10 mg L^{-1}. It indicates that the low concentration is more conducive to demonstrating the capability of imprinted sites on selective recognition and rebinding of CIP. The phenomenon is consistent with the apparent interference caused by competitors at the high concentration (> 50 mg L^{-1}). The intrinsic reason should be that the high concentration promotes a shift of the equilibrium towards saturation. Considering the limited number of imprinted sites on MIM, the non-specific rebinding will, therefore, be enhanced at the high concentration, thus weakening the specificity dominated by specific rebinding. Compared with MIM, the as-obtained PAM, as expected, shows no obvious specificity towards CIP because of the absence of a template during the polymerization.

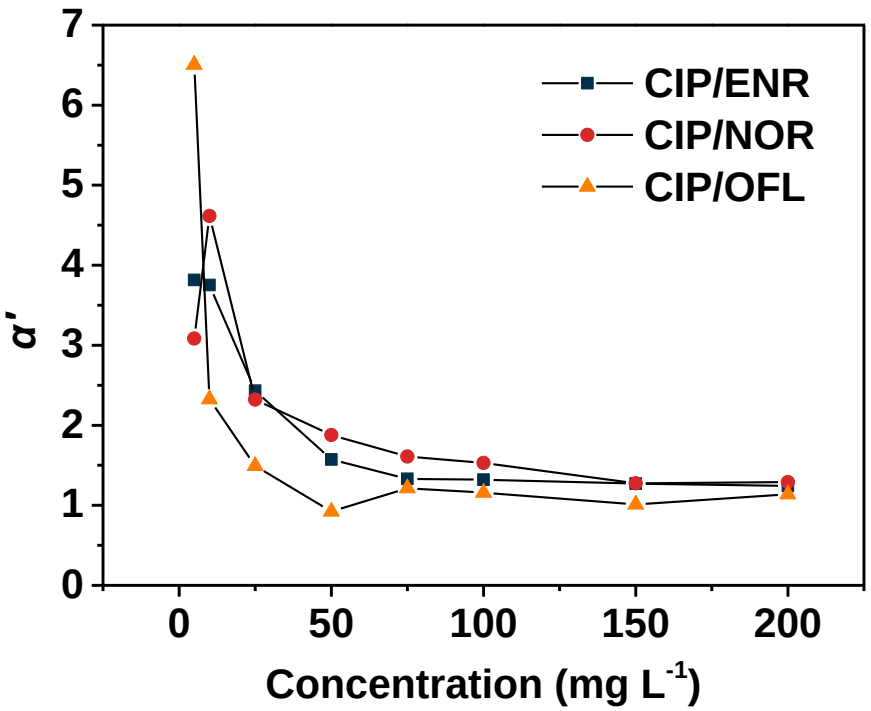

Fig. 7-10 Relative separation factors (*α′*) onto MIM and PAM.

To eliminate the interference of non-specific rebinding, relative separation factors (α') obtained by MIM and PAM were further explored. Fig. 7-10 shows that the relative separation factors are positively high when the concentration is below 50 mg L^{-1} but exhibits negativity above this concentration. It confirms that the specific rebinding is dominant at low concentrations, while non-specific rebinding gradually becomes dominant at high concentrations. As a result, the MIM will exhibit better performance when the concentration is lower than 50 mg L^{-1}, especially below 10 mg L^{-1}. Since the reported concentration range of CIP and its analogues in real samples is generally within 5 mg L^{-1} [6-11], the resulting MIM exactly shows the suitable pertinence and applicability. Static allocation coefficient, separation factors and relative separation factors are summarized in Table 7-1 in detail.

Further, the imprinting factors at the optimum concentration (10 mg L^{-1}) were explored under different pH values. Fig. 7-11 shows that the rebinding capacity of CIP on both MIM and PAM increased first and then decreased.

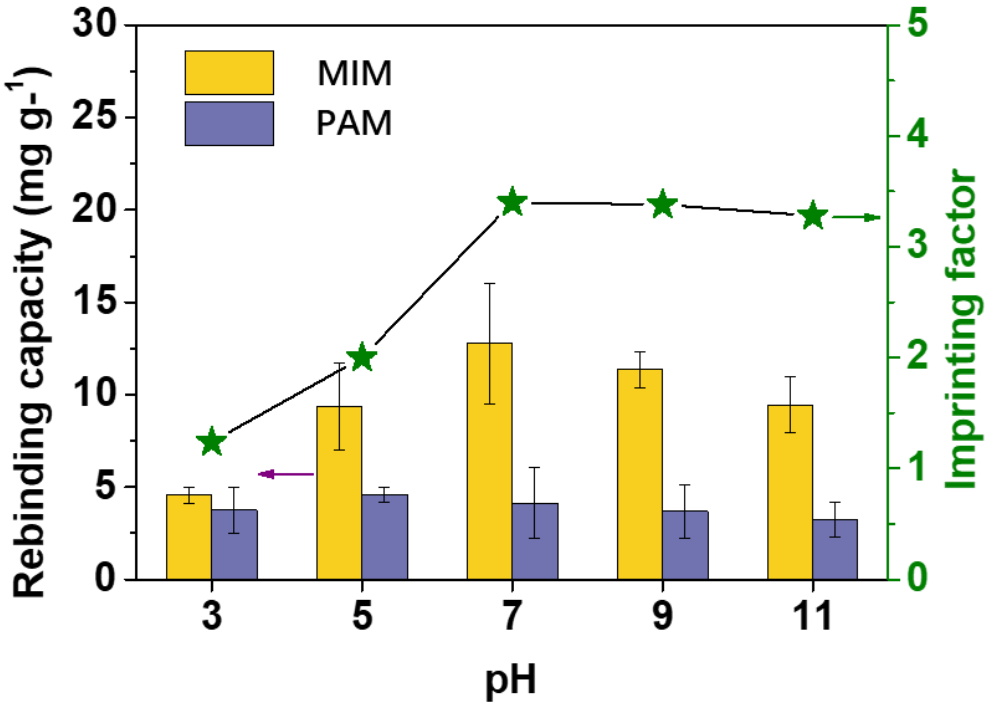

Fig. 7-11 Rebinding capacities and imprinting factors achieved by MIM and PAM

For the PAM, the best performance is achieved at pH = 5. It should result from that the PAM

is dominated by the negative charge under an acidic condition. The combination of H^+ and the –NH– group makes the CIP exhibit a cationic state and be conducive to binding with PAM [12]. However, the performance significantly declines when pH < 5. It should be ascribed to the competition of excessive H+ with the CIP based on the protonation effect. In contrast, the optimum rebinding capacity of MIM is obtained at pH = 7. The difference between MIM and PAM should be attributed to the fact that the imprinting polymerization is carried out in a neutral environment. The resulting caves (imprinted sites) are most matched with the molecular structure of neutral CIP, thus showing a better rebinding performance. As a result, the optimum imprinting factor (3.40) could be achieved at pH = 7.

Table 7-1 Static allocation coefficient (K, L g^{-1}), separation factors (α) and relative separation factors (α') onto MIM and PAM (10 mg L^{-1}).

Molecule	Membrane	K (L g^{-1})	α	α'
CIP	MIM	1.7096	-	-
	PAM	0.5033	-	
ENR	MIM	0.2998	5.70	3.75
	PAM	0.3312	1.52	
NOR	MIM	0.5916	2.89	4.59
	PAM	0.8037	0.63	
OFL	MIM	0.2065	8.28	2.33
	PAM	0.1414	3.56	

7.2 Permeation performance comparison

In chapter 6, a mixed solution with 10 mg L^{-1} of CIP, ENR, NOR and OFL was employed for the permeation investigations onto the MIM. For comparison, the same experiment also operated onto the PAM. The typical static permeation was performed on MIM and PAM, respectively.

In Fig 7-12 (left), the concentration evolution in the permeate and dialysate of MIM is

depicted. Notably, a distinct disparity emerges in the equilibrium times of CIP (36 h) and non-targets (24 h). This discrepancy signifies a pronounced delay in achieving equilibrium for CIP permeation onto MIM, indicating the membrane's substantial retarding effect on CIP. Simultaneously, the equilibrium concentration of CIP proves to be considerably lower than that of the non-targets, underscoring MIM's robust rebinding effect on CIP within the mixed system. These findings align with the deductions drawn from selective rebinding experiments. Thus, it can be reasonably inferred that MIM effectively impedes the permeation of CIP by virtue of its capacity for selective recognition and subsequent rebinding to CIP.

On the other hand, PAM exhibits contrasting behavior with comparable equilibrium concentrations and nearly identical equilibrium times for both CIP and non-targets, as shown in Fig. 7-12 (right). This observation suggests that achieving effective separation is challenging on PAM in terms of both time and concentration due to the absence of selective recognition sites. In light of this inference, Fig. 7-13 depicts the mechanism of selective separation on MIM.

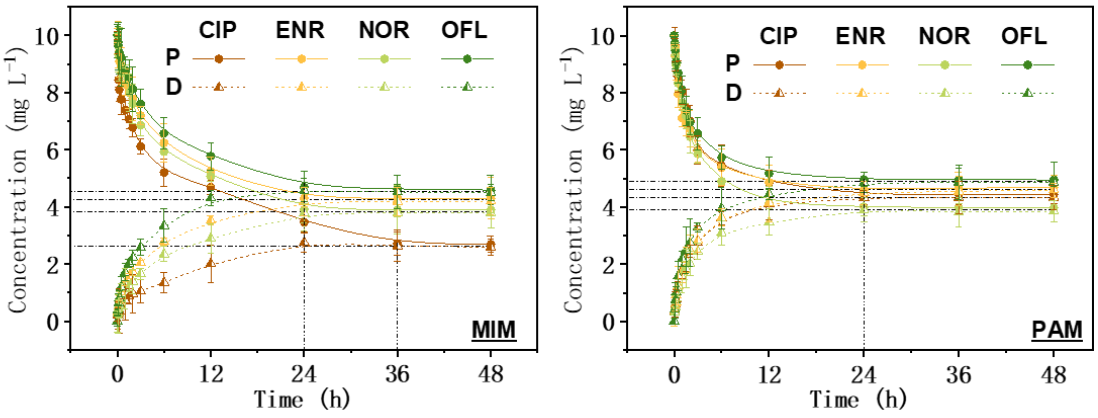

Fig. 7-12 Comparison of permeation performance of target and non-targets onto MIM and PAM

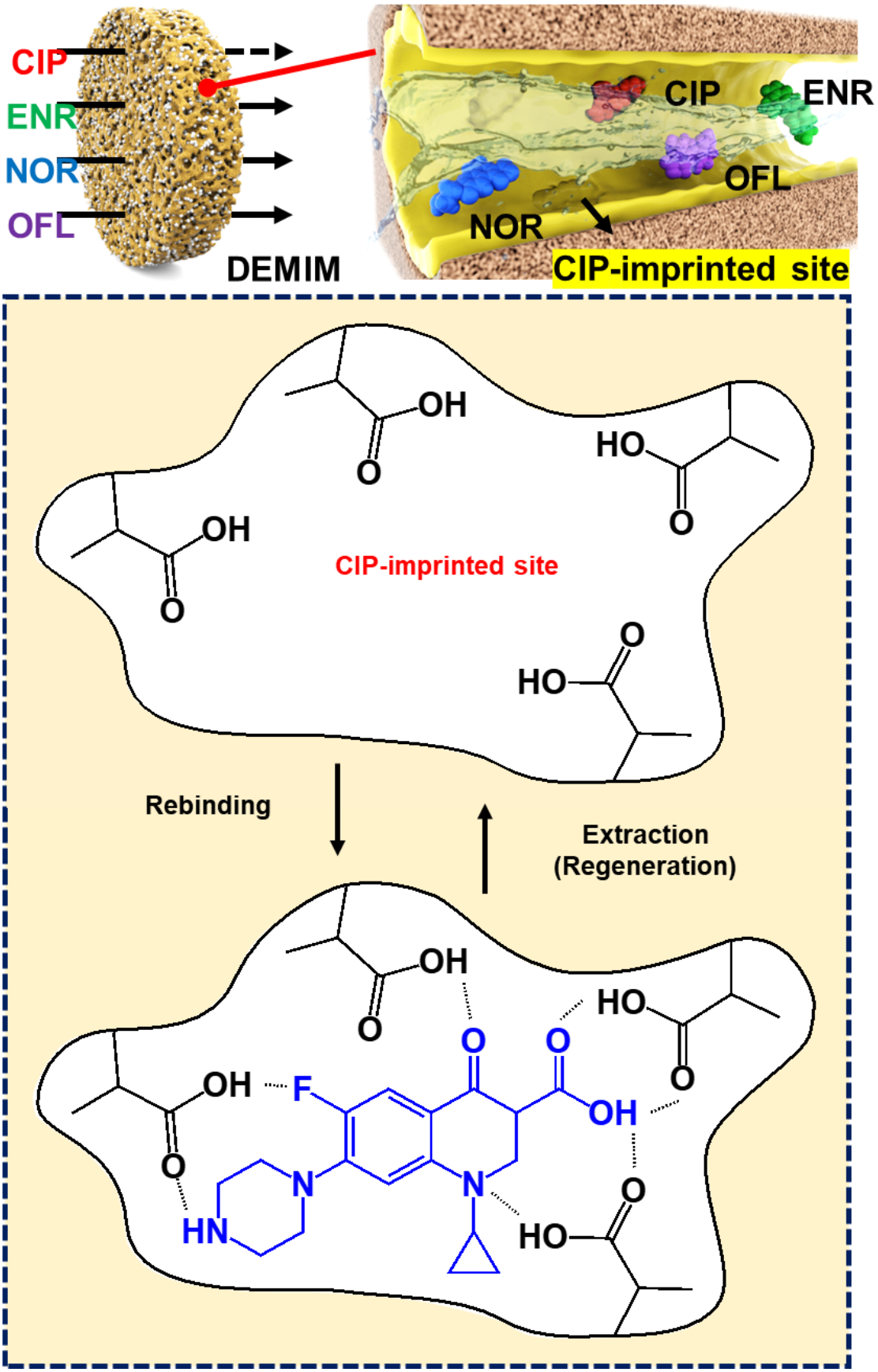

Fig. 7-13 Schematics illustrating the selective separation based on MIM

Next, I compare the permeation fluxes (J) of CIP and non-targets to gain deeper insights. The evolution curves of CIP and non-targets on MIM exhibit significant variations, particularly within the first 24 hours, owing to their distinct permeabilities (Fig. 7-14 left). In contrast, the permeation fluxes on PAM show minimal differences (Fig. 7-14 right). Consequently, the feasibility of achieving selective separation through the specially designed MIM is confirmed. It is important to note that the permeation fluxes of non-targets on PAM are higher than those on MIM. This phenomenon can be attributed to the structural complementarity, which plays a crucial role in the selective recognition and rebinding by the imprinted sites. Since the selected non-targets closely resemble CIP, the inevitable matching leads to enhanced rebinding and reduced permeability of the non-targets. Nevertheless, the stronger recognition and rebinding towards CIP ensure effective separation between CIP and non-targets.

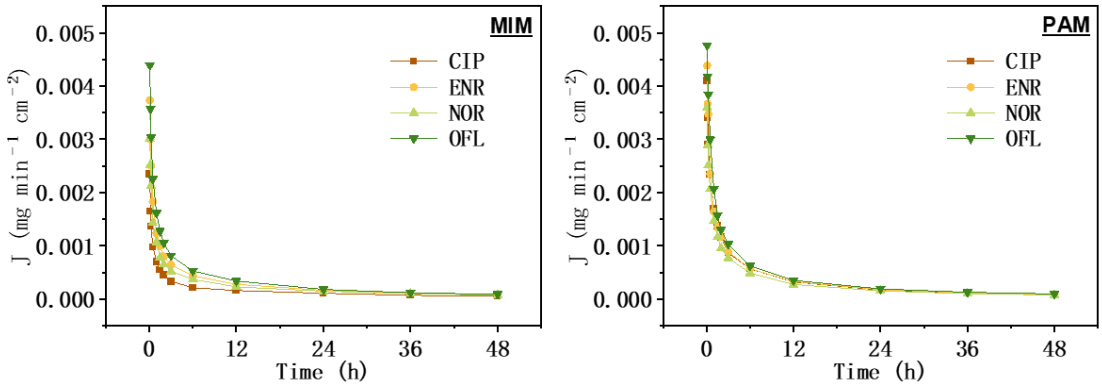

Fig. 7-14 Comparison of permeation flux of target and non-targets onto MIM and PAM

To investigate the optimal operating conditions, I further analyze the evolution of the permeability coefficient (P). In the case of MIM (Fig. 7-15 left), both CIP and non-targets show a decreasing trend in the permeability coefficient during the first 3 hours. This can be attributed to the initial rapid diffusion of molecules driven by the concentration gradient, followed by the specific rebinding of CIP and the non-specific rebinding of non-targets facilitated by the imprinted sites, which hinder their permeability. As the concentration difference between the permeate and dialysate decreases and the retarding ability strengthens, the permeability coefficients decline. Subsequently, the permeability coefficients increase as the system approaches equilibrium rebinding. During this process, the retarding effect on CIP persists

longer than on non-targets due to the stronger interaction between the imprinted site and CIP. Consequently, the maximum permeability coefficient for CIP is reached more slowly (at 36 hours) compared to non-targets (at 24 hours). Conversely, for PAM (Fig. 7-15 right), the permeability coefficients of both CIP and non-targets reach their maximum simultaneously (at 24 hours) due to the lack of selectivity. Based on this analysis, superior selective separation can be achieved when the permeability of non-targets remains active while the permeability of CIP is suppressed (at 24 hours). Table 7-2 provides a summary of the permselectivity coefficients (β) for MIM and PAM, highlighting the impressive permselectivity exhibited by MIM, with coefficients ranging from 9.50 to 12.50.

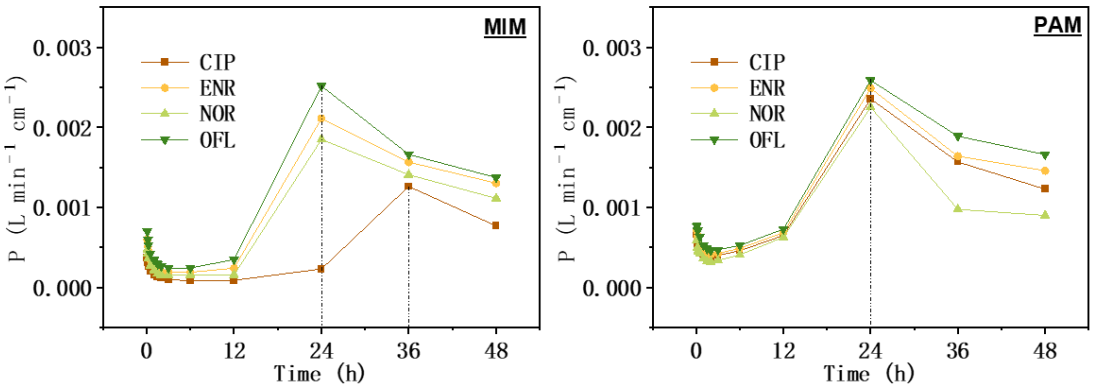

Fig. 7-15 permeability coefficient of target and non-targets onto MIM and PAM

Table 7-2 Parameters of selective permeation onto MIM and PAM (24 h)

Membrane	Molecule	$J \times 10^4$ (mg min^{-1} cm^{-2})	P (L min^{-1} cm^{-1})	β
MIM	CIP	1.0836	0.0002	-
	ENR	1.6459	0.0021	10.50
	NOR	1.4886	0.0019	9.50
	OFL	1.8016	0.0025	12.50
PAM	CIP	1.7006	0.0024	-
	ENR	1.7659	0.0025	1.04
	NOR	1.5353	0.0023	0.96
	OFL	1.9077	0.0026	1.08

7.3 Performance evaluation

For a comprehensive evaluation of the performance, multi-dimensional comparisons were performed between MIM and reported researches, focusing on the rebinding capacity, imprinting factor, selectivity, regeneration property and anti-fouling performance.

Table 7-3 Performance comparison between MIM and reported CIP-imprinted materials

Material	Rebinding capacity	Imprinting factor	Selectivity[a]
MMIPs	33.18 mg g^{-1}	1.69	CIP/ENR = 1.26 CIP/NOR = 1.08 CIP/OFL = 1.10
MIP	9.57 mg g^{-1}	3.88	CIP/LOM = 1.55 CIP/SMZ = 3.03 CIP/N-Py = 1.67
MIP	11.53 mg g^{-1}	1.35	CIP/GAT = 1.48 CIP/CHL = 2.32 CIP/TC = 2.92
MGO@$MSiO_2$	27.02 mg g^{-1}	3.00	CIP/ENR = 1.14 CIP/NOR = 1.05 CIP/OFL = 2.26
MIM	121.12 mg g^{-1}	3.40	CIP/ENR = 3.75 CIP/NOR = 4.59 CIP/OFL = 2.33

[a] The selectivity was evaluated according to the relative separation factors (α').

As shown in Table 7-3, the superior rebinding capacity that is much higher than that of reported CIP-imprinted materials, together with the remarkable imprinting factor (3.40), is obtained on MIM. It indicates that the PDA-embedded strategy provides the possibility of integrating the numerous CIP-imprinted sites in an interpenetrating-bicontinuous porous sleeve.

As a result, better selectivity can be achieved on MIM. Moreover, the performance of MIM is also compared with similar MIMs for the evaluation of membrane performance. As summarized in Table 7-4, MIM exhibits impressive permselectivity to the congeneric membranes, which is even better than our previous work [13]. The result is attributed to the design of the PDA-embedded porous sleeve, which increases the time for the liquid to flow through the inner space of the membrane. It ensures enough time for the target to approach the imprinted site. The efficient specific rebinding and permselectivity can be, therefore, achieved on the MIM. Importantly, the as-obtained MIM also shows comparable regenerative performance and a wider-available anti-fouling performance. Based on the above analysis, the as-constructed MIM demonstrates better comprehensive properties than similar materials with wider application prospects.

Table 7-4 Performance comparison between MIM of this research and other reported MIMs

Membrane	Selectivity[a]	Regeneration performance	Antifouling performance
m-MIM	1.51-1.82	9% of decline (9 cycles)	-
CBMIMs	1.65-1.87	-	5-20 mg L^{-1} of pollutant
MIM7	2.66	11.43% of decline (5 cycles)	-
MAPSP	2.03-2.15	4% of decline (6 cycles)	-
C/A/D-MIMs	1.65-2.08	3.8%-7.4% of fluctuation (10 cycles)	50-200 mg L^{-1} of pollutant
MIM	9.50-12.50	8.4-10.8% of fluctuation (10 cycles)	5-200 mg L^{-1} of pollutant

[a] The selectivity was evaluated according to the permselectivity coefficients (β).

Therefore, MIMs hold significant promise as a cutting-edge solution for the removal of antibiotics from wastewater in medical buildings. These advanced membranes, designed with molecular recognition sites tailored to specific antibiotic molecules, exhibit exceptional

selectivity and adsorption capacities. This technology not only addresses the pressing issue of antibiotic pollution but also offers a sustainable and efficient approach to safeguarding environmental and public health within medical buildings. As the demand for effective wastewater treatment in healthcare settings continues to grow, MIMs stand out as a transformative technology capable of mitigating the environmental impact of antibiotic discharge and enhancing the quality of treated effluents.

Reference

[1] B. Park, S.H. Yun, C.Y. Cho, Y.C. Kim, J.C. Shin, H.G. Jeon, Y.H. Huh, I. Hwang, K.Y. Baik, Y.I. Lee, H.S. Uhm, G.S. Cho, E.H. Choi, Surface plasmon excitation in semitransparent inverted polymer photovoltaic devices and their applications as label-free optical sensors, Light: Sci. Appl. 3 (2014) e222-e222.

[2] J. Lu, Y.-Y. Qin, Y.-L. Wu, M.-N. Chen, C. Sun, Z.-X. Han, Y.-S. Yan, C.-X. Li, Y. Yan, Mimetic-core-shell design on molecularly imprinted membranes providing an antifouling and high-selective surface, Chem. Eng. J. 417 (2021) 128085.

[3] J. Lu, Y. Wu, X. Lin, J. Gao, H. Dong, L. Chen, Y. Qin, L. Wang, Y. Yan, Anti-fouling and thermosensitive ion-imprinted nanocomposite membranes based on grapheme oxide and silicon dioxide for selectively separating europium ions, J. Hazard. Mater. 353 (2018) 244-253.

[4] F. Pincella, K. Isozaki, K. Miki, A visible light-driven plasmonic photocatalyst, Light: Sci. Appl. 3 (2014) e133-e133.

[5] Y. Qin, H. Li, J. Lu, Y. Yan, Z. Lu, X. Liu, Enhanced photocatalytic performance of MoS2 modified by AgVO3 from improved generation of reactive oxygen species, Chinese J. Catal. 39 (2018) 1470-1483.

[6] L. Tong, P. Li, Y. Wang, K. Zhu, Analysis of veterinary antibiotic residues in swine wastewater and environmental water samples using optimized SPE-LC/MS/MS, Chemosphere 74 (2009) 1090-1097.

[7] R.H. Lindberg, P. Wennberg, M.I. Johansson, M. Tysklind, B.A.V. Andersson, Screening of human antibiotic substances and determination of weekly mass flows in five sewage treatment

plants in sweden, Environ. Sci. Technol. 39 (2005) 3421-3429.

[8] R. Rosal, A. Rodríguez, J.A. Perdigón-Melón, A. Petre, E. García-Calvo, M.J. Gómez, A. Agüera, A.R. Fernández-Alba, Occurrence of emerging pollutants in urban wastewater and their removal through biological treatment followed by ozonation, Water Res. 44 (2010) 578-588.

[9] N. Vieno, T. Tuhkanen, L. Kronberg, Elimination of pharmaceuticals in sewage treatment plants in Finland, Water Res. 41 (2007) 1001-1012.

[10] X. Van Doorslaer, J. Dewulf, H. Van Langenhove, K. Demeestere, Fluoroquinolone antibiotics: An emerging class of environmental micropollutants, Sci. Total Environ. 500-501 (2014) 250-269.

[11] S. Babić, M. Periša, I. Škorić, Photolytic degradation of norfloxacin, enrofloxacin and ciprofloxacin in various aqueous media, Chemosphere 91 (2013) 1635-1642.

[12] D. Vasudevan, G.L. Bruland, B.S. Torrance, V.G. Upchurch, A.A. MacKay, pH-dependent ciprofloxacin sorption to soils: Interaction mechanisms and soil factors influencing sorption, Geoderma 151 (2009) 68-76.

[13] J. Lu, Y.-Y. Qin, Y.-L. Wu, Z. Zhu, M.-N. Chen, Y.-S. Yan, C.-X. Li, Bio-synthesis of molecularly imprinted membrane with photo-regeneration availability for selective separation applications, Mater. Today Chem. 24 (2022) 100836. https://doi.org/10.1016/j.mtchem.2022.100836.

Chapter 8

CONCLUSION AND PROSPECT

8.1 Conclusion

With the increasing use of antibiotics and the rising concentration of antibiotics in medical wastewater, the treatment of antibiotics in wastewater from medical buildings has become increasingly important. Between 2000 and 2015, antibiotic consumption increased by 65%, and the antibiotic consumption rate increased by 39%. Among the various methods for treating antibiotics in wastewater, membrane separation technology has been our focus of research due to its high treatment efficiency, strong operational flexibility, sustainability, and relatively mature technology. However, traditional membrane treatment techniques face a trade-off between membrane flux and treatment performance, resulting in certain limitations in treatment efficiency. The objective of this study is to explore improvements in membrane technology to increase membrane flux while ensuring an increase in treatment performance. Additionally, I aim to meet the requirements for selective separation to further enhance the treatment efficiency of antibiotics in medical wastewater from medical buildings.

The main works and results can be summarized as follows:

In Chapter 1, RESEARCH BACKGROUND AND PURPOSE OF THE STUDY, the research backgrounds of the increasing use of antibiotics and the rising concentration of antibiotics in medical wastewater are introduced in chapter 1, including the sources and distribution of antibiotics in the environment. As well as the antibiotic pollution in water resources. Then the hazards of antibiotics pollution to the environment, creature and human beings is well introduced. Researching the treatment technologies for antibiotics in medical building wastewater is of great importance. At last, the research purpose and logical framework is shown in order to support reviewers understand the content of this paper.

In Chapter 2, LITERATURE REVIEW OF ANTIBIOTIC REMOVAL, this chapter provides a comprehensive overview of past research on the removal of antibiotics from wastewater. The focus is on three primary treatment methods: biological treatment, oxidation methods, and physical methods. The biological treatment approach is cost-effective and can achieve high removal efficiencies but sensitive to environmental conditions, and have the potential for the development of antibiotic-resistant bacteria. The oxidation methods have high treatment

efficiency but its energy and cost consumption are high, too. Physical methods, particularly membrane separation technology, offers high removal efficiencies, compatibility and the potential for resource recovery. Therefore, the treatment of antibiotics by membrane technology is the focus of this study.

In Chapter 3, METHODOLOGY, in this chapter, the design of membrane synthesis methods was explored. The aim was to enhance both membrane flux and adsorption efficiency. To achieve this, the membrane thickness was increased, and a sacrificial template method was utilized to enhance the interconnected pore structure within the membrane. To address the issue of pore size affecting treatment efficiency, a plan was devised to synthesize a polymer layer on the inner and outer surfaces of the membrane to absorb antibiotic molecules. In order to ensure that the synthesized materials meet our requirements, a design for the characterization methods of the membrane materials was established. This involved conducting a series of material property characterizations, including scanning electron microscopy (SEM), X-ray photoelectron spectroscopy (XPS), Fourier-transform infrared spectroscopy (FTIR), in-situ diffuse reflectance infrared Fourier transform spectroscopy (In-situ DRIFT) and so on.

In Chapter 4, DATA RESOURCE AND MEMBRANE PERFORMANCE ANALYSIS, this chapter focused on the planning and design of testing methods for membrane performance, with ciprofloxacin selected as the target molecule for testing. The testing methods were carefully planned to evaluate the efficacy of the membranes in adsorbing and permeating ciprofloxacin. The adsorption capacity would provide insights into the membrane's ability to remove the target molecule from the solution, while the permeation tests would assess the membrane's ability to allow or restrict the passage of the molecule through its structure. By conducting these tests and employing the provided calculation methods, the performance of the synthesized membranes could be quantitatively evaluated.

In Chapter 5, POLYMERIZATION ADSORPTION MEMBRANE, in this chapter, the synthesis of the Polymerization Adsorption Membrane (PAM) was performed. After determining the materials and characterization equipment, the PVDF-βCD-dopamine membrane (VCDM) was synthesized as a precursor, followed by ethylene modification and

subsequent polymerization to obtain the desired PAM. The membrane was then subjected to material characterization, confirming the success of each reaction step. The performance testing began with isothermal adsorption tests, which revealed that the adsorption capacity of the PAM for ciprofloxacin (CIP) reached 22.04 mg g^{-1}. Furthermore, the adsorption sites on the PAM exhibited a uniform and monolayer distribution, confirming its adsorption capability for CIP molecules. Subsequently, permeation adsorption experiments were conducted, and it was observed that the equilibrium of CIP molecules in solution was reached after 24 hours. This indicated that the PAM had an inhibitory effect on the permeation of CIP within 24 hours.

In chapter 6, MOLECULARLY IMPRINTED MEMBRANE, in this chapter, to maximize membrane utilization and address real antibiotic discharge scenarios, I enhanced the absorption capacity of the PAM membrane for a specific antibiotic molecule among various types. Through modification during synthesis, the final step incorporated molecular imprinting technology, using ciprofloxacin (CIP) as the template, resulting in the creation of a Molecularly Imprinted Membrane (MIM). Material characterization confirmed the successful synthesis at each step. In adsorption performance tests, the MIM exhibited an impressive adsorption capacity of 121.12 mg g-1 for CIP molecules. The membrane surface demonstrated a uniform monolayer distribution of adsorption sites, with a coexistence of chemical adsorption and physical diffusion. Subsequently, selective adsorption and permeation experiments were conducted with four structurally similar but different types of antibiotics, including CIP. The results revealed that the MIM possessed significantly higher absorption capacity for CIP molecules compared to the other three types. The inhibitory effect on CIP permeation lasted for 36 hours, surpassing the 24-hour mark observed for the other types. These findings demonstrate the strong inhibitory and adsorption capabilities of the MIM specifically for CIP molecules.

In chapter 7, PERFORMANCE COMPARISON, in this chapter, in order to evaluate the performance enhancement achieved by incorporating molecular imprinting technology, a comparison of the Molecularly Imprinted Membrane (MIM) and the Polyacrylamide (PAM) membrane was conducted. Additionally, the PAM membrane was subjected to adsorption and permeation experiments involving four structurally similar but different types of antibiotics. The results of the comparison indicated that the MIM is far superior to PAM in terms of

adsorption capacity, permeation inhibition, adsorption selectivity and permeation selectivity, highlighting the role played by the imprinting sites on the membrane surface. Then regeneration performance and anti-fouling tests were performed on the MIM, demonstrating comparable regenerative properties and a wider range of resistance to fouling. Taking all the findings into consideration, the as-constructed MIM exhibited superior comprehensive properties compared to similar materials, thus presenting promising prospects for broader applications.

In chapter 8, CONCLUSION AND PROSPECT, a summarized of each Chapter is concluded.

To enhance the efficiency of antibiotic removal in medical wastewater treatment, I proposed the design of a thicker membrane material with larger interconnected pores. Additionally, I attempted to synthesize a layer of adsorptive polymer on the membrane surface to enhance its affinity for antibiotic molecules. Through this approach, I successfully synthesized polymerization adsorption membrane (PAM) and tested their performance using Ciprofloxacin (CIP) as a model antibiotic. The results demonstrated the presence of adsorption capacity and permeation inhibition for CIP molecules on the PAM. Furthermore, to meet the demand for selective adsorption of specific types of antibiotic molecules, I introduced molecular imprinting technology onto the PAM membrane. This resulted in the synthesis of a Molecularly Imprinted Membrane (MIM) using CIP as a template. The MIM exhibited significantly improved absorption capacity and permeation inhibition for CIP molecules. Notably, the impressive rebinding selectivity (α = 2.89-8.28) and permselectivity (β = 9.50-12.50) highlighted the superior selective separation capabilities of the MIM.

8.2 Prospect

The use of molecularly imprinted membranes for the treatment of antibiotics in water from medical building holds promising prospects for the future. There are four key aspects to consider:

Adsorption Capacity: Continued research efforts will focus on enhancing the adsorption capacity of molecularly imprinted membranes. By optimizing material synthesis and structural design, I can improve the membrane's ability to effectively adsorb target antibiotic molecules,

leading to higher removal efficiencies and lower residual concentrations.

Selectivity: Future studies will prioritize the selectivity of molecularly imprinted membranes. Through adjustments in the ratio and structure of imprint templates and functional monomers, high selectivity for different antibiotics can be achieved. This will enhance treatment effectiveness while minimizing interference from other substances in the environment.

Treatment Efficiency: Advancements will be made in improving the treatment efficiency of molecularly imprinted membranes. By optimizing membrane structure and flux, the mass transfer rate of antibiotic molecules within the membrane can be enhanced, resulting in faster treatment processes and increased removal efficiencies in water bodies.

Cost Reduction: As technology progresses and economies of scale come into play, it is expected that the production costs of molecularly imprinted membranes will decrease. Additionally, the development of new materials and process improvements will further contribute to reducing the overall manufacturing costs, making molecularly imprinted membrane technology more commercially viable.